DOTTORATO DI RICERCA IN INGEGNERIA CIVILE PER L'AMBIENTE ED IL TERRITORIO
XI Ciclo - Nuova Serie (2009-2012)
DIPARTIMENTO DI INGEGNERIA CIVILE, UNIVERSITÀ DEGLI STUDI DI SALERNO

A METHODOLOGICAL APPROACH FOR THE ANALYSIS OF SHALLOW LANDSLIDES IN NON-COLLAPSIBLE SOILS

UN APPROCCIO METODOLOGICO PER L'ANALISI DELLE FRANE SUPERFICIALI IN TERRENI NON COLLASSABILI

MARIANTONIETTA CIURLEO

Relatore:
PROF. ING. LEONARDO CASCINI

Coordinatore
PROF. ING. LEONARDO CASCINI

Correlatori:
PROF. ING. GIUSEPPE SORBINO

PROF. DOTT. SILVIO DI NOCERA

ING. GIOVANNI GULLÀ

On the front cover: Typical examples of shallow landslides in fine-grained soils. Catanzaro, Calabria (Italy).

A METHODOLOGICAL APPROACH FOR THE ANALYSIS OF SHALLOW LANDSLIDES IN NON-COLLAPSIBLE SOILS

INDEX

INDEX OF FIGURES

INDEX OF TABLES

SOMMARIO

Le frane superficiali in terreni a grana fine non collassabili sono tra i fenomeni naturali che, per il loro simultaneo verificarsi in aree di grande estensione, comportano spesso rilevanti perdite di suolo agricolo con conseguenti ingenti danni economici.
Nonostante la rilevanza delle conseguenze si deve, tuttavia, osservare che la letteratura scientifica, da sempre molto attenta all'analisi dei fenomeni franosi superficiali in terreni collassabili, ha dedicato fino ad ora un'attenzione molto limitata ai fenomeni superficiali in suoli non collassabili. Inoltre i pochi lavori disponibili si basano, infatti, sull'uso di approcci mono-disciplinari che forniscono utili indicazioni di carattere specifico, ma spesso introducono drastiche semplificazioni finendo per trascurare aspetti talora rilevanti. Aspetti, questi ultimi, che possono essere ben evidenziati soltanto facendo riferimento ad un approccio multidisciplinare e multi scalare (di tipo induttivo o deduttivo), come messo già in evidenza da alcuni autori in contesti geo-ambientali molto diversi tra loro sede di fenomeni franosi da mediamente profondi a profondi.
In un panorama così delineato, che risulta ricco in termini di approcci disponibili ma carente con riferimento alle frane superficiali in terreni non collassabili, la presente tesi intende fornire un contributo metodologico per l'inquadramento dei fenomeni oggetto di studio in un contesto organico di riferimento che consenta, allo stesso tempo, di fornire risposte specifiche ad alcuni dei molteplici e complessi quesiti che sorgono nell'analisi dell'innesco di questi fenomeni.
La metodologia proposta è stata testata e validata in un'area dell'Italia meridionale, sede di una franosità superficiale diffusa della quale si sono analizzati i fattori predisponenti e le cause innescanti passando dalla piccola scala, alla quale si sono utilizzati i modelli di tipo geologico, fino alla grande scala per la quale si è fatto ricorso alle analisi geotecniche sia su area vasta e sia a scala di versante.
L'approccio che si è privilegiato ha consentito, da un lato, di individuare nelle principali strutture tettoniche, nelle linee di drenaggio e nella litologia i fattori predisponenti l'evoluzione morfologica dei rilievi alle scale medio piccole, dall'altro di caratterizzare le frane a grande scala ed a

scala di dettaglio individuandone i meccanismi di innesco ed indagando alcuni aspetti specifici quali le proprietà meccaniche ed idrauliche del mezzo ed il regime delle pressioni neutre in sito.
In particolare, a grande scala sono stati individuati ed analizzati tre principali meccanismi di innesco che differiscono per caratteristiche morfometriche, entità dei volumi mobilitati e risultano non casualmente distribuiti sui versanti.
Successivamente, per i principali meccanismi di innesco, si è condotta una modellazione (saturo-parzialmente saturo) del regime delle acque sotterranee che ha fornito gli elementi di partenza per le analisi di stabilità che si sono svolte con i metodi dell'equilibrio limite e quelli fisicamente basati.
La validità complessiva dei risultati conseguiti evidenzia l'efficacia dell'approccio proposto e ne incoraggia l'uso anche in contesti geo-ambientali differenti da quello nel quale è stato testato e calibrato. A tale fine, al termine della tesi si sviluppano considerazioni di carattere generale che sono supportate da applicazioni preliminari a casi di studio ben noti nella letteratura scientifica internazionale.

ABSTRACT

Shallow landslides in non-collapsible, fine-grained soils are natural phenomena which, due to their simultaneous occurrence over large areas, often cause agricultural production loss, with enormous economic damage.
Although the scientific community has offered in depth analyses of landslides in collapsible soils, shallow landslides in non-collapsible soils, have been paid very little attention in spite of their consequences. The few works available in scientific literature are based on monodisciplinary approaches which provide useful specific information on these phenomena; yet, at the same time, they also oversimplify the problem, often neglecting some relevant issues. Such issues can be best highlighted and addressed following a multisisciplinary and multiscalar (deductive or inductive) approach, as some authors have evidenced in very different geological and environmental contexts affected by medium- to deep - seated landslides.
Within such a context, rich in approaches but lacking in references to shallow landslides in non-collapsible soils, the present thesis seeks to offer a methodological contribution for creating a homogeneous reference framework for the phenomena examined. At the same time, this work seeks to answer specific questions concerning the ways in which these phenomena are triggered.
The proposed methodology has been tested and validated over an area in southern Italy, in which shallow landslides are very frequent. The predisposing factors and the triggering causes have been analysed going from small scale, through geological models, to large scale by means of geotechnical analyses performed at slope and large scale.
On the one hand, this approach allowed to identify the predisposing factors of the morphological evolution of the reliefs in the main tectonic structures, drainage lines and in the main lithology; on the other hand it allowed the characterization of large scale and detailed scale landslides by identifying their triggering mechanisms, and by investigating specific aspects such as the hydraulic and mechanic properties of the soil and the pore water pressure regime in situ.

In particular, three main triggering mechanisms have been identified and analysed at large scale which differ in terms of morphometric characteristics, volumes involved, and which do not show a casual slope distribution.
Subsequently, a (saturated and unsaturated) modelling of groundwater regime for these mechanisms has been performed which provided the input data for stability analysis carried out through physically based and limit-equilibrium methods.
The overall validity of the results obtained highlights the efficacy of the methodology applied and recommends its use in geo-environmental contexts which differ from the one in which this methodology has been tested and validated. For this purpose, at the end of the present thesis, a series of general considerations have been discussed by making use of preliminary applications to internationally well-known case studies available in scientific literature.

ACKNOWLEDGEMENTS

At the end of this long, hard work, I am deeply grateful to the University of Salerno, where my research has been carried out, and to its teaching staff. In particular, I profoundly thank Professor Leonardo Cascini for making me join his team since the very beginning of my PhD programme. To him, I would like to offer my most sincere gratitude for guiding me and believing in me in spite of the difficulties encountered along the way.
A special thanks goes to Prof. Silvio Di Nocera, who encouraged me to deal with subjects I had not previously studied. Our constant conversations on my research topic gave me the opportunity to improve my knowledge.
I am also indebted to Ing. Gullà for his availability and competent advice despite the distance.

This work could not have been possible without the late Prof. Giuseppe Sorbino, whose memory I will always keep not only for our significant conversations on the topic of unsaturated soils, but mostly for teaching me never to give up in the face of difficulties.

I would like to acknowledge Ing. Foresta for his help during my laboratory analyses and *in situ* investigations. I will always remember the seven rounds of investigation programme we had in mid-August.
In addition, I am thankful to Prof. Ferlisi for his discretion and support.
I would also like to thank all my friends from the Civil Engineering Department: Dario, Claudia, Livia, Giovanna and, Maria for always making me feel at home.
My gratitude also goes to all my friends at the CNR-IRPI in Cosenza, Sarah, Gino and Luigi. The latter deserves a special thanks for encouraging me to carry on with my research work with passion and for supporting me through hard times.
Last but not least, from the bottom of my heart, I am grateful to my parents and to Giusy and Domenico Andrea for their help, encouragement and trust. They all gave me a reason to keep going and never surrender.

ABOUT THE AUTHOR

Mariantonietta Ciurleo graduated in Civil Engineering at the University of Calabria with 110/110 cum laude.
During her PhD programme she has developed research topics related to the analysis of predisposing and triggering factors of shallow landslides in fine-grained soils. These phenomena stand out for their spectacular features essentially when they occur as multiple landslides over large areas. To deepen these issues, she has undertaken training and research activities at the University of Salerno and some in leading national research Institutions such as CNR-IRPI in Cosenza (National Council Research). She attended also the postgraduate school LARAM (LAndslide Risk Assessment and Mitigation).

Mariantonietta Ciurleo si laurea in Ingegneria Civile, presso l'Università degli Studi della Calabria con la votazione di 110/110 e lode. Durante il corso di dottorato sviluppa tematiche inerenti l'analisi dei fattori predisponenti e delle cause innescanti le frane superficiali nei terreni a grana fine. Tali fenomeni risultano di grande interesse per il loro verificarsi come eventi multipli su aree di rilevante estensione.
Al fine di approfondire tali tematiche, svolge attività di ricerca presso l'Università di Salerno in collaborazione con il CNR-IRPI di Cosenza e frequenta i corsi nell'ambito della scuola di alta formazione LARAM (LAndslide Risk Assessment and Mitigation).

1 INTRODUCTION

Landslides are one of the main problems in the world due to their consequences in terms of both victims and damage to properties. Several databases discuss the relevance of the topic, as for instance MunichRe and OFDA/CRED; in particular, in the latter, mass movements are considered one of the most frequent natural disasters in the world. Among these, shallow landslides in collapsible soils often cause the worst consequences, since they occur simultaneously over large areas and because of their high velocity and great magnitude. These characteristics are essentially due to static liquefaction phenomena under critical rainfall condition or dynamic liquefaction (Olivares and Picarelli, 2003; Musso and Olivares, 2004; Wang et al., 2002), which are favoured by the metastable structure of the involved soils.

Given the relevance of the topic, many efforts have been devoted to study in depth several relevant topics, and scientific literature provides significant contributions on shallow landslides in collapsible soils.

Similar efforts have not been devoted to shallow landslides involving non-collapsible soils that are characterized by a totally different triggering and evolution stage and they do not suffer a large decrease in bulk volume as a consequence of failure. Nonetheless, they occur simultaneously over large areas and, after a certain period of time, they rapidly evolve causing the destruction of property as, for instance, in the case of New Zealand described by Crozier (2005).

Other significant examples are discussed by Aleotti et al. 1996, Meisina 2006, Lim et al. 1996, Eigenbrod et al. 1999, Pasuto 1998, Eden and Mitchell 1969, Roger and Selby 1980, Gullà et al. 2006, Gullà et al. 2008, Leoni 2008.

These examples confirm that, currently, the knowledge of these phenomena is poor and does not allow to classify, understand and properly manage the risk related to landslides. Moreover, as argued in the present thesis, these landslides are also underestimated since they are often considered as erosional processes in many scientific papers. Consequently, damage prevention is extremely difficult since

susceptibility and hazard maps are not properly developed or are not developed at all.
The present thesis aims at offering a contribution to fill this gap in the study of shallow landslides, particularly as the soil has been defined an inestimable resource by the European Union, and this kind of phenomena produces a consistent loss of this resource as Crozier et al (2005), Glade et al (2005) have confirmed with reference to other non-European countries such as New Zealand.
In particular, the purpose of this thesis is to offer a general framework of analysis based on a simple and coherent methodology which can clarify, and thus quantify, the predisposing and triggering factors of shallow landslides in clayey soils.
Particularly, chapter 2 reviews the scientific literature on shallow landslides in fine-grained soil summarizing definitions, types of phenomena, the general features of the involved soils, the methodologies used to analyse this kind of phenomena and the unsolved questions on several topics.
Chapter 3 discusses the reference framework for an advanced analysis of the open questions posed in chapter 2.
In Chapter 4, an integrated methodological approach to analyse this kind of phenomena is introduced. This approach goes from small to large scales and reinterprets what is currently available in literature in order to delineate and correlate the predisposing factors (at small-medium scale) to the triggering causes (at large and detailed scale) of shallow landslides.
Chapter 5 presents a relevant case study of shallow landslides in fine-grained soils triggered by rainfall, devoting particular attention to the cartographic database; the landslides inventory; in situ investigations and laboratory tests used to characterize the geotechnical properties of soils.
Chapter 6 describes a sample area, where the methodology proposed in chapter 4 is tested through a small scale analysis with the aim to identify and quantify the predisposing factors of the geo-morphological evolution of the study area.
Chapter 7 focuses on the use of a heuristic method to identify the morphological evolution of the reliefs identifying the necessary input data to develop a statistical analysis at medium scale.
Chapter 8 deals with the morphological evolution of hollows at large scale, and at detailed scale identifies three different triggering mechanisms on the basis of a landslide inventory, the available cartographic data base and in-situ evidence.

Then, for each of these mechanisms the predisposing factors and the triggering mechanisms are analysed through evolution models at slope scale.
In Chapter 9, the quantification and validation of the triggering mechanisms identified in chapter 8 is pursued at slope scale through accurate geotechnical analyses. Particular attention is given to the hydraulic behaviour of the soil at both scales of macro and meso-structure.
Chapter 10 addresses the modelling of the triggering stage for shallow landslides induced by rainfall. Among the available approaches, uncoupled geotechnical models are used with particular reference to the modelling of pore water pressure and instability conditions. In particular, starting from the results of the analysis at slope scale, several modelling over large areas are carried out to investigate the limit-equilibrium conditions for each cell of the surface.
On the basis of the results obtained for the sample area, chapter 11 develops some general considerations within the general framework of Chapters 2 and 4, suggesting the necessary research developments to further investigate some relevant open questions.
Finally, the conclusions are outlined in chapter 12.

2 LITERATURE REVIEW ON SHALLOW LANDSLIDE IN FINE-GRAINED SOILS

The scientific literature on shallow landslides deals with multiple issues such as landslides morphometric characteristics, soil properties, kinematic evolution, duration and intensity of rainfalls. The papers analyzed in this thesis testify to the use of several approaches to study these phenomena and highlight the main role played by the collapsibility of the involved soils on the genesis, typology and kinematic evolution of shallow landslides (Campbell 1974, Cascini 2004, Cascini et al. 2005, Fannin 2000, Guzzetti et al. 2008).

Moreover, the papers dealing with collapsible soils address several issues such as the identification of the landslides source area, predisposing and triggering factors, mechanisms and modeling of the failure and post-failure stages and runout distance etc. (Corominas, 1996; Corominas et al., 2003; Pastor et al., 2003 a,b; Rahardjio et al., 2001; Wang et al., 2003).

On the contrary, the scientific literature on shallow landslides in non-collapsible soils is much more complex due to several reasons essentially related to the heterogeneity of the available studies. Many of them usually deal with geological, geotechnical, hydrological, statistical issues; however, no studies or methods are available to analyze all the landslides-related factors such as landslide mechanisms, the soils involved and the triggering factors of shallow landslides. Other studies deal with the main aspects of the genesis, types, classification, methods of analysis but the landslides inventory, the susceptibility and hazard assessment are not adequately introduced and developed according to the most advanced procedures available in literature.

Given the lack of knowledge on the topic, the following sections provide the basic elements for a correct classification of landslides. Initially, the definitions, the typologies and the geotechnical properties of the phenomena involving non-collapsible soils are introduced; subsequently, the methodologies available in literature to analyse the triggering stage are discussed.

DEFINITION AND TYPES

About thirty papers listed in Table 2.1 deal with shallow landslides in non-collapsible soils. These works introduce different definitions and typologies of landslides that can affect different soils according to various mechanisms. The latter have been studied through the application of the different methodologies characterising different disciplinary approaches.

Table 2.1 Reference papers for the analysis of shallow landslides in non-collapsible soils.

Authors	Continent	Country	Region	SL	ML	Types
Eden and Mitchell 1969	America	Canada	-			Rapid flow
Rogers and Selby 1980	Oceania	New Zealand	North Island		x	Slide
Aleotti et al. 1996	Europe	Italia	Piemonte		x	Soil slip
Lim et al. 1996	Asia	Singapore	-	x		Earth flow
Crosta et al. 1997	Europe	Italia	Lombardia e	x		Soil slip
Pasuto and Silvano 1998	Europe	Italia	Veneto	x		Soil slip
Eigenbrod and Kaluza 1999	America	Canada	Ontario	x		Shallow translational and rotational
Antronico and Gulla 2000	Europe	Italia	Calabria		x	Soil slip
Antronico et al. 2001	Europe	Italia	Calabria		x	Soil slip
Borga et al. 2002	Europe	Italia	Dolomiti		x	Shallow landslides
Borga et al. 2002	Europe	Italia	Bacino di Vauz			Shallow landslides
Antronico et al. 2004	Europe	Italia	Calabria		x	Soil slip
Brian et al. 2004	-	-	-	x		Shallow landslides
Gullà et al. 2004	Europe	Italia	Calabria		x	Soil slip
Sorriso-Valvo et al. 2004	Europe	Italia	Calabria		x	Soil slip
Crozier 2005	Oceania	New Zealand	North Island		x	Soil SLip
Gullà et al. 2005	Europe	Italia	Calabria			-
Shakoora and Smithmyerb 2005	USA	Ohio	-		x	Shallow translational and rotational
Gullà et al. 2006	Europe	Italia	Calabria		x	Shallow landslides
Meisina 2006	Europe	Italia	Lombardia		x	Shallow translational and rotational
Claessens et al. 2007	Oceania	New	North Island		x	Earth flow
Meisina and Scarabelli 2007	Europe	Italia	Lomabardia		x	Shallow translational and rotational
Gullà et al. 2008	Europe	Italia	Calabria		x	Shallow landslides
Guzzetti et al. 2008	Europe	-	-			all Type
Leoni 2008	Europe	Italia	Emilia-Romagna		x	Soil slip
van Asch and Malet 2009	Europe	Francia	Barcellonette	x		Earth flow

SL: single landslide; ML: multiple landslides.

Indeed, and unsurprisingly, different definitions and different proposals for studying the same phenomena are available in scientific literature. However, despite the relevant differences concerning the differentiation and characterization of landslides, some general features can be recognized as argued by Crozier (2005), Gullà et al. (2004, 2005, 2006), Hicks (1995).

In particular, at slope scale, Campbell (1975) defines these phenomena as soil slips, and now, this term is used almost universally in scientific literature to indicate fast shallow instabilities phenomena involving

superficial covers. Other authors offer different definitions, such as earth flows, shallow translational slides, fast-shallow sliding flow.
Whatever their classification, these landslides generally affect relatively small areas, they are between 3 m and 15 m wide and between 10 m and 100 m long depending on their localization on the slope. The sliding surface can reach depths varying between a few centimeters and 3 meters, although some authors define as 'shallow' those landslides with a maximum depth of 10 m. Typical examples of single phenomena occurring along the slope are shown in Figure 2.1.

Figure 2.1 Typical examples of shallow landslides in clay soils. (a) New Zealand (Brooks et al. 2002); (b) Catanzaro (2004).

At any rate, these phenomena, involving thin covers, stand out for their spectacular features essentially when they occur as multiple landslides over large areas. Notwithstanding the diffusion of multiple landslides (two or more triggered surfaces), only 2% of papers provide useful

information about the number of triggered failures over large areas (Crozier 2005, Gullà et al. 2004, 2005, 2006).
With regards to the disasters occurred in New Zealand in 2004, Crozier (2005), defines these phenomena as MORSLE (Multiple Occurrence Regional Shallow Landslides Events). Here, these events, which are also present in other parts of the world Figure 2.2., occur two or three times a year on average (Crozier, 2005).

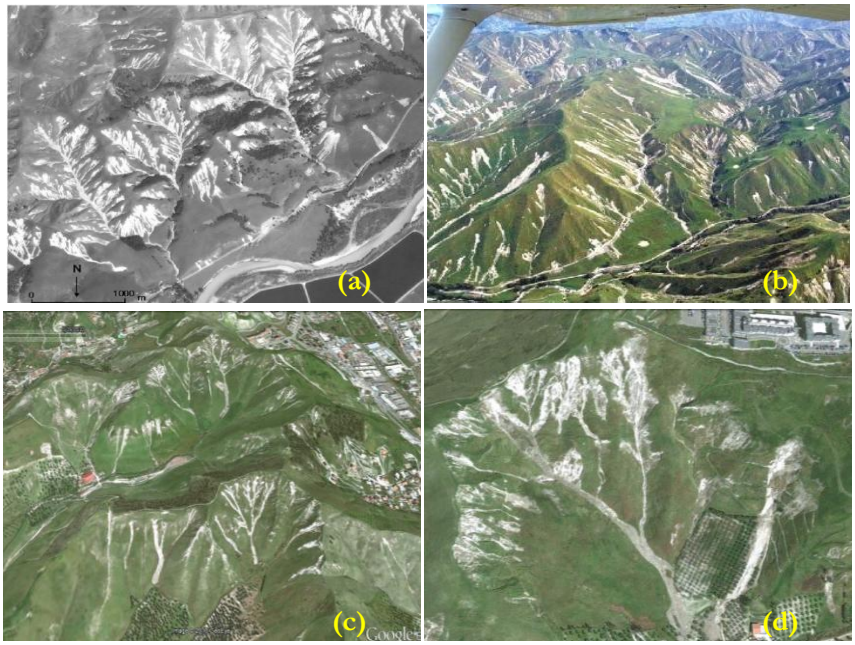

Figure 2.2 Multiple rainfall-triggered shallow landslides. (a) Air photo of July 1977, Wairarapa, North Island, New Zealand (Crozier, 2005); (b) Air photo of events in New Zealand in February 2004 (Hancox & Wright, 2005); 3D view from Google Earth, March 2010, Catanzaro, Calabria, Italy: (c) general view (d) typical phenomena in a morphological hollow.

Many authors recognise that deforestation acts as a predisposing factor in shallow landslides over large areas. (Hicks 1995, Page et al. 2000, Crozier 2005). Hicks (1995) claims that a 50-80% reduction in mass movements affecting pastures can occur if broadleaved trees are kept at a distance of 12 m or closer; he also argues that mass movements can be reduced by 10-20% planting trees on unstable slopes, Figure 2.3 (Crozier, 2005).

The role of different kind of trees is also analysed by other authors, and exotic conifers seem to reduce mass movement by 90% Crozier (2005). According to the author, this level of protection can be reached by appropriately evaluating tree density for young or mature trees (1000 stems per hectare for young trees and 300 for mature trees).

Figure 2.3 Stabilising effect of close planting of pines and riparian planting of poplars, Gisborne District, North Island, New Zealand (Crozier 2005).

INVOLVED SOILS

All the features discussed in the previous section (definitions, typologies, morfometry, etc.) and the mechanisms characterizing the triggering and the evolution stages of shallow landslides are strictly related to the geotechnical properties of the involved soils. These properties drastically differ from those of collapsible soils, even though a clear distinction between collapsible and non-collapsible soils is not usually provided in the papers analysed. Indeed, since the distinction between collapsible and non-collapsible soils represents a key issue and a starting point in the accurate analysis of shallow landslides, this issue is now going to be discussed by referring to (Rogers, 1994) and (Michell and Soga 2005).

Michell and Soga (2005) define as collapsible soils those materials susceptible to large decreases in bulk volume when they become saturated.
Rogers (1994), referring to natural and compacted soils, Figure 2.4, defines as collapsible soils those characterized by distinct geotechnical properties that include an open (metastable) structure resulting in low bulk density, high void ratio and high porosity, geologically young deposit, lately altered deposit, significant sensitivity, and weak inter-particle bonding.

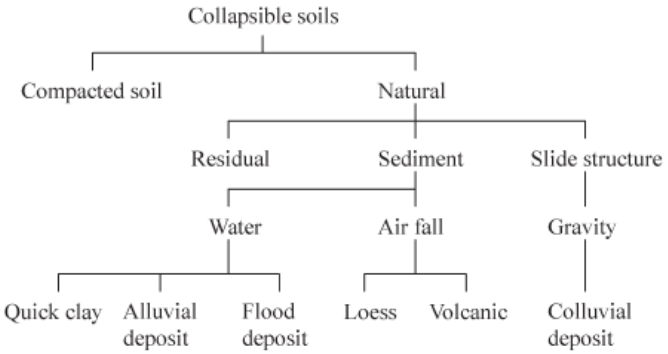

Figure 2.4 A family of collapsible soils (Rogers 1994).

To quantify their collapsibility, several authors introduce the collapse potential of soils and provide general criteria for its estimation(Denisov 1951, Clevenger 1958, Priklonski 1952, Gibbs 1961, Feda 1964, Benites 1968, Handy 1973); some of them are summarized in Das 2007, Table 2.2.
Table 2.2 highlights that originally the criteria proposed to estimate the collapse were based on index properties (Denisov 1951, Clevenger 1958, Proklonski 1952).
In particular, Denisov (1951) used the coefficient of subsidence, Priklonski (1952) the liquidity index, while Clevenger (1958) the dry unit weight, and finally the Soviet Building refers to L parameter which depends on the in situ void ratio and the void ratio at liquid limit.
Gibbs (1961) introduced a collapse ratio based on the ratio between the water content at full saturation and the liquid limit.
Other methods summarised in Table 2.2 are based on the content of clay or silt, on the value of the degree of saturation, and on porosity (Feda

1964, Benites 1968, Handy 1973 and Czechslovak Standard from Klukanova and Frankovaska 1994).
The criteria reported in Figure 2.4 and in Table 2.2 were used to confirm that the phenomena investigated in these papers can effectively be classified as shallow landslides in non-collapsible soils.

Table 2.2 Criteria for collapse potential (Das 2007; Lutenegger 1988)

Investigator	Year	Criteria
Denisov	1951	Coefficient of subsidence: $K = \frac{e_{LL}}{e_0}$ K=0.5–0.75→highly collapsible K=1.0→noncollapsible loam K=1.5–2.0→ noncollapsible soil
Clevenger	1958	If dry unit weight is less than 12.6 kN/m^3 (80 lb/ft^3)→large settlement If dry unit weight is larger than 14 kN/m^3 (90 lb/ft^3)→small settlement
Priklonski	1952	$K_D = \frac{\omega_n - PL}{PI}$ K_D<0→highly collapsible soils K_D>0.5→non-collapsible soils K_D>0→swelling soils
Gibbs	1961	Collapse ratio $R = \frac{\omega_{sat}}{LL}$ This was put into graph form
Soviet Building Code	1962	$L = \frac{e_o - e_{LL}}{1 + e_o}$ For natural degree of saturation <60%, if L>−0.1, the soil is a collapsing soil
Feda	1964	$K_L = \frac{\left(\omega_n/S\right) - PL}{PI}$ For S<100%, if K_L>0.85, the soil is considered collapsible
Benites	1968	A dispersion test in which 2g of soil are dropped into 12 ml of distilled water and specimen is timed until dispersed; dispersion times for 20 to 30s were obtained for collapsing Arizona soils
Handy	1973	Iowa loess with clay (<0.002mm) contents: <16%: high probability of collapse 16–24%: probability of collapse 24–32%: <50% probability of collapse >32% usually safe from collapse
South Africa Criteria (Brink 1958)	n/a	Aeolian sand: $CP = \frac{1672 - \gamma_d}{22} < 0$ not collapse Mixed origin: $CP = \frac{1590 - \gamma_d}{18.9} < 0$ not collapse
Czechslovak Standard	n/a	Collapse may occur when Silt % > 60% Clay% < 15% S < 60% and LL < 32% n > 40 % Wn < 13%

However, these types of soils must be considered as complex soils due to the weathering grade of the covers which influences the triggering mechanisms, the seepage process, the pore pressure regime, the hydraulic properties and the shear strength of the soils.
Given the relevance of the weathering process for the work carried out in the present thesis, the most important aspects of weathering are now going to be summarized.

2.2.1 Weathering process

Many authors have studied the weathering process, from Polynov (1937), who describes it as "the change of rocks from the massive to the clastic

state" to Cascini (1992), who identifies six weathering classes for crystalline rocks.
Starting from the definition given by Polynov (1937), Ollier (1984) describes weathering as "the breakdown and alteration of materials near the earth's surface to product that are more in equilibrium with newly imposed physic-chemical conditions".
Generally, weathering can be considered as a destructive process due to both physical and chemical phenomena. The present thesis focuses on physical weathering, which can be defined as the breakdown of materials by entirely mechanical methods brought about by a variety of causes. Different kinds of physical weathering are present in nature: sheeting, unloading and spalling, induced fracture, crystal growth, insolation weathering, moisture swelling, slaking, cavitation, abrasion, mechanical collapse, colloid plucking, soil ripening (Ollier, 1984).
Slaking is one of the most common kinds of weathering involving non-collapsible soil and it consists of the alternate process of rocks wetting and drying. Some interesting experiments on slaking were carried out by several authors such us (Dunn and Hudec 1966, Kennard et al. 1967, Ollier 1984; Gullà et al. 2005). After analysing the experiments results carried out by M.A. Condon using samples of different geomaterials (sandstone, siltstone, shale and mudstone) subjected to cycles of alternate wetting and drying Ollier (1984) observes that the degradation effects produced by these cycles are more evident in fine-grained soils(see also Gullà et al., 2005).
Slaking produces two types of disintegration: a minor disintegration due to flaking, and a major disintegration due to the splitting of the sample into two or more large pieces. (Ollier, 1984) observes that "the cracking zone was concentrated along the bedding planes and cleavage planes when these were present"
For Kennard et al. (1967) the most important part of the cycle is drying, because it leads to negative pore pressure and, consequently, to tensile failure.
Many authors studied the failure mechanism caused by drying processes, from a molecular viewpoint (Dunn an Hudec 1966, Kennard et al. 1967, Ollier 1984) both in laboratory tests or in situ state (Gullà et al. 2005, Meisina 2006).
Ollier (1984) asserted that a possible explanation for slaking is provided by the mechanism of 'ordered-water' molecular pressure. Due to its chemical configuration, water is considered as a polar liquid and can be

regarded as a magnet. When positively charged, water molecules are attracted to the negatively charged surface of a clay or other material: as a result, they become oriented around clay fragments, but remain disordered in bulk water. When the clay material is drained, the ordered configuration of water remains, so that when the wetting process takes places again, another layer of ordered water builds up along the clay surface (Fig. 2.5).

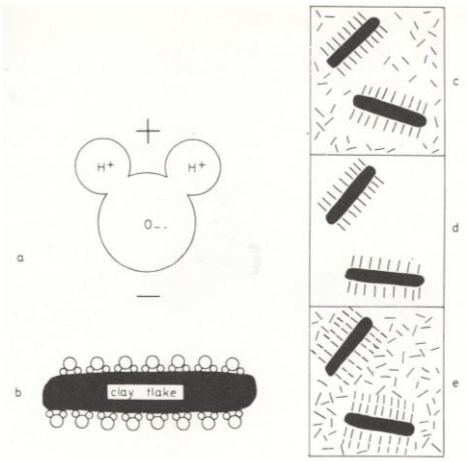

Figure 2.5 Ordered water weathering: a) A molecule of water, b) water molecules become oriented, c) water is ordered around clay fragments and remains disordered in bulk water, e) renewed wetting builds up another layer of ordered water.

During repeated wetting and drying processes, water molecules become increasingly ordered and exert an expansive force that pushes against the confining walls.
Gullà et al. 2005, carrying out an experimental study, reproduces in laboratory wetting-drying and freezing-thawing cycles to characterize the weathered clay soils responsible for shallow landslides and to investigate how slaking affects the mechanical behaviour of natural clays in the superficial layers. The authors observe a significant variation in geotechnical properties, especially in the first month of tests.
Meisina (2006) investigates the role of shrinkage cracks on the hydraulic conductivity of a weathered clay and, consequently, in mass movements. He underlines the importance of in situ typical cracks network compared with geotechnical properties.

Due to their complexity, weathered soils are characterised by peculiar features at micro- and macro- scale. Here, only some features strongly affecting their mechanical behaviour are reviewed.
As far as the micro-scale characteristics are concerned, Gullà et al. (2008a) observes that physically weathering produces a variation in the morphology of clay minerals, especially on mica minerals. The slightly weathered mica (Fig. 2.6a) of the natural (intact) silt sample shows a smooth basal surface with etch pits of submicrometer size, whereas secondary minerals are attached to the edge. During the weathering and the degradation processes, mica minerals have a tendency to open the reticular sheets and gradually lose K+ ions toward the top part. This result indicates that illitization has occurred, and such K-depleted inter-layers in the mica minerals will be referred to hereafter as illite/ smectite-like inter-layers. The mica mineral of the silt sample degraded in laboratory (Fig. 2.6b) is slightly deformed, with secondary minerals present in the lower part and at the edge of the grain. One of the secondary minerals is identified qualitatively as an illite and/or smectite-like silicate, as indicated by its morphology and composition (revealed by SEMEDS).

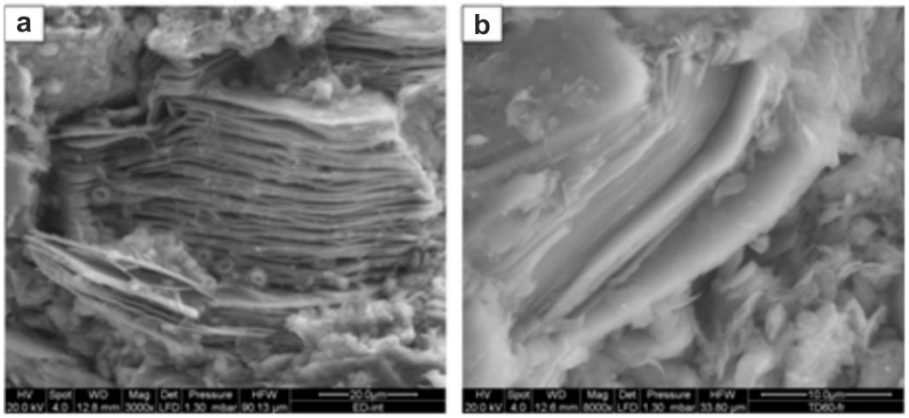

Figure 2.6 SEM images from grains of two different fine grained soil samples: a) natural (intact) silt sample, b) silt sample degraded in laboratory (Gullà et al., 2008a).

From a chemical and mineralogical point of view, the XRD patterns of natural (intact) silt samples and silt samples degraded in the laboratory do not show substantial mineralogical differences (Fig. 2.7a); only a <2 μm fraction of these samples shows a small variation related to the illite

and illite-smectite mixed layers (I-S) content (Fig. 2.7b). These slight differences are probably a consequence of laboratory degradation treatments (cycles of saturation, drying, wetting and freezing) Gullà et al., (2008).

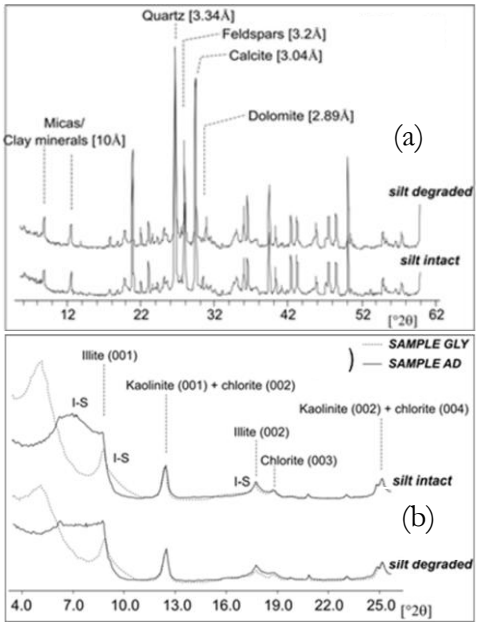

Figure 2.7 (a) The XRD patterns of silt samples degraded in laboratory and natural (intact) silt samples whole-rocks, (b) The XRD patterns of the air dried (AD) and ethylene glycol solvated (GLY) <2 μm fraction specimens of silt samples degraded in laboratory and natural (intact) silt samples (Gullà et al., 2008).

Gullà et al. (2006) assert that the degradation cycles do not cause any change in the index soil properties, Table 2.3, while the compressibility and the peak shear strength of natural clays show significant changes.

Table 2.3 Comparison between the index properties of intact weathered test materials (Gullà et al. 2006).

State	w_L (%)	w_P (%)	IP (%)	CF (%)
Intact	51.47	29.33	22.14	55
D1	52.39	31.05	21.34	55
D7	51.47	29.33	22.14	55
D30	51.59	28.79	22.80	58
D60	51.60	28.80	22.85	57
D90	51.65	28.82	22.83	58

With regards to this issue, Gullà et al. (2005) compared the one-dimensional compression curves of the intact, weathered and reconstituted clay. The authors noted that the curves of weathered specimens go towards that of the reconstituted one and the void ratios increase with the duration of the cycles of degradation.

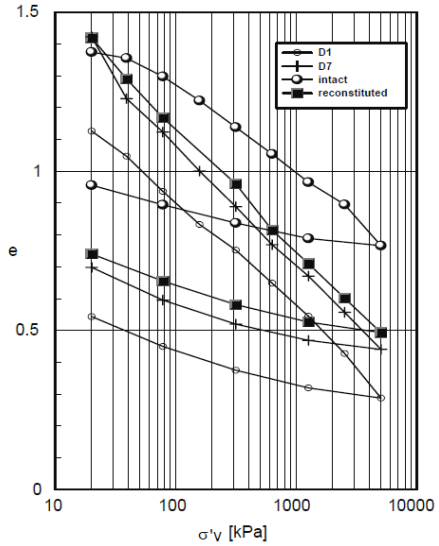

Figure 2.8 Oedometer curves of intact, weathered and reconstituted clay (Gullà et al., 2006).

With reference to shear stress, Gullà et al. (2005) show that the stress-displacement curves of intact clays exhibit a much greater shear strength than the shear strength of those weathered. The intact clay shows peak shear strength well defined that decreases with the displacement; by contrast, the weathered clays do not show such decay and the peak shear

strength goes to asymptotic value with increase of displacement, Figure 2.9.

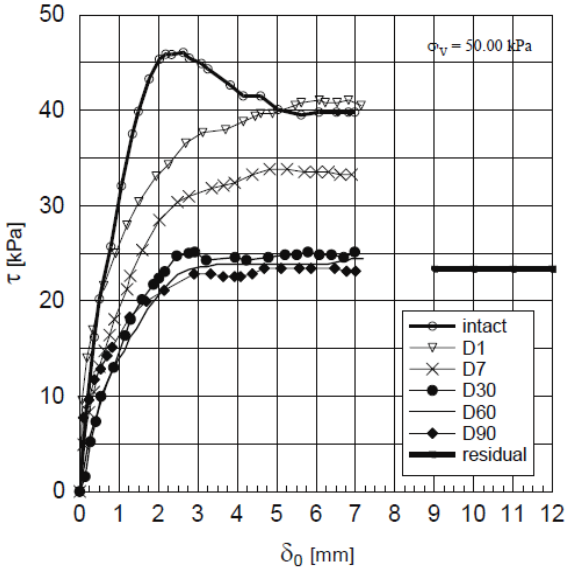

Figure 2.9 Stress-displacement relationships of intact and weathered specimens compared with residual shear strength (Gullà et al., 2006).

The peak shear strength reductions are pronounced in the first month of degradation; subsequently, they could be essentially regarded as constant. The peak shear strengths of the specimens subjected to 30-day, 60- day and 90-day cycles of degradation are similar to each other (Gullà et al., 2008).

The authors observed that the shear strength envelopes for intact and degraded clay show considerable differences, Figure 2.10. By increasing the number of degradation cycles, the strength envelopes of the weathered specimens are close to those of the reconstituted specimens.

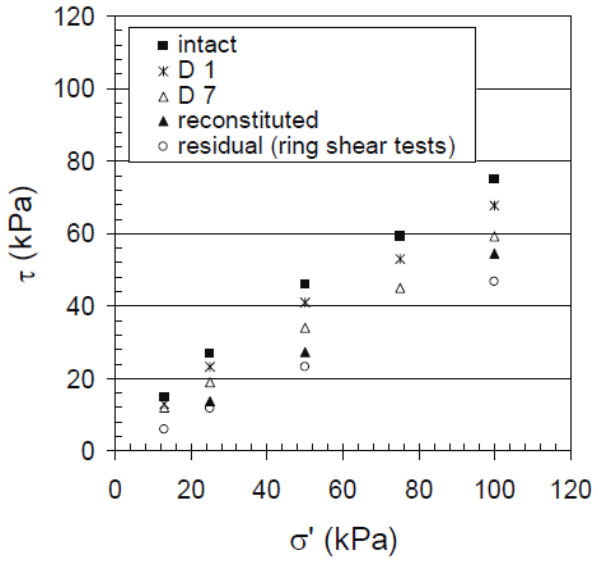

Figure 2.10 Strength envelopes of intact and weathered clay compared with reconstituted and residual envelopes.

INPUT DATA AND METHODS OF ANALYSIS IN THE SCIENTIFIC LITERATURE

Figure 2.11 shows that about 70 % of the papers analysed makes use of mono-disciplinary approaches, and about 30% of multidisciplinary approaches, being the percentage calculated on a total of about 30 papers examined.

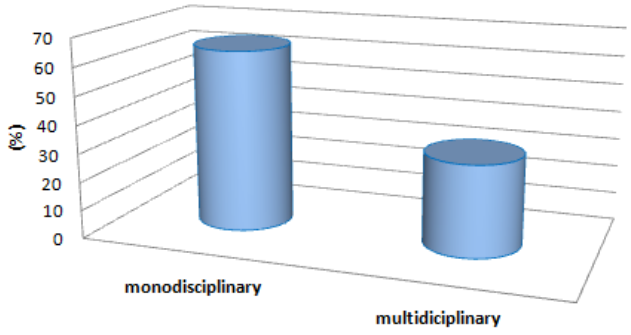

Figure 2.11 Approaches used in scientific literature.

With reference to monodisciplinary approaches, several available studies separately analyse hydrological, geological and geomorphological characters as (M. J. Crozier et al. 2005, Antronico et al. 2000, Sorriso Valvo et al. 2004, Guzzetti et al. 2008); others studies essentially focus on geotechnical and numerical aspects as in the case of (Lim et al. 1996, Eigenbrod et al 1999, Claessens et al. 2007, Eden et al. 1969).
The work by Lim et al. (1996) is of great interest given the high number of in situ investigations carried out in an area of 200 m^2 where 36 "jet fill" tensiometers were installed to monitor the role of negative pore-water pressures on slope stability conditions, Figure 2.12.

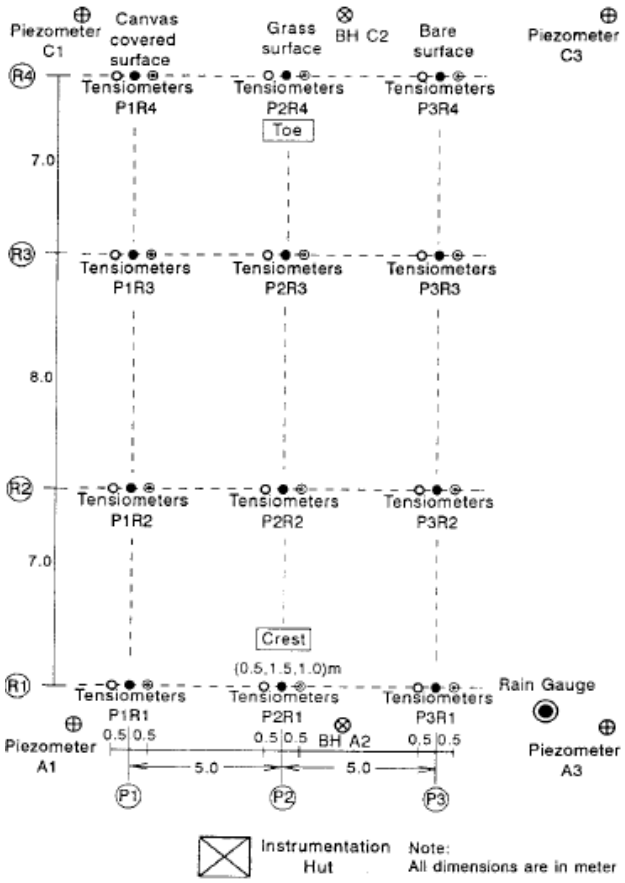

Figure 2.12 Instrumentation layout. Measurements in meters (Lim et al., 1996).

Analysing the change in matrix suction under different vegetative condition (canvas over grass, grass and bare slope) or in response to changes in climatic conditions, Figure 2.13, the author highlights some similarities in the characteristics of in situ matrix suction variations under three different surface conditions, Figure 2.14.

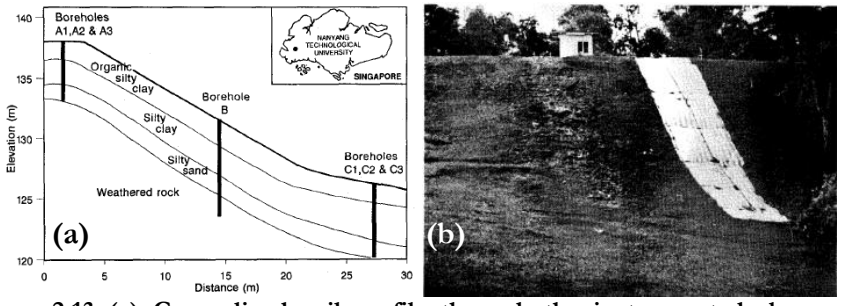

Figure 2.13 (a) Generalized soil profile through the instrumented slope; (b) Ground surface condition on the instrumented slope (Lim et al. 1996).

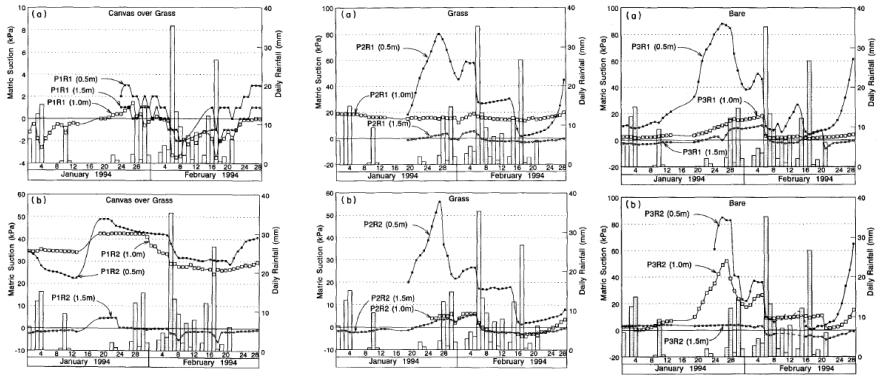

Figure 2.14 In situ matrix suction measurement in the slope with canvas over grass, grass and bare surface (Lim et al., 1996).

Figure 2.14 shows that maximum change in matrix suction often occurs near the ground surface (i.e. at a depth of 0.5m), and the magnitude of the changes generally decreases with depth. The variation in matrix suction due to periodic wetting and drying is most significant in the bare slope section and least significant in the canvas-covered slope. Changes in climate conditions result in variations in the matrix suction profile with depth (in this case, the ground surface is the first to be affected) and time. The variation of the matrix suction profile is less significant under the canvas-covered section than under the grassed-covered and bare

sections of the slope. A perched water table appears to have developed in the instrumented slope at a depth of about 1.5 m below the ground surface during rainy periods.

In situ data acquisition is the starting point in a more complex process aimed at the understanding of the triggering mechanism(s) of shallow landslides in fine-grained soils which must necessarily be investigated by means of geotechnical models. For example, Eigenbrod and Kaluza (1999), with reference to shallow ground movements occurred in Ontario, propose an analysis of slope movements on one of the grassy slopes in the valley, Figure 2.15.

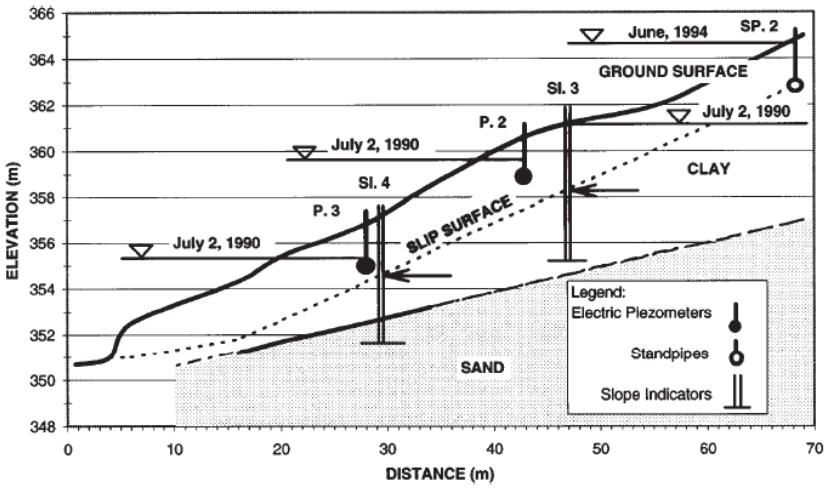

Figure 2.15 Geological section of slope with location of slip surface (Eigenbrod and Kaluza, 1999).

The authors monitored and examined the phenomenon since 1989 with 19 test holes, two test pits, and various field instruments such as slope-indicator casings, electrical piezometers, stand pipes, and thermistors.
Once the geotechnical properties of involved soils were known, and after measuring the piezometric pressures in the upper fractured clay zone, the authors performed a back analysis starting from the maximum values usually reached in early summer, i.e. at the same time when ground movements occurred. The authors, using a pore-pressure coefficient r_u = 0.5 (water pressure/total overburden pressure), indicated reactivated

movements at fully softened strength conditions (c' = 0, φ'= 30°), Figure 2.16.

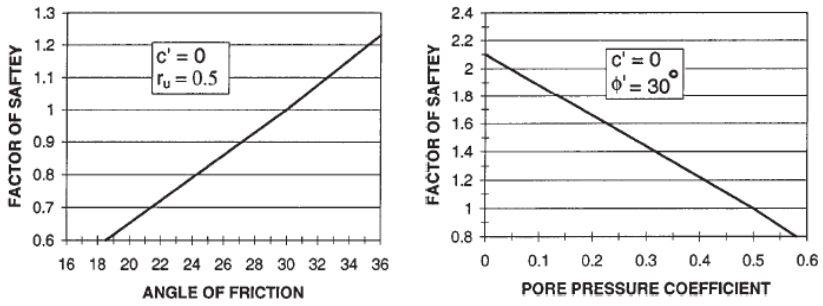

Figure 2.16 Slope stability analysis. (a) Factor of safety versus angle of friction. (b) Factor of safety versus pore-water pressure coefficient at slip surface (Eigenbrod and Kaluza, 1999).

The monodisciplinary approaches previously summarized usually provide excellent solutions but they do not offer a general framework for the analysis of shallow landslides in fine-grained soils since they investigate only some features of these phenomena and solve specific problems. Generally, this kind of goal can be reached through a multidisciplinary approach which, combining at least two disciplines, can offer a complete solution to the problem by enhancing the potentiality of each discipline.

The majority of multidisciplinary studies analysed in this thesis mix hydrological and geotechnical aspects identifying the critical rainfall by means of a back analysis of the rainfall events occurred, and subsequently modelling the stability conditions of the landslides phenomena.

Other studies combine geological and geomorphological aspects identifying a morpho-evolutional model associated with geotechnical information. For example, Antronico et al. 2001 identify some typical elements of shallow landslides by calculating the morphometric parameters of the slopes affected by such superficial phenomena. The same authors underline the presence of an uncommon ADZ3 weathered material, where surface instabilities occur, which is in contact with an AIZ3 material, Figure 2.17, with intervals of LSZ3 sands levels

From a phenomenological point of view, the surveys carried out in situ by the authors over 10 years of research, coupled with the photo-

documentation available, allowed to the define a typical morpho-evolutive model for complex shallow landslides (10 m long, with a scarp width of about 8 m) localised on open slopes having a slope angle between 38°-40°.

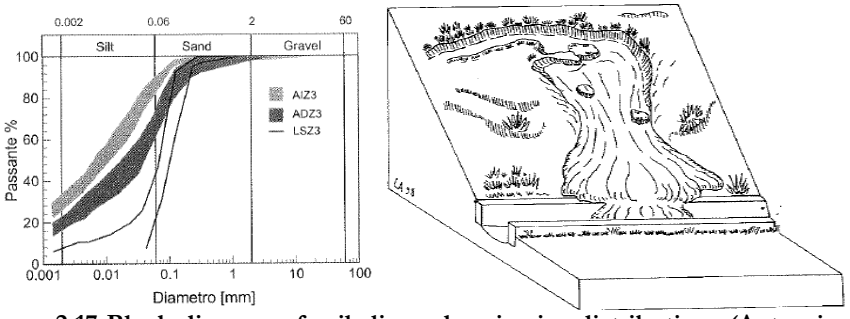

Figure 2.17 Block diagram of soil slip and grain size distributions (Antronico et al., 2001).

Meisina (2006) confirms the influence of weathered thickness on the triggering and the evolution of such phenomena, proposing a methodology for the identification and mapping of weathered clay soils responsible for shallow landslides. Such methodology can also determine geological, geomorphological and geotechnical characteristics of weathered clay soils associated to shallow landslides. The proposed method is based on the integration of intensive field work together with laboratory tests, in order to define areas that may be regarded as homogeneous from the geomorphologic and engineering geological point of view in terms of shallow slope instability, Figure 2.18.
This methodology, useful for studies to be developed at scales between 1:10,000-1:5000, requires a deep knowledge of the lithological and geological characteristics of the area.

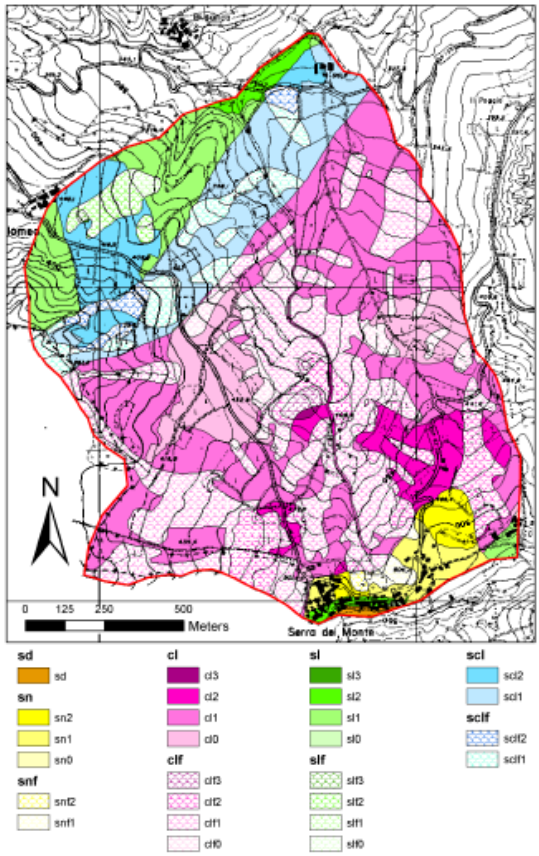

Figure 2.18 Engineering geological unit map (Meisina, 2006).

The papers previously summarized do not make use of geotechnical models for the back analysis of the phenomena occurred in the test area, although the back analysis is a fundamental step to quantify the failure stage. For this purpose, the work developed by Borga et al. 2002 uses simple models such as the limit-equilibrium model for an infinite slope and manages to provide useful information on the role played by several factors such as root cohesion (Cr), soil cohesion (C_s), slope angle (θ), vertical soil depth (D), the vertical height of the water table within the soil layer (Dw),as confirmed by the formula used to calculate the factor of safety expressed by:

$$FS = \frac{C_r + C_s + [\rho_s g(D - D_w)\cos^2\theta + (\rho_s g - \rho_w g)D_w \cos^2\theta + W\cos\theta]\tan\phi}{D\rho_s g \sin\theta\cos\theta + W\sin\theta} \quad (1)$$

The overall results obtained using eq. (1) are described in Figure 2.19 which illustrates the relative importance of each variable taken into account in slope stability analysis. Figure 2.19 shows that the root strength increases the factor of safety FS if the depth of the soil increases, while soil depth, groundwater–soil depth ratio and tree surcharge will decrease the FS if the slope angle increases.

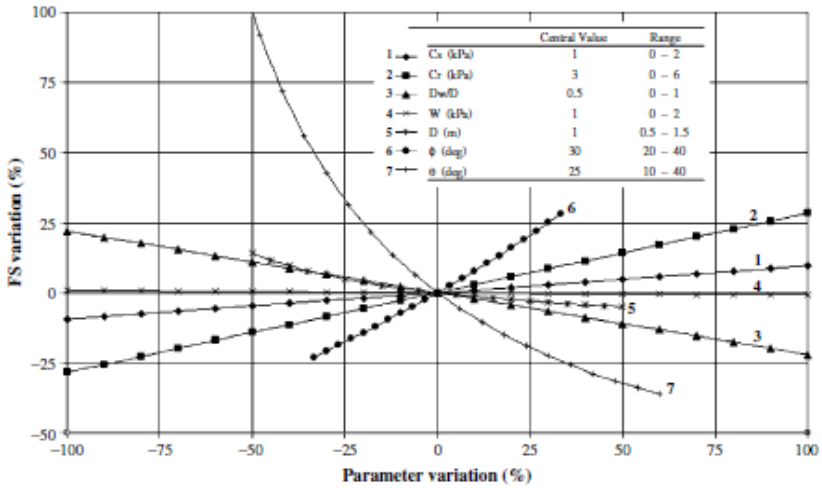

Figure 2.19 Sensitivity plot for the infinite slope equation (Borga et al., 2002).

Despite the use of a multidisciplinary approach, none of the previous papers provide a general framework for the identification of the predisposing factors and of the triggering causes of shallow landslides. These phenomena can be better investigated by a multi-scale approach that necessarily combines different scales of analysis and, consequently, different disciplines; this approach enhances the potentialities of each single discipline as it has been demonstrated by (Calvello et al. 2012, Cascini et al. 2005a) analyzing shallow landslides in collapsible pyroclastic soils of the Campania region in southern Italy.

Lasciare bianca questa pagina solo se (come in questo caso) il capitolo precedente finisce in una pagina dispari. Questo per garantire che ogni nuovo capitolo inizi su una pagina a destra (ovvero dispari).

3 REFERENCE FRAMEWORKS FOR AN ADVANCED ANALYSIS OF THE OPEN QUESTIONS

> "It is important for the user not only to acknowledge the source of his terminology but also to realise that the dividing lines in most classifications represent an indistinct transition in nature" (Crozier, 1986)

The literature review on shallow landslides highlights many open questions which cannot be easily answered given the lack of knowledge on specific key points.
For instance, considering that failure and post failure stages may greatly vary in time and space, can this kind of phenomena be included into a landslide classification already available in literature? Moreover, due to the large extension of areas affected by shallow landslides, how can the landslides inventory be easily developed and updated?
As regards the analysis of these phenomena, can a multidisciplinary approach be useful to develop a back analysis of past events? If so, which type of approach can be applied at different scales? Given the absence of specific proposals in literature, can susceptibility and hazard be assessed using qualitative and/or quantitative approaches?
This chapter summarizes the available studies which try to provide an answer to these questions, while specific answers are provided in the following chapters and then utilized to develop a methodological approach that can be used also in different geo-environmental contexts.

3.1 LANDSLIDES CLASSIFICATION

The identification of a valid classification system for shallow landslides in non-collapsible soils is one of the most difficult problems to solve considering that more than one hundred proposals exist in literature for every kind of landslides , among which the most known are: Skempton

1953, Blong 1973, Jahns 1978, Varnes 1978, Crozier 1986, Walker et al. 1987, Hutchinson 1988, Cruden and Varnes 1996, Leroueil et al. 1996, Hungr et al. 2001.
However, despite the numerous classification systems proposed for landslides, Crozier 1986 observes that *"the Proliferation of classifications in recent years ... has unintentionally defeated one of the principal purposes of the exercise; that is, the provision of clear and unambiguous terminology"* (Walker et al. 1987). Following Crozier 1986, and in order to avoid errors and misunderstanding, the present section refers to the simplest and clearest available landslides classification systems, and only the aspects and the mechanisms compatible with shallow landslides phenomena examined will now be discussed.
To this aim, one of the simplest proposals that can be used is the one developed by Blong (1973) who recognises four types of landslides, three of which are of interest for this thesis, i.e. slide, flow and slump or rotational slide (Fig. 3.1). With reference to the rates of movements Blong (1973) does not indicate the qualitative range of variation, but generally the range proposed by Jahns (1978) is used.

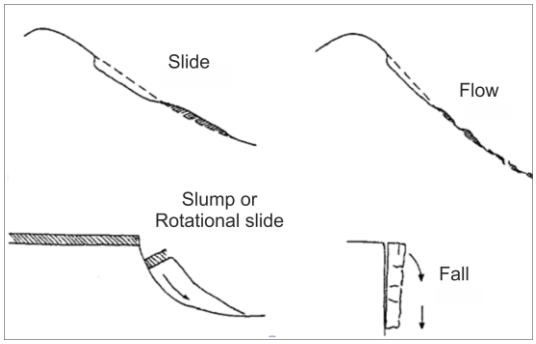

Figure 3.1 A simple classification of landslide (Blong 1973).

Slides are characterised by a planar surface generally parallel to the ground profile, translated in nature. The failed material fails down the slope as blocks of material usually with vegetative roots. The rates of movements range from mm/sec to m/sec.
Slump or rotational slides present curvilinear shear planes, they usually extend in depth rather than length while the failed material remains intact and only few blocks can be produced. Due to the presence of a complex stratigraphy in nature, these types of failure are very difficult to

find in natural slopes but very common in man-made excavation and fills instead. Their rates of movements range from mm/y to meters/day.
Flows, like slides, are characterised by a planar surface of rupture generally parallel to the original ground profile. Flows are likely to extend in length rather than depth. Their rates of movement range from cm/min to m/sec.
Further elements can be provided by the classification proposed by Varnes (1978), Figure 3.2, who identifies different mechanisms depending on the type of movement and on the material.

TYPE OF MOVEMENT		TYPE OF MATERIAL		
		BEDROCK	ENGINEERING SOILS	
			Predominantly coarse	Predominantly fine
FALLS		Rock fall	Debris fall	Earth fall
TOPPLES		Rock topple	Debris topple	Earth topple
SLIDES	ROTATIONAL	Rock slide	Debris slide	Earth slide
	TRANSLATIONAL			
LATERAL SPREADS		Rock spread	Debris spread	Earth spread
FLOWS		Rock flow (deep creep)	Debris flow (soil creep)	Earth flow
COMPLEX		Combination of two or more principal types of movement		

Figure 3.2 Slope movement, types and processes (Varnes 1978).

With reference to the type of movement, the author recognises the difficulties to classify natural landslides on the basis of a single type of mechanism; for this reason, he integrates the main categories by introducing a complex failures type. He also defines the terms 'multiple movements' and 'compound movements', whereby by multiple movements he means that a series of failures of the same type occur repeatedly one after the other. "Compound movements", instead, are those landslides in which "the failure surface is formed of a combination of curved and planar elements" With reference to the material, the author introduces bedrock and engineering soils (earth and debris). (Varnes 1978).
Referring to the schemes suggested by Blong and Varnes, additional elements of analysis have been added by Skempton (1953) who introduced a morphometric classification based on the ratio between the maximum thickness of a landslide (depth D) and its maximum length in the direction of maximum slope (L). On the basis of the D/L ratio he

recognized three different phenomena: slide, flow and rotational slide Table 3.1.

Table 3.1 Typical D/L ratio for various landslides types (Walker et al., 1987).

Landslide type	D/L %
Slides	5 - 10
Flows	0.5 - 3.0
Slumps	15 - 30

Based on data in Skempton (1953),Crozier (1973) Selby (1967), and East (1978).

From a geotechnical point of view, classification systems giving useful indications can be found in Hutchinson (1988) who takes into account the history of the movement, in terms of geotechnical parameters involved in the failure (c' and φ'), and the time to failure, in terms of pore pressure regime, Table 3.2.

Table 3.2 Geotechnical classification in terms of soil fabric and pore-water pressure conditions (Hutchinson 1988)

Soil fabric conditions (affecting c' and Φ')	Pore-water pressure conditions on slip surface (affecting u)
1. FIRST-TIME SLIDES IN PREVIOUSLY UNSHEARED GROUND: soil fabric tends to be random (or partly orientated as a result of depositional history) and shear strength parameters are at peak or between peak and residual values.	A. SHORT-TERM (undrained) - no equalisation of excess pore-water pressure set up by the changes in total stress.
2. SLIDES ON PRE-EXISTING SHEARS associated with:	B. INTERMEDIATE - partial equalisation of excess pore-water pressures. Delayed failures of cuttings in stiff clay (Vaughan and Walbanke 1973) are usually in this category.
2.1. Re-activation of earlier landslides.	C. LONG-TERM (drained) - complete equalisation of excess pore-water pressures to steady seepage values.
2.2. Initiation of landsliding on pre-existing shears produced by processes other than earlier landsliding, i.e:	Note that combinations of A, B & C can occur at different times in the same landslide. A particularly dangerous type of slide is that in which long-term, steady seepage conditions (C) exist up to failure but during failure undrained conditions (A) apply, i.e. a drained/undrained failure. The quick clay slide at Furre, central Norway (Hutchinson 1961) provides at an example.
a) Tectonics	
b) Glacitectonics	
c) Gelifluction of clays	
d) Other periglacial processes	
e) Rebound	
f) Non-uniform swelling	
In these cases the soil fabric at the slip surface is highly orientated in the slip direction, and shear strength parameters are or about residual value.	

In addition, , Leroueil et al. (1996) define, four different stages of slope movements Figure 3.3 (a).

- "pre-failure stage, when the soil is essentially overconsolidated and intact";
- "the onset of failure characterized by the formation of a continuous shear band or surface through the entire soil mass";
- "the post-failure stage which includes movement of the soil mass involved in the landslide, from just after failure and until it essentially stops";
- "The reactivation stage, when the soil mass slides along one several pre-existing shear surfaces; this reactivation can be occasional or continuous with seasonal variation of the rate of movement".

This scheme is only a part of a much more complex process that has led Leroueil et al. 1996 to consider the use of a 3-D matrix for the classification of landslides Figure 3.3 (b).
This matrix has three axes: one for the type of movement, one for the materials and one for the stages of movement, Figure 3.3 (b).
In order to take into account the mechanical characteristics of the materials involved, Leroueil et al. (1996) expand the number of types of material considered by Varnes (1978) and divide the rocks in hard and soft rocks, and the soils into two main classes (saturated and unsaturated soils), Figure 3.3 (c).

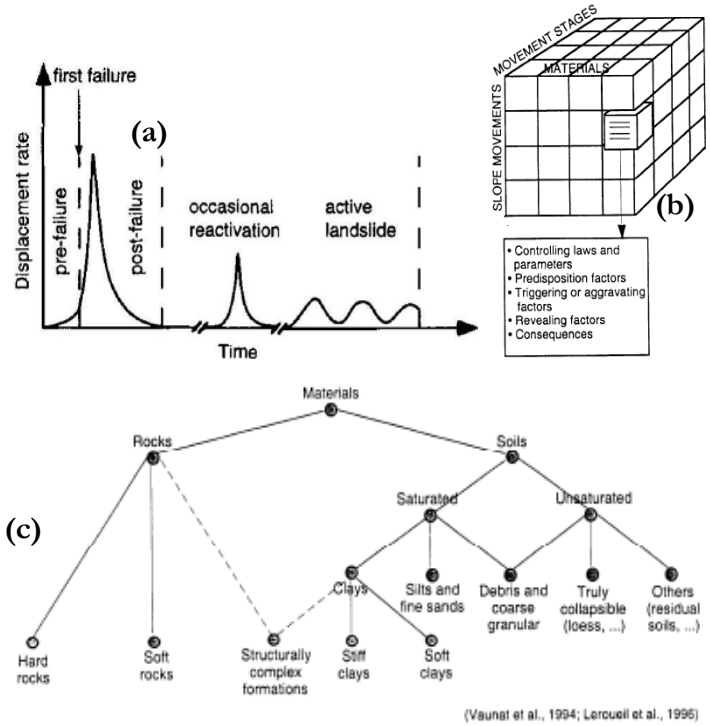

Figure 3.3 Geotechnical characterisation of slope movements (Leroueil et al., 1996): (a) different stage of slope movements (b) schematic slope movement characterization (c) types of material considered in the characterization.

It should be pointed out that all the previous classification systems, which can be used to properly classify shallow landslides in fine-grained soils, do not take into account the most relevant factors of these phenomena, i.e. their spatial diffusion over large areas, Figure 2.2.
To solve this problem, some proposals are available in scientific literature and, among these, the one developed by Carrara et al. (1985) - who proposes the use of the term "landslide zone" for those slopes affected by diffused and poorly detectable mass movements – is adopted in this thesis.

3.2 LANDSLIDE INVENTORY

A landslide inventory map records the location, classification, volume, activity and the date of occurrence, and the types of mass movements

when known (Pašek 1975, Hansen 1984a, 1984b, McCalpin 1984, Wieczorek 1984, Guzzetti et al. 2000, Fell et al., 2008a, 2008b, Cascini 2008).

Generally, the mapped landslides may be divided into their components: scarp, rupture surface and mass or deposit (Fell et al., 2008b). On the basis of these and many other elements, several methods can be used to develop a landslides inventory: "standard methods" such as manual image interpretation using digital stereo images coupled with field investigations, or more innovative methods, such as automatic identification based on either elevation or spectral information, or a combination of both.

A complete list of landslides inventory mapping techniques are proposed by Van Westen et al. (2008), Figure 3.4 who introduce six groups of landslides inventory techniques, i.e. image interpretation, (semi) automatic classification based on spectral information or on altitude information, field investigation, archive studies, dating methods and monitoring networks.

Group	Technique	Description	Scale			
			Regional	Medium	Large	Detailed
Image interpretation	Stereo aerial photographs	Analog format or digital image interpretation with single or multi-temporal data set	M	H	H	H
	High Resolution satellite images	With monoscopic or stereoscopic images, and single or multi-temporal data set	M	H	H	H
	LiDAR shaded relief maps	Single or multi-temporal data set from bare earth model.	L	M	H	H
	Radar images	Single data set	L	M	M	M
(Semi) automated classification based on spectral characteristics	Aerial photographs	Image ratioing, thresholding	M	H	H	H
	Medium resolution multi spectral images	Single data images, with pixel based image classification or image segmentation	H	H	H	M
		Multiple date images, with pixel based image classification or image segmentation	H	H	H	M
	Using combinations of optical and radar data	Either use image fusion techniques or multi-sensor image classification, either pixel based or object based	M	M	M	M
(Semi) automated classification based on altitude characteristics	InSAR	Radar Interferometry for information over larger areas	M	M	M	M
		Permanent scatterers for pointwise displacement data	H	H	H	H
	LiDAR	Overlaying of LiDAR DEMs from different periods	L	L	M	H
	Photogrammetry	Overlaying of DEMs from airphotos or high resolution satellite images for different periods	L	M	H	H
Field investigation methods	Field mapping	Conventional method	M	H	H	H
		Using Mobile GIS and GPS for attribute data collection	L	H	H	H
	Interviews	Using questionnaires, workshops etc.	L	M	H	H
Archive studies	Newspaper archives	Historic study of newspaper, books and other archives	H	H	H	H
	Road maintenance organizations	Relate maintenance information along linear features with possible cause by landslides	L	M	H	H
	Fire brigade/police	Extracting landslide occurrence from logbooks on accidents	L	M	H	H
Dating methods for landslides	Direct dating method	Dendrochronology, radiocarbon dating etc.	L	L	L	M
	Indirect dating methods	Pollen analysis, lichenometry and other indirect methods,	L	L	L	L
Monitoring networks	Extensometer etc.	Continuous information on movement velocity using extensometers, surface tiltmeters, inclinometers, piezometers	–	–	L	H
	EDM	Network of Electronic Distance Measurements, repeated regularly	–	–	L	H
	GPS	Network of Differential GPS measurements, repeated regularly	–	–	L	H
	Total stations	Network of theodolite measurements, repeated regularly	–	–	L	H
	Ground-based InSAR	Using ground-based radar with slide rail, repeated regularly	–	–	L	H
	Terrestrial LiDAR	Using terrestrial laser scanning, repeated regularly	–	–	L	H

Figure 3.4 Overview of techniques used to landslides inventory. H, M, L indicated the applicability of each technique for small, medium, large and detailed mapping scales. (H=highly applicable, M=moderately applicable, and L=Less applicable) (van Westen et al., 2008).

The selection of a specific technique depends on the purpose of the inventory, on the extent of the study area, on the data output resolution, and also on the visibility of landslides at any scale. However, due to the morphometric characteristics of shallow landslides and their spatial-temporal evolution, a landslide inventory map cannot be developed using all the methods currently available in scientific literature. For this reason, only the methods considered useful for the studied phenomena are analysed in this section, while for specific information readers can directly refer to Van Westen (2008).

Until recently, image interpretation by means of Stereoscopic aerial photographs, combined with field investigations, has been the main source for landslide inventory mapping (Van Westen and Lulie Getahun, 2003, Tribe and Leir, 2004; Metternicht et al., 2005).

In the last few years, the birth of the GIS system made the use of aerial photographs easier since the interpretation of stereo images can be done digitally, by using two scanned stereo images, or one image combined with a DEM to produce an artificial stereo image (VanWesten, 2004).

Although aerial photographs accurately depict details of a landslide, they are often not available in a multi-temporal sequence for the majority of landslide-prone areas in the world. Due to the high availability of data at a relatively low cost in most countries of the world, satellite images have become an alternative source of data for the detection and mapping of landslides, allowing a synoptic appreciation of the context within which phenomena occur, especially in terms of land cover dynamics (Martha 2011).

New opportunities are offered at present by the advent of Google Earth, which provides satellite multi-temporal images of different places in the world (Guzzetti et al. 2012).

One of the most recent methods is the use of LiDAR (Light Detection And Ranging) DEM to obtain digital representations of the topographic surface for areas ranging from a few hectares to thousands of square kilometres (Guzzetti et al. 2012, Shan and Toth 2009).

This technique uses a laser sensor mounted on an airplane or helicopter to measure the distance from the instrument and several points located on the topographic surface (more than 100 points per square meters can be measured, depending on the sensor characteristics, flight height and speed, and terrain geometry (Razak et al. 2011).

In Italy, an Extraordinary Plan of Environmental Remote Sensing has been realized to establish a data-base representative of the national

territory, especially with respect to its configuration and to its relationship with the environment. In particular, the project provides the acquisition of data produced by the remote sensing technique with laser-scanning LiDAR (from an aerial platform) and the interferometric technique (from satellite platform), and the subsequent classification of such data in the National Geoportal database. Currently, this information is available only for a part of the Italian territory, most countries in the world do not have similar data.

Obviously, the preparation of landslide inventory maps using automatic methods is preferable over manual approaches with the aim to obtain rapid results over large areas, and in those areas where these phenomena repeatedly occur. The most common methods used for landslides mapping are change detection, image fusion and objected oriented analysis (OOA). These methods are largely used for large landslides and several examples are reported by Martha (2011) with reference to the landslides occurred in different areas of the Himalayas.

At present, the resolution of these methods is still too low to ensure their use for small landslides, in fact, the methods are based on raster data composed by pixels and in some cases the pixel dimension represents one or more landslides (the smallest pixel has a dimension of 5.8 m) Nichol and Wong (2005). In the future, if improved in resolution, these techniques can be used for the automatic mapping of very small landslides.

Obviously, landslides mapping is a function of the scale of analysis, a common element to every scale is usually represented by drainage lines, those at small scale (≤1:100,000) play an important role on the geomorphological evolution of the area, while at detailed scale they offer an exact identification of the triggering zones.

3.3 METHODS OF SUSCEPTIBILITY ZONING

Landslide susceptibility represents the first step in a more complex process called risk management process, which consists of three parts: risk analysis, risk assessment, risk management, Figure 3.5.

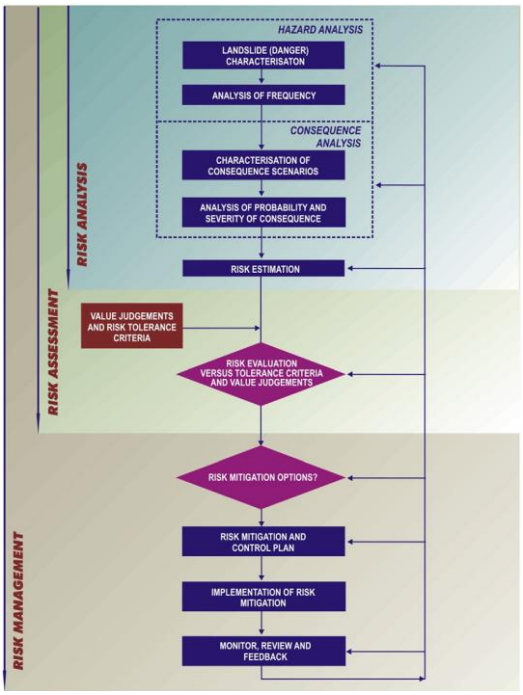

Figure 3.5 General framework of landslide risk management (Fell et al., 2008a).

Landslides susceptibility has been given different definitions in scientific literature (Brabb 1984; Soeters e Van Westen 1996, Fell et al., 2008a) although the most common is the one proposed by Fell et al., 2008a who define susceptibility as:

"A quantitative or qualitative assessment of the classification, volume (or area), and spatial distribution of landslides which exist or potentially may occur in an area. Susceptibility may also include a description of the velocity and intensity of the existing or potential landsliding. Although it is expected that landsliding will occur more frequently in the most susceptible areas, in the susceptibility analysis, time frame is explicitly not taken into account."

Starting from the consideration that susceptibility is a function of a landslides type, the first part of the definition highlights the need to classify landslides and to indicate their dimensions.

A significant classification of the methodologies used for the evaluation of landslide susceptibility has been proposed by Soeters and Van Westen (1996) and by Fell et al., (2008a). On the basis of this classification, methodologies can be divided into "qualitative" and

"quantitative". Despite the lack of proposals for shallow landslides in non-collapsible soils, in the present work the methodologies available in literature are summarized underlining the advantages and disadvantages of their use.

Qualitative methods are essentially subjective and provide a descriptive evaluation of susceptibility. Quantitative methods provide a numerical value in terms of spatial probability of landslides occurrence.

Another distinction can be made between direct and indirect methods (Guzzetti et al. 1999, 2005). Direct methods are based on experience and knowledge and expertise. Indirect methods are based on the identification of a direct or indirect interrelation between landslides distribution and landslides predisposing factors.

The most common methods are generally grouped into three categories (Carrara 1992; Guzzetti et al. 1999; Soeters and Van Westen 1996): heuristic methods, statistic methods and deterministic methods.

Heuristic methods are qualitative and are based on the expert's judgment. These methods combine the landslides inventory map with geomorphologic settings. Two types of heuristic analysis can be distinguished: geomorphic analysis and qualitative map combination.

Geomorphic analysis, also known as direct mapping method, is based on the expert's judgment and on the use of reasoning by analogy. The main advantage of this method is its simplicity, but the results obtained for one area cannot be applied to different areas. Qualitative map combination, also known as indirect method, is based on the overlapping of index maps. The expert assigns weighting values to different parameters maps. The overlapping of these maps, obtained by summing the weighted values of each map, allows to define the susceptibility values which can be grouped into susceptibility classes.

The advantages in the use of this method are that the expert's knowledge can be included and the high flexibility in both input and output data. Yet, the subjectivity in the attribution of weight can be considered the main disadvantage of this method.

Statistical methods try to overcome the problem of subjectivity and non-exportability of heuristic methods. Statistical methods are based on the statistical correlation between the principal factors that contribute to

landslides and the past and present landslides inventory in order to evaluate the potential distribution of failures (Carrara 1983; Carrara et al. 1995; Chung & Fabbri 2003; Corominas et al. 2003).

Deterministic methods are based on the physical laws controlling a landslide. Initially, deterministic methods were applied to a single phenomenon through the use of standard and advanced geotechnical methods (such as limit-equilibrium methods or stress strain analysis). Geotechnical methods need several data concerning the geotechnical and hydraulic properties of soil, stratigraphy and pore water pressure regime. Despite the problems related to the collection of data, in the last few years the use of deterministic models has considerably increased especially in combination with GIS techniques which allow to evaluate factors of safety over large areas (Van Westen, 1996).

In Table 3.3, Cascini (2008) summarized the methods, the procedures and all the input data necessary to calculate landslide susceptibility.

Table 3.3 – Methods required for the inventory of existing landslides and characterization of potential landslides (Cascini 2008 mod.)

Method	**Input** / **Procedure**	**Topography, Landslide Inventory, Geology, Geomorphology**	**Adding Soil classification and depth, Terrain units**	**Adding Hydrogeology and Geotechnics**
Basic	Heuristic or empirical methods	*		
Intermediate	Statistical analyses	*	*	
Sophisticated	Deterministic (physically based or geotechnical) models	*	*	*

The selection of one method over another depends on several factors such as: availability, quality and accuracy of data, scale of zoning, the output requirements, etc. All these aspects are well introduced and discussed in the Guidelines of JTC-1 (Fell et al., 2008) which are hereafter summarized considering their overall value for a definition of

the methods and of the input data that must be used given the complexity of the phenomena under investigation .

3.4 THE GUIDELINES OF JTC-1

The knowledge concerning landslide susceptibility and hazard zoning (especially as tools for a correct land-use planning) has increased considerably over the last few decades (Cascini et al. 2002, 2005). However, the lack of standard procedures has restricted the use of susceptibility zoning maps. The JTC-1, the Joint Technical Committee on Landslides and Engineered Slopes, has filled this gap by proposing the Guidelines for Landslide Susceptibility, Hazard and Risk Zoning for land-use planning.

JTC-1 guidelines do not deal with multiple occurrence shallow landslides, nonetheless, they provide international standards for the methods, the levels, the scales and the types of zoning (Casini 2008).

The guidelines group the methods for inventory and susceptibility maps available in scientific literature into three different categories: basic, intermediate and advanced. On the basis of the methods adopted, three different zoning levels (preliminary, intermediate and advanced) can be obtained.

For instance, when basic methods are exclusively used, only a preliminary zoning level can be obtained; while intermediate and advanced methods can allow the improvement of the zoning level according to the combinations shown in Table 3.4.

Table 3.4 Levels of activity required for susceptibility levels (Fell et al.,, 2008a mod.)

Type of zoning	Risk zoning Hazard zoning Susceptibility zoning Inventory mapping			
Zoning level	Inventory of existing landslides	Characterization of potential landslides	Travel distance and velocity	Frequency assessment
Preliminary Intermediate Advanced	Basic[1] [2] Intermediate Advanced	Basic[1] [2] Intermediate Advanced to intermediate	Basic[1] Intermediate[2] Intermediate Intermediate to advanced	Basic[1,2] Intermediate Intermediate to advanced

The use of different methods and the achievement of different levels of zoning depend on the scale of analysis and on the purpose of zoning, as reported in Table 3.5 (Fell et al., 2008a).

Table 3.5 Recommended types and levels of zoning and zoning map scales related to landslide zoning purpose (Fell et al.,, 2008a mod.)

Purpose	Type of zoning		Zoning level			Applicable zoning map scales
	Inventory	Susceptibility	Preliminary	Intermediate	Advanced	
Regional zoning						
Information	X	X	X			1:25,000 to 1:250,000
Advisory	X	X	X	(X)		
Statutory	Not recommended					
Local zoning						
Information	X	X	X	(X)		1:5000 to 1:25,000
Advisory	(X)	X	X	X	X	
Statutory		(X)		X	X	
Site-specific zoning						
Information	Not recommended					1:5000 to 1:1000
Advisory	Not commonly used					
Statutory		(X)		X	X	
Design		(X)		(X)	X	

Notes: X = applicable; (X) = may be applicable.

Specific information on the zoning methods will be provided in the subsequent chapters, while for additional information readers can refer to Fell et al., 2008a, Cascini 2008, Cotecchia et al. 2012.

With reference to the landslides inventory, the commentary of JTC-1 guidelines underlines the difficulties linked to landslides mapping at several scales and suggests the essential data to create an inventory. For example:

(a) At scale 1:50,000 to 1:100,000 landslides smaller than 4 ha may be represented by a dot. It is unnecessary and impossible to distinguish between landslide scarp features and the resulting mass or deposit. At this scale, landslides are only classified.

(b) At scale 1:10,000 to 1:25,000 landslides smaller than 1600 m^2 are represented by a dot. Minor and lateral scarps may be distinguished, as well as up-slope deformations such as tension cracks or minor landslides.

(c) a Landslides inventory at a scale greater than 1:5000 is used for site specific or local zoning.

JTC-1 guidelines propose the use of common descriptors which are independent of the adopted scale and zoning level for landslide susceptibility zoning maps in order to obtain the degree of landslide susceptibility necessary to compare different geo-environmental contexts.

A standardization of the descriptions of landslide susceptibility is very complex, given the difficulties arising from assessing whether a given landslide occurs and from the objective quantification of the factors (topographical, geological, geotechnical and climatic) which trigger landslides. The descriptors also depend on landslide types and, with reference to small landslides on natural slopes, some typical examples are reported by Fell et al., (2008a), Table 3.6.

Table 3.6 Examples of landslide susceptibility mapping descriptors (Fell et al.,, 2008a mod.)

Susceptibility descriptors	Small landslides on natural slopes
(a) Quantitative susceptibility descriptors	
	Scores of contributing factors obtained from data treatment techniques
	Factor of safety values from stability models
(b) Qualitative susceptibility descriptors	
	# of landslides per square kilometre
	% of area covered by landslides deposits
	Overlapping of index maps with or without weighting

Generally, at small scale a susceptibility zoning, made by using qualitative descriptors, is considered subjective because it depends on the expert's opinion, a fact which often leads to a map difficult to justify or reproduce systematically (Fell et al.,, 2008a).
At large scale, detailed susceptibility maps may be created on geotechnical models by obtaining a factor of safety. These approaches need geotechnical and pore water pressure parameters for a single slope or large area. For the analysis of multiple occurrence shallow landslides, usually the factor of safety may be established, on large area, in a GIS system by pixel cells, and the results may be referred to susceptibility depending on the calculated factor of safety. Given the complexity of the geotechnical conditions in slopes, these methods are unreliable unless calibrated by means of a correlation with the landslide inventory (Fell et al., 2008a).
In some situations it may be sufficient to simply use two susceptibility descriptors: "susceptible" and "not susceptible" (Fell et al.,, 2008a).
The guidelines of JTC-1 underline possible mistakes in developing the landslides susceptibility zoning due to imprecise input data (inventory, topographical, geological and geomorphological maps), uncertainly due to used methods, inexperience of the person that carried out the studies.

Moreover, the guidelines suggest that intermediate and advanced levels of zoning are more reliable than preliminary level of zoning.
Considering the suggestion provided by Fell et al. (2008a) and the characteristics of shallow landslides in non-collapsible soils, it is clear that the application of an integrated approach at various scales calls for a clear view of the problem and the individuation of the potentialities and the limits of each scale. For this reason, in the following section, examples of a multi-levels approach provided in scientific literature are introduced and discussed.

3.5 THE MULTI-LEVELS APPROACH

An analysis at different scales, or hierarchical approach, has been used for many years in mineral exploration due to financial reasons (Pan and Harris, 2000b). Recently, it has been applied to susceptibility landslides mapping and, in general, to landslides risk assessment (Castellanos Abella 2008).
A multi-levels approach can be developed following two different alternatives, i.e. from small to large scale (Cascini 2008, Gullà et al 2008) or from large to small scale (Cotecchia et al. 2012). The first approach implies the passage from regional to detailed scale and appears to be more convenient since the size of the significant area to be investigated in depth decreases, going from small to large area. The second method seems more precise since the information collected on a few number of landslides at slope scale is progressively exported over the entire area to be studied at small scale, thus obtaining considerable information for susceptibility and hazard zoning; examples of this procedure are given by (Guzzetti et al., 1994; Guzzetti and Tonelli 2004, Cotecchia et al., 2012).
As it concerns the input data, the methods to be used and the usefulness of the studies developed at different scales, in Cascini (2008) each scale is connected with the purpose of zoning (information, advisory, statutory and design) and with the zoning methods, zoning levels and types of zoning, Table 3.7.

Table 3.7 Methods, levels and types of zoning at different scales (Cascini, 2008).

Scale description	Indicative range of scales	Zoning methods			Zoning levels			Types of zoning		Purpose
		Basic	Intermediate	Sophisticated	Preliminary	Intermediate	Advanced	Susceptibility	Hazard	
Small	< 1:100,000	*			*			*		Regional zoning - Information
Medium	1:100,000 to 1:25,000	*	(*)		*	(*)		*	(*)	Regional zoning - Information - Advisory
Large	1:25,000 to 1:5,000	*	*	*	*	*	*	*	*	Local zoning - Information - Advisory - Statutory
Detailed	> 1:5,000	[*]	(*)	*	[*]	(*)	*	(*)	*	Site specific zoning - Information - Advisory - Statutory - Design

Notes: * applicable; (*) may be applicable; [*] not recommended or not commonly used

At small scale (<1:100,000), considering Table 3.7, only basic methods can be used and preliminary level of zoning can be pursued.
At medium scale (from 1:100,000 to 1:25,000) basic and intermediate methods can be used and preliminary and intermediate levels of zoning can be obtained.
At large scales (from 1:25,000 to 1:5000) all levels of zoning are possible using basic, intermediate and advanced methods.
Finally, at detailed scale an advanced level of zoning is advisable. This level of zoning requires the availability of advanced data set to use deterministic procedures.
However, the type of analysis, level and scale depends not only on the purpose of zoning but also on the complexity of the landslides features, on the homogeneity of the terrain, on the spatial variability of the causal factors and on geotechnical parameters (Cascini, 2008).

Cotecchia et al. (2012) propose a methodology divided in two phases defined as: phase I (preliminary) and phase II (applicative).
In phase I, the methodology includes the creation of a large regional database, initially using the available data which have been previously critically analyzed in order to check their reliability and for their

homogenization. In phase I of analysis, the authors proposed a multi-level analysis at slope scale, identifying three different levels of investigation based on the geological, hydrological and mechanical characters of landslides (level I, level II, level III), Table 3.8.

Table 3.8 Scales and levels of analysis (Cotecchia et al. 2012 mod.).

Scale description		Indicative range of scale	Geo-hydrological and mechanical levels of analysis	Deterministic methods according to the guidelines of JTC-1
large area	small	<1:100,000	I	basic
	medium	1:100,000-1:25,000		
medium area	large	1:25,000-1:5,000	I-II	analytical advanced
slope	detailed	>1:5,000	I-II-III	numerical advanced

As it can be inferred from Table 3.8, for each scale of analysis, the authors use the same variation range proposed by Cascini (2008) recommending the application of advanced methods at medium and large scale.

In particular, at small and medium scales, the authors suggest the application of a Level I analysis following a preliminary deterministic method, while at large scale they propose to combine level I and II analyses following an advanced analytic deterministic method; at detailed scale, instead, they suggest the application of a level III analysis following an advanced numerical deterministic method. Level I and II analyses, appearing simultaneously at different scales, show a degree of detail which varies according to the scale.

The cascading application of the three methods described allows to define and analyze both the representative geo-hydrological and mechanical properties (GMi) and landslides mechanisms (Mi).

Phase II of analysis consists of the evaluation of susceptibility and hazard zoning at large scale. To pursue this aim, the authors applied the results obtained at slope to large area following two hypotheses. In the first, in any area with a limited extension and with sufficiently homogeneous hydrogeological and mechanical characters, recurrent hydrogeological and mechanical properties can be identified, more specifically, the combinations between GMi (i = 1…n) and Mi (i = 1…n) are limited in number. According to the second hypothesis, the connections between the hydro-geological and the mechanical properties of the slopes and the landslides mechanisms must be equally limited in number.

Several examples concerning the application of JTC-1 guidelines, on the basis of a multi-scale approach, are proposed in literature; some of them

(Cascini, 2008, Gullà et al. 2008, Santaloia et al. 2012 and Lollino et al. 2012) are hereafter summarized.

3.5.1 Examples of Small and medium scales

An interesting example of a preliminary level of susceptibility zoning at small scale (1:100.000) is provided by Cascini (2008) who develops the susceptibility zoning map Figure 3.6(c) by simply overlapping the geological map Figure 3.6(a) with a very accurate landslide inventory, based on Varnes' classification, developed at 1:25,000 scale Figure 3.6(b). This inventory map allows to clearly distinguish several areas affected by slow moving landslides of different volume or potentially affected by fast landslides that can occur over a well-defined slope or over large areas with huge consequences in terms of victims and economic damage.

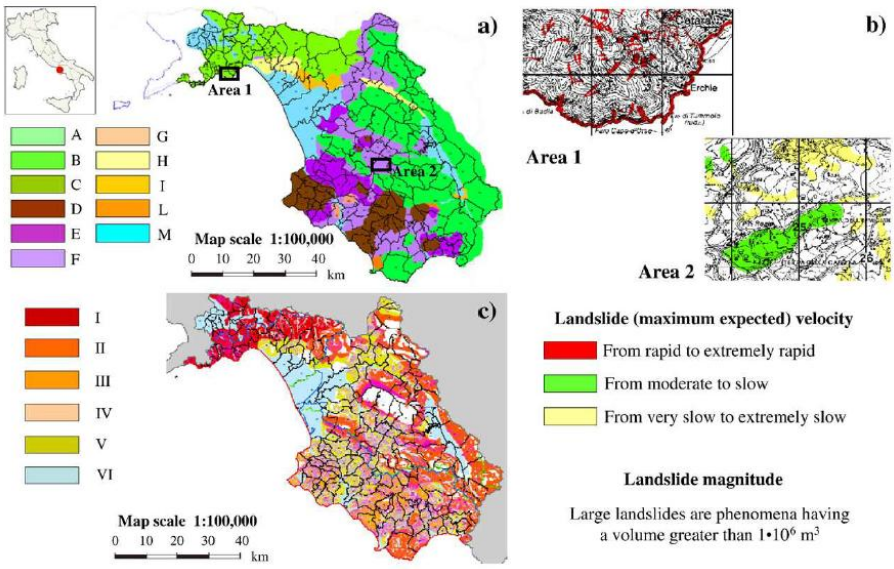

Figure 3.6 (a) Geological map of Salerno province; (b) Part of landslides inventory map and classes of landslides intensity and magnitude; (c) Susceptibility zoning map at small scale (Cascini 2008).

The same author, once again following the guidelines of JTC-1, uses the preliminary level of zoning at medium scale (1:25,000), over a territory of about 12,000 km^2. In particular, the author obtains a susceptibility zoning map by simply overlapping several thematic maps among which the

landslides inventory map, developed at 1:25,000 scale using Varnes' classification, and the geomorphological map developed at the same scale, Figure 3.7.

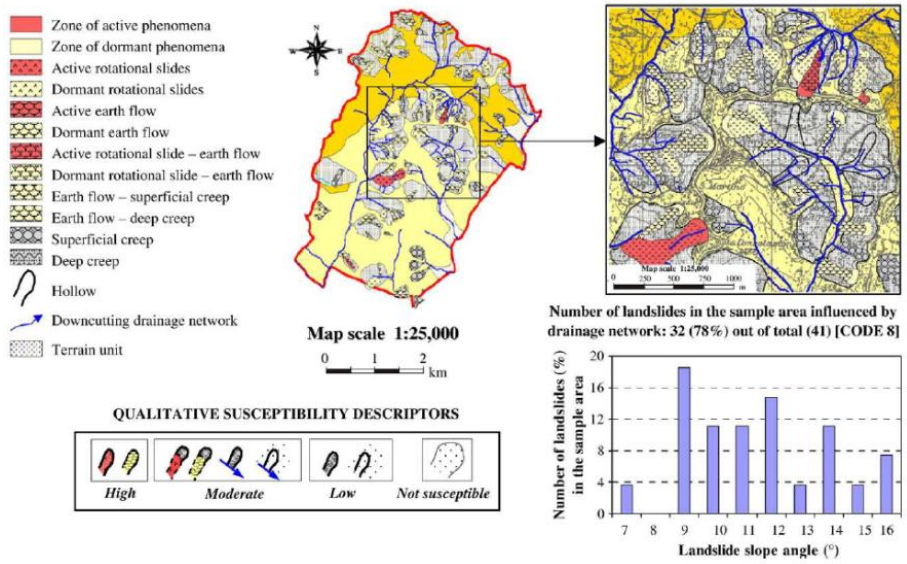

Figure 3.7 – Preliminary susceptibility zoning at medium scale for the area framed with the black square in the Figure (Cascini 2008).

In this case, the geomorphological map represents the key factor in the differentiation of instability phenomena and their mechanical characterization.
Subsequently, in a sample area, the author introduces the factor $Ri=fli/fi$, similar to the one adopted by Coe et al. 2004. For every homogeneous geolithological complex initially identified with *i*, fli is the ratio between the number of large landslides mapped inside the *i* code and the total number of mapped landslides in the sample area, fi is the ratio between the area of the *i* code and the whole study area.
On the basis of the Ri ratio, of the types and of the state of activity of the instability phenomena, of the geomorphological map and of the slope angle, Cascini (2008) identifies three landslides susceptibility classes: high, moderate and low susceptibility, Figure 3.7.
The procedure adopted also allows to discover a strict relationship between the drainage network and creeping and existing landslides, Figure 3.7, considering that 78% of phenomena interact, at the toe, with streams.

A significant example specifically related to shallow landslides is provided by Gullà et al. (2008) who propose a methodology to identify susceptibility and triggering scenarios at a regional scale. The author used an intermediate approach to analyze shallow landslides susceptibility and triggering scenarios in the Calabria region (15,075 km^2 extension). This approach was combined with an available database linked to a GIS created to support the various steps of spatial data management and manipulation. The data used by the authors to identify shallow landslides predisposing factors were: 40-m digital terrain model, outcropping lithology; soils; land use and inventory map. With reference to the outcropping lithology, the authors, referring to the geotechnical characteristics of the geomaterial, identify two main kinds of covers: prevalently coarse-grained or fine-grained covers. Soilscapes have been drawn from soil maps; and finally, the land use map has been employed without any prior processing. The inventory map considered in this process includes more than 30,000 instabilities of the past.
The approach was carried out into two phases related to two different levels of analysis: at the first level, three different susceptibility maps have been provided; at the second level of analysis, the areas susceptible to shallow landslides events have been better identified by overlapping the single susceptibility maps. The results of the second level of analysis showed five different susceptibility classes for shallow landslide events over the regional territory. More specifically, 8,9% of the regional territory is characterized by very high susceptibility, 14,3% by high susceptibility, 15% by moderate susceptibility, 3,6% by low susceptibility, and finally, about 58% by very low susceptibility.
Finally, the maps of two significant shallow landslide events of the past, and their related rainfalls, have been used to identify the relevant rainfall triggering scenarios.
The complete procedure used by the authors is reported in Figure 3.8, see Gullà et al. (2008) for a detailed explanation.

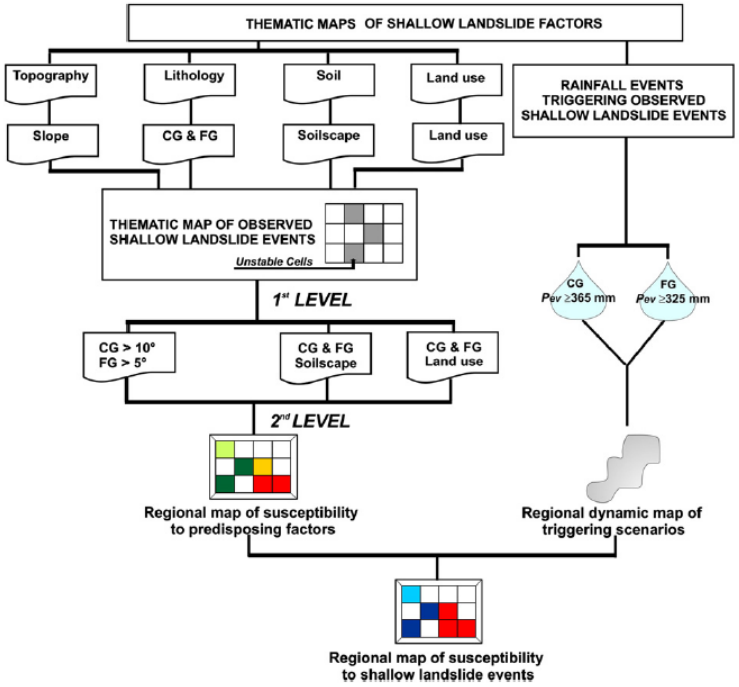

Figure 3.8 Procedure used to identify and classify areas susceptible to shallow landsliding events at a regional scale (Gullà et al., 2008).

Following the procedure summarized in the previous section, Santaloia et al. (2012b), propose, at small scale, a level I analysis of on the Apulia-Lucanian front, which consists in the collection, summary and critical analysis of all the available geological and geotechnical data managed using GIS procedure. As a result, the authors identify and interpret the landslides mechanisms and their causal factors that are subsequently verified through a level II analysis carried out on different sample areas using the limit-equilibrium methods. The results obtained for two sites underline that limit-equilibrium analysis, performed with data obtained at medium slope scale, allows the quantitative check of the geo-mechanical characters indentified at level I of analysis. Particularly, level II analysis gives indications about the predisposing and triggering factors of the landslides and, at slope scale, allows to better identify the location of the slip surface or the location of the toe or the head of the landslide.

3.5.2 Examples of analysis on large, detailed and REV scales

Several examples of landslides susceptibility zoning at large and detailed scale are available in literature, among which those proposed by (Cascini et al. 2008, Sorbino et al. 2009, Lollino et al. 2012) are particularly interesting.

At large scale, Cascini (2008) uses a qualitative approach based on the analysis of the geological, geomorphological setting and on an inventory map. With reference to the geological setting, and, in particular, to gneissic cover, the author firstly identifies six weathering classes of gneissic unit that are respectively called: class VI (residual soil and colluviums), class V (completely weathered, gneiss), class IV (highly weathered gneiss), class III (moderately weathered gneiss), class II (slightly weathered gneiss), class I (fresh gneiss). This classification allows to distinguish between existing and potential landslides (hollows) involving soils (classes V and VI, and landslides in debris) and instability phenomena involving weak and/or hard rocks (classes III and IV, and sometimes V).

Improved knowledge is then obtained by overlapping the areal extension of the weathering grade, the areas prone to instability phenomena (landslides and hollows), the structural elements and/or the active stream down cutting on the bedrock . For example, for class V and VI the author shows that about 90% of the landslide-prone areas are influenced by drainage networks and/or tectonic structures. This information allows to define qualitative susceptibility descriptors and, therefore, to distinguish between areas characterized by high, moderate and low landsliding susceptibility.

Sorbino et al., 2009 use a quantitative approach based on distributed physically-based models to simulate limit-equilibrium conditions on a large area. This model represents a powerful tool to analyze the triggering stage of shallow landslides, as in the case of flow-like landslides occurring in pyroclastic soil in the Campania region (southern Italy). In particular, the author uses saturated and unsaturated TRIGRS models (which are introduced and discussed in chapter 10) to calibrate and validate some significant hydraulic parameters at slope scale that are subsequently used for modelling the potential instability phenomena at large scale over larger areas For this purpose, a success-index and an error-index, defined by Sorbino et al. (2007), are used to test the validity of the modelling performed. The results obtained for the case study, in

addition to those coming from an application carried out on an area in California, confirm the potentialities of such a method.

Cotecchia et al (2012) use a quantitative approach based on advanced geotechnical numerical methods, such as the finite elements method (FEM) or the finite differences method (FDM), applied to specific sections and subsequently exported at large scale. At this scale, the authors define a level III analysis which requires a thorough interpretation of complex systems, such as landslides, on a physical and mechanical basis, the use of strain stress analysis at slope scale and the rational use of monitoring techniques. With regard to this, Santaloia et al. (2012) suggest that geognostic investigations must be planned and developed at Level III when the results of level I and II analyses are complete. In Table 3.9 all the types of in situ and laboratory investigations as it concerns all three levels of analysis suggested by the authors are summarized.

Table 3.9 Suggested investigations for the geo-hydro-mechanical characterization (Santaloia et al. 2012 a mod.).

In situ investigations	Laboratory tests
(a) Detailed geological surveys	(a) Multi-temporal air photo interpretation
(b) Geotechnical surveys	(b) definition of the absolute age of the organic substance present in the landslide bodies
(c) Permeability measurements (Lugeon and Lefranc) and in situ suction measurements	(c) Meso-structure analysis for complex lithotypes
(d) Geophysical analysis	(d) Laboratory geotechnical analysis
(e) Topographical monitoring	(e) Mechanical tests
(f) Rainfall gauge and thermometer	
(g) Structural damages analysis	

In particular, the analysis at large scale consists of a geognostic investigation, with intact samples taken to perform the mechanical characterization through laboratory tests. Such characterization is necessary to obtain the basic input data for a geotechnical numerical modeling. For example, laboratory tests aimed at the characterization of shear strength are essential to develop limit-equilibrium analysis, while the constitutive laws of the materials cannot be disregarded when stress-strain analyses must be carried out. Furthermore, monitoring stations must be installed for analysis at Level III based on the results obtained at

level I., Table 3.9. This table also summarises the useful surveys for analyses at levels I, II.
The relevance of timely and spatially well-planned in situ investigations is underlined also by Cascini et al. 1991, 1992 who carried out three different investigations in 1981, 1983 and 1987, to study a complex landslide in weathered gneiss. The data acquired during the first investigation were used to establish reliable cross sections that allowed both i) the assessment of slope susceptibility to landslides on the basis of geological criteria only and ii) the individuation of some preliminary data regarding the groundwater regime and the displacement of the slope affected by the landslide. On the basis of the knowledge acquired, the other two investigations were performed to gather further insight into the groundwater regime and to characterize the geotechnical properties of the soils involved in the landslide.
This kind of information is fundamental, as pointed out by many authors, among which Picarelli (1991) and D'Elia et al. (1998) who propose a rational framework for the study of the behaviour of a geo-material relating to its structure. These authors identifies different aspects that require further investigation at different scales, as suggested in Figure 3.9. In particular, they identify:
(a) the microstructure, visible at a microscope, which is principally related to soil particles, their arrangement and the possible bonding between particles;
(b) the mesostructure which is related to the size of laboratory samples (centimetres to decimetres). It includes fissures, and pockets or laminae of soils of different grain sizes;
(c) the macrostructure which is a structure typical of engineering works (metres to tens of metres). It is generally characterized by bedding planes, joints and major heterogeneities;
(d) the megastructure which is related to the geological scale (tens of metres to kilometres). It includes faults, folds and other geological features. At slope scale, all these types of structures interact to provide the global behaviour of geomaterials; consequently, a good understanding of landslides can be obtained only from a multidisciplinary approach (Leroueil et al., 2001).

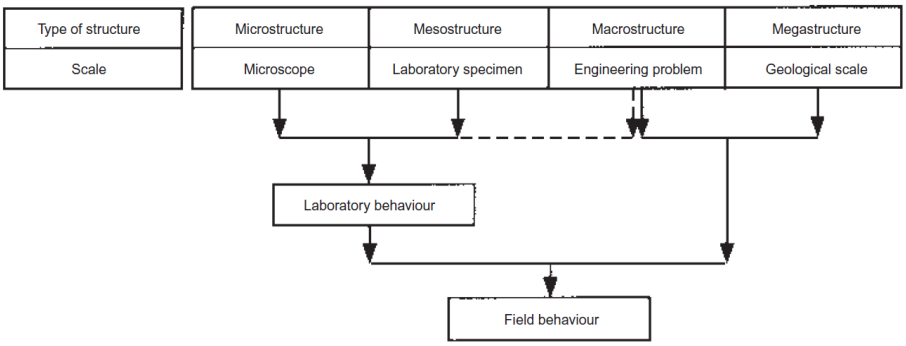

Figure 3.9 Relation between structure and material behaviour (Picarelli 1991 and D'Elia et al., 1998).

4 THE PROPOSED APPROACH

The literature on the topic underlines how landslides can be investigated with different aims and using various methodologies at different topographic scales. In addition, significant contributions are available, which highlight the potentialities of studies carried out at multi-scale level through a deductive approach Cascini (2008) or an inductive one Cotecchia et al. (2012).
In particular, Cascini (2008) provides a preliminary development of studies at small scale that progressively move on to larger scales. By contrast, Cotecchia et al. (2012) use a multi-scale approach at slope scale, analyses several slopes affected by single landslide, and then they use the obtained results at large scale.
Whatever the modalities to perform the analyses, the complete absence in literature of proposals focusing on shallow landslides must be pointed out and, as underlined in chapter 2, the existing contributions essentially refer to a single scale of analysis, while only a few are developed using a multi-scale approach.
Within the present chapter, an integrated methodological approach for such phenomena going from small to large scale is proposed which reinterprets what is currently available in literature; this approach also aims at developing a general framework that is able to delineate and correlate the predisposing factors (at small-medium scale) to the triggering causes of the landslide (at large and detailed scale).

4.1 GENERAL FRAMEWORK

The proposed methodological approach (which to speak metaphorically, can be compared to a puzzle) is characterized by three subsequent steps; each of them provides a significant element and, once completed, it allows to establish a connection between all the predisposing factors and the triggering causes of the landslides, Figure 4.1(a). This approach differs from others insofar as it uses two distinct phases for each step, in turn referring to a specific scale of analysis: Phase I in which

predisposing factors and/or triggering causes depending on the scale of analysis are identified; and phase II in which the factors or causes are quantified.
From an operational point of view, the proposed methodology starts from small scale following a logical process that considers the output of Phase II of each scale as the input of Phase I of the scale that follows. Such conditions enable a strict evaluation of both the validity of the methodology used and of the obtained results.
As far as the analysis at small scale is concerned, Phase I consists of the application of qualitative heuristic methods such as geological, geo-morphological and structural analyses. Phase II consists of the quantification of the factors identified in the previous phase through quantitative heuristic methods such as the "quantitative map combination". This step principally aims at identifying the general conditions which are able to produce diffused shallow landslides in an area.
The analysis at medium scale, following what has been developed at small scale, includes a preliminary phase of improvement of the input data which aims at identifying both the areas of interest for the present study and the predisposing factors of the landslide that are analyzed with the use of a slope evolution model. Given the scale of reference, a good inventory of landslide phenomena is paramount for this aim which, as Fell et al., (2008) suggest, should be acquired at a larger scale than the one deployed in the analysis.
Phase II should quantify the landslides predisposing factors individuated at the end of the Phase I by applying statistical methods. Given that this goal requires relevant efforts beyond the scope of the present thesis, only Phase I will be analyzed and discussed.

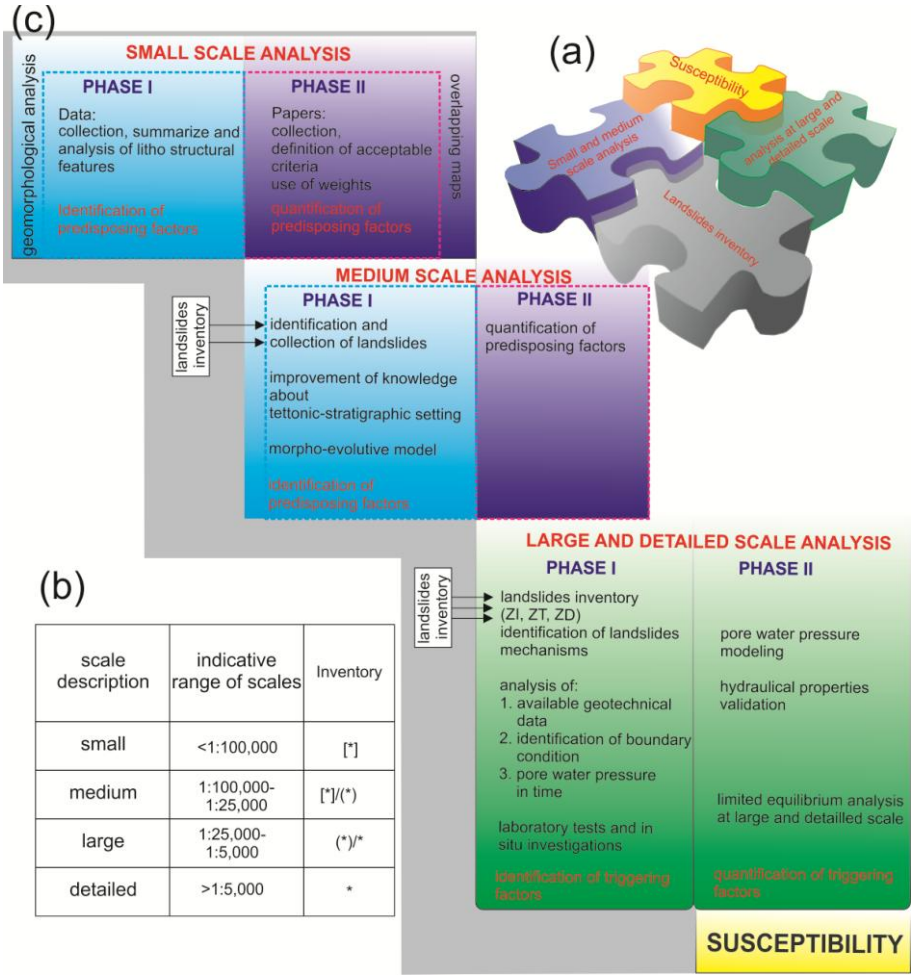

Figure 4.1 General framework for landslides susceptibility map

Finally, the analyses at large and detail scale are characterized by specifically geotechnical analysis. The collected geotechnical data derive from in situ investigations and laboratory tests and they must allow the characterization of the mechanical properties of the lithotypes involved in landsliding and the definition of the pore water regime that are absolutely necessary to perform geotechnical analyses performed to identify the triggering causes of a landslide.

Phase II-analysis focuses on the quantification of the triggering causes which can be obtained either through traditional geotechnical models or

through advanced ones such as, for example, physically-based models and/or stress strain analyses.
It is worth noting that the methodology specifically proposed for the analysis of the shallow landslides is particularly versatile insofar as it can be applied to different phenomena than those studied here. However, considering the aims of the present thesis, this chapter exclusively focuses on the applicability of such a methodology to shallow landslides in non-collapsible soils.

4.2 APPLICABILITY TO SHALLOW LANDSLIDES

The starting point for each study aimed at assessing landslides susceptibility is represented by the inventory map which must be as complete and accurate as possible, i.e. it must contain all the useful information for carrying out studies at different topographic scales. Obviously, the inventory map cannot, and must not, leave aside the characteristics of a landslide, such as its dimension and its evolution over time.
All that considered, it is clear that shallow landslides in non-collapsible soils, given their small dimensions, are more difficult to map as the topographic reference becomes smaller and smaller Figure4.1(b). In fact, at small scale (1:100,000), the studied phenomena are neither visible nor can they be mapped and, in such a case, several authors recommend to represent such phenomena through the use of dots with attributed characteristics (typologies and state of activity). As a consequence, the absence of well-defined landslide boundaries only provides information to be used for the analysis of the landslide density in an area. Moreover, through the use of geological and qualitative and quantitative morphological analyses, useful insight can be obtained on the predisposing factors of the landsliding.
Also, at medium scale (1:25,000) landslides cannot be mapped since the boundaries of the phenomena are not clearly distinguishable at this scale. On the contrary, the boundaries and the main morphological elements of the landslides can be recognized and mapped at large and detailed scale. For this reason, the author propose the development of two different inventory maps, one of which devoted to analyze the

phenomena at medium scale, while another is aimed at performing advanced studies at large and detailed scale.
Bearing in mind these necessary preliminary remarks, the elements required for the proposed methodology are hereafter outlined by referring, in general, to the selected area, i.e. the Catanzaro Graben, which is described in detail in chapter 6.

4.2.1 Small and intermediate scales

The reference area extends for about 2000 km^2; within this area two different analyses in two different phases must be developed. Phase I concerns the identification of predisposing factors, and Phase II concerns their quantification.
Given the aims to be pursued, Phase I must necessarily consist of an accurate collection, analysis and summary of the geological, morphological and structural data available in technical and scientific literature. On the one hand, the complexity of this phase evidently depends on the geological and structural complexity of the studied area; on the other hand, it depends on whether scientific contributions describing a credible and unambiguous reference framework are available.
In the case under investigation, van Dijk and Okkes (1991) lists three different geological schemes, respectively proposed by Dubois (1970, 1976), Amodio Morelli et al. (1976), Lorenzoni et al. (1978), to reproduce the evolution model of the northern part of Calabria Figure 4.2.

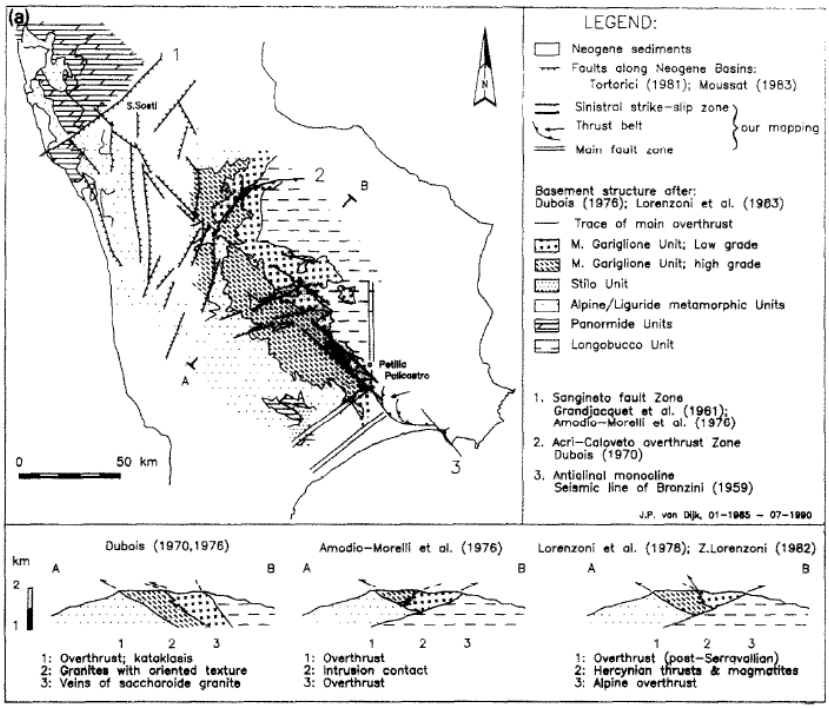

Figure 4.2 (a) Compilation of geological data concerning the Petilia-Sosti fault zone in Northern Calabria.(van Dijk 1991).

The study by Van Dijk and Okkes (1991) stresses how complex a small scale analysis of this area is. Therefore, in accordance with the JTC-1 guidelines, the available thematic maps have been remade by applying subsequent simplifications of input data available at greater detailed scales. The starting input data are represented by a map of the main lithological distributions at scale1:100,000, a map of the main tectonic structures, and that of the main water courses visible at that scale. An accurate analysis of the outcropping lithologies, of the tectonic structures, and of the consequent uplifts in each structural sector, together with the hydrological trend of the rivers, offers useful clues to identifying the predisposing factors of the overall morphological evolution of a landslide area. Therefore, the identification of the predisposing factors has to be followed by the quantification of the same data through a sequence analysis going from Phase I, which has just been discussed, to Phase II, which consists of the use of a quantitative map combination (see paragraph 6.4). Phase II includes two further phases: i) collection and analyses of the works available on the use of combined

index maps in a context similar to the one under investigation; ii) identification and validation of the reliability criteria of the work and, finally, use of the weights available in literature.
The results obtained at the end of Phase II analysis at scale 1:100,000 constitute the input data of phase I of landslide susceptibility analysis at intermediate scale (1:25,000), which is dedicated to determine the predisposing factors of the landslide conditions in the area.
For the implementation of phase I, a DEM with a reliability ≥ 25 m, a geological map at scale 1:25,000, a map of the main tectonic structures, and, above all, an inventory map of landslide phenomena developed at a greater detailed scale are necessary. Such basic parameters have to be used to identify the predisposing factors through geomorphological analyses; the latter, given the peculiar characteristics of the phenomena under investigation, must necessarily aim at defining a slopes evolution model which enables a subsequent zoning of the studied area into zones with a different landslide susceptibility.
To sum up, the analysis of the collected information must offer a morphological characterization of the areas mostly affected by shallow landslides; and, at small scale, a quantification of the predisposing factors to shallow landslides in the area through morphological and geomorphological elements. The aim of this analysis is to identify the zones to be investigated at a greater detailed scale through a semi-automatic process.

4.2.2 Large and site scales

Given the objectives pursued at these scales, the analyses must necessarily include the identification, mapping and validation of the landslide mechanisms in the area under investigation. Because of the intrinsic characteristics of the studied phenomena, accurate surveys of the territory, and the availability of temporal sequences of satellite images from Google Earth can be decisive in mapping of the phenomena studied. Phase I begins with the identification, mapping and classification of landslides, and it continues with the interpretation of landslide mechanisms deriving from morphological analyses supported by the collection, the summary and the analysis of geotechnical data. Phase II consists of the validation of landslides mechanisms pointed out in the previous phase.

The necessary data for the analysis are a topographic and geological-structural map at scale 1:5000, the inventory map of the landslide at the same scale or a greater detailed scale, a synthesis of the available geotechnical data. An accurate analysis of the main outcropping lithologies, together with a knowledge of the geotechnical data, such as borehole drills, negative and positive pore water pressures measured in situ, shear strength parameters, hydraulic parameters, can allow the identification of typical successive stratigraphic layers highlighting the presence of weathered, fissured material over an intact bedrock.
The hydraulic characterization of the involved lithotypes, although necessary to understand the triggering mechanisms, is particularly difficult given the intrinsic characteristics of the soils involved, and typical values available in literature represent a good starting point for an advanced characterization of the soil.
The identification of the landslide mechanisms, the characterization of degraded lithotypes on the basis of the available geotechnical data, the performance and interpretation of the geotechnical analyses necessary to investigate specific aspects such as shear strength and the hydraulic properties of the materials are significant moments in Phase II-analysis. This analysis aims at calibrating geotechnical parameters and at validating the triggering mechanisms identified. In the first case, it is likely to encounter considerable difficulties in the calibration of hydraulic parameters provided by lab tests. Often, such calibration cannot leave aside the knowledge of a material's hydraulic behavior at the scale of the macrostructure which can be determined by installing adequate equipment in situ.
A correct identification of the pore pressure regime at significant dates can also be very complex. Such identification, together with an in-depth knowledge of the geotechnical properties of the involved soils, constitutes the starting point for the modeling of limit-equilibrium conditions, and, more importantly, for the quantification of the mechanisms identified on a phenomenological basis in Phase I of the analysis.

5 THE TEST AREA

The potentialities of the methodology proposed and discussed in the previous chapter have been tested in an area which has long been affected by shallow landslides in non-collapsible soils. Since this methodology uses a multi-scale approach, a gradually smaller reference area has been considered going from small to large scale.

In particular, at small scale, the reference area has an extension of 2000 km^2, it is located in the central-southern part of Calabria (south of Italy), and falls within the provinces of Catanzaro and Crotone. To the north, the area borders the Sila massif, while to the south it borders the Serre massif, to the east and the west it is delimited by the Ionian and the Tyrrhenian seas respectively.

At medium scale, a 150 km^2 a wide portion of territory in the city of Catanzaro has been considered; its borders are the Sila massif to the north and the Ionian sea to the south, it is delimited to the east and west by the watersheds of the basins located to the hydrographical left and right of the Corace and Fiumarella rivers.

Finally, two morphological hollows - respectively located near the city of Catanzaro, i.e. the St. Antonio area and that of the University of Magna Graecia - have been chosen at large and detailed scales, Figure 5.1.

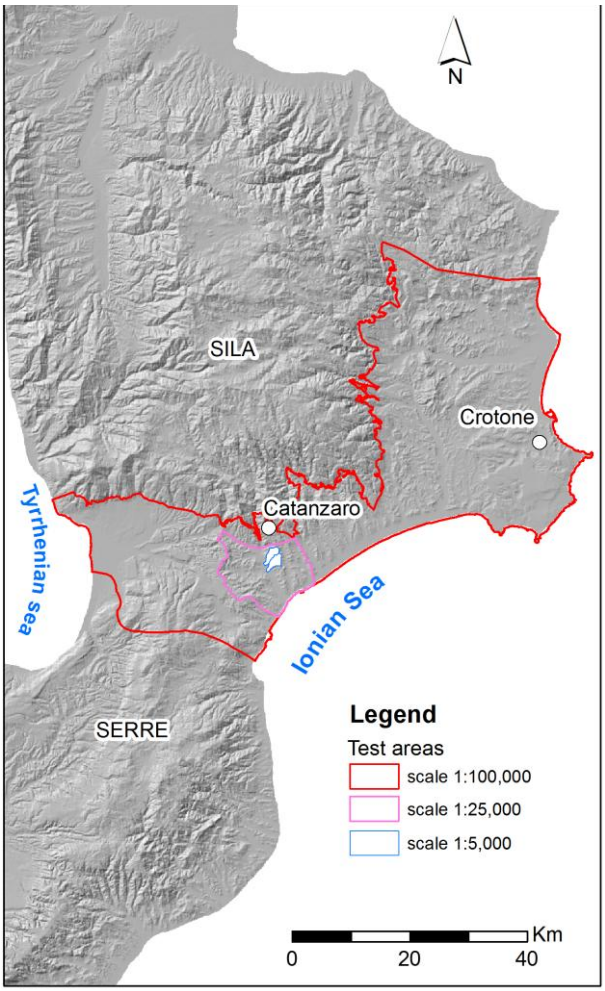

Figure 5.1 Test areas at different scales.

The initial database available for all these test areas, in situ investigations and lab tests performed to develop the analyses, together with all the different elements acquired to obtain scientifically significant results, are summarized in the present chapter.

5.1 THE AVAILABLE DATABASE

At each scale, the proposed methodology requires the use of a reliable dataset concerning: topography, geology and geomorphology, hydrogeology and surface flows, landslides inventory and geotechnical properties.

Topographic data can usually be found as topographic maps, available in digital or hardcopy form, showing the ground surface with its features and objects, such as rivers, buildings and roads. These data are not fixed, since they refer to the time when they were created and they can be modified as a consequence of the natural slope evolution due to different causes.

In the present thesis, digital topographic maps (at 1:100,000. 1:25,000, 1:5,000 and 1:1,000 scales) easily supported by a GIS system, are used also to obtain a digital numerical representation of the soil surface through the construction of a Digital Terrain Model (DTM) (Wilson & Gallant, 2000). DTMs have been used in geotechnical modelling and for the acquisition of the parameters generally used in GIS procedures such as, for instance, slope angle, curvature, flow direction etc.

The larger the scale of reference becomes, the more accurate the DTM must be, especially in this case study where the dimensions of shallow landslides are very small. Consequently, whenever possible, the influence of input data on the obtained results must be tested from large to detailed scale. This is possible for a 4 km^2-wide portion of territory where the use of a DTM at scale1:5,000 is compared to a LIDAR with 1mx1m cells. The comparison between the two sets of input data, as it will subsequently be shown in detail, reveals the existence of significant differences at a topographic level that can significantly affect, at this scale the output data of the performed analysis.

As far as the geological and geomorphological aspects are concerned, at small scale (1:100,000), the morpho-structural characteristics that determine the overall morphology of the area, by originating tectonic depressions (graben) and morphological highs (horst), have been investigated using a structural geological map at scale 1:100,000 proposed by Van Dijk. This map represents the principal tectonic lineations that originate the localization of the horst and the graben in the area and individuate the main contact zones between stratigraphic successions of different geological ages.

The geological input data have been taken from a geological map at scale 1:50,000 by Antronico et al. (2001), available for a portion of the area under investigation only, and from the regional geological map at scale 1:25,000, available for the whole test area. The inhomogeneity of such data, in terms of both scale of analysis and of area coverage, required the realization of an original map of the principal lithological distributions. This map shows the existence of different lithotypes in the study area characterised by physically and mechanically homogeneous features.
A knowledge of both the main outcropping lithologies and the main tectonic lineaments visible at small scale is extremely useful to draw detailed information, at medium scale, on morphological hollows, on the distribution of past landslides, on cracks, discontinuities, and all the morphological features which characterise the landscape affected by landsliding. Of course, the more accurate the input data, the greater the possibility to see and distinguish the alternations between hollows and ridges governing the localization of the phenomena that must be studied.
Starting from these input data, the main stratigraphic contacts at large scale are obtained though photo interpretation and in situ investigations that can identify the presence of soil thickness characterised by a diffuse pattern of cracks. The latter play a significant role in the morphological and evolutionary dynamics of the territory.
For this purpose, a map of degraded thickness is created on the basis of an entirely new criterion that uses a thorough reading of both the topographic maps and the landslides triggering mechanisms hypothesized and introduced for shallow landslides. The map of degraded thickness is validated through simple in situ investigations, mainly based on the use of a steel bar with a 1.4 cm diameter, 200 cm long and placed in the ground at a maximum depth of 130 cm (with a hammer weight of 6 Kg falling through a distance of 70 cm), Figure 5.2.

Figure 5.2 In situ investigations with steel bar.

5.1.1 Groundwater system

Generally, the definition of groundwater systems is one of the most complex aspects to analyse since it requires a large number of information for each scale of analysis. In particular, at small scale, hydrogeology allows the understanding of the main features of groundwater systems (deep and subsurface water circulation), generally resulting in a map of the distribution of underground flows and springs (perennial, seasonal, temporary). At large scale, in order to assess the deep and surface regime, several sites need to be monitored for a long time to obtain useful data.

Currently no useful research for the present study exists in the area between the Sila and the Serre massifs in Calabria, and only a particularly limited number of sites have been properly monitored for a long period of time. In particular, the Explanatory Notes of the Hydrogeological Map of Southern Italy at scale 1:250,000 (Celico et al. 2010) can be used as a reference at small scale; on the other hand, the paper written by Gullà et al. (2004) offers significant data at slope scale but, unfortunately, it refers to one monitored station only.

Given the aim of the present work, the gaps existing in scientific literature cannot be filled due to the difficulties deriving from the

homogeneity of the outcropping soils (mostly fine-grained soil). Therefore, only simple hypotheses can be developed as regards the subsurface flow considering both the localization of the main tectonic structures and their associated cracking zones which inevitably influence the surface water circulation.
Instead, as far as the latter is concerned, greater insight can be obtained through the use of the available DTM. Of course, the more accurate the DTM, the more precise is the computation of surface water circulation.

5.1.2 Landslides Inventory

A landslides inventory map is the starting point for any study aimed at defining landslide susceptibility and hazard. This map must be properly developed since it is greatly influenced by the scale of the analysis. At small scale, shallow landslides are not visible, at medium scale, instead, only landslides area can be distinguished. Finally, at large and detailed scale, these landslides are clearly visible and can be mapped. However, the rapid evolution of these phenomena, which undergo substantial morphometric changes over time, make the updating of the inventory through traditional techniques extremely difficult.
The systematic lack of adequate inventory maps for shallow landslides testifies to such difficulties. The PAI inventory map of the Regional Basin Authority created as part of the Authority Plan for Hydrogeological Hazard (so called PAI in Italian) Decree Law 180/'98 (known as Decreto Sarno) at scale 1:10,000 is the only official document available for the entire study area (Fig. 5.3) however, this map cannot be used in the present study as explained in chapters 6 and 7. Consequently, the landslides have been inventoried using as input data the aerial photos and the multi-temporal satellite images from Google Earth, following the method suggested by Van Westen et al. (2008), as described in chapter 3.

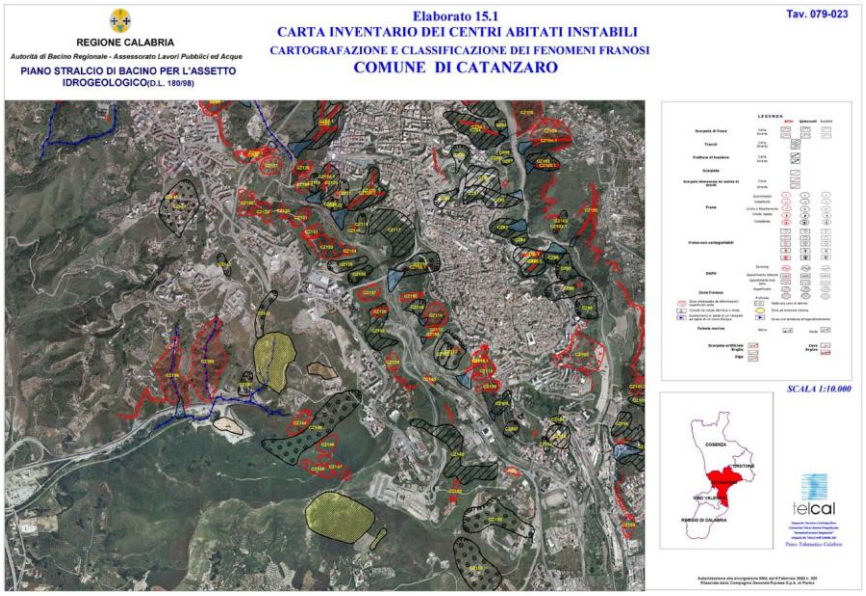

Figure 5.3 An example of PAI landslides inventory map.

5.1.3 In situ investigations and laboratory tests

The geotechnical characterization of the lithotypes present in the soil could not be carried out in the present work due to the intrinsic complexity of both the soils and the shallow landslides. However, such a characterization is important for the quantification of triggering mechanisms through geotechnical numerical modelling. Consequently, the strategy pursued here is based on the integration of the data available in literature with those deriving from the tests and investigations performed during the present study.

Among the data available in literature, the vast database of the CNR-IRPI in Cosenza has been used. This database contains microstructural information, in addition to that which can be collected at the scale of the mesostructure, and which can be summarized as index properties of the materials involved, shear strength parameters and information collected at the macrostructure on the pore water pressure regime.

The database is used operating a distinction between intact and weathered material on the basis of the depth of the samples used for lab

tests, as it is believed that at a depth of about 3 m, the soil analysed can reasonably be considered weathered. Below 3 m, the available database shows substantial differences existing between index properties and shear strength, as a result of which the presence of a presumably intact base formation can be hypothesized. The information contained in the CNR-IRPI database in relation to this formation is compatible with that collected by Cascini et al. 2010 in a different study area. For more detailed information, please refer to chapters 8 and 9 of the present work.

In this thesis, the mechanical characterization of the involved soils is performed through standard lab tests for the characterization of shear strength behaviour in saturated conditions and through advanced tests to obtain some indications on the hydraulic behaviour of the soil.

While an accurate description of standard tests can be found in the most important manuals, this paragraph focuses on "advanced" tests which have been performed with a Richards pressure plate, a volumetric pressure plate extractor and a suction controlled oedometer apparatus used in the lab experimentation phase.

In the tests with Richards pressure plate and with the extractor, samples of the same dimensions as those used for the tests with the oedometer have been used (56 mm diameter and 20 mm high). The samples have been placed inside the same hollow punches used during sampling. Once the air pressure chamber has been closed, the equipment has been pressurized to guarantee the beginning of the equalization phase. The (transitory) equalization stage begins, which will finish only when the conditions of the samples from within reach an equilibrium with the conditions imposed from without. At the end of this stage, the water volumes exchanged by the samples can be measured.

In the case of the extractor, the water volumes exchanged can be measured by monitoring the water level in the drainage circuits; in the case of Richards plate, instead, they can be measured weighting the samples before and after the equalization stage.

Both tests have been performed applying subsequent suction values to which the same values for water content correspond.

Only drying tests can be performed with Richards plate. Instead, both drying and wetting tests can be performed with the extractor: in the case of drying, suction values are progressively increased, whereas in the case of wetting, these values are progressively reduced.

Only the stages strictly related to the calculation of the Soil Water Characteristic Curve have been completed with the suction controlled oedometer apparatus. The test performed with this apparatus included only the phases which are directly involved in the measurement of the initial suction, in the application of an assigned suction value and in the reduction of the suction applied. The measurement of the initial suction immediately follows the sample assembling, pore water pressure is measured in a closed system through pressure transducers. When the initial conditions are known, an assigned suction value is applied and a transitory process begins, during which the sample either releases or absorbs water. This process can be considered complete when the measured variations in water content are less than 0.04% (Sivakumar, 1993). During such a process, air bubbles form in the circuit; they are periodically eliminated thanks to a peristaltic pump. For each increase in suction, the value of water content is measured at the end of each equalization phase. By putting the water content values and the suction values in a diagram, the Soil Water Characteristic Curve θ-Ψ is obtained.
If a wetting curve must be calculated, repeated decreases in suction are performed with a consequent increase in water content in the sample.
The hydraulic properties of the soils have also been calculated through in situ investigations by means of a Guelph permeameter, which is essentially a Mariotte's bottle made up of three transparent plastic cylinders which are inserted one within the other and sustained by a tripod. This device can establish a transient tri-dimensional infiltration process, with a constant, load within a small radium cylindrical hole opened in the soil, Figure 5.4. When the transient infiltration process becomes steady state, the test finishes and the formulas available in literature can be applied to estimate the conductivity value at stationary flow.

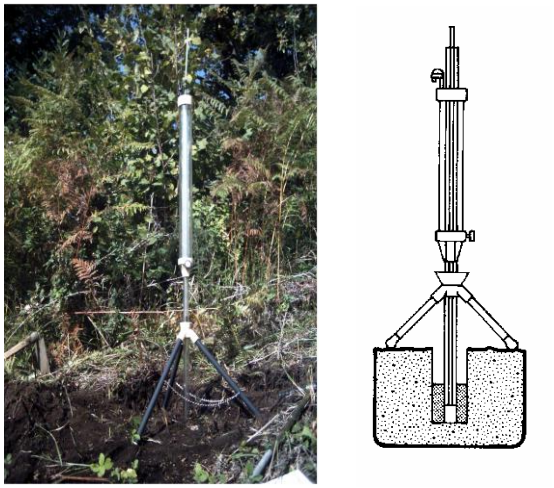

Figure 5.4 Guelph permeameter.

5.2 THE MONITORED TEST SITE

Monitoring multiple occurrence shallow landslides, such as the ones under investigation, is very difficult given the rapid evolution of these phenomena over a few years. It is therefore practically impossible to install fixed equipment which would be damaged and rendered useless after a very short time.

An alternative to a common monitoring system is therefore necessary, and could consist of a series of installations, procedures and models that are used for a large scale analysis of the triggering causes and of the evolution of mass movements.

Within such a purview, a limited number of fixed instruments can be used and they can be located in different sectors of the study area which have been stable for a long time. The monitoring data come from two different monitoring systems one of which essentially refers to piezometric measurements analysed and modelled by Cascini et al. 2010 who investigated part of an area particularly interesting for the present study. The other is provided by Gullà et al. 2004, who provide an integrated measurement, from 2001 to 2004, of climate conditions and of positive and negative pore water pressures.

In order to obtain further monitoring data, a monitoring station has been installed to measure the environmental parameters and the negative pore water pressures, Figure 5.5.

Figure 5.5 Monitoring station.

This station is made up of the following basic components: a datalogger for data logging and storage; a power supply system for every component of the station; sensors for measuring meteorological and climatic parameters, in particular, temperature, humidity, and atmospheric pressure, a rain gauge placed on a steel support to measure precipitation, and five Jet Fill' tensiometers used for measuring negative pore water pressures, placed at depths of 0.10 m, 0.15m, 0.30m,0.45m and 1.20 m, respectively, Figure 5.5.
The datalogger has been programmed with a 15-minute logging interval, except for the rain gauge for which the interval is 15 minutes until an increment of 0.2. mm is registered whereby the logging takes place every 5 minutes, Figure 5.5.
The download and transfer procedure of input data from the datalogger has been performed with a modem, by means of a GSM remote telephonic connection. This modem, in turn, is connected to a digital switch, Figure 5.6, from which the modem can be switched on or off.

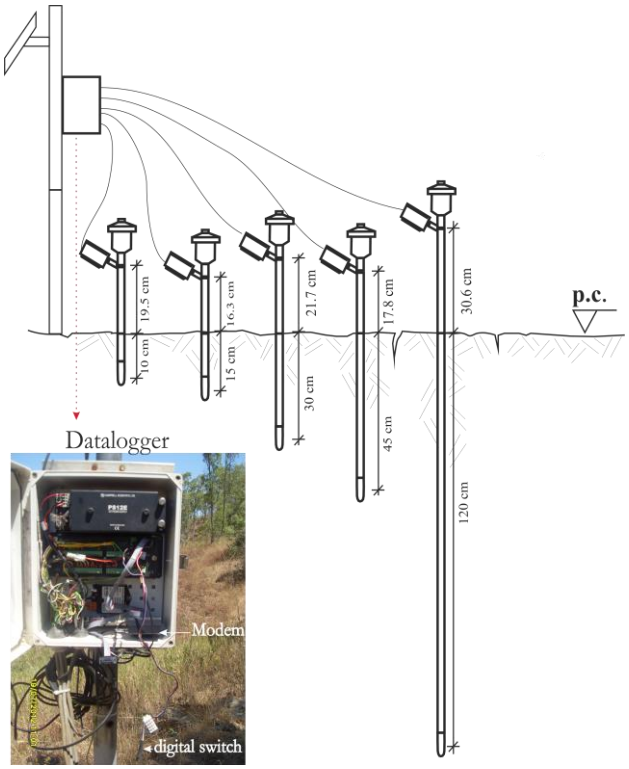

Figure 5.6 Jet Fill' tensiometers layout.

The calibration of the system, which is very complex as to what concerns the measurement of negative pore pressures is currently under progress in another study area.
The data recorder by the station with a logging interval of 15 minutes have been re-elaborated in order to obtain the same daily information.
Daily data used by Gullà et al. 2004 which refer to the values logged by the tensiometers at 7 a.m. have been used as pore water pressure data.
Both maximum and minimum daily temperature and relative humidity have been calculated.
The precipitation data recorded have been re-elaborated as daily cumulated rainfall, while an average wind velocity has been taken into account.
The data thus re-elaborated will be used, in chapters 9 and 10, for the definition of the characteristic hydraulic properties of the superficial

weathered layers and for the identification of the initial predisposing conditions of shallow landslide triggering at both slope and large scales.

6 SMALL SCALE ANALYSIS

The small scale analysis is aimed at describing the main geological and morphological characteristics of a significantly wide area in the Calabria region (southern Italy) where shallow landslides are a relevant issue due to their diffusion.
An overview is possible if an in-depth analysis of the available geological and geomorphological documentation is done. In addition, the analysis has to include the PAI inventory map at scale 1:10,000 mentioned in chapter 5.
Following the methodological approach proposed and described in Chapter 4, two distinct phases of analysis have been developed. Phase 1 identifies the predisposing factors of the geo-morphological evolution of the test area, establishing their role on the triggering and the evolution of the shallow landslides. In phase II, such factors are quantified by means of a quantitative map combination. The main results of this analysis are described in the following sections.

6.1 GEOLOGICAL SETTING OF THE CALABRIA REGION

The Calabria region is made up of crystalline–metamorphic nappe units, defined as Calabrian Arc (Amodio-Morelli et al., 1976; Tortorici 1982). This is a well-developed arc-shaped structure of the circum-Mediterranean orogenic belt originating in the collision between the African and the European plates between late Cretaceous and Palaeogene (Amodio-Morelli et al., 1976; Tortorici 1982), Figure 6.1.
Beginning in late Pliocene, the arc underwent a phase of severe isostatic uplift, which is still active today (Tortorici et al., 1995). The uplift produced a large rift-zone between eastern Sicily and northern Calabria called "Calabrian-Sicilian rift-zone" (Monaco et al., 1997; Monaco and Tortorici, 2000). The geometry of the rift-zone is clearly outlined by the distribution of the most destructive epicentres of the crustal earthquakes in the region, Figure 6.2 (Postpischl 1985; Boschi et al. 1995, 1997).

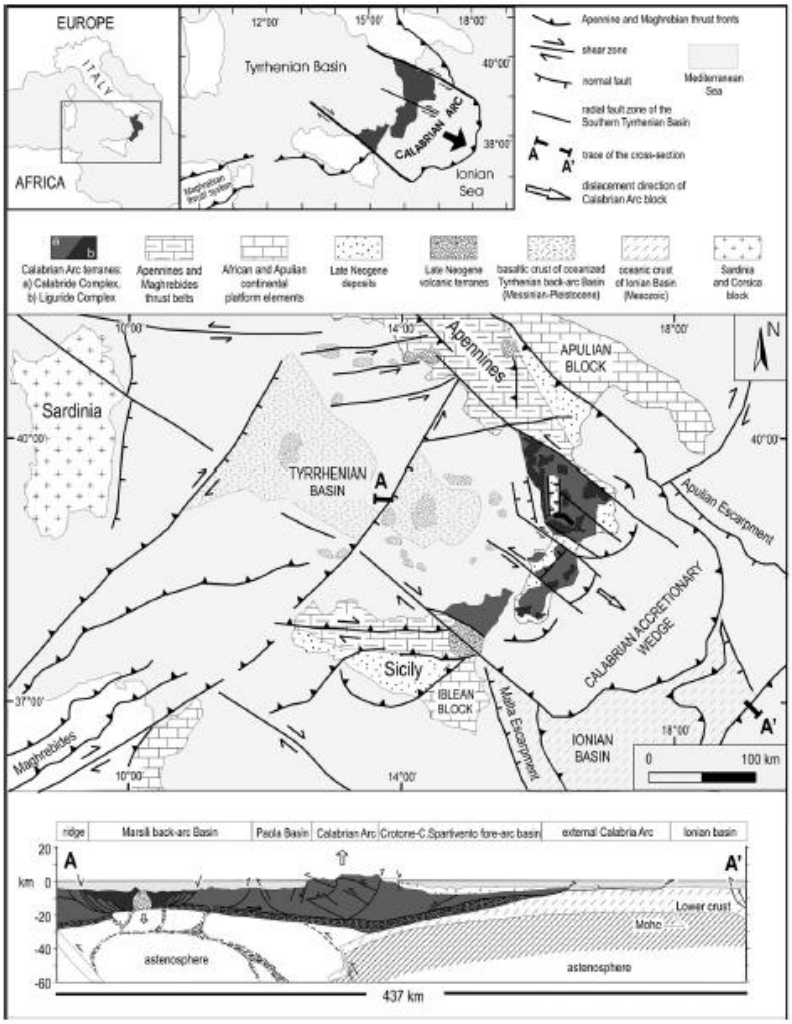

Figure 6.1 Geological sketch-map of the Central Mediterranean area, with geological section at the bottom. At the top, location of the study area, and tectonic simplified sketch of the Calabrian Arc (Tansi et al., 2007).

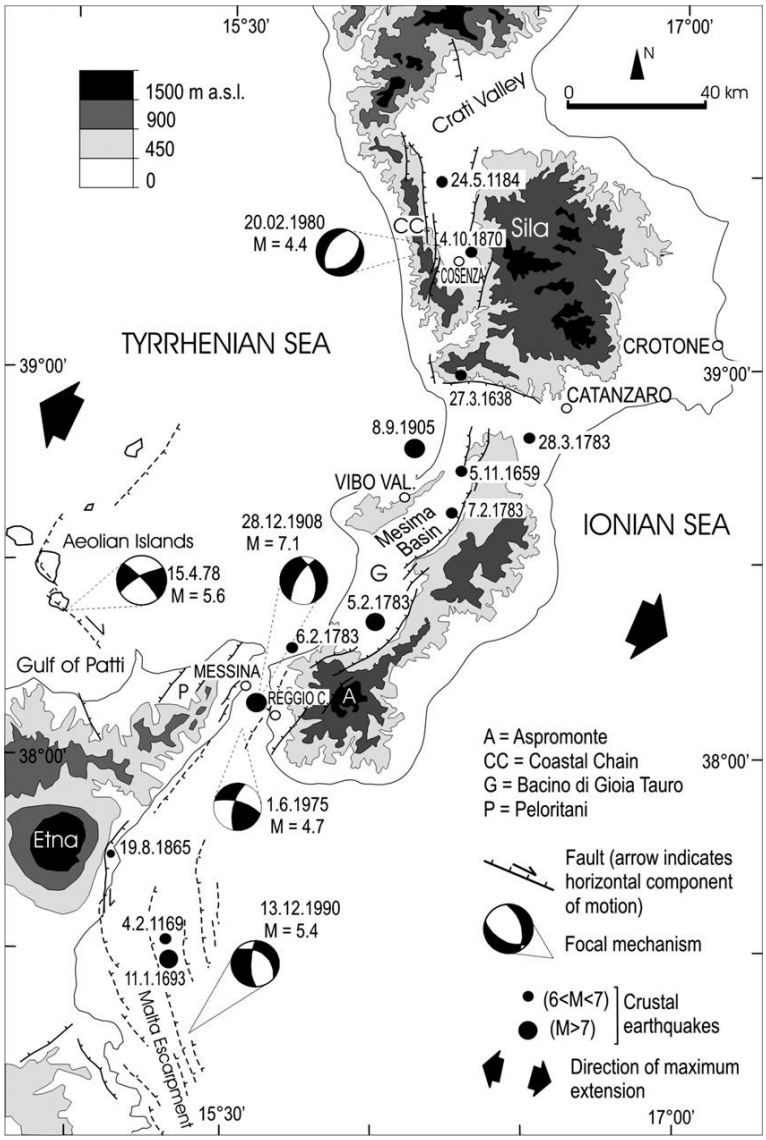

Figure 6.2 Calabrian-Sicilian rift-zone (Monaco and Tortorici, 2000, modified). Crustal earthquakes (depth < 35 km) since 1000 a.d. are also shown (Postpischl, 1985; Boschi et al., 1995).

During Late Pliocene-Early Quaternary, several fault systems have developed along the Calabrian Arc. These fault systems are the results of an intense uplift to which the Calabria Region has been subject.

According to Ghisetti (1979), these fault systems caused the fragmentation of the Calabrian Arc into nine zones: (1) Paola and Gioia Tauro peri-Tyrrhenian basins; (2) Pollino Massif, Coastal Chain, Capo Vaticano and Mt. Peloritani highs; (3) Crati and Mesima basins; (4) Sila, Serre and Aspromonte highs; (5) Crotone-Capo Spartivento peri-Ionian basins; (6) Sibari basin; (7) Catanzaro basin; (8) Siderno basin; (9) Messina basin, Figure 6.3 (A).
Sorriso and Tansi (1996) identified the main regional morphotectonic structures and uplift rate in Calabria during the Quaternary Era. The different uplift rate caused a continuous increase in slope energy with an attendant deepening of drainage lines which preserve a high magnitude of landslides movements and erosional process, Figure 6.3(B).

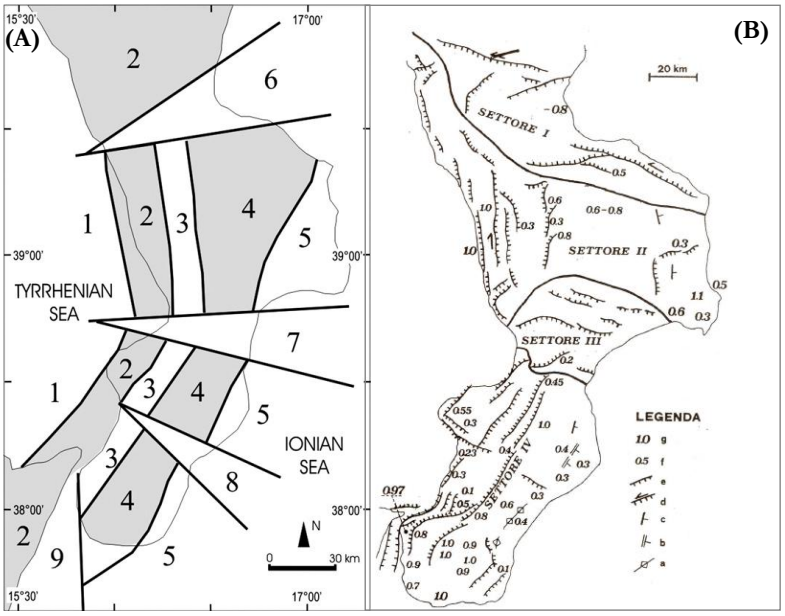

Figure 6.3 (A) Late Pliocene-Early Quaternary block-segmentation of the Calabrian Arc (Ghisetti, 1979, modified). Black lines indicate the main faults. (B) main morpho-neotectonic structures and uplift rate in Calabria during the Quaternary. Legend: g) and f) average uplift rate during 1my and 40 ky-125 ky. e), d), c), b), a) main structural features.

Figure 6.3 (B) shows four morphotectonic sectors. Sector I is characterised by left-lateral strike-slip faults which have been active since middle Pleistocene and which, taken together, constitute the Pollino Line

(Monaco and Tansi 1992). The uplift rate over the last 0.7 MY is of about 1 mm/y for higher blocks, while a subsiding area has been identified in the Crati Basin. (Sorriso and Tansi 1996).
Sector II coincides with the horst-graben system of the Coastal Chain-Sila Massif, characterised by predominantly N-S faults. The maximum uplift rates in this sector in the last MY were of about 1 mm/y affecting the Coastal Chain, while the maximum uplift rate in the Sila Massif was 0.8 mm/y. In the Crati graben, an uplift rate of 0.3 mm/y has been estimated, while in the Crotone area, the maximum uplift rate has been 1.1 mm/y in the last 120 ky.
Sector III corresponds to the Catanzaro graben and is characterised by individual faults with an average direction N 110°-120°. The north side of the graben is characterised by the important Lamezia-Catanzaro fault, while its southern side by the Maida-Girifalco-Squillace fault line. An 0.2 mm/y uplift rate has been calculated for the Catanzaro graben.
Sector IV is characterised by a series of faults with a NE-SW direction which uplifts the Serre-Aspromonte highs. Here the tectonic uplift is particularly complex. A maximum uplift of 1 mm/y both in the last MY and in the last 120 ky has been recorded. A 1.1 mm/y in the Gioa Tauro Plain is particularly significant; the maximum uplift for Mount Porro is also worth noting, which amounts to 0.55 mm/y and has been even greater in the last MY.
From a geological point of view the main outcropping lithotypes identify by (Sorriso-Valvo and Tansi 1996), at regional scale, are: limestone and dolomites, medium and high acid metamorphic rocks, acid intrusive Paleozoic rocks, cemented detritic sediments, mainly clastic sedimentary rocks (siltstone and mudstone), medium and low grade metamorphic ophiolites, pelitic sediments with evaporitic layers, from very low to medium metamorphic rocks, flysch and flysch-like soils, Figure 6.4.

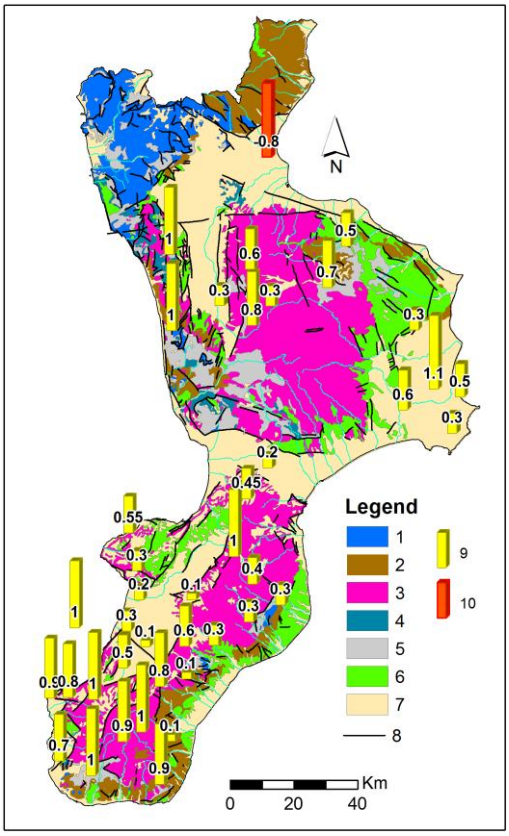

Figure 6.4 Litho-structural map. Legend: 1) Mesozoic–Paleogene carbonatic units of the Appennine Range and Mesozoic rocks cover of Alpine units in south Calabria (limestone and dolomites); 2) Mesozoic and Tertiary flysh–type sequences (flysch and flysch-like soils); 3) Paleozoic medium- to high-grade metamorphic and intrusive rocks of the Alpine units derived from continental crust (gneiss and granitoid rocks); Paleozoic and Mesozoic very low to low-grade metamorphic rocks at places with ophiolites, 4) ophiolitic rocks, 5) low grade metamorphic rocks (schist and phyllite); 6) pelitic sediments with evaporitic layers (Miocene); 7) sandstone, sand and clay (Pliocene-Quaternary) (Sorriso-Valvo and Tansi 1996 mod.)

6.2 GEOMORPHOLOGICAL SETTING OF THE CALABRIA REGION

The Pollino Massif constitutes the northern boundary of Calabria. The Massif's highest peaks are 2250 m high and the massif goes from East to

West, forming a continuum from the Ionian to the Tyrrhenian sea. The morphology of the region presents very steep slopes and deep fluvial incisions with gorges and canyons. A carsic morphology predominates in these areas. On the Ionian side, along a N-S-oriented zone, the morphology presents arenites and argillites with several landslides and gravitational slidings which can be quite deep at times.
South of Pollino, the Coastal Chain, the Crati basin and the Sila Massif morphological systems can be found. The first constitutes a wide mountain system which is fairly young from a tectonic evolutionary point of view. Its morphology is very rocky and presents very steep slopes which become hilly only at its basement.
On the coast, typical terraces and characteristic alluvial fans can be found (Sorriso-Valvo and Sylvester 1993).
The Crati basin, which goes from Cosenza to the Plain of Sibari, is an asymmetric graben with several faults at its border, some of which are still active. It is filled with Plio-Quaternary sediments (Lanzafame and Tortorici, 1981). This area is morphologically hilly and is characterised by a dense fluvial system whose main basin is that of the Crati river. Alluvial fans and marine and continental deposits are typical of this area, while on the side of the Sila Massif several landslides affecting quaternary sands and deeply degraded crystalline rock-based soils can be observed. (Cascini et al., 1992).
The Sila is a box-shaped massif characterized by a plateau standing at an average altitude of 1200 m a.s.l., whose highest peak is M. Botte Donato at 1930 m.
At the toe of Sila massif the Catanzaro Graben can be found, while the souther part of the Region includes the Serre–Aspromonte system N-S oriented.

6.3 THE CATANZARO GRABEN AND THE CROTONE STUDY AREA

The study area at small scale Figure 6.5 is represented by the Catanzaro Graben where sedimentary deposits (sandstones and clays) prevail and are systematically affected by shallow landslides along the slopes. These deposits are post-orogenic soils which have formed after the

development of the Calabrian Arc in a predominantly distensive tectonic regime.
The study area has a total surface of 2000 Km^2, 58% of which is flat, 42% is hilly and the highest altitude is below 600 m, with peaks of 900 m only at the boundaries of the test area (which are not included in the study). The latter falls between the Sector II and Sector III.

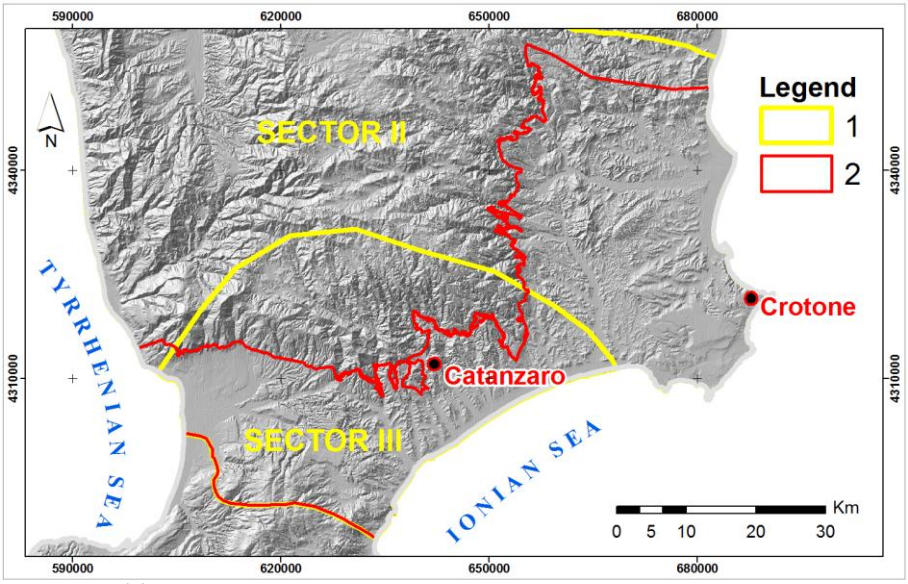

Figure 6.5 The test area at 1:100,000 scale. Legend: (1) area test, (2) morpho-tectonic sectors.

The boundaries of the Crotone Basin are represented by two major NW trending left-lateral shear zones, the Rossano–San Nicola shear zone (north) and the Petilia–Sosti shear zone (south) Figure 6.6 (Van Dijk, 2000).
The stratigraphy of the Crotone Basin was described by Van Dijk (1990), Zecchin et al. (2004). Three main tectonostratigraphic units are recognizable: a Serravallian to Early Messinian unit, a Middle Messinian to Lower Pliocene unit, and a Middle Pliocene to Pleistocene unit (Zecchin et al., 2004).

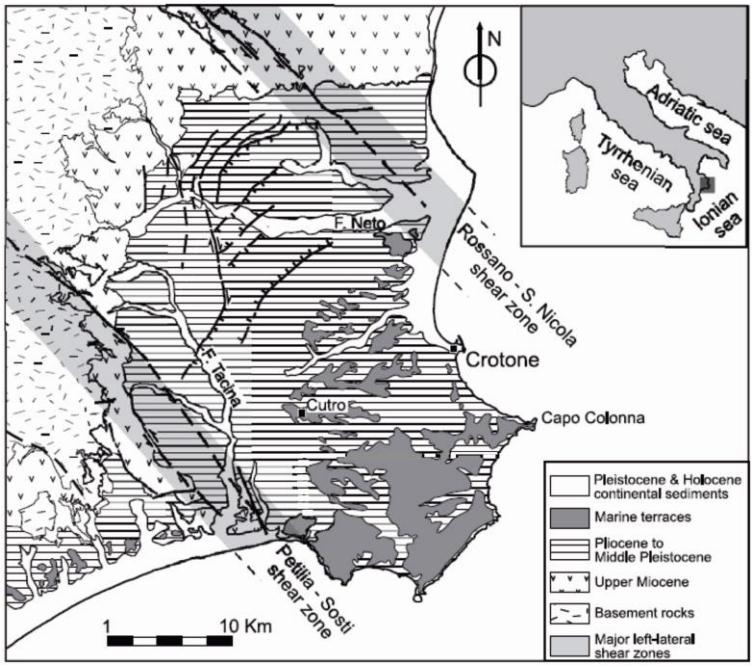

Figure 6.6 Geological sketch-map of Crotone Basin with location of the study area. The two NW-trending shear zones that bound the basin should be noted (Massari et al., 2002).

The Catanzaro Graben is a Plio-Holocene tectonic depression, filled by marine and continental clastic deposits, and structured by NW-SE trending normal left lateral faults (Van Dijk et al., 2000). These two fault systems are known as the "Lamezia-Catanzaro", and the "Maida-Girifalco-Squillace",
On its northern and southern sides, the graben is bounded by paleozoic crystalline-metamorphic rocks of the Sila and Serre horsts respectively, Figure 6.7.

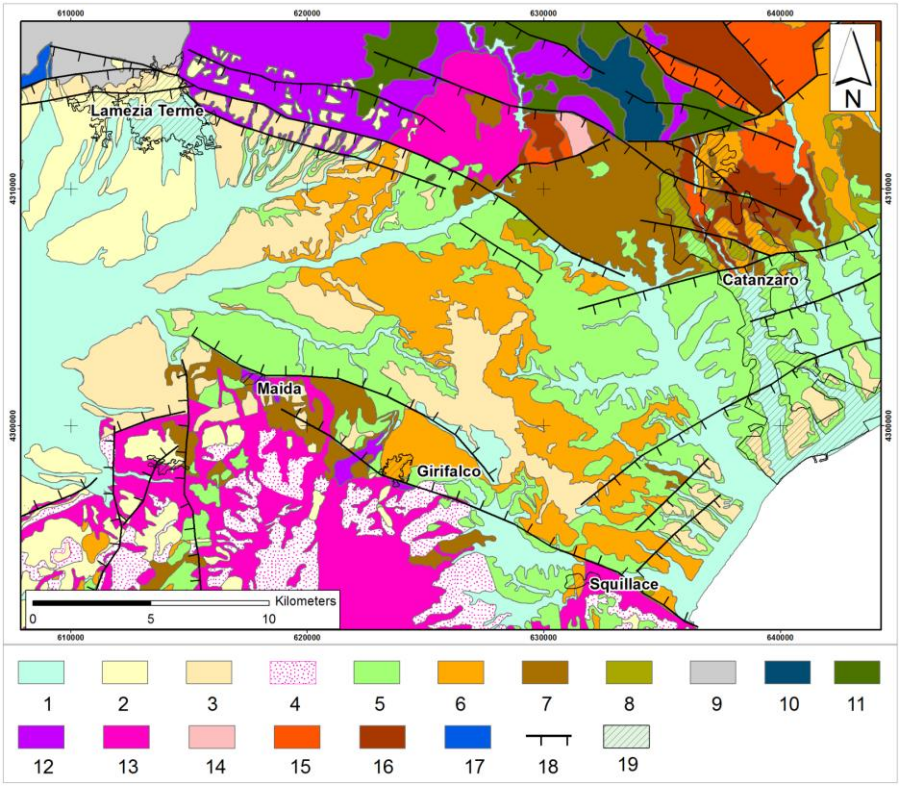

Figure 6.7 Litho-structural and mass movements map of Catanzaro Graben, 1:50,000 scale. Legend: 1) alluvial deposits, landslides deposits, dunes and eolian sand (Olocene); 2) continental terraced deposits (Pleistocene); 3) marine terraced deposits (Pleistocene); 4) weathering cover (Pleistocene); 5) clayey deposits (late Miocene- middle-late Pliocene); 6) sandy and sandstone deposits (Late Miocene-middle-late Pliocene); 7) conglomeratic deposits (Late Miocene-middle-late Pliocene); 8) bioclastic and evaporitic rocks (Late Miocene); 9) Frido Units (Late Cretaceous): metamorphic rocks (facies HP-LT) of oceanic basins; 10) Gimigliano Units (Jurassic–early Cretaceous): Ophiolithic rocks with sediments of Frido unit; 11) Bagni Unit (Paleozoico): medium grade metamorphic rocks; 12) Castagna Units (Paleozoico): gneiss, paragneiss, biotite-gneiss, micascisti; 13) Polia-Copanello units (Paleozoico): gneiss kinzigitici; 14) Stilo Units: cover (Late Triassico-Cretaceo); 15) Stilo Units: granitoid basement (Paleozoico); 16) Stilo Units: metamorphic basement; 17) Panormidi Unit (Triassico): carbonatic rocks; 18) normal fault; 19) residential area (Antronico et al. 2001 mod.).

6.4 SMALL SCALE ANALYSIS OF THE STUDY AREA

As it has been underlined in the previous chapters, due to their morphometric characteristics, shallow landslides at 1:100,000 scale can be only represented by means of dots with attributed characteristics. Therefore, small scale analysis can be only performed to identify potential correlations between Calabria's complex geological history and the areas which are generally affected by the landslides under investigation. To this aim, the principal lithological, stratigraphic and tectonic factors governing the overall morphological evolution of the region are analysed in Phase I via an heuristic approach that interprets, processes and examines the basic geological data. These factors are quantified in Phase II by means of a quantitative map combination. The input data and the results obtained through these studies are summarized in the following sections.

6.4.1 Phase I

The input data in Phase I are the PAI landslide inventory map of the residential areas affected by instabilities at 1:10,000 scale, the regional geological map at 1:25,000 scale (CASMEZ, 1967), the structural geological map at 1:100,000 scale proposed by Van Dijk, the fluvial system map derived from the topographical map at 1:100,000:

The PAI landslide inventory map of the residential areas affected by instabilities at scale 1:10,000 is the only official document available for the entire study area. Due to their size, at small scale the landslides are schematized through dots, Figure 6.8

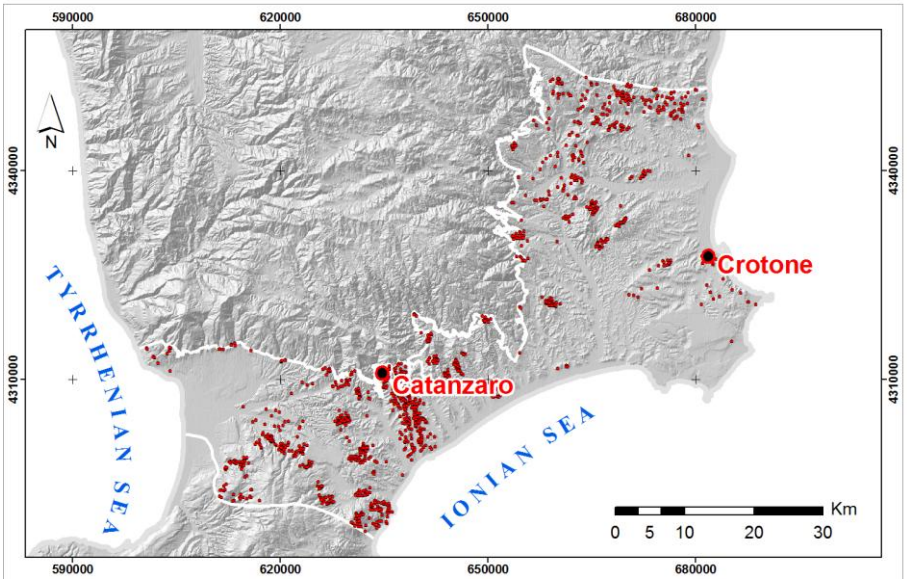

Figure 6.8 Landslides inventory map at 1:100,000 scale.

The regional geological map at scale 1:25,000 (CASMEZ, 1967), of which two excerpts are shown in Figure 6.9 was used as a starting point to develop a new lithological map, Figure 6.10, in which several stratigraphic and tectonic-stratigraphic outcropping units are grouped on the basis of the lithological types.

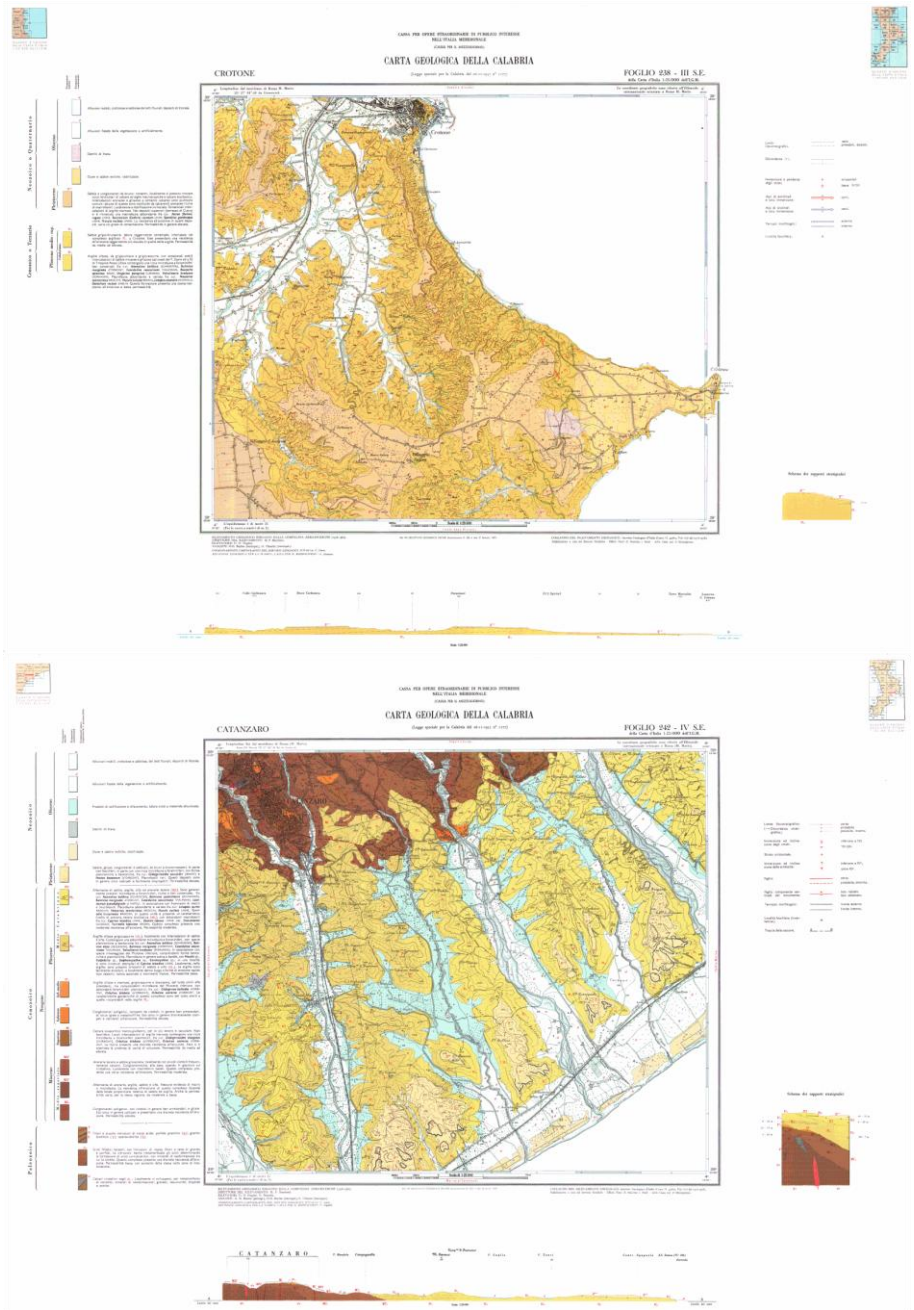

Figure 6.9 Two examples of the regional geological map. (A) Crotone Basin and (B) Catanzaro Graben.

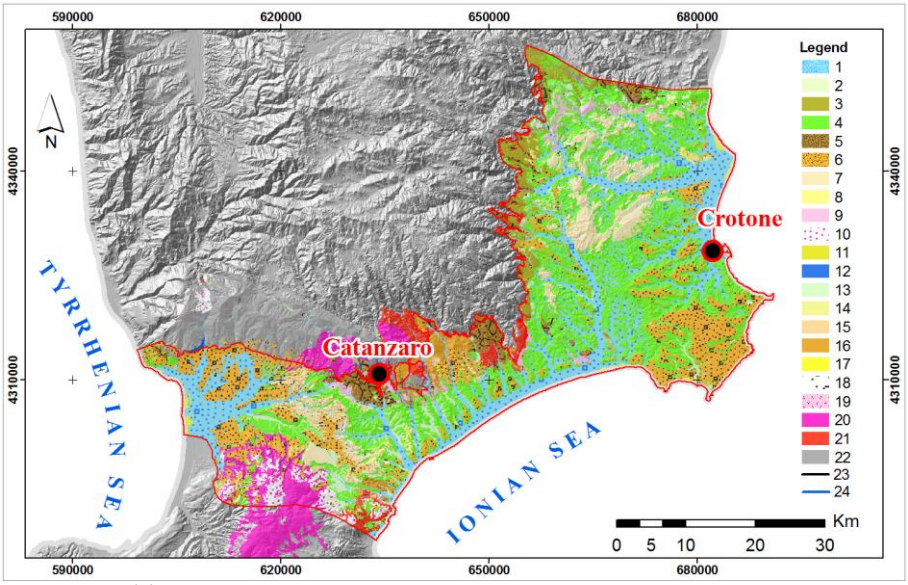

Figure 6.10 The Lithological map of the test area. (1) gravel deposits (2) sand and gravel deposits (3) sandstone deposits (4) clay and silt deposits (5) conglomeratic deposits (6) conglomeratic and sand deposits (7) sandstones and sand deposits (8) sand and clay deposits (9) evaporitic and bioclastic rocks (10) residual soils (11) limestones (12) limestone and dolomites (13) colluvial soils (14) fine-grained soils (15) corse-grained soils (16) sandstones deposits (17) sand deposits (18) landslides debris (19) gypsum (20) gneiss (21) granitoid rocks (22) schists.

The lithological map groups physically and mechanically homogeneous lithostratigraphic units thus allowing to identify 22 different lithotypes in the study area.

The analysis of the lithological map shows the presence in the study area of a Palaeozoic crystalline basement mainly constituted by outcropping gneiss, schists and granitoids at the foot of the Sila and the Serre Massifs. Along the pediment linking the Sila Massif and the sedimentary basins of the Catanzaro Graben and the Crotone area, discordant sedimentary Miocene rocks, which are made up of a succession of conglomerites, arenites and evaporitic limestone, unconformably lies Palaeozoic crystalline basement. Upwards, the Miocene succession becomes a Plio-Pleistocene post-orogenic sedimentary succession composed of marine deposits originally coming from the Catanzaro and Crotone basins. Specifically, in their lower part, these lithotypes consist of thick clay deposits (about 800 m for the Catanzaro basin and 1200 m for the

Crotone one, Appendix A AGIP boreholes, Fig. A.1, A2) which in their higher parts turn into mainly sand deposits dating back to the Lower Pleistocene.
Mainly sand and gravel terraced deposits can be found at the end of the succession, which are well preserved in the area of Crotone, become sporadic in the transitional area between Crotone basin and the Catanzaro one, and then reappear in the form of preserved terraces in the central part of the Catanzaro graben area.

The structural geological map developed by Van Dyjk (1991); Figure 6.11, shows an initial fault system with a NW-SE direction characterises the northern and southern boundaries of the study area. Such faults delimit the tectonic depression of Catanzaro Graben. A second fault system NE-SW located at the Amato basin predominates in the transition area between the Catanzaro and Crotone basins, where a series of terraced faults dipping towards the Ionian Sea. In the same area, a local horst is present, delimited by two shear zones which isolate, identify and preserve the structural high of Isola Capo Rizzuto. Such a structure highlights how the uplift and the related evolution of the slopes in the Catanzaro area have occurred and continue to occur at different velocities.

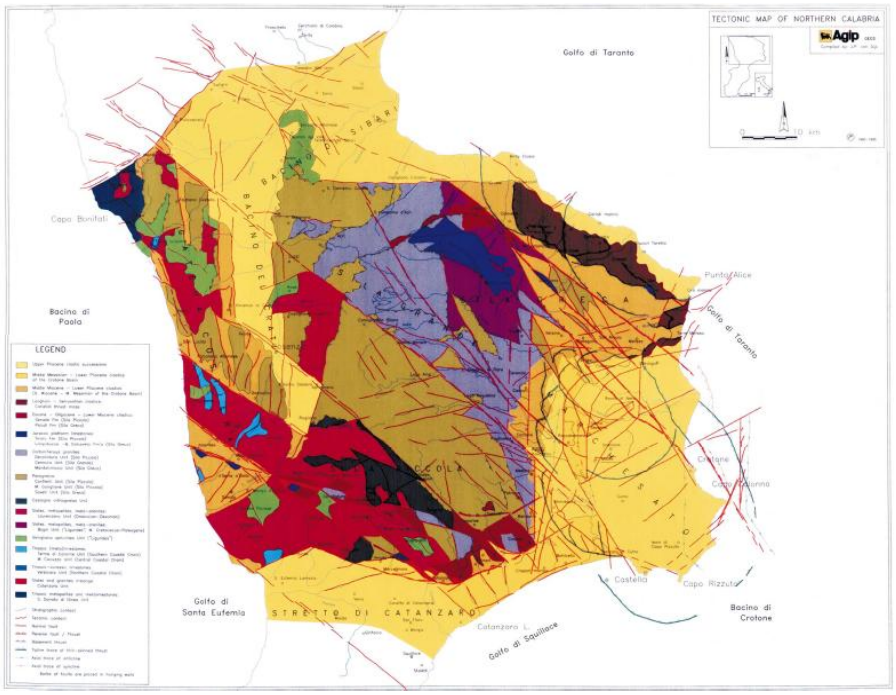

Figure 6.11 Schematic tectonic map of Northern Calabria (Van Dijk 2000).

The fluvial system map highlights the fluvial system originated as a results of the different uplifts in the study area, together with the outcropping lithotypes and their stratigraphic and tectonic characteristics. Such a system is influenced by the local horst in the Crotone area, and by the Sila and Serre horsts in the Catanzaro graben; the rivers with the highest gradient are present in the area located between Catanzaro and Crotone which directly flow into the Ionian Sea (Sellia Marina area), Figure 6.12.

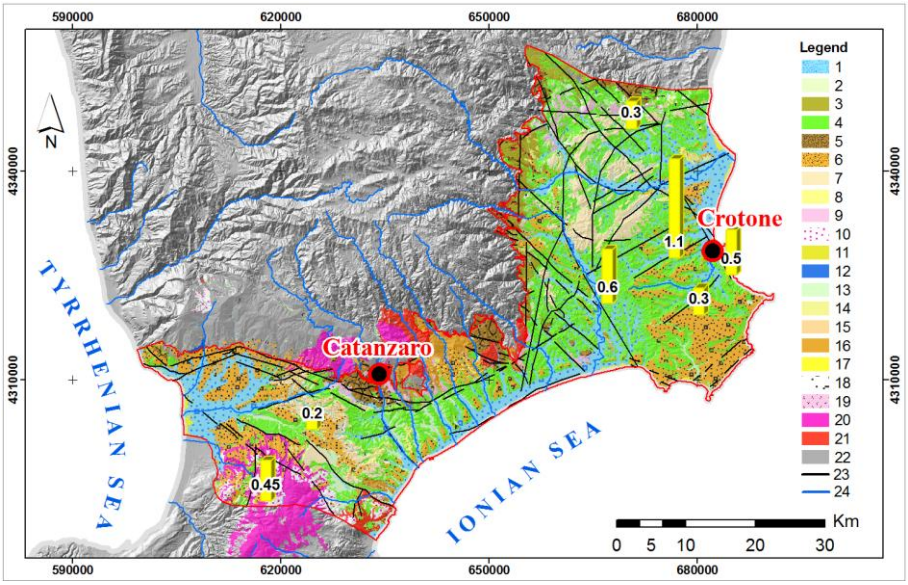

Figure 6.12 Main drainage line at 1:100,000 scale. Legend: from 1) to 22) see legend Figure 6.11, 23) main faults, 24) drainage lines.

The information so far analysed, gathered from an in-depth analysis and re-interpretation of the main basic data available, allows to identify three sub-zones A1, A2 and A3 within the test area, Figure 6.13.
Sub-zone A1 falls within the graben, it includes a portion of territory whose northern and southern boundaries are the Sila Horst and the Serre Horst respectively. The N-W boundary of sub-zones A2 borders the Sila Horst, while its S-E boundary is the sea and is constituted by a series of dipping faults. Finally, sub-zones A3 is bound by the Sila Horst to N-W and by the local Crotone horst to S-E.

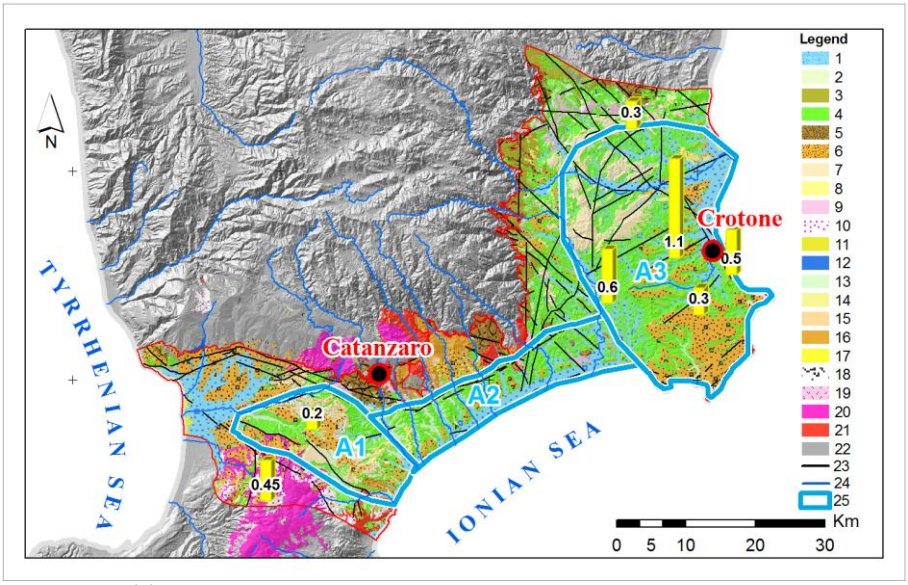

Figure 6.13 The sub-sectors A1, A2 and A3. Legend: from 1) to 24) see legend Figure 6.12, 25) the sub-sectors.

In order to investigate the relationship between landsliding and the geological evolution of the three sectors in Figure 6.13, a landslide density map has been created by cross-referencing the information gathered from the PAI landslide inventory. This map has been realized though a radial basis method for interpolation proposed by Chapman and Hall (1986), and currently implemented by the ArcGis software, Figure 6.14

The figure clearly highlights that the area mostly affected by landslides is the one between sectors A1 and A2, even though it does not provide any information on the role played by each of the three factors on landsliding. The quantitative determination of these roles is the main goal of the Phase II analysis, which is described in the following section.

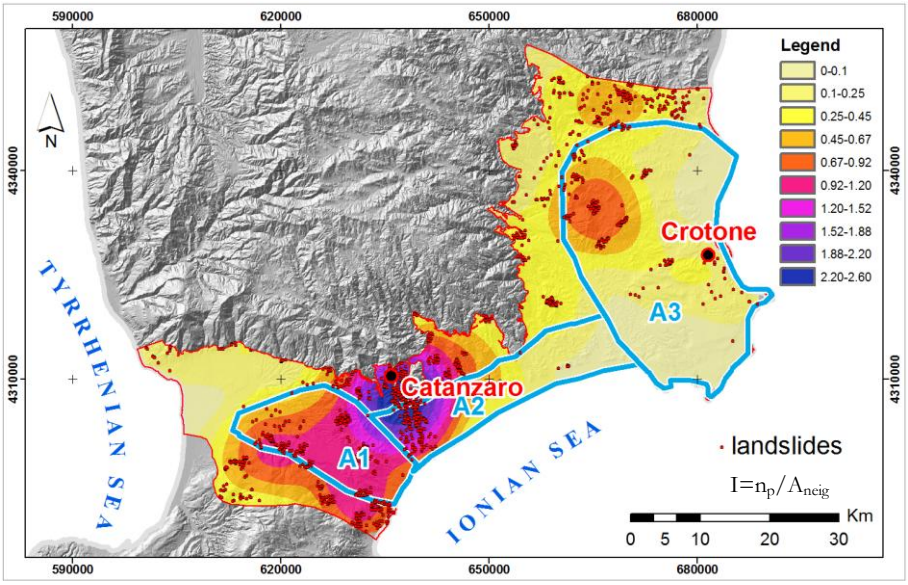

Figure 6.14 Landslide density map. I= landslides index, n_p=number of points, A_{neig}= neighbor area. In legend: the number of shallow landslides per square kilometer.

6.4.2 Phase II

The quantification of the role that each of the predisposing factors plays on the overall evolution of the area at a very small scale for such small landslides can be pursued through a series of procedures universally adopted to analyse landslide susceptibility and hazard zoning, such as the qualitative map combination which allows to overcome the problem of the "hidden rules" in geomorphic mapping.

Experts in the field use their experience to assign certain weights to the different themes, each of them regarded as representative of a factor predisposing the overall evolution of the area. The sum of the weights given to each predisposing factor allows the quantification of the same factors by means of numerical values. These factors can be subsequently grouped into different landslide classes, Figure 6.15.

The availability of GIS systems further simplifies the proposed procedure and speeds up the repetitive calculations necessary for the combination of a great variety of maps and of the attributes to be taken into account. The user of this system can test the significance of each

parametric map and decide on the final input maps in an iterative way. (Soeter and van Westen 1996).
Following Soeter and van Westan (1996), the GIS procedure used in the analysis can be summarized as follows:

- Classification of each map into a number of relevant classes;
- Combination of the selected parametric maps with the inventory map through a map crossing process in order to produce a cross-tabulation through the definition of the spatial correlations between the parametric maps and the inventory map;
- Calculation of weighted values based on Cross-tabulation data;
- Definition of weighted values to the various parametric maps or otherwise identification of decisional rules to be applied to the maps in order to produce a classification of the results obtained into susceptibility classes.

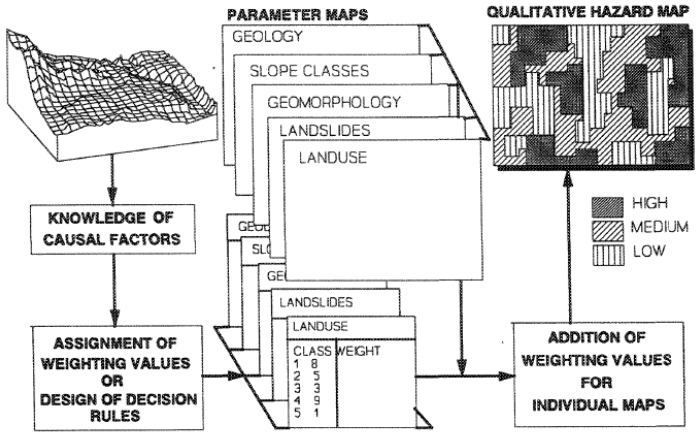

Figure 6.15 Quantitative map combination.

One of the main difficulties in the application of quantitative map combination lies in the definition of the weights that have to be assigned to each theme taken into consideration, which necessarily has to go hand in hand with a knowledge of a good landslides inventory.
The PAI inventory available for the Calabria region has been compiled for residential areas and small villages with more than 200 inhabitants, therefore underestimating the areas affected by landslides. Despite the lack of input data, the results obtained in Phase I have enabled to choose

those weights that could better express the overall level of landslide susceptibility of the area. Within this context, the literature available on the subject of small scale landslide susceptibility zoning has been used to single out a reference work. This work had to satisfy two applicability criteria at the same time: (i) use of an inventory map of the whole area at medium scale; (ii) analysis carried out in a similar geological context and representative of the case study.
The work by Del Monte et al. 1996 satisfies both criteria starting from a landslide inventory at scale 1:5000 on the Trionto basin, Figure 6.16(A), which presents a stratigraphic succession characterized by clay comparable to those in the Catanzaro and the Crotone areas, Figure 6.16 (B).

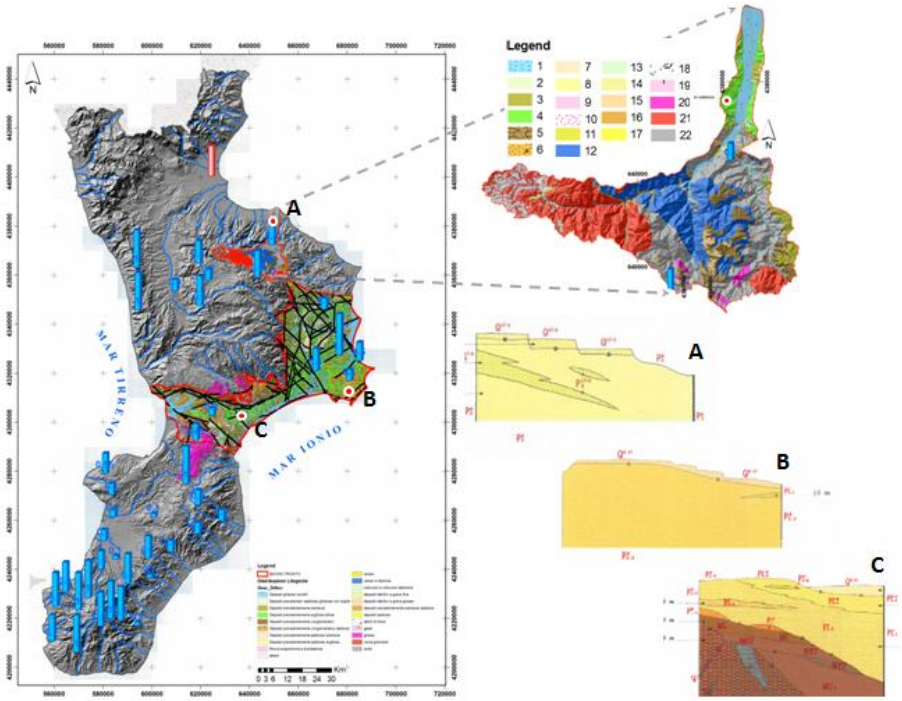

Figure 6.16 Trionto basin. Legend: from 1) to 22) see legend Figure 6.12, A), B), C) Soil stratigraphy.

Once the criteria of applicability have been tested, the predisposing factors identified by Del Monte et al., 2002 and the attendant weighted values have been used. These authors identify four predisposing factors in relation to the evolution of mass movements only: lithology, slope,

drainage density and soil use. They assign a different weight to each factor on the basis of the percentage of the area affected by mass movements. They identify six lithological classes assigning a minimum weighted value to alluvial deposits and the maximum one to clay. They also identify five slope classes assigning maximum weight to those slope classes with a gradient higher than 20°, and five classes of drainage density (the total length of all the streams and rivers in a drainage basin divided for the total area of the drainage basin) assigning maximum value to those basins with a drainage density between 2 and 4, Table 6.1.

Table 6.1 Weights used by Del Monte et al. 2002

Lithologies	**W**
Alluvial deposits	1
Clay	37
Sand, gravel and conglomerates	8
Grey limestone, marl and sandstone	15
Phyllite, micashist and gneiss	16
Granite and granodiorite	3
Slope gradient	**W**
0<S≤10	5
10<S≤20	5
20<S≤30	12
30<S≤40	12
S>45	14
Drainage density	**W**
0<D≤2	0
2<D≤4	27
4<D≤6	17
6<D≤8	7
D>8	7

Soil use has not been taken into account as a predisposing factor since, given the scale of analysis 1:100,000 and the objectives that can be pursued at this scale, it is considered marginal compared to the other factors previously mentioned. By contrast, the weight of the relative uplift rate is paramount insofar as the role of the dynamics of the slope evolution has been pointed out in Phase I analysis. The criterion chosen for associating weights to the factor taken into consideration lies in the difference between the mean uplift rates. Within this purview, three classes of analysis are defined Du=0, Du=0.2 e Du=0.6, typical of the three sectors identified (A1, A2, A3).

In Figure 6.17, the themes used and divided into classes of associated weights are shown.
The weights thus identified have been added up in order to produce a map of the morphological evolution of the test area, Figure 6.18.

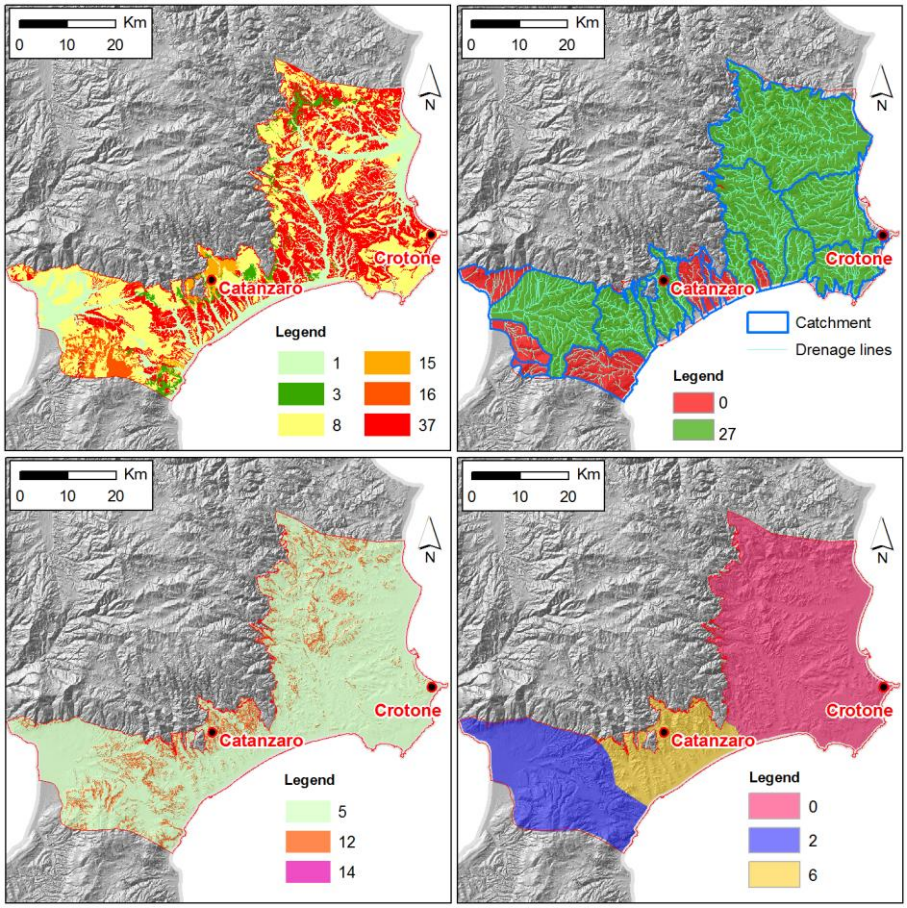

Figure 6.17 (a) lithology, (b) drainage density, (c) slope, (d) differential uplift.

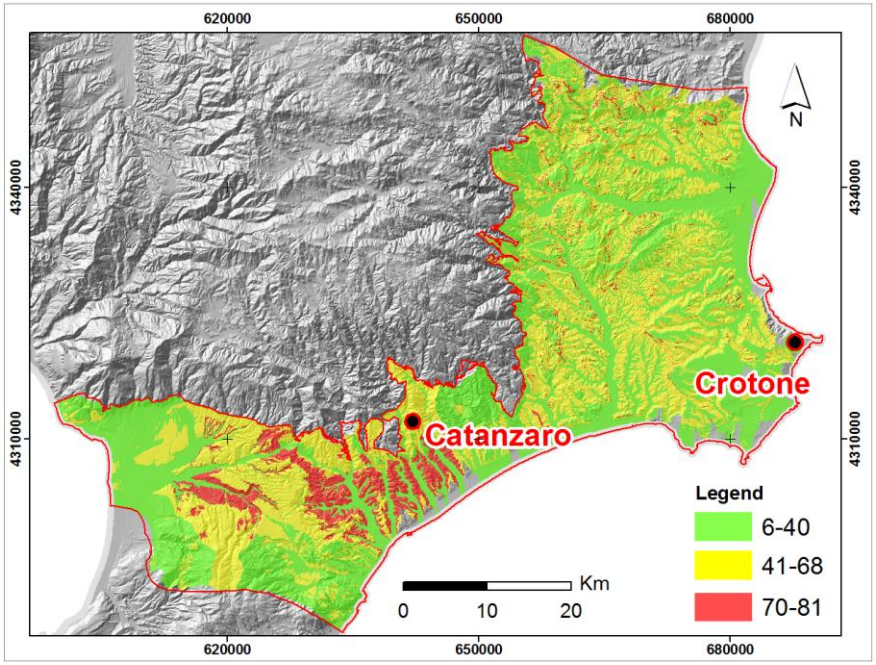

Figure 6.18 Geo-morphological evolution map.

Figure 6.18 highlights that the zone with the greatest evolution (in red in the Figure) is the one located near the city of Catanzaro in which clays predominate. This zone is characterized by basins with a drainage density between 2 and 4 and highly affected by the uplift of the Sila Massif.
The greatest limit of quantitative map combination resides in the arbitrariness with which the weights are assigned. However, by following the procedure proposed here, this model tends to be less influenced by the subjectivity of the field expert assigning the weights, since the same weights identified by other authors have been used in a different area.
To sum up, the results of the analysis demonstrate that, within a very wide area (about 2000 Km^2), the adopted method automatically identifies a section of the area (150 km^2) which is smaller but with a more rapid morphological evolution that is essentially related to the differential uplifts produced by an active tectonics; the prevalent lithotypes; and the characteristics of the fluvial system.

7 MEDIUM SCALE ANALYSIS

On the basis of the general framework proposed for the present work, the analysis at medium scale (1:25,000) follows the one carried out at small scale which, at the end of Phase II, quantifies the predisposing factors of shallow landslides in both the Catanzaro graben and the Crotone basin. The methodological approach proposed generally at medium scale consists of the identification and quantification of the factors predisposing the evolution of the reliefs in fine-grained soils.
For this purpose, Phase I of the analysis focuses on the identification of the predisposing factors on the basis of geological and geomorphological input data together with the necessary information deriving at this scale from the landslide inventory.
Phase II should quantify the landslides predisposing factors individuated at the end of the Phase I analysis and this goal can be pursued by applying statistical methods, for instance multivariate analysis, which are commonly used at medium scale. Given that this goal requires relevant efforts beyond the scope of the present thesis, in the following section only Phase I will be analyzed and discussed.

7.1 PHASE I: TEST AREA AND INPUT DATA

The test area at medium scale is located within the widest area analyzed at small scale. It has an overall surface of 150 km^2, borders the Sila Massif to the north, the Serre Massif to the south-west and the Ionian Sea to the south-east (Fig. 7.1).

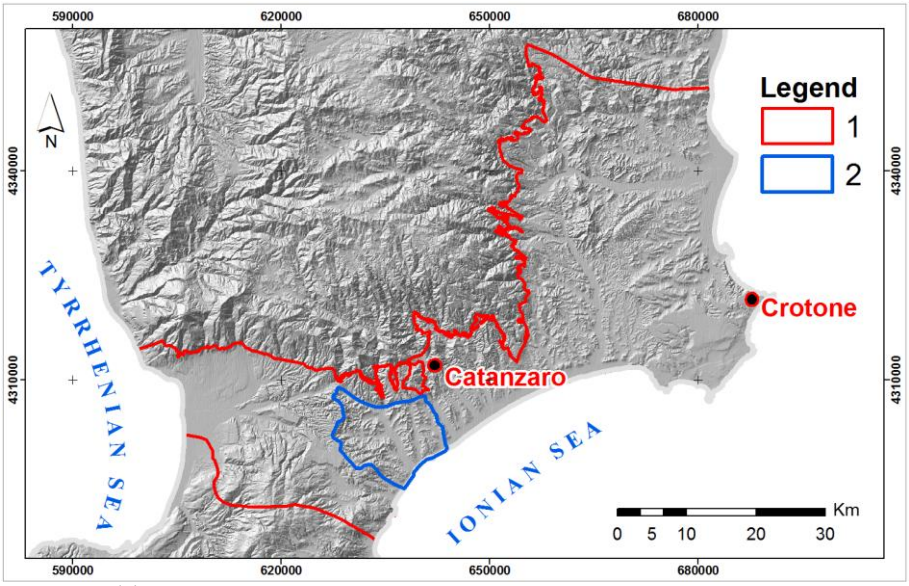

Figure 7.1 Test area at 1:25,000 scale. Legend: (1) test area at 1:100,000 scale, (2) test area at 1:25,000 scale.

Within this area, the analyses are performed on the basis of the following themes:

- Geology and tectonics (at scales 1:50,000 and 1:25,000);
- Landslides inventory maps(a scale 1:10,000);
- 20m x 20m cells DTM.

The input data for these issues and the subsequent elaborations developed to reach the fixed goal are introduced and discussed in the following sections.

7.1.1 Geology and tectonic

A thorough investigation of geological and tectonic aspects has been carried out starting from the map of the lithological structure and of the mass movements in the Catanzaro Graben area (scale 1:50,000), (Antronico et al, 2001), Figure 7.2.
Further information on the geological features of the area have been taken from the Geological Map of Calabria (scale 1:25,000) (table 242).

Within this basic reference framework, geological details on the lithological, structural and morphological features of the study area have been acquired through photo interpretation validated by subsequent specific surveys in situ. The main characteristics of all these maps are now summarized.

The Map of the lithological structure and of the mass movements in the Catanzaro Graben area (scale 1:50.000)

Generally, along the northern boundary of the graben (that of the "Lamezia-Catanzaro" fault corresponding to the southern slopes of the Sila massif) the map shows some outcropping crystalline rocks belonging to the Cretaceous-Paleogenic Alpine Chain unit, mainly composed of phyllite, schists, gneiss (Frido unit, Gimigliano unit, Bagni unit, Polia Copanello unit, Castagna unit and Stilo unit). On top of these crystalline rocks, some High Miocene trasgressive deposits principally composed of conglomerates, evaporites and bioclasts can be found (Amodio-Morelli et al., 1976).

In the central section of the Catanzaro graben, post-orogenic Plio-Pleistocenic deposits outcrop, mainly constituted by silt, marl and sand clays, sand and sandstone and Pleistocenic terraced deposits, the latter mainly composed of sandy gravel Figure 7.2. The Olocenic alluvial deposits of the Amato river, of the Corace river and their affluents occupy a large portion of the study area Figure7.2.

The southern section of the Stretta di Catanzaro area corresponds to the northern side of the Serre massif horst, where Palaeozoic crystalline rocks outcrop, mainly represented by medium and high metamorphic gneiss, which belong to the Castagna and Polia-Copanello Units (Amodio-Morelli et al., 1976), Figure 7.2.

The southern border of the Catanzaro graben is structurally less articulated that the northern border, since it is delimited by WNW-ESE direction dipping towards NNE "Maida-Girifalco.Squillace" fault, Figure 7.2. This structure is responsible for the uplift of the Palaeozoic metamorphic rocks of the Polia-Copanello and Castagna units, as opposed to the Tortonian-Quaternary depositional sediments of the Catanzaro Graben.

Right to the south of this fault, the predominant systems are the extensional faults belonging to the fault system N-S - NNE-SSO, which are the most recent tectonic elements, Figure 7.2.

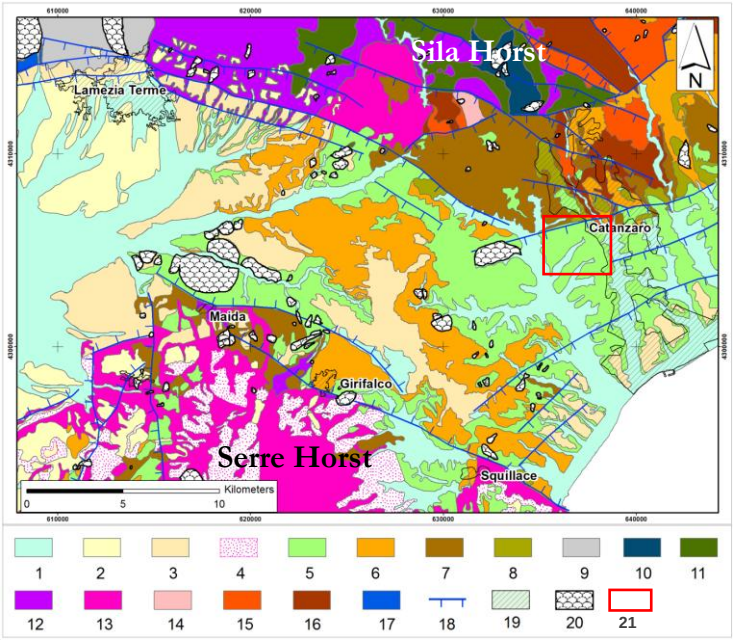

Figure 7.2 Litho-structural and mass movements map of Catanzaro Graben, 1:50,000 scale. Legend: 1) alluvial deposits, landslides deposits, dunes and eolian sand (Olocene); 2) continental terraced deposits (Pleistocene); 3) marine terraced deposits (Pleistocene); 4) weathering cover (Pleistocene); 5) clayey deposits (late Miocene- middle-late Pliocene); 6) sandy and sandstone deposits (Late Miocene-middle-late Pliocene); 7) conglomeratic deposits (Late Miocene-middle-late Pliocene); 8) bioclastic and evaporitic rocks (Late Miocene); 9) Frido Units (Late Cretaceous): metamorphic rocks (facies HP-LT) of oceanic basins; 10) Gimigliano Units (Jurassic–early Cretaceous): Ophiolithic rocks with sediments of Frido unit; 11) Bagni Unit (Paleozoico): medium grade metamorphic rocks; 12) Castagna Units (Paleozoico): gneiss, paragneiss, biotite-gneiss , micascisti; 13) Polia-Copanello units (Paleozoico): gneiss kinzigitici; 14) Stilo Units: cover (Late Triassico-Cretaceo); 15) Stilo Units: granitoid basement (Paleozoico); 16) Stilo Units: metamorphic basement; 17) Panormidi Unit (Triassico): carbonatic rocks; 18) normal fault; 19) residential area; 20) Landslides; 21) Van Dijk study area (from Antronico et al. 2001 mod.).

With regard to the structural complexity of the northern section of the graben, Van Dijk and Okkes (1991) reconstructs at a greater scale (1:20,000) a geological section which is particularly representative of the overall structural context: this section allows to distinguish clearly the tectonic contacts between chain units and post-orogenic sediments, Figure7.3.

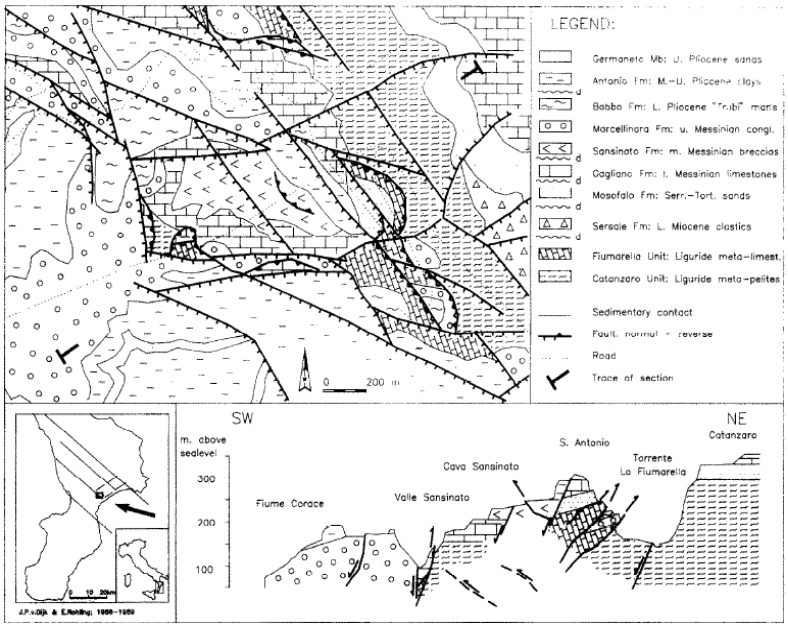

Figure 7.3 Geological map and structural section of the Catanzaro area in the central part of Calabria (Van Dijk and Okkes, 1991).

All these faults refer to a left-lateral strike-slip faults that has locally given rise to traspressional and trastensional regimes. Such a fault system can be associated to a deep transform fault dividing southern Calabria more or less at the level of the Catanzaro graben. Such a fault, called the Catanzaro fault, is well known in the seaside area, where it has been revealed by deep reflection seismic (Finetti and Del Ben, 1986).
The seismic highlights a very recent incision due to regional uplift which has begun in High Miocene which involved the Miocene and Pliocene levels. This uplift caused the formation of a submarine canyon located near the Corace fault (Fig. 7.4).

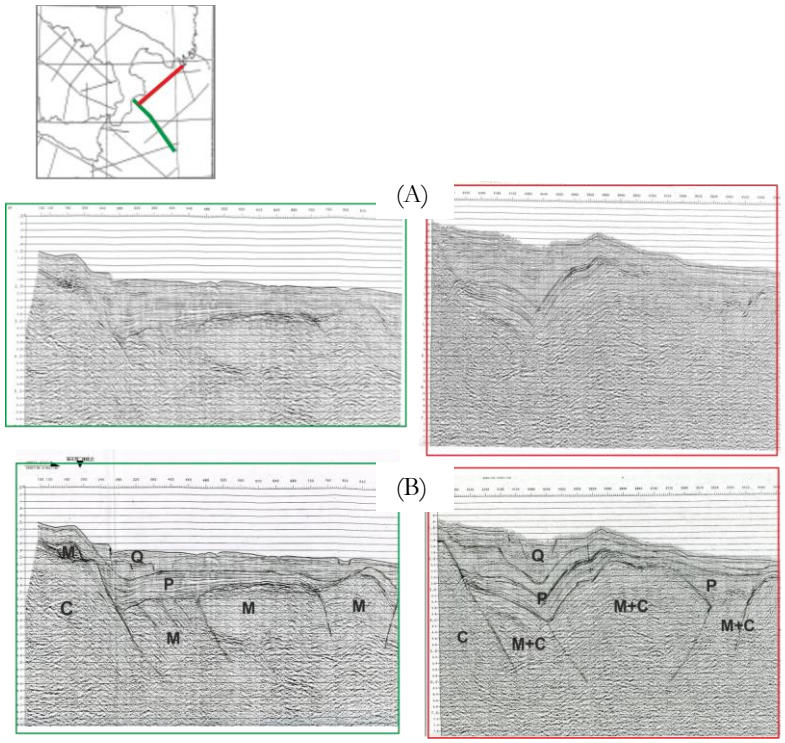

Figure 7.4 Deep reflection seismic (AGIP). Legend: A) original data, B) re-elaborated data: C (Crystalline), M (Miocene); P (Pliocene); Q (Quaternary).

7.1.1.1 The Geological Map of Calabria region (scale 1:25,000)

Within such a well-defined geological context, the analysis at scale 1:25,000 has redefined the lithological contacts between the main outcropping lithologies evidencing the significant presence of Miocenic marine deposits such as polygenic conglomerates, sandstone, clays, sands and silts, arenites and sandstone, yellow-white evaporitic limestone. In the central section, Pliocene clastic marine deposits can be found: among these are polygenic conglomerates, light blue-grey silty and marl clays from the Lower Middle Pleistocene and the Middle-Calabrian, sands, silts, clays and sandstone. Finally in the southern section, the predominant formations date back to the Pleistocene: sand, gravel, brown and red-brown conglomerates.

Along the main rivers and flat areas fluvial deposits with gravel and gravelly sands, eluvial and colluvial deposits, dunes and eolian sand are

predominant. This map also provides information on where significant landslide deposits can be found in some areas, Figure 6.9 (B).

7.1.1.2 New elements for the morphological and lithological structure of the study area *(1:25,000).*

The lithological information and the structural elements available in the geological map at 1:25,000 scale have been verified and updated using aerial photo interpretation and in situ investigations.
With reference to the lithological information, the adopted procedure allowed to redraw the contours of the main lithologies. In particular, light blue-grey silty clays were found at the bottom of the sedimentary succession (Pa_{2-3}), with intercalations of sands and silts (Ps_{2-3}). Towards the top of the succession an alternation of sands, clays, silts and soft sandstone are found (Ps-a_{2-3}). Towards the top, the Ps-a_{2-3} turn into sand, gravel, brown and red-brown conglomerates (Q s-cl).
With reference to macro-structural aspects, new elements have been acquired through the interpretation of aerial photo images available at scale 1:33,000 (1991, black-and-white IGM flight) that allowed to identify some relevant structural elements in the study area (Panizza, 1992; Burbank and Anderson, 2001). The resulting profile confirms the structural complexity already highlighted by Van Dijk and Okkes (1991) (Figure 7.3), and reveals the presence of normal faults with a NW-SE, direction linked to the tectonic system of the Catanzaro graben, overlapping with faults with a NE-SW direction, Figure 7.5.
Specifically, in Figure 7.5, a series of structures with a NE-SW are arranged into a stepwise system mainly dipping toward SE. Also, the fault of the Corace river is present, which has a NW-SE direction and is presumably the continuation of the Catanzaro-Lamezia master fault.

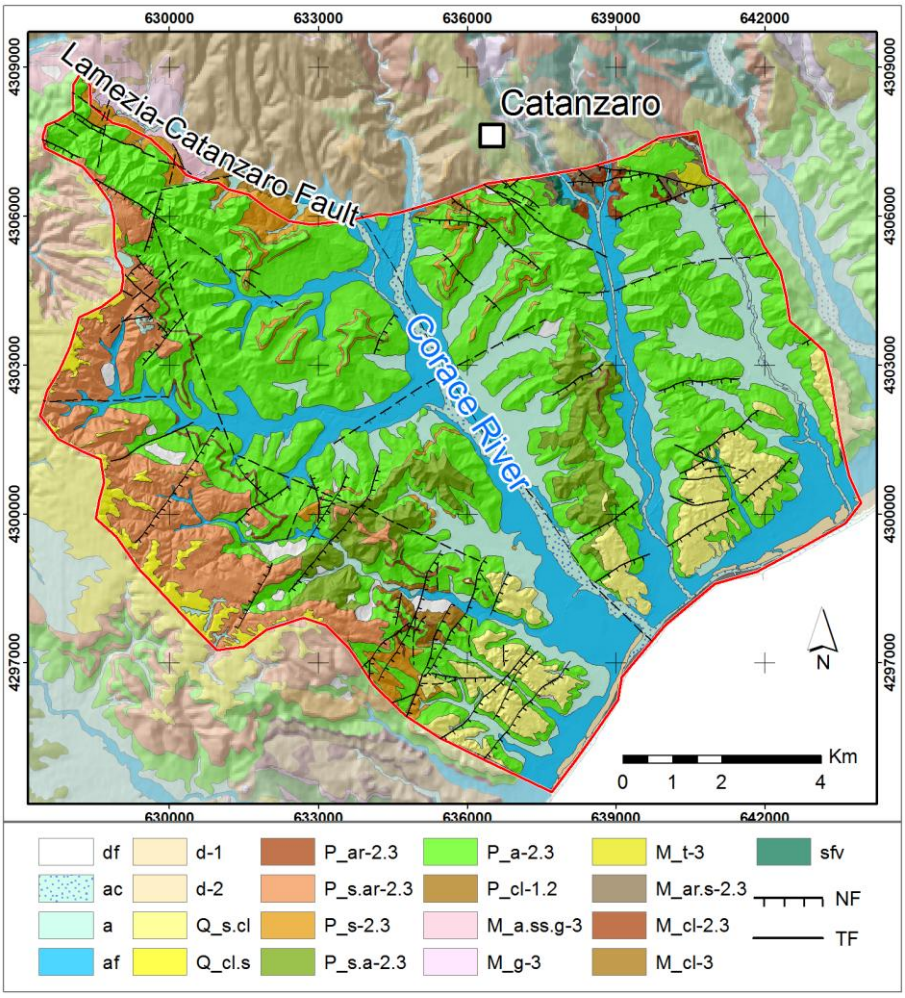

Figure 7.5 Geological map of the test area. Legend: df) landslides debris; ac) alluvial deposits; a) colluvial deposits; af) old alluvial deposits; d-1) and d-2) aeolian sands and sand dunes; Q_s.cl and Q_cl.s) quaternary sands, gravels, brown and red-brown conglomerates; P_ar-2.3) Pliocene sandstones; P_s.ar-2.3) Pliocene sands and sandstones; P_s-2.3) Pliocene sands and silts; P_s.a-2.3) Pliocene sands, clays, silts and soft sandstones; P_a-2.3) Pliocene light blue-grey silty clays; P_cl-1.2) Pliocene conglomerates; M_a.ss.g) and M_g-3) Miocene evaporitic marls and gypsum; M_t-3) Miocene evaporitic limestones; M_ar.s-2.3) Miocene sandstones and sands; M_cl-2.3) and M-cl-3) Miocene conglomerates; sfv) Paleozoic schists and phillytes; NF) normal fault TF) fault with undetermined kinematics.

7.1.2 Landslides inventory map (scale 1:10,000)

The PAI inventory map already introduced in chapter 6, Figure 7.6, essentially refers to residential areas and small villages with more than 200 inhabitants. From a technical point of view, it distinguishes between mappable and unmappable landslides, depending on the latter's dimensions. Mappable landslides are represented by polygons whose shapes are well defined but do not show reference to their morphological features. By contrast, unmappable landslides are indicated by means of symbols and indicated as "unstable areas" (deep-seated landslide area, DLA, and shallow landslide area, SLA). Finally in those areas notoriously affected by shallow landslides, a distinction is made between *creep zones* (CZ) and *deep erosional zones* (DEI).

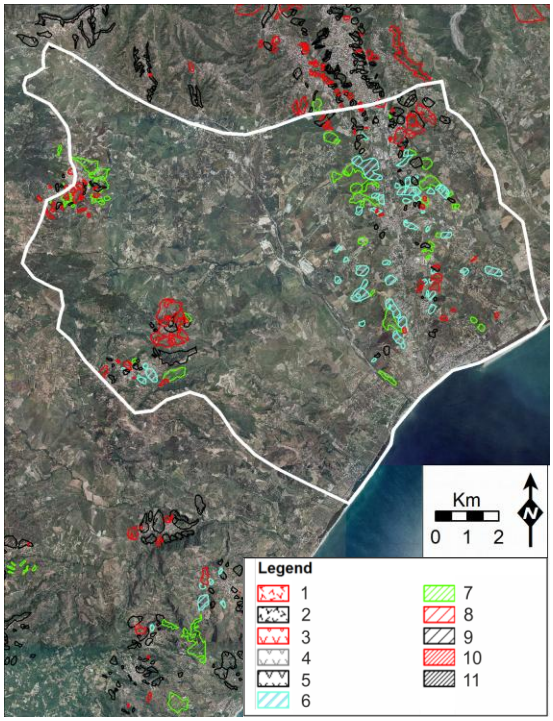

Figure 7.6 PAI landslides inventory map. Legend: 1) active complex landslide; 2) dormant complex landslide; 3) active slide; 4) inactive slide; 5) dormant slide; 6) shallow slow moving deformation; 7) area of intense erosion; 8) active deep landslide zone; 9) dormant deep landslide zone; 10) active shallow landslide zone; 11) dormant shallow landslide zone.

Given the limits of the PAI landslides inventory, which only provides data for urbanized areas, and the need for an inventory covering the entire test area, a new landslide inventory map was created first using the aerial images at scale1:33,000. The aerial photos interpretation allows to identify the typical diagnostic elements (scarp, landslide body and debris accumulation zone) of large size landslides (Gullà et al, 2008), while it does not provide any information on shallow landslides since they were not present in 1991 at the time of the IGN flight.
In order to map these shallow landslides, which are the focus of this work, the images dating back to 2010 available on Google Earth have been used. These images allows mapping, with a good accuracy the boundaries of shallow landslide areas occurred during the winters of 2008-2009 and 2009-2010, Figure 7.7.

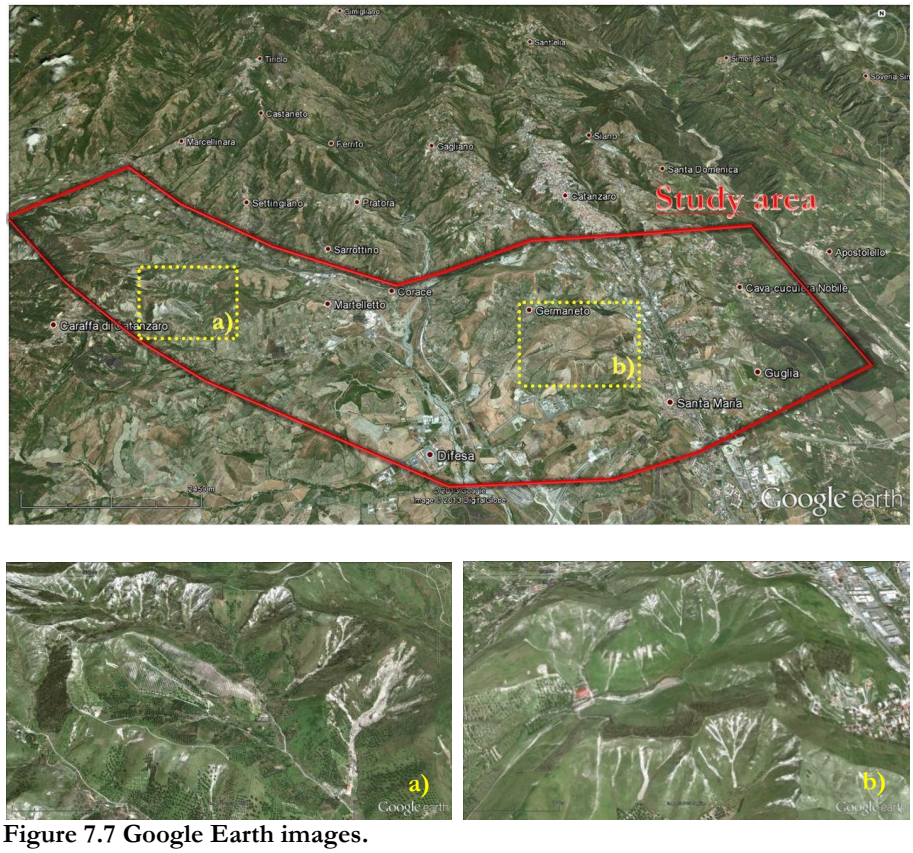

Figure 7.7 Google Earth images.

The landslides inventory, obtained using the two procedures Figure 7.8, highlights that: i) both large and shallow landslides prevalently occur at the northern border of the area, at the foot of the Sila massif where clay deposits are predominant and ii) shallow landslides mostly occur within well-defined morphological hollows. On the contrary, the southern border of the study area, where sands and conglomerates prevail, are essentially affected by large size landslides.

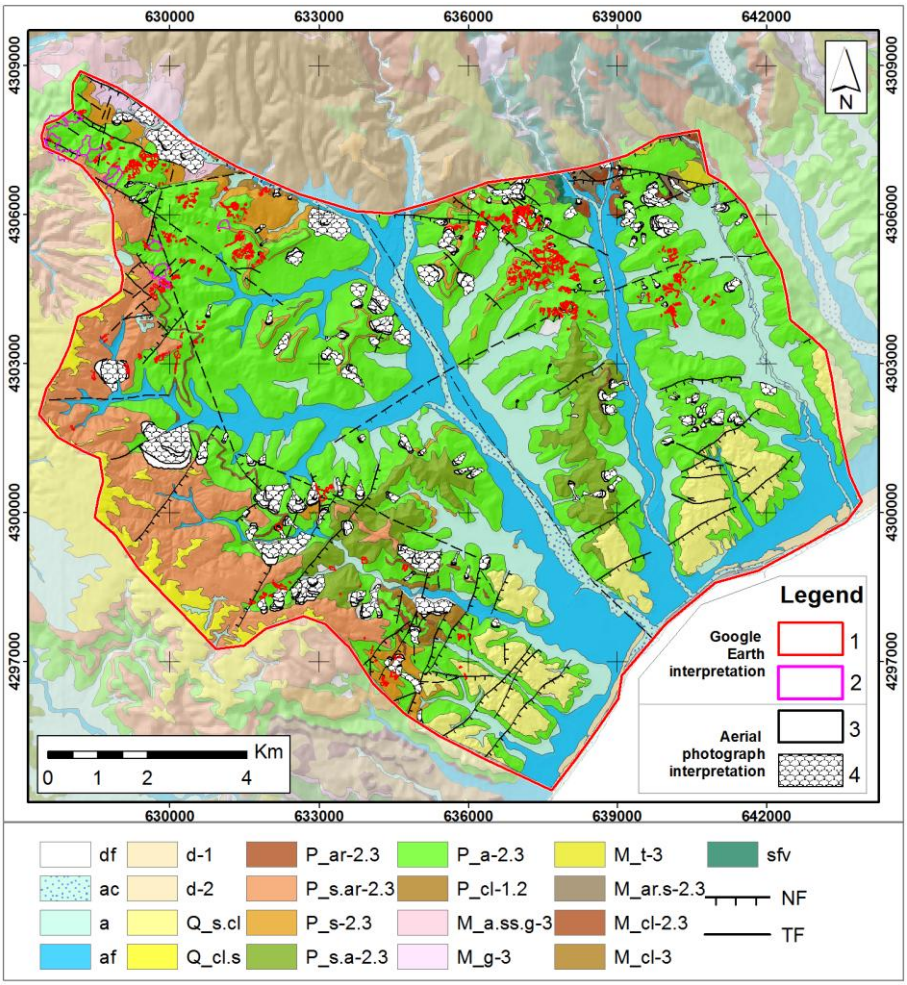

Figure 7.8 Landslides inventory and geological maps of the study area. For the geological legend see Figure 7.5. Landslide inventory legend: 1) shallow landslides, 2) erosional process both visible form google earth; 3) landslides scarp, 4) landslide body both visible from aerial image interpretation.

7.1.3 DTM

This model has been obtained starting from the elevated contour lines on the topographic map available at scale 1:5000 using the triangulation necessary for the realization of TIN (Triangular Irregular Networks). These are a series of triangles which satisfy the Delaunay criterion (each triangle's circumscribing circle contains no points from the dataset in its interior) constituted by elevated vertices or mass points spatially distributed which represent the morphology of a land surface. The higher the triangulation density, the greater the resolution of input data, Figure 7.9. The resulting triangulation has been subsequently transformed into a GRID made up of a series of cells spread over a 20mx20m dimensional plane.
Therefore, this model can be considered accurate at the scale of analysis, following the recommendations given by (Fell et al.„ 2008) who highlight the relationship existing between the scale of analysis and that of the input data. They also underline that the input data at medium scale must possess an accuracy of 1:25,000 or greater.

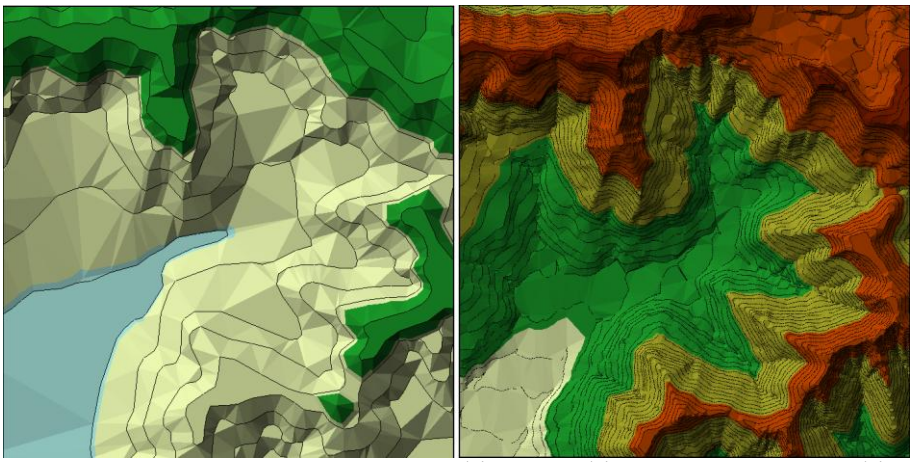

Figure 7.9 Comparison of the different DTMs. A) DTM 25x25 m cells, B) DTM 5x5 m cells.

7.2 LANDSLIDES PREDISPOSING FACTORS AND NEO-TECTONIC EVOLUTION OF THE STUDY AREA.

In order to identify the landslide predisposing factors influenced by the tectonic evolution over the last 5my, a geological map has been created, Figure 7.10, which also records the updated temporal data available in the geological map n 580 "*Soverato*"of the CARG project (CNR, 2012) obtained through in situ surveys at scale 1:25.000, (available on line at: http://www.isprambiente.gov.it/Media/carg/580_SOVERATO/Foglio.html).

The most significant data concerning the activity of tectonic lineations (active faults) delimiting some areas here called morpho-structures (Mescrjakov 1968; Demaugeot, 1973; Ollier,1981, Carraro 1976, Bartolini and Peccerillo 2002, Panizza 2005) are illustrated in the map in Figure 7.10. In the study area, four morpho-structures have been identified, each referring to a single sector of analysis.

Each sector is characterized by two-digit ID codes. The first digit refers to the geological period of surfacing (1= lower Pliocene, 2= lower Pleistocene, 3= Middle Pleistocene), while the second refers to the uplift rate qualitatively defined on the basis of scientific literature.

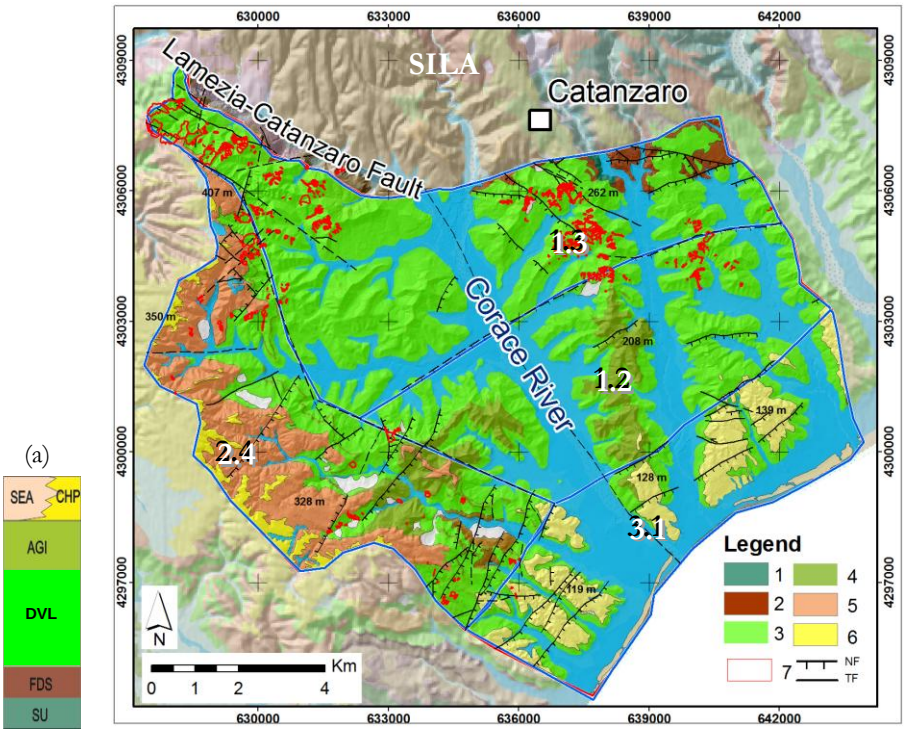

Figure 7.10 Geological map at 1:25,000 scale. 1) Sila Unit (SU): granitoid rocks, phyllites and mica-schists; 2) Messinian evaporitic Unit (FDS); 3) blue-gray clays lower Pliocene-upper Pliocene-Pleistocene (DVL); 4) clay with sand lower Pleistocene (AGI); 5) sand, gravel and conglomerates Middle Pleistocene (SEA); 6) Sand Upper Pliocene (CHT). 7) shallow landslides; NF normal faults, TF strike-slip faults; in withe the ID codes.

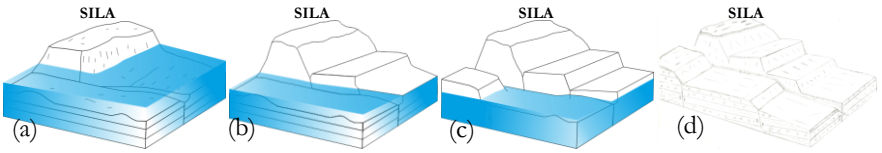

Figure 7.11 Morpho-evolution model.

To interpret more clearly the neo-tectonic evolution of these four sectors, the methodology applied in the Neo-tectonic Project of the Southern Italy (Ciaranfi el al., 1983) is used.
The temporal division in which the neo-tectonic events must be framed has been updated using the time intervals recently adopted in the S. CARG "Soverato", Appendix A (Fig. A.3). The expression 'time

intervals' here refers to the deposition periods elapsed between two greater uplift periods.
Interval I: the upper time limit for this interval date back to 5300 my and corresponds to the Messinian-Zanclean (Upper Miocene-lower Pliocene) period. The study area was completely submerged by the sea, Figure 7.11 a. A connection between the Ionian and the Tyrrhenian Seas took place. The Sila and the Aspromonte horsts were uplifting.
Interval II: dating from 5300 my to 1800 my Zanclean-Gelasian (Pliocene-lower Pleistocene). The uplift of the Sila horst involved the evaporitic soils of the Upper Miocene, the surfacing of subsectors 1.3 and 1.2 occurred with the identification of the watershed between the Ionian and the Tyrrhenian Seas.
During Upper Pliocene (Zanclean), a greater uplift occurred which determined a different evolution in sectors 1.3 and 1.2, with the complete surfacing of blue clays in sector 1.3 (DVL).
The stratigraphic succession of sector 1.3 is reported in Catanzaro borehole (up to a depth of 800 m), performed in 1980 a few kilometers east of the city of Catanzaro in the attempt to find hydrocarbons (Cfr Appendix A, Fig. A1)
At the end of the Lower Pleistocene interval (Gelasian), in the areas near the Ionian coast, marine sediments are mainly influenced by detritic sediments originated by the erosion of the Sila and Serre, as shown in the stratigraphy of sector 2.4 (Figure 7.10 a) in which sand layers outcrop on blue clay.
Interval III: 1.8 - 0.12 ky the uplift of sectors 1.3 and 1.2 continued and sectors 2.4, where gravels and conglomerated prevail, rapidly surfaced.
Interval IV: 0.12ky - to present is a forecast of the Sila and Serre horsts which have reached their current tectonic conditions.
In order to find some relationships, if existing, between landslides and the morphological evolution of the study area, the density index proposed by Coe et al. (2004), has been estimated for the entire area, (Fig. 7.12). The Figure highlights that instability phenomena concentrate within subsectors 1.3 and 2.4, i.e. the sectors located near the Sila and Serre horsts which, for this reason, are characterized by a more intense uplift caused by the various faults systems(N-S, E-W, NW-SE, NE-SW). This uplift, together with the various perpendicular fault systems produced a higher slope energy, a deepening of the stream network and the formation of the hollows, which are the morphological elements where both shallow and deep-seated landslides are more frequent.

$$I_i = \left[\frac{\frac{Area_i(f)}{Area_i}}{\frac{Area\_tot(f)}{Area\_tot}} \right]$$

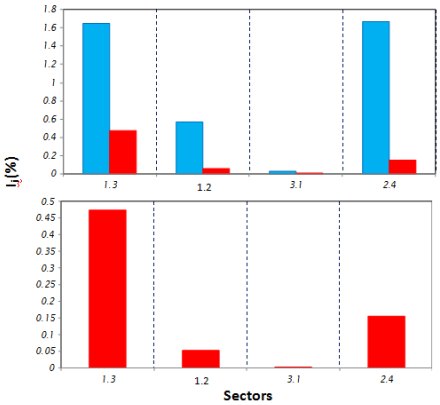

Figure 7.12 Landslides Index. In blue deep seated landslides, in red shallow landslides.

8 SLOPE EVOLUTION MODELS AT LARGE AND DETAILED SCALES

The analysis at medium scale identifies the morphological hollows located at the toe of the Sila massif as the predominant elements in the evolution of the reliefs essentially caused by deep-seated and shallow landslides.
Indeed, the study of the most representative morphological hollows at large and detailed scale is a key factor for a better understanding of the genesis and evolution of shallow landslides.
Following the proposed procedure, the study carried out at these scales has been subdivided into two phases, respectively the identification of the prevailing landslide mechanisms (phase I) and the quantification of these mechanisms through geotechnical engineering analyses (phase II).
Given the importance and complexity of each phase, this chapter initially focuses on phase I and, specifically, on i) the identification of the predisposing and triggering factors of the hollows evolution and on ii) the definition of the triggering mechanisms of shallow landslides that, at this scale, can be identified, mapped and classified. Then, both the predisposing factors and the triggering mechanisms are put in a general reference scheme which is based on the slope evolution models at detailed scale.
The calibration, the validation and the application of the slope evolution model (phase II) will be developed and discussed in chapters 9 and 10.

8.1 EVOLUTION OF THE MORPHOLOGICAL HOLLOWS

The main reasons for high landslide susceptibility of the morphological hollows are an intense tectonic activity and the greatest concentration of elements causing the erosion of the clayey lithotypes, i.e. the prevailing soils along the slopes.
These factors concentrate at the toe of the Sila Massif and, particularly, in two hollows located near the city of Catanzaro in the San'Antonio

area, and near the area where the Magna Graecia University and the University Policlinic are located, Figure8.1.
Both hollows show mainly clayey outcropping deposits locally interrupted by a dense alternation of silts and sands which can even be a few metres thick. The two hollows are lithologically and stratigraphically homogeneous, while they are structurally heterogeneous as a result of a different overall morphological evolution caused by a different distribution of tectonic lineations.
Diffused shallow and deep-seated landslides characterize the hollow in the St. Antonio area, whereas the hollow of Magna Graecia University is essentially affected by shallow landslides, Figure 8.2.

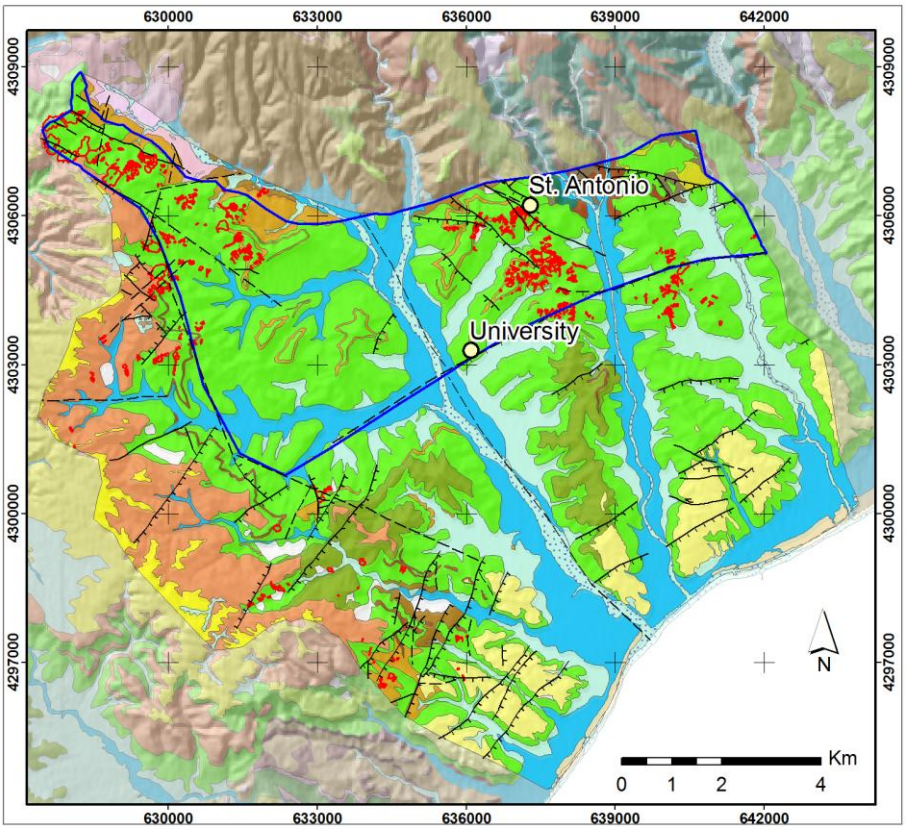

Figure 8.1 St. Antonio and Magna Graecia University areas.

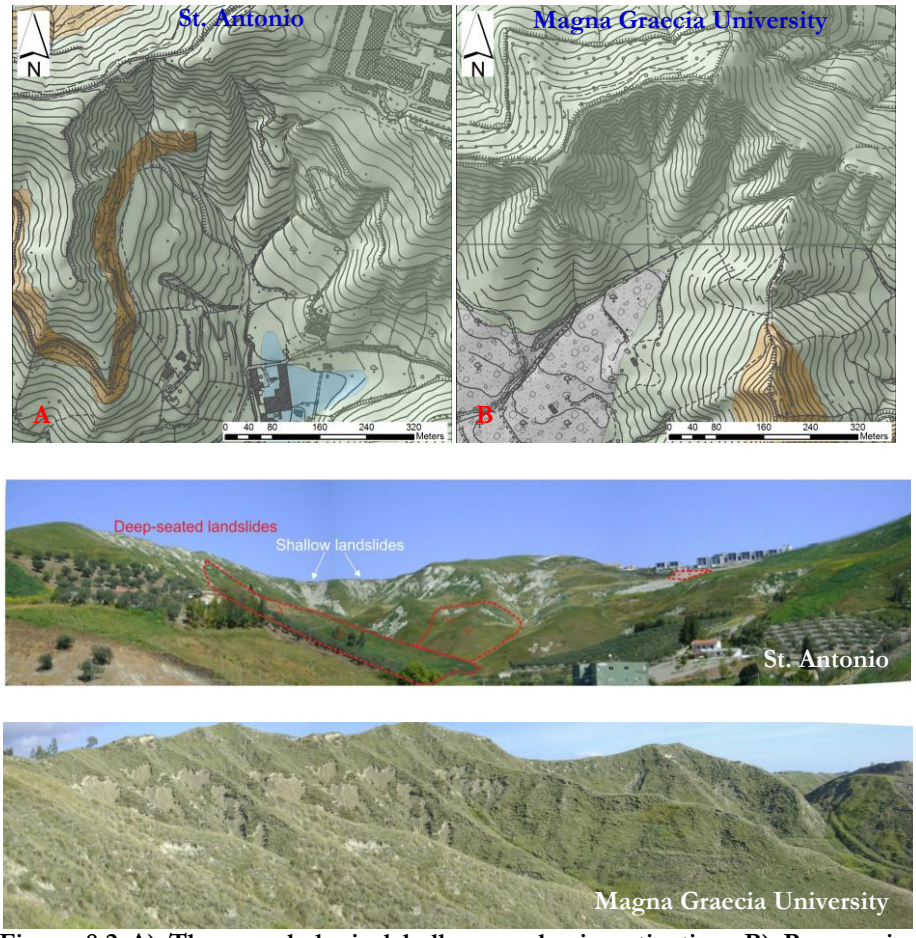

Figure 8.2 A) The morphological hollows under investigation. B) Panoramic photos of St. Antonio and Magna Graecia Univeristy areas.

Only through an accurate analysis of the official documents recording the occurrence of significant phenomena in these two hollows caused by critical rainfall, it was possible to infer that shallow landslides rapidly evolve in space and time. The rapid evolution of landslides makes traditional inventory mapping, generally based on aerial photo-interpretation, difficult.

Such a difficulty can be overcome by using temporally-sequenced images available on Google Earth from 2001 to 2010 (Fig. 8.3). However, these images, due to their low resolution, must be accurately verified trough detailed in situ investigations.

The analysis of the available sequence of images shows that the first landslide event was triggered in 2001 along the upper part of the slopes, near some of the main drainage lines. In 2006, such landslides became more diffused, appearing as new triggers or involving wider sections of the hollows. In 2010, as a result of a more intense rainfall event than those occurred in the previous years, landslides affected the entire hollows including the drainage lines where the runout of the unstable masses can be clearly observed.
Although the resolution of the images is not particularly high, a landslide inventory map can be developed using Google Earth imagery. The temporal sequence of these images shows a very complex evolution process which begins as a single event and subsequently turns into multiple events affecting the entire hollow (Fig. 8.3). Moreover, it can be observed that:

- landslides tend to be quickly hidden by vegetation, as clearly shown by comparing images dating back to 2010 and 2011, in Figure 8.4;

- the main drainage lines – appearing along the principal tectonic lineations (or along their associated deep cracks) and dividing the main hollow into smaller hollows limited by secondary watersheds – play a key role at this scale, and they are also significant at other scales too.

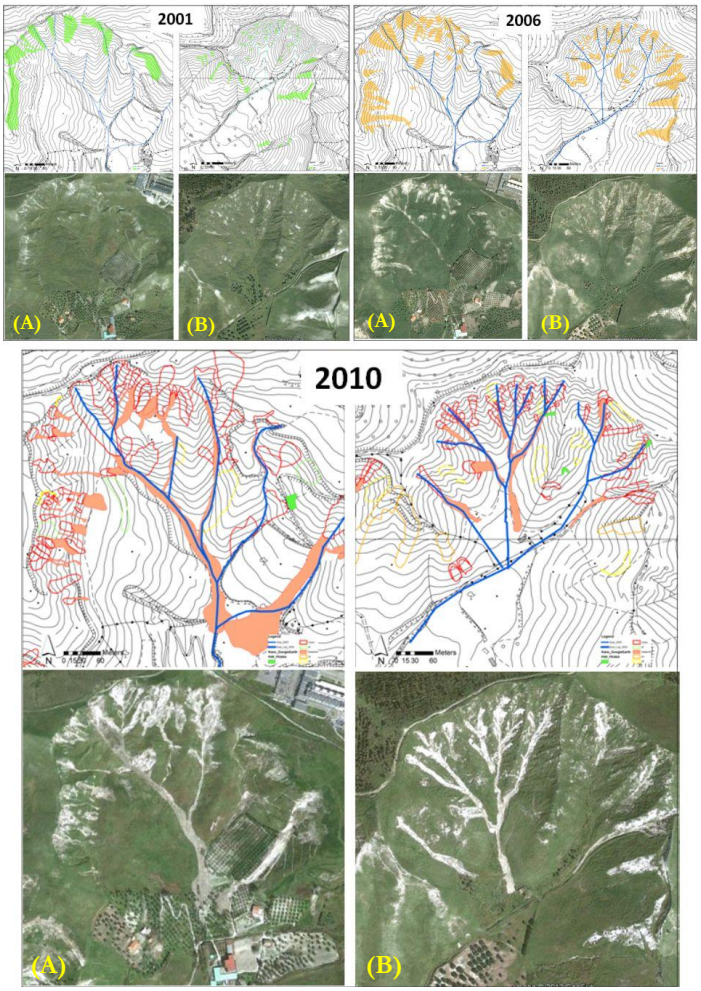

Figure 8.3 Temporal sequence of Google Earth images. A) St. Antonio area, B) Magna Graecia University.

Figure 8.4 Google Earth images of St. Antonio area.

In conclusion, the elements acquired show that the events involving the morphological hollows are very complex events which begin in the drainage lines. In turn, the morphological evolution of the hollows entails the thinning and/or the total dismantling of the secondary ridges that progressively widen the hollows, Figure 8.5.

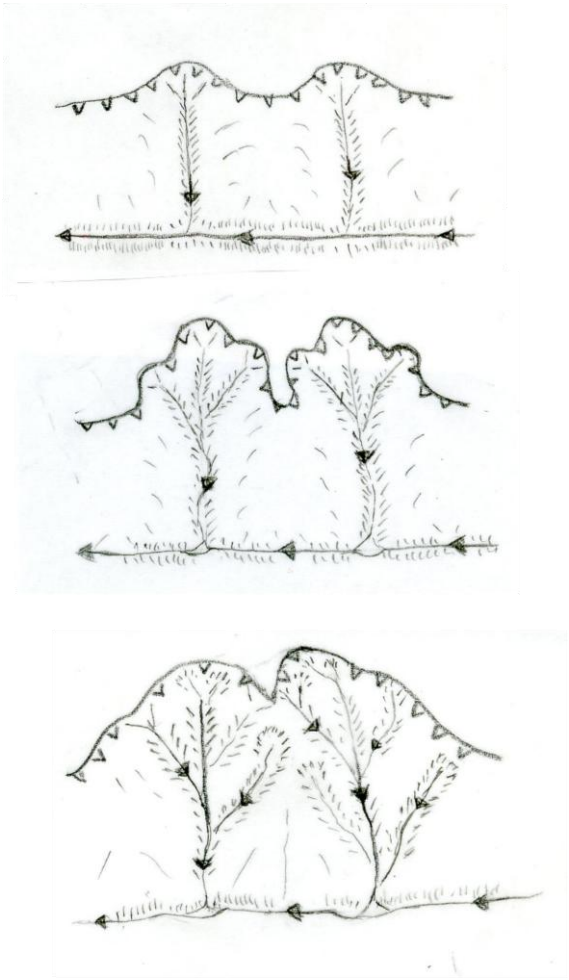

Figure 8.5 Hollows evolution model.

8.2 THE LANDSLIDES CLASSIFICATION AND MECHANISMS

In spite of the complex evolutions of the hollows highlighted in the previous paragraphs, it can be initially observed that the main morphological characteristics of the phenomena occurred can be identified on the basis of the available classification systems. Moreover, considering that they are not randomly located along the slope and that they evolve following a well-defined temporal trend, the shallow landslides in the test area can be described using appropriate slope

evolution models. Therefore, both the classification of these phenomena and their slope evolution models are now going to be introduced and discussed.

8.2.1 Shallow landslides classification

The classification of the phenomena observed in the test area can be obtained by referring to the proposals provided by Varnes (1978) and Leroueil et al. (1996). For this purpose, and focusing only on the event occurred in the winter 2009-2010, the contours identified by means of Google Earth have been verified through in situ surveys for an exact determination of their typical morphological elements. Moreover, available geotechnical data set discussed in detail in the next chapter have been used to provide an exact classification of the materials involved.
According to Varnes (1978), the phenomena investigated can be generally classified as translational and/or complex slides. Following Leroueil et al.1996, who divide the types of materials into 9 classes and identify several failure stages (Figure 8.6), clay and silt are the materials involved in the first failure stage of landslides which however, only in some parts of the hollows, can be classified as post-failure stage.

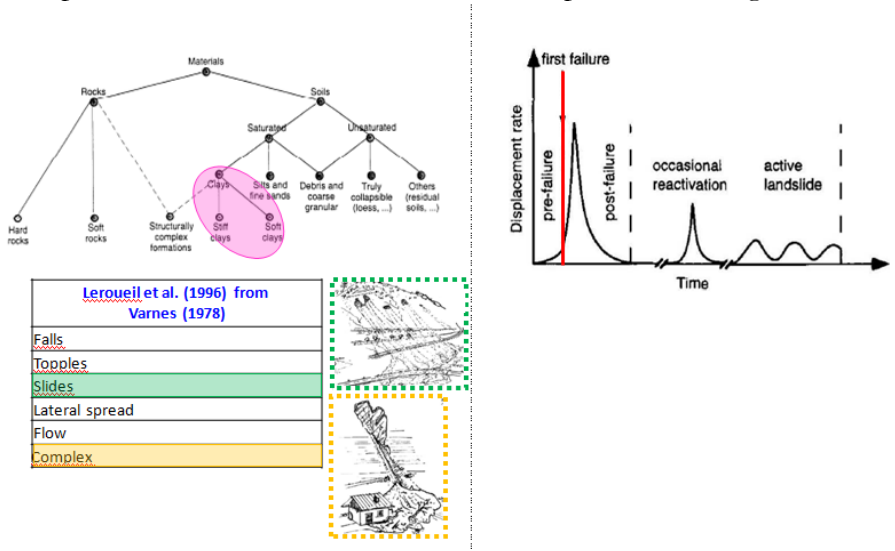

Figure 8.6 Shallow landslides classification. a) involved soils, b) different stages, c) types of movements. (Leroueil et al., 1996 mod.).

Moreover, Leroueil et al. (1996) also recommend the use of a data sheet for a complete analysis of shallow landslides in order to explain the laws governing these events, their predisposing factors, their triggering and their aggravating factors, their revealing factors and the consequences of slope movements.
For this purpose, following the methodology initially formulated by Vaunat et al. (1992), and subsequently used by Leroueil et al. (1996), it is necessary to identify:

(a) the laws and the parameters controlling the phenomenon, for example the Mohr-Coulomb criterion, and c' and φ' at the failure stage. Given that such reference values vary depending on the state of activity, in the case under examination they can be considered equal to the peak values of the materials involved;
(b) the predisposing factors providing information about the current situation of the landslide and determining the slope response to the occurrence of a triggering factor (for example the presence of a weak layer).
(c) the triggering factors that lead to failure, or the aggravating factors that produce a significant modification of the stability conditions or of the rate of movement. The correct identification of these factors requires specific analyses, listed in Table 8.1, and subdivided into three classes: those that contribute to an increase in the shear stress, those that contribute to a decrease in shear strength, and those that can influence both shear stress and strength. As discussed in the next chapter, in the case under investigation here, infiltration and degradation mainly contribute to the decrease in shear strength;
(d) the revealing factors that provide evidence of the slope movements which do not generally influence the process (presence of cracks for example), even though their role must be clearly understood and highlighted.

Table 8.1 Common triggering or aggravating factors.

Increase in shear stress
Erosion and excavation at the toe
Surcharging at the crest
Rapid drawdown
Fall of rock (Bovis & Dagg, 1992; Lacerda, 1997)
Earthquake (Sassa, 1996)
Decrease in strength
Infiltration due to rainfall, snow melt, irrigation water leakage from utilities
Pile driving
Weathering
Fatigue due to cyclic loading
Physico-chemical changes
Possible increase in shear stress and decrease in strength
Vibrations and earthquake shaking that can generate excess pore pressure
Swinging of trees due to wind gusts
Thunderstorm lightning (Lacerda, 1997)
Storm waves

8.2.2 Slope evolution models for shallow landslides

Once the shallow landslides in the test area have been classified, it is necessary to describe their evolution in space and time using, if possible, the slope evolution model currently available in literature.
However, given the aim of the present study, only few works are available on the triggering mechanisms and the evolution of shallow landslides in non-collapsible soils, and among them the most useful are the ones written by (Rogers and Selby, 1980; Gullà et al., 2001).
Rogers and Selby (1980) examine the translational slides triggered in the North Island of New Zealand, by short and intense rainfall events during the dry seasons. Eye-witness accounts indicate that slides usually begin with a bulging of the toe of the slope and subsequently separate from the soil above the failure along a tension crack. Over a period from 15 minutes to two hours the mass slides moves over the failure plane as either debris avalanche or flow, Figure 8.7(A).
Gullà et al. (2004) introduce, in their evolution model, the role played by degraded covers identifying three different evolution stages: a) initially a sliding failure of the soil located in the degraded cover takes place; b) in the sliding stage, the material can become a mixture of mud and clods of various sizes flowing fast downwards; c) after the failure, soil degradation reoccurs along the ground surface. Generally, this last stage represents the end and the beginning of a single cycle of the slope evolution model

proposed by the authors, even though, in some cases, the unstable mass is not dislocated and the instability is testified by a fracture at the top of the slope (Gullà et al. 2001b).

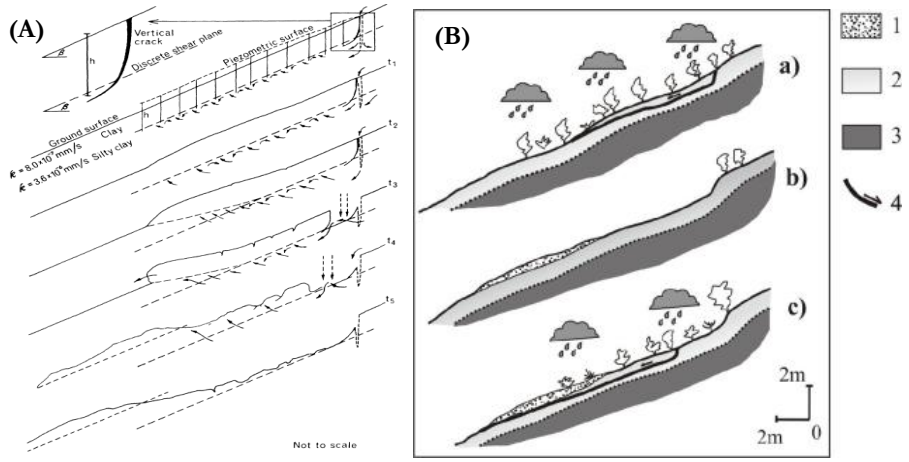

Figure 8.7 Evolution model of the slope for soil slip, (A) Rogers and Selby (1980); (B) Gullà et al. (2004). Legend: 1) Landslide deposit; 2) degraded soil; 3) intact soil; 4) sliding surface. a) sliding - initial stage; b) flowing - intermediate stage; c) soil degradation end start stage.

The models available in scientific literature allow to identify some of the features of the mechanisms observed in the study area. Yet, these mechanisms require a specific model able to take into account all the phases of the morphological evolution described in section 8.2.1.
Therefore, starting from the evolution models already discussed and considering the main aspects of shallow landslides, three new mechanisms have been identified which are tagged MORSLE1, MORSLE2, MORSLE3, using the acronym already created by Crozier 2005 to indicate multiple occurrence regional shallow landslides events.
The main characteristics of these mechanisms are strictly related to their different location along the slope, which also affects their evolution and magnitude.
Specifically, MORSLE1, Figure 8.8, can be classified as an earth slide; it is always located at the top of the open slopes either on old landslides deposits or near a change in slope gradient. It is usually shaped as a rectangle along the maximum gradient direction; this mechanism has a few meters wide triggering area and a total length of generally less than 10m. The sliding surface is located at a maximum depth of 0.80 m from

the ground surface and, quite often, the first failure stage is preceded by the opening of cracks at the top of the slope, while just after the first failure stage the unstable mass dislocates from the landslide source area.

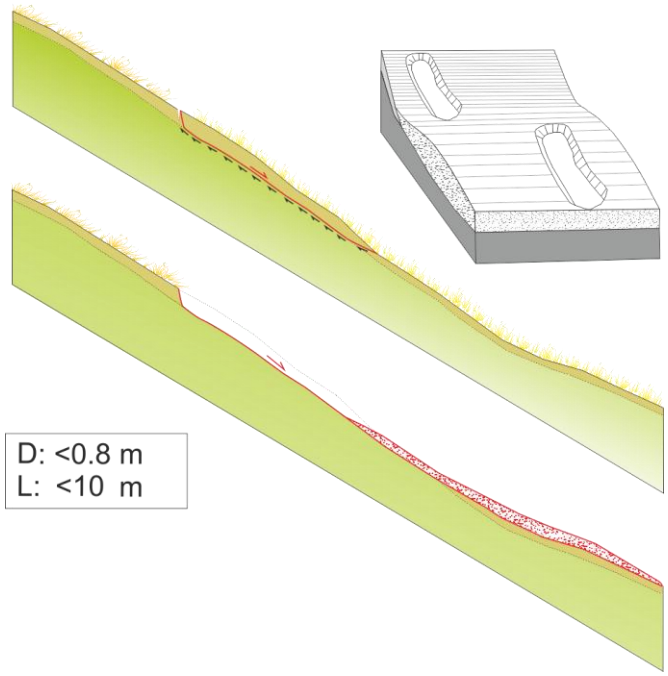

Figure 8.8 Slope evolution model (MORSLE 1).

MORSLE2, Figure 8.9, can be classified as a complex earth slide-earth flow phenomenon; it is usually located in the upper part of secondary morphological hollows limited by secondary watersheds. It has a typically oblong shape, it is a few meters large and between 10m and 50 m long. The sliding surface is at a maximum depth of 1.5 m from the ground surface. This mechanism has a very rapid triggering stage, and the volume involved in the landsliding is distributed along the main axis of the hollow, even though secondary phenomena can occur along the lateral flanks.

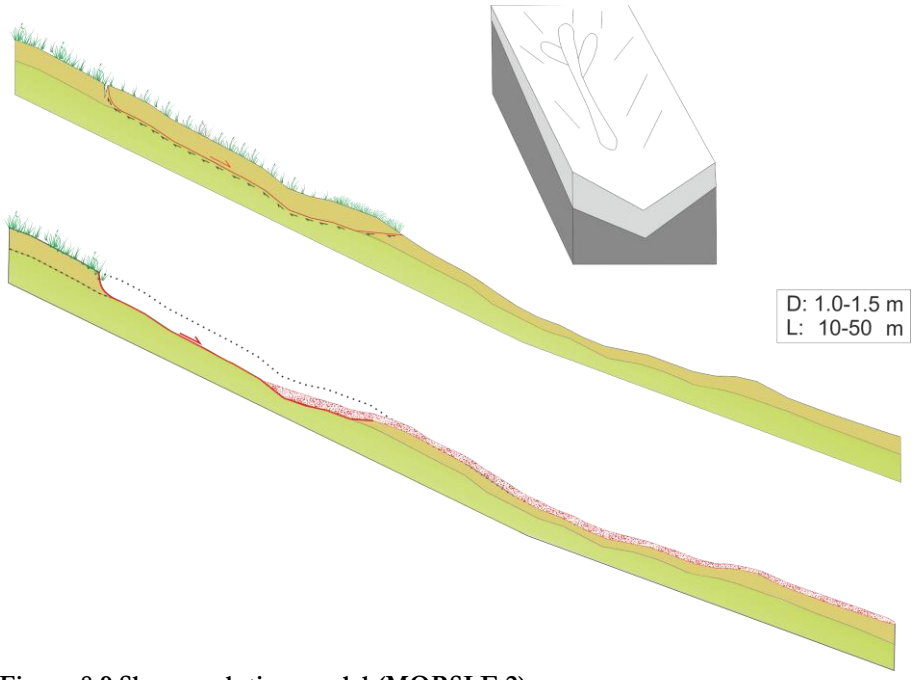

Figure 8.9 Slope evolution model (MORSLE 2).

MORSLE3 generally occurs within morphological hollows wider and deeper than those affected by the ones previously described. Usually, the areas involved are between 10 m and 30 m wide and between 50 m and 100 m long, while the maximum depth of the sliding surface is 3 m and takes place over a longer timespan than the other mechanisms. In this case, the weathering process involves greater depths and volumes than the ones observed in the other mechanisms; it starts with the opening of a tension crack at the top of the slope and it is accelerated by a pattern of cracks inside the landslide body which facilitates the infiltration of runoff water, Figure 8.10.

For instance, by observing Figure 8.10 the formation of an initial visible crack before the occurrence of the phenomenon can be observed, which can be dated back to 2001. This date can be reasonably taken as the beginning of the formation of an incomplete sliding surface.

In 2005, the tension crack located at the top of the slope became more evident and an accurate zoom of the Google Earth image allows to define the formation of the landslides boundary.

In 2006, the Google Earth image seems to show the formation of secondary steps on the topographic surface. These steps have been observed through in situ surveys carried out in 2010 with reference to similar phenomena occurred in the St. Antonio area, and shown in Figure 8.10.
In 2009, the main landslide scarp appeared, but the complete evolution of this phenomenon took place in 2010 following a rotational translational slide movement type upslope which evolved into an earth flow along the main drainage lines.

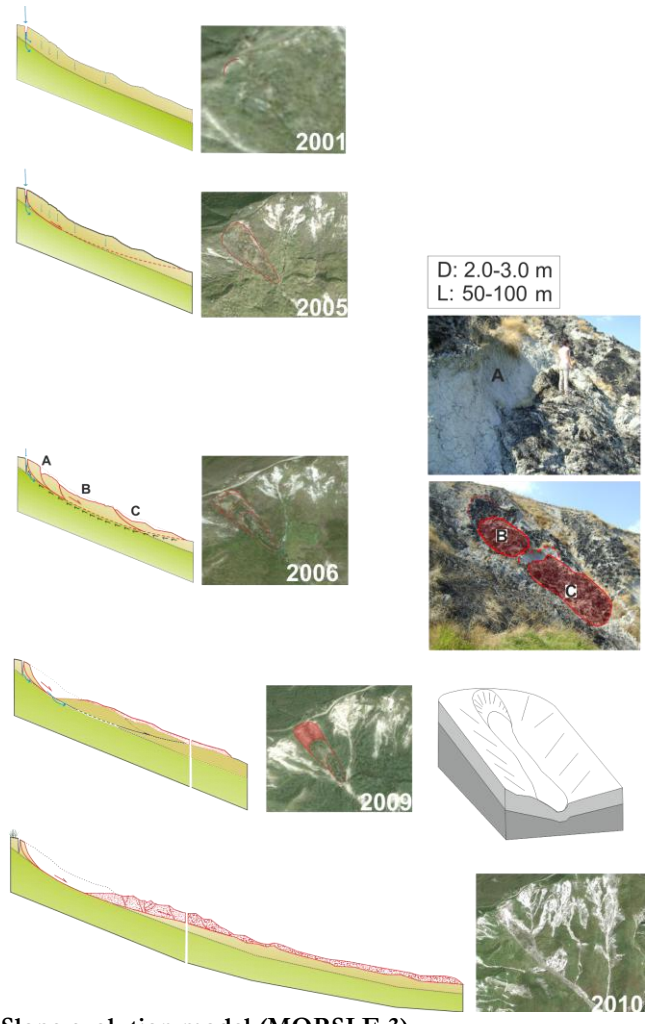

Figure 8.10 Slope evolution model (MORSLE 3).

Once the triggering mechanisms have been defined and localized along the slope, Figure 8.11, it is interesting to observe that the morphological evolution of the hollows, apparently chaotic and disordered, occurs following an evolution scheme strictly influenced by well-defined causal factors (Popescu, 2002) such as surface and subsurface runoff.

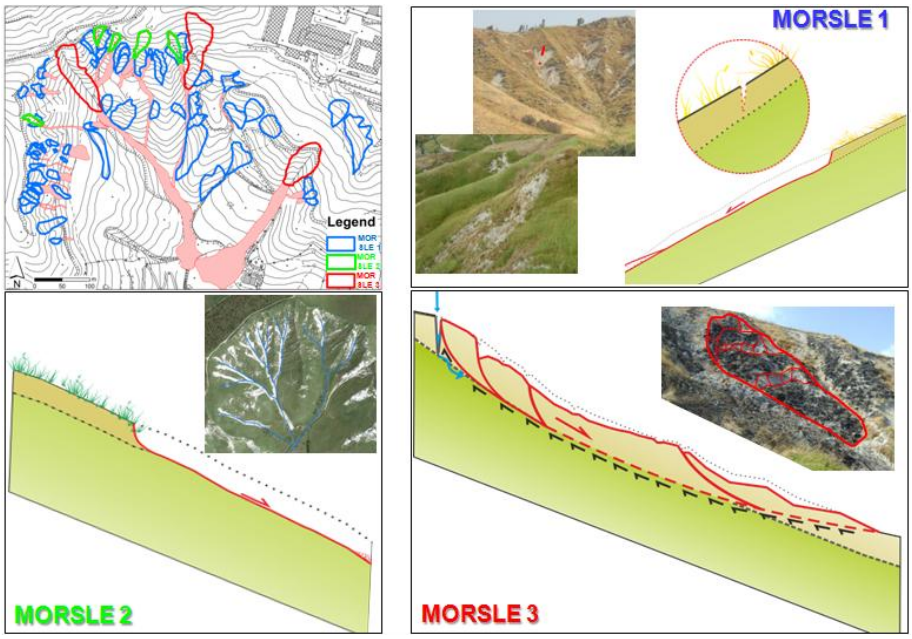

Figure 8.11 Spatial distribution of the triggering mechanisms.

The main casual factors visible at 1:5000 scale are summarized in Figure 8.12. This figure shows that surface and subsurface runoff is influenced by the slope morphology; i.e. in the upper part of the slopes, it is characterized by straight lines, whereas a convergent radial flowing into the main drainage line can be observed in the hollows Figure 8.12 a,b.
The effects of the surface and subsurface runoff on the slope stability conditions are magnified by the effects caused by the wind and solar irradiation which both depend on the slope aspect. All these factors accelerate the formation of a cracks pattern, whose dimensions and features vary according to their position on the slope, thus accelerating physical weathering which strongly affects all the mechanisms previously defined, Figure 8.12 c.

Considering the relevant role played by the cracks pattern on the slope stability conditions, the characteristics of such cracks have been verified by in situ investigations which evidenced that along the open slope, the cracks pattern is characterized by a maximum depth value of 0.80 m.
The cracks are more homogenous and less deep along the ridges where only few fractures, 0.2 m deep at the most, can be found.
The cracks are more pronounced and deeper in morphological hollows, from the few available data it reasonable to think that their maximum depth is 1.5 m.

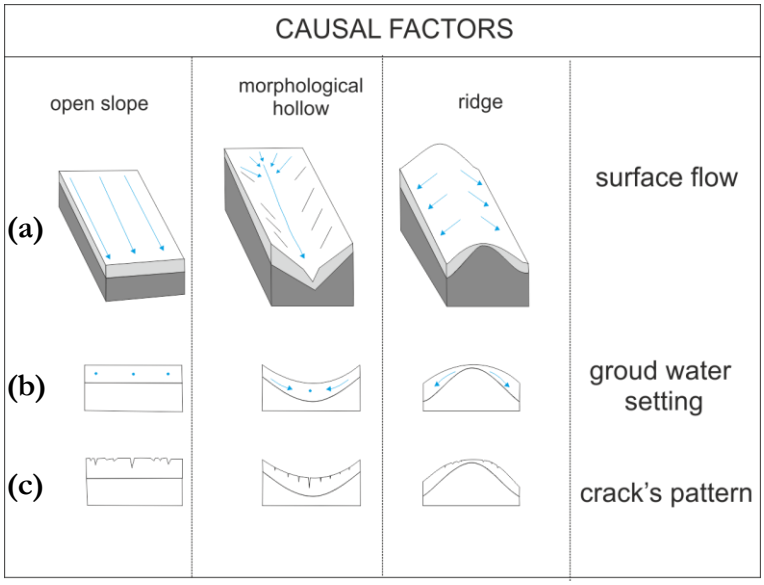

Figure 8.12 Causal factors of slide and complex landslides.

8.3 THE GEOTECHNICAL DATA SET.

The available dataset includes in situ investigations and laboratory tests performed within scientific research works and/or technical activities.
The spatial distribution of all the available in situ investigations is summarized in Figure 8.13.
In particular, the data available from the boreholes performed in the Murano area and St. Antonio area revealed the presence of a stratigraphic succession mainly composed of silts with clay with some

sporadic sands intercalations in the silts (Gullà et al. 2004, e Cascini et al. 2010), Figure 8.13.

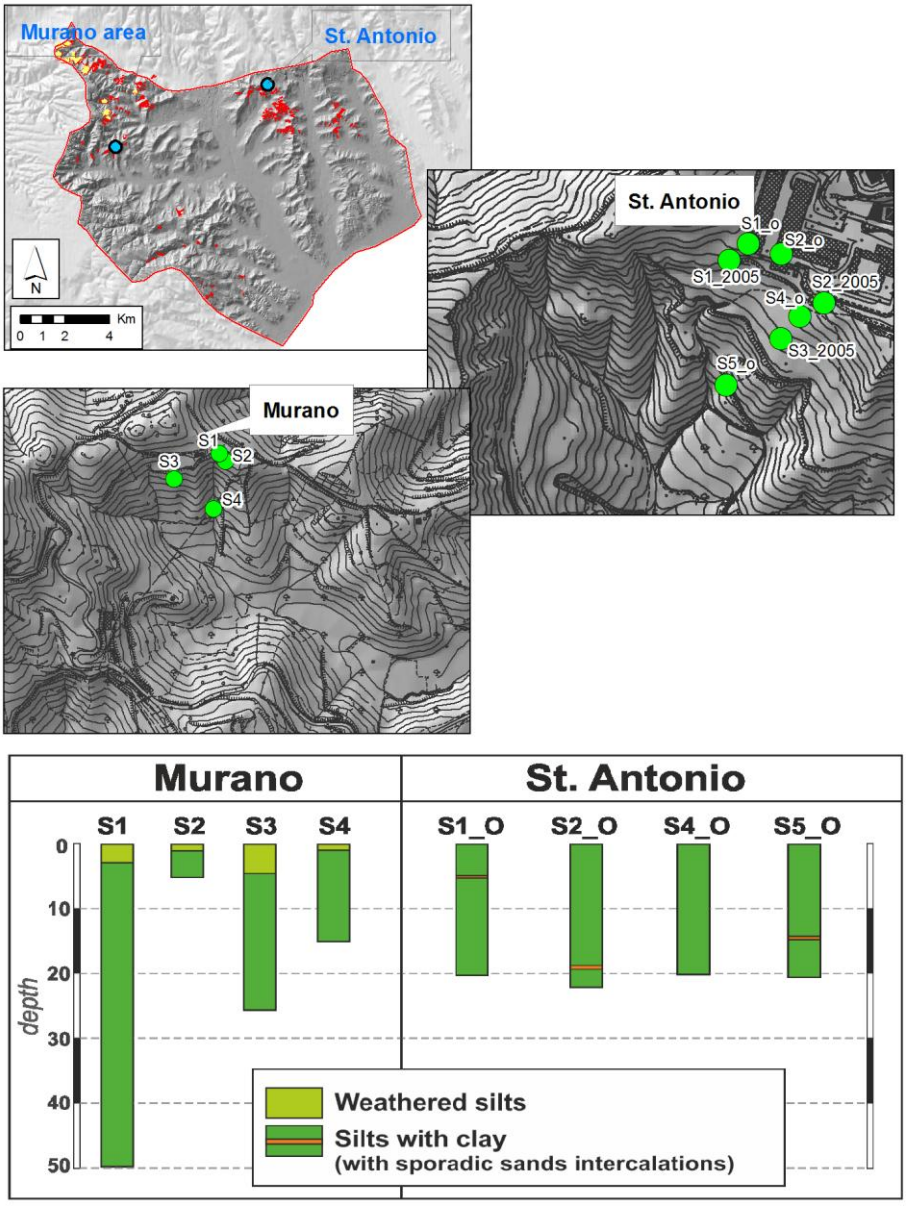

Figure 8.13 Spatial distribution of in-situ investigations and soil stratigraphy.

The available physical and mechanical properties of the soils derive from i) a laboratory testing programme performed at the CNR-IRPI in Cosenza on undisturbed and degraded samples and ii) from a technical investigation discussed in Cascini et al. 2010.
In terms of shear strength, Figure 8.14, all the data collected show a great variability in the values of both shear strength parameters, which range, respectively, between 3-50 kPa as it concerns the effective cohesion c', and between 18°-40° for the peak friction angle.

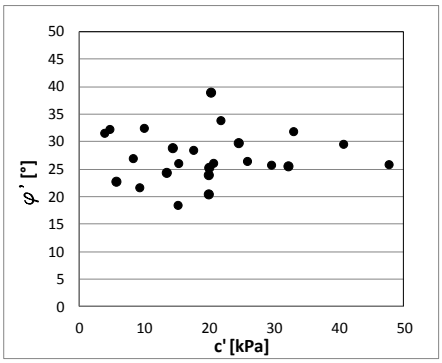

Figure 8.14 Shear strength properties.

On the contrary, little information exists about the hydraulic properties of the materials involved in landslides for which the database of the CNR-IRPI of Cosenza provide a mean permeability varying between $3.1x10^{-8}$ m/s – $7.65x10^{-7}$ m/s.
Given the relevance of the hydraulic parameters for modelling rainfall infiltration in the slope during wet periods, a laboratory programme was developed by performing advanced tests on unsaturated undisturbed specimens, introduced and discussed in the next chapter.

9 INPUT DATA FOR THE GEOTECHNICAL ANALYSIS

Phase II of the analysis at large and detailed scale aims at quantifying and calibrating the triggering mechanisms of shallow landslides in the test area; this goal will be pursued by means of geotechnical analyses requiring several and accurate input data in order to provide reliable output results.
Considering the relevance of these mechanisms, this chapter focuses on the input data of the geotechnical analyses, initially referring to the available data set that derives from in situ investigations, land surveys and laboratory tests carried out at the CNR-IRPI Operational Unit in Cosenza. Subsequently, a specific investigation programme developed to better understand the soils involved in the landslides is illustrated. Specifically, the cracks pattern in situ has been analysed considering its influence on the mechanical and hydraulic properties of clayey soils; moreover, advanced laboratory tests have been performed to characterize directly these soils in both undisturbed and degraded conditions, the latter induced by wetting and drying cycles to reproduce the conditions observed in situ.

9.1 GENERAL FEATURE OF THE CLAYEY COVERS

The previous chapters highlighted that i) mass movements essentially involve physically degraded lithotypes characterized by diffused pattern of fractures and fissures and that ii) the formation of cracks is generally attributed, in literature, to an external or internal mechanical stresses, due to an alternate process of wetting and drying, which produces a fragmentation when these stresses are equal to the soil shear strength.
Whatever their origin, it is well known that soils cracks drastically modify the infiltration of water from the ground surface and this issue is investigated by several authors who analyse the spatial and depth

distribution of cracks in fine-grained soils (Towner, 1987; Dexter, 1988; Blight, 1997; Meisina, 2006).
In particular, Dexter (1988) provides a conceptual model for the development of desiccation cracks, Figure 9.1 (A) which start from tensile stresses acting in the horizontal direction in the soil. When these tensile stresses become equal to the tensile strength of the soil, primary cracks due to vertical desiccation occur, Figure 9.1 (B), Towner (1987). The author asserts that when the primary cracks reach a certain width (probably 5 mm), air convection currents occur in the soil and the process of drying involves the vertical crack faces also causing secondary (horizontal) cracks, Figure 9.1 (C), (Ritchie and Adams, 1974). Further drying can produce tertiary cracking, Figure 9.1 (D). To sum up, tensile stresses develop during drying, causing the creation of primary, secondary and tertiary cracks.
Blight (1997), evaluates the stress state in situ during a drying process induced in a clayey soil by a slow evaporation phenomenon and underlines that the open vertical cracks are generally continuous until a depth of 1m from ground surface. By contrast, the cracks up to 1.5 m deep are often discontinuous ending with inclined fissures that are not present at depths less than 0.5 m.

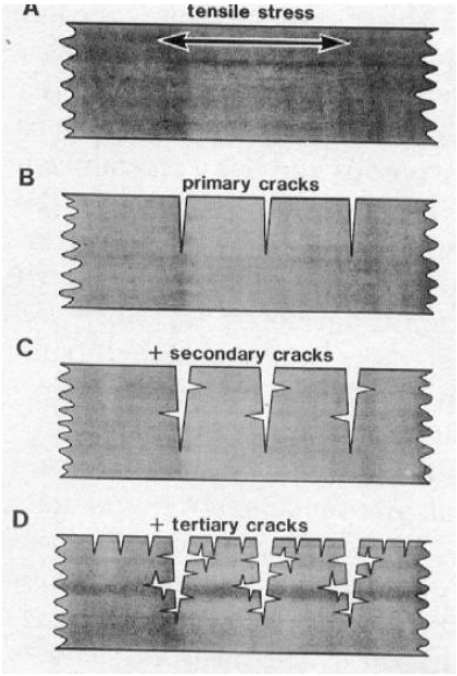

Figure 9.1 Conceptual model describing the development of primary, secondary and tertiary cracks, resulting from the build up of tensile stresses on drying (Dexter 1988).

With reference to the spatial distribution of the shrinkage cracks, defined as primary cracks in Figure 9.1(B), Towner (1987) affirms that the formation of cracks depend on the velocity of the drying process. Slow drying tends to produce wide cracks with large spacing, whereas rapid drying tends to produce a greater number of narrower cracks with smaller spacing. These cracks tend to form a hexagonal-type pattern on the soil surface.

A typical pattern of shrinkage cracks on the ground surface is described by Blight (1997), Figure 9.2, who shows both deep primary and shallower secondary cracks. It must be noted that most of the cracks intersections are orthogonal, and the cracks pattern is more square than hexagonal. Similar observations have been reported by Corte & Higashi (1964) and Lachenbruch (1962).

Figure 9.2 Cracking pattern in a desiccated soil surface (Blight 1997).

The geometrical characteristics of the cracks network in swelling soils in a drought period is provided by Meisina (2006), who identifies near-vertical shrinkage cracks, Figure 9.3, extending almost to the depth of the seasonal moisture change in the ground and reaching a value of 1.4-1.9 m, respectively for silty clay and clayey silt. In this case, the author observes that the cracks were wide open until a depth of 0.5–0.8 m, where the soil was in an unsaturated state and the water content was below the shrinkage limit.

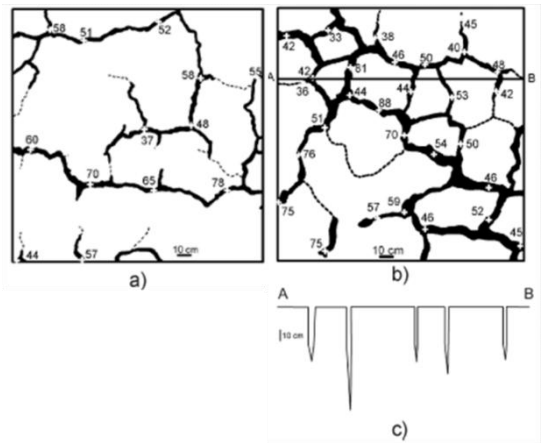

Figure 9.3. Crack pattern at the soil surface. (a) soil with grass; (b) soil ploughed in spring; (c) cross-section showing the crack depth (Meisina 2006).

A similar trend for the cracks pattern is observed in a measured field of about 2 m long and 1 m wide which is located in the upper part of a

slope within the St. Antonio test area. Here, the fractures form almost regular quadrangles, are wide (the maximum measured width is about 0.05 m) and reach a maximum depth of about 0.50 m, Figure 9.4, although the little information available along the slope, in some points of the morphological hollow, indicate that the cracks can reach a maximum depth of about 1.5m.

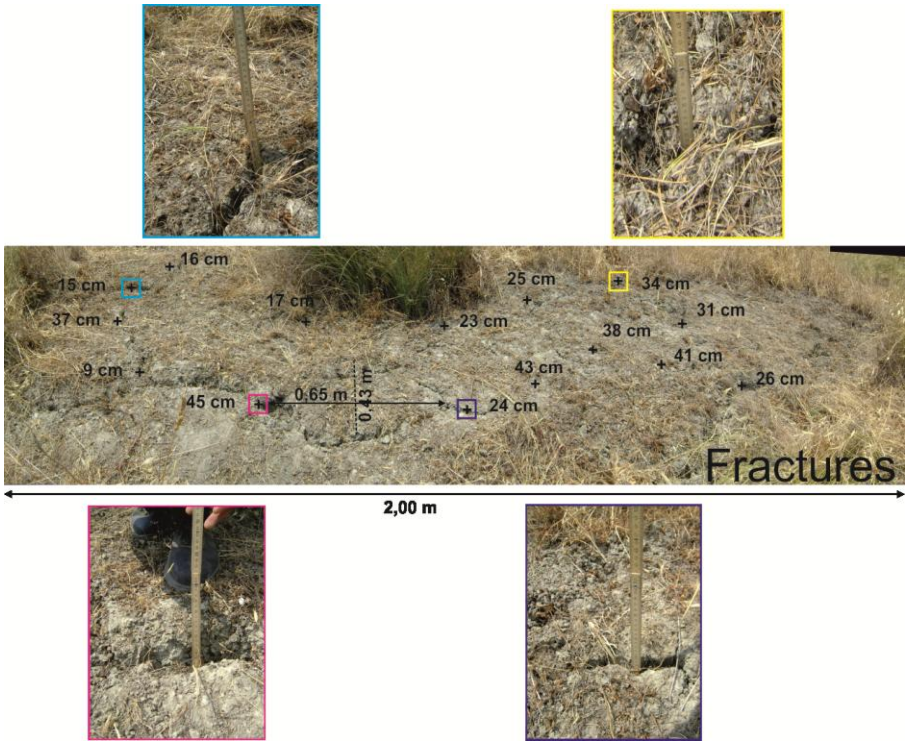

Figure 9.4 Pattern of fractures mesured in the test area.

9.2 MICRO, MESO AND MACRO STRUCTURES

The geotechnical characterization of a predominantly clayey lithotype, which is physical weathered (degraded) and affected by a combination of cracks (i.e. fractures and fissures), is very a difficult task and requires a complex experimental programme due to i) the different features of the soil at micro and macro scale and ii) their variability over time as a consequence of drying and wetting cycles.

Indeed, in order to obtain consistent results from a geotechnical point of view, an integrated multiscale approach, like the one shown in Figure 9.5, has been selected and used in this thesis.

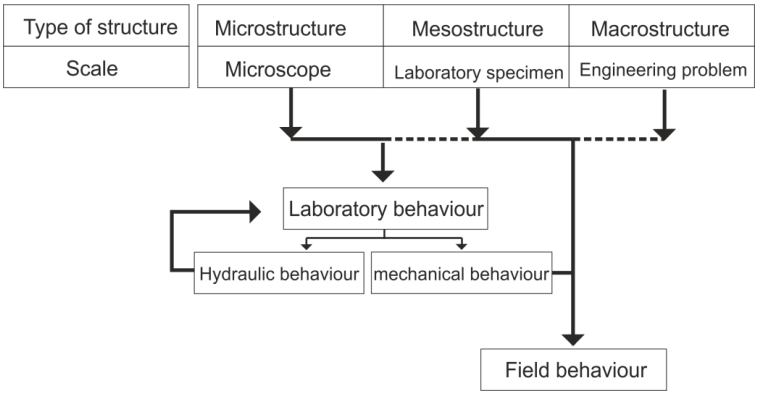

Figure 9.5 Metodological approach proposed for the geotechnical analysis (Picarelli 1991 and D'Elia et al. 1998, mod.).

Referring to the microstructure, the XRD lab tests developed by (Gullà et al.,2008) highlight the presence of certain minerals notoriously able to influence the hydraulic behavior of the soil, even though they do not evidence any substantial difference between intact and degraded soils, Figure 9.6.
As far as the mesostructure is concerned, useful information can be obtained by laboratory tests carried out to assess the shear strength of both degraded and intact soils characterized by a limited variability in both cohesion and friction angle (Gullà et al. 2006). By contrast, as regards the hydraulic properties, the usual dimension of the specimens in the lab is representative of the matrix behavior of the intact soil only. On the contrary, degraded fissured soil requires further experiments to be carried out in the lab on soil specimens subjected to drying-wetting cycles and in situ to investigate the role played by these properties at the scale of the macrostructure.

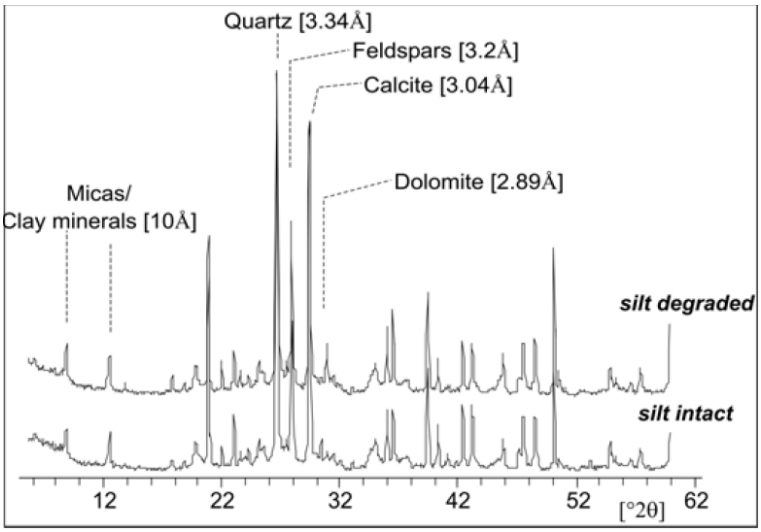

Figure 9.6 The XRD patterns of silt samples degraded in laboratory and natural (intact) silt samples whole-rocks (Gullà et al., 2008).

9.3 GEOTECHNICAL AND HYDRAULIC PROPERTIES OF THE SOIL

The present section introduces and discusses the main experimental data available in literature and the additional experiments and/or analyses developed in this thesis to understand and to model the mechanical and hydraulic behaviour of a soil which is degraded, fissured and fractured at slope scale. The data available in literature are those collected by the CNR_IRPI in Cosenza in the Murano area and by Cascini (2010) in the St. Antonio area, already introduced in paragraph 8.3. Further data derive from the experiments carried out on specimens collected in the Monachella site located in the town of San Floro, Figure 9.7.

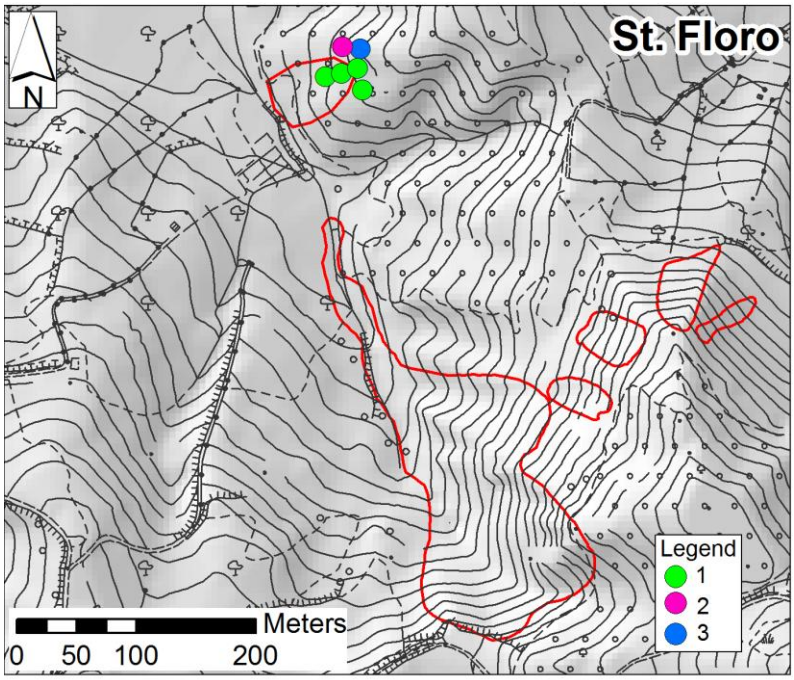

Figure 9.7 Spatial distribution of in situ and laboratory test. 1) soil specimens taking, 2) monitoring station, 3) Guelph permemeter test.

9.3.1 Grain size distribution and index properties

Typical grain size, index properties, plasticity and activity diagrams referring to the samples collected in the Murano area, the St. Antonio area and the new acquisition data obtained in San Floro area, are shown in Figure 9.8-9.10. On the basis of the available data, the soil can be classified as inorganic, inactive clay having high plasticity and high liquidity limit.

As regards the grain size of the soil, this is typical of clay with silt up to a depth of 3 m from ground surface; and of silt with clay and silt with sandy clay at greater depths. As far as the saturated unit weight is concerned, it ranges between 19.1 kN/m^3 - 24.8 kN/m^3, with the highest values recorded at a depth of about 14 m in a section where the material is believed to be intact. The natural unit weight varies between 17.0 kN/m^3 and 20.8 kN/m^3 in the first few meters below ground level, and then stays at 20 kN/m^3 in the following meters. The dry unit weight shows a variation range between 13.7 kN/m^3 and 17.5 kN/m^3 along the

surface layers, and subsequently reaches a constant value of 17 kN/m^3 in the following meters. As far as void indexes are concerned, a minimum value of 0.57 and a maximum one of 1.3 is recorded in the layers with degraded material; 0.8 is the maximum value recorded in the layers with intact material. Finally, the initial saturation degree of the tested samples ranges between 68% -100%.

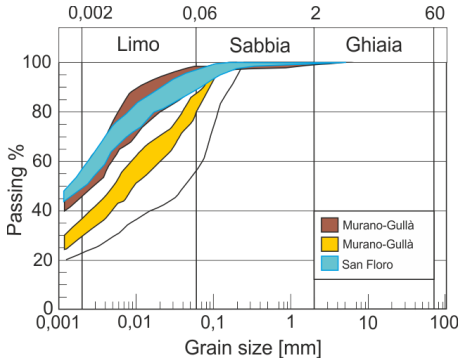

Figure 9.8 Grain size distributions.

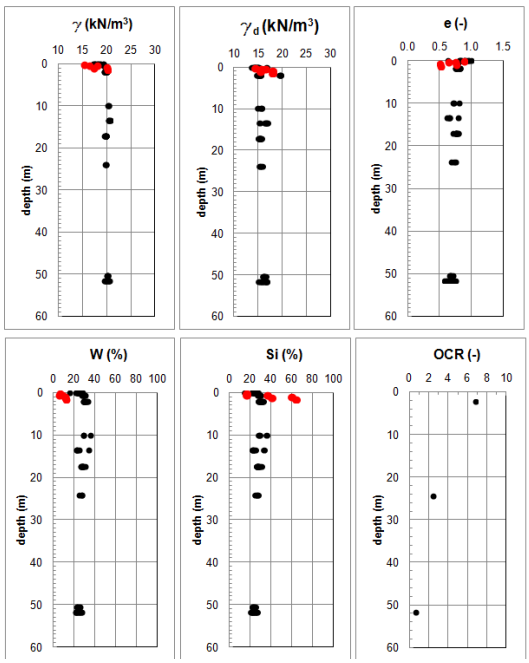

Figure 9.9 Trends of the main index properties with depth, in black available data, in red new acquisition data.

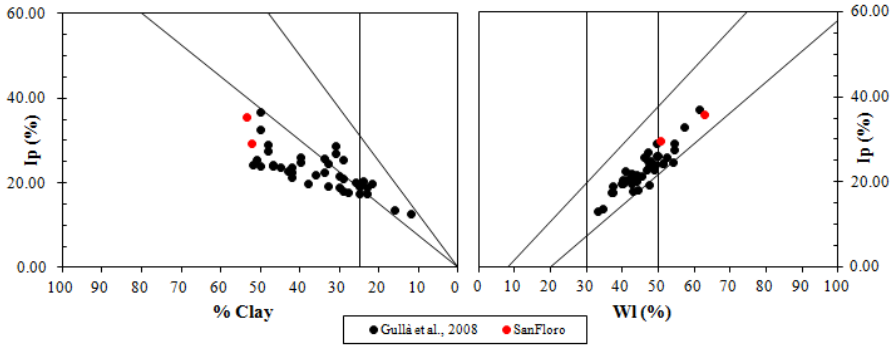

Figura 9.10 Activity and plasticity chart. In black available data, in red new acquisition data.

9.3.2 Shear strength properties

In the area investigated by Gullà (2005) and Cascini (2010) the shear strength envelops, obtained by testing saturated undisturbed specimens collected at different depths, are bounded by an upper limit having a cohesion value c'_p= 57 kPa and a friction angle φ'_p=29,4°, and by a lower limit with a cohesion value c'_p= 13,5 kPa and a friction angle φ'_p=24,4°, Figure 9.11.

In order to obtain greater insight on the shear strength properties of the most superficial layers, only the values of the specimens collected at depth less than 5 m from the ground surface are shown in Figure 9.12.

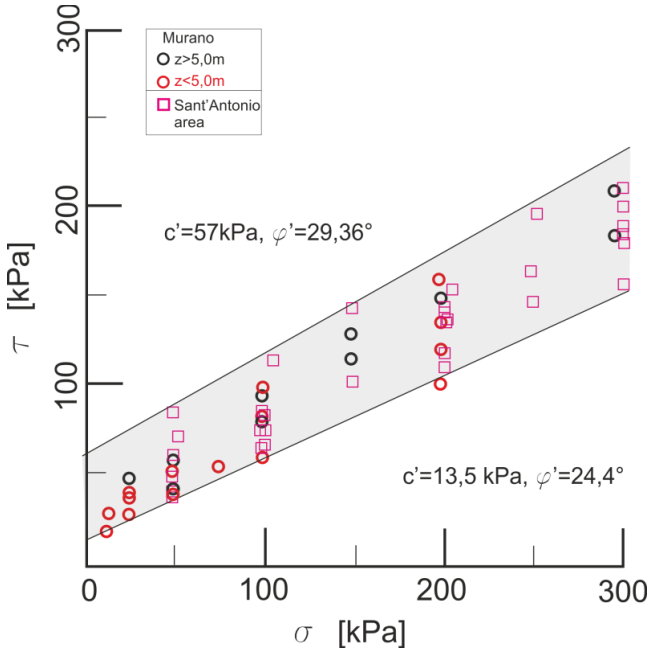

Figure 9.11 Strength envelopes of intact and degraded clay.

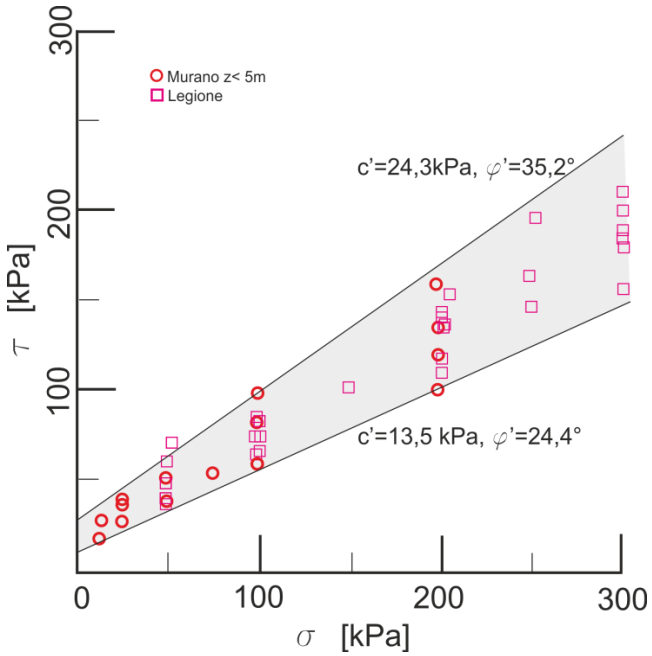

Figure 9.12 Strength envelopes of degraded clay.

This figure indicates c'_p= 24.3 kPa and φ'_p=35.2°, as the upper limit, and c'_p= 13.5 kPa e φ'_p=24.4° as the lower limit.
In order to verify the similarity of the soils present in the St. Antonio area with those tested in literature, some saturated shear strength tests have been performed on superficial undisturbed specimens collected in the St. Antonio area. The test have been performed until a maximum normal effective stress of 100 kPa, which is representative of the soils involved in landslides.
Figure 9.13 shows that the experimental results obtained from the samples collected in St. Antonio area do not entirely fall within the range identified by the available data and reported in Figure 9.12. In particular, the lower limit of shear strength envelop identified by lab tests made on the St. Antonio samples is characterized by the pairs c'_p= 5,1 kPa and φ'_p=28°. This pair identifies a limit which is lower than those reported in Figure 9.12 (i.e. c'_p= 13,5 kPa e φ'_p=24,4°) but comparable with the range of envelopes identified by Gullà et al. (2004) with reference to soil specimens submitted to frequent wetting-drying and freezing-thawing cycles in laboratory, Figure 9.13.

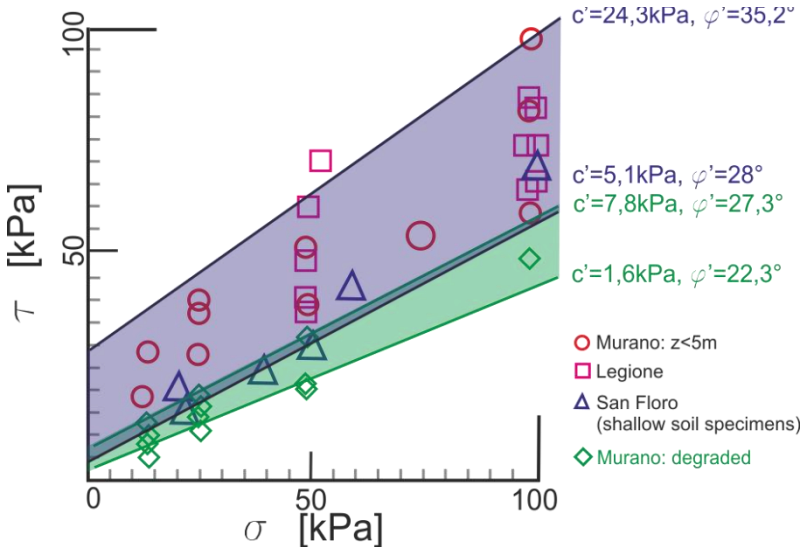

Figure 9.13. Strength envelopes of degraded and artificially degraded clay.

9.3.3 Hydraulic properties

The database available at the CNR- IRPI (Cosenza) is extremely useful as it concerns the shear strength properties of the soils involved in landslides, but it does not provide sufficient information to define the hydraulic properties that are only indirectly estimated on the basis of oedometric tests. In particular, by referring to an effective vertical stress compatible with a maximum depth present in situ of about 5 m, permeability coefficient values are estimated in the range $3.1x10^{-8}$ m/s – $7.65x10^{-7}$ m/s, i.e. typical values for fine-grained materials which, however, are not representative of the real in situ situation.
Indeed, a specific experimental programme has been developed to determine the soil water characteristic curves which are important to model rainfall infiltration and evapotranspiration phenomena during wet and dry periods, Figure 9.14.

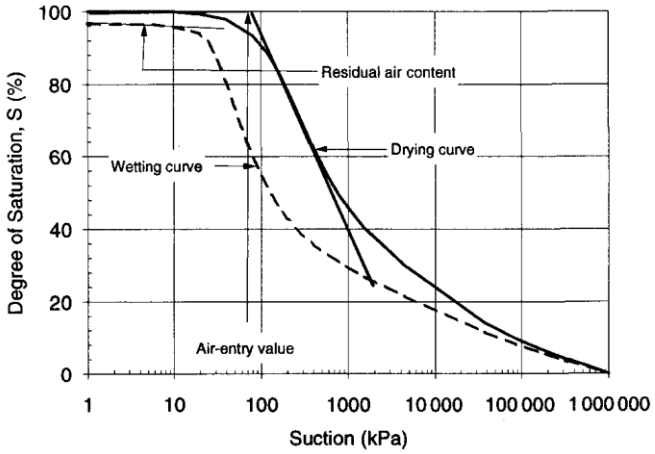

Figure 9.14 Typical soil-water characteristic curve features for the drying and wetting of soil (Vanapalli et al., 1996).

The experimental programme has been developed using standard and advanced equipment including a volumetric pressure plate extractor, a Richards pressure plate and a suction controlled oedometer apparatus used to test undisturbed superficial soil specimens with a diameter of about 6 cm, taken up to a depth of 0.80 m.
Four soil water characteristic curves were obtained in Richards pressure plate, one in the suction controlled oedometer apparatus and one in the volumetric pressure plate extractor (Fig. 9.15).

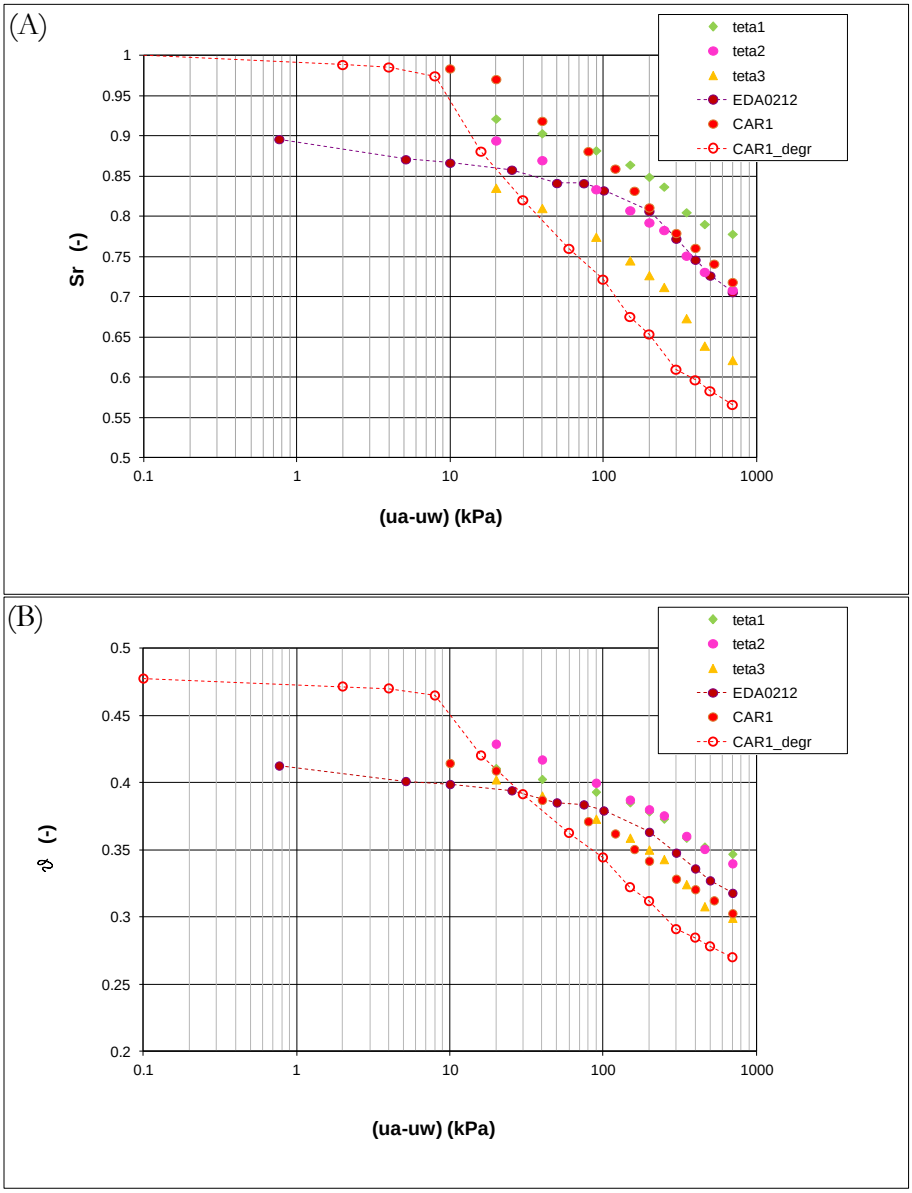

Figure 9.15 Soil water characateristic curves.

In order to determine the role played by physical weathering, one of the soil specimens, tagged EDO0112, has been flooded to reach the total saturation condition for about one month at the end of a first phase of drying; subsequently, the specimen was submitted to a new process of

drying in the Richards pressure plate. Figure 9.16 (A) shows the degradation at the end of the first drying cycle in Richards pressure plate and highlights the formation of a large fracture of about 2mm, near to the metal ring, and some small fissures inside. Afterwards, the specimen was dried at a temperature of 105° and then flooded, Figure 9.16 (B); it is interesting to observe that only a few minutes later the fractures and fissures completely closed. Finally, a new drying cycle in the Richards pressure plate caused a complex pattern of fractures and fissures, some of which coincided with those formed in the previous phase while some other were new formations.

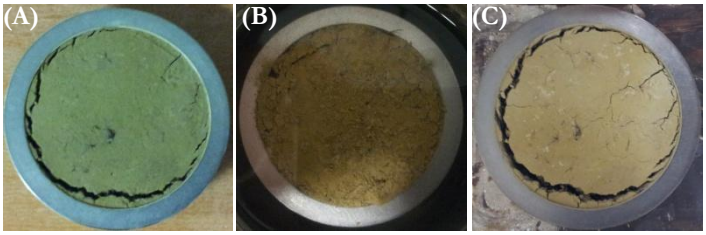

Figure 9.16 (A) Soil sample after a first drying cycle in Richards pressure plate (B) Soil sample after wetting (C) Soil sample after a second drying cycle in Richards pressure plate.

The soil water characteristic curve (θ-ψ and S-ψ) obtained at the end of the artificial drying and wetting cycles shows a slight bimodal trend and a significant decrease in both water content and saturation degree for low suction values, Figure 9.16 (car1_degr).
The experimental results have been interpolated referring to the well known equation proposed by Van Genuchten 1980, who assumes:

$$\Theta = \left[\frac{1}{1+(p\psi)^n}\right]^m$$

where:

Θ is the normalized (or dimensionless) water content (i.e., $\Theta=(\theta_s- \theta_r)/(\theta_s- \theta_r)$ where θ_s and θ_r are the saturated and residual volumetric water contents, respectively)
ψ is the suction, and p, n, m represent three different soil parameters.

The interpolated curves thus obtained are shown in Figure 9.17 together with the optimized fitting parameters. With reference to the soil specimen submitted to drying and wetting cycles (red dotted line), the interpolation function shows an air-entry value of about 16 kPa which differs from the ones previously obtained (ranging from 26 kPa to 100 kPa), Figure 9.17.

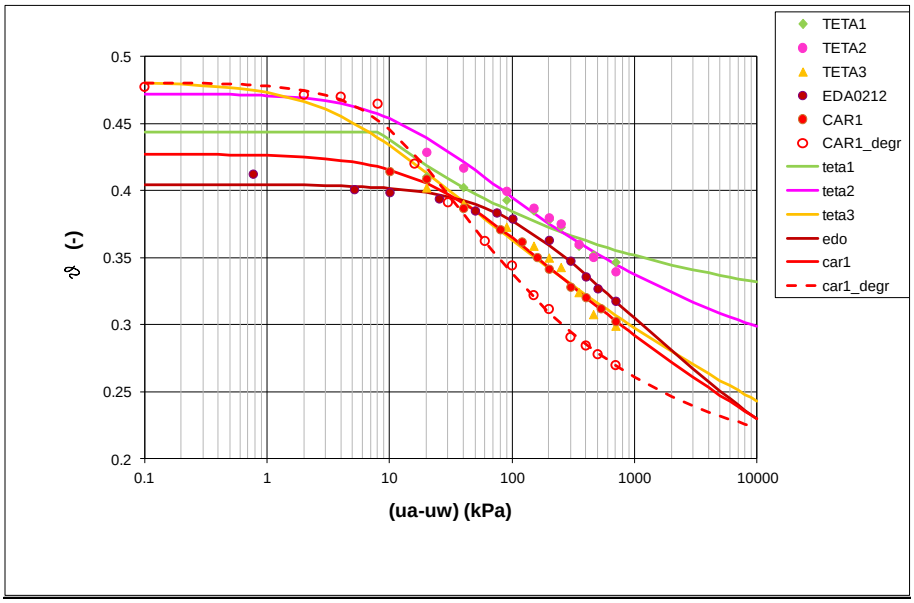

Curva	θs	θr	α	n	R^2	Model
TETA1	0.4344	0.2856	0.02955	1.2782	0.95192	van Genuchten
TETA2	0.4724	0.2289	0.06835	1.1908	0.98062	van Genuchten
TETA3	0.4806	0.0000	0.23890	1.0875	0.97946	van Genuchten
EDO	0.4045	0.00002	0.00863	1.1268	0.98754	van Genuchten
CAR1	0.4273	0.0002	0.03775	1.1043	0.99736	van Genuchten
CAR1_degr	0.4804	0.1900	0.07453	1.3267	0.99600	van Genuchten

Figure 9.17 Interpolated curves and experimental data, in table: the optimized fitting parameters.

Referring to van Genuchten (1980), the curves obtained for the hydraulic conductivity are shown in Figure 9.18.

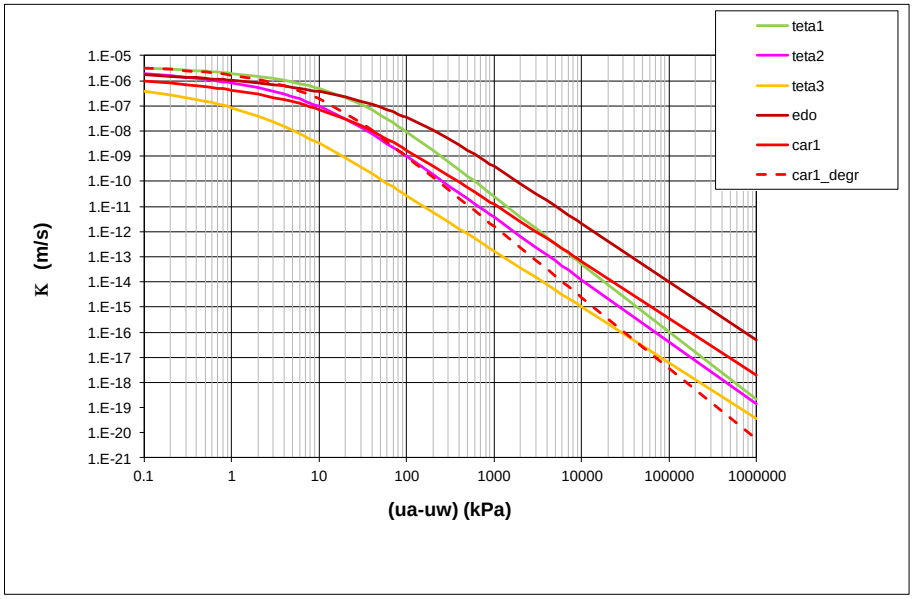

Figure 9.18 Hydraulic conducivity functions.

9.4 CALIBRATION AND VALIDATION OF THE HYDRAULIC PROPERTIES

9.4.1 LAB Parameters

The curves obtained through laboratory tests sometimes require calibration before they are used to solve engineering problems. The calibration is particularly necessary in the case studied here due to the complexity of the soils involved in shallow landslides, as it has been discussed in the previous sections. To this end, the necessary calibration can be obtained through a back-analysis of a set of data acquired in situ as in the case of the monitored station located in the Murano area, where a rain gauge and several "Jetfill" in-place tensiometers were installed along the same vertical at various depths from the ground surface (0.10 m; 0.15 m; 0.30m; 0.45m, 1.20m), Figure 9.19.
The in situ measurements indicate: soil suction values between 0 kPa and 80kPa; a strict correlation between pore water pressure regimes and daily rainfalls up to a depth of 0.45 m; and pore water pressure values next to

0 in the months between October and May at a depth of 1.20 m, where the minimum value is only reached in the months of July and August.

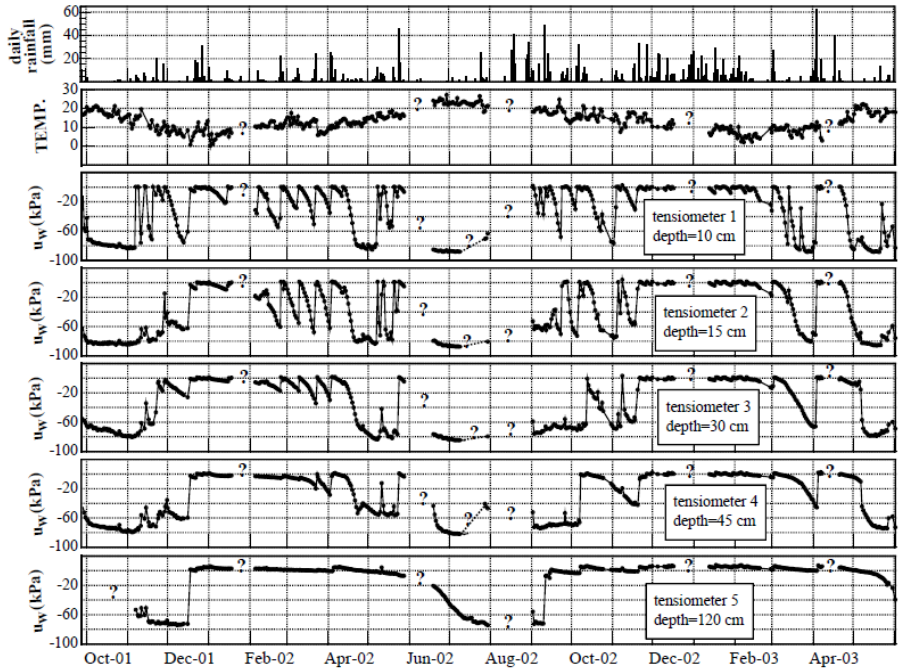

Figure 9.19 Daily values of rain depth, temperature, pore pressure resulting from the tensiometers. "?" No available data (Gullà et al., 2004).

Starting from these data, the pore water pressure regime has been analysed through the finite element code (VADOSE/W della GeoSlope 2007), by using the characteristic curves and the hydraulic conductivity functions previously discussed, and by referring to the stratigraphic section shown in Figure 9.20. This section is around 50 m long and characterized by the presence of two different layers as found out through borehole and laboratory tests, Figure 9.21. Initial and boundary conditions were obtained referring to tensiometer located at a depth of 1,20m (Figure 9.19) while, the boundary condition at the ground surface, using the climatic data provided by the monitoring station (from December 2001 to July 2002), listed partially in Table 9.1 and reported in full in App. B (Fig. B1).

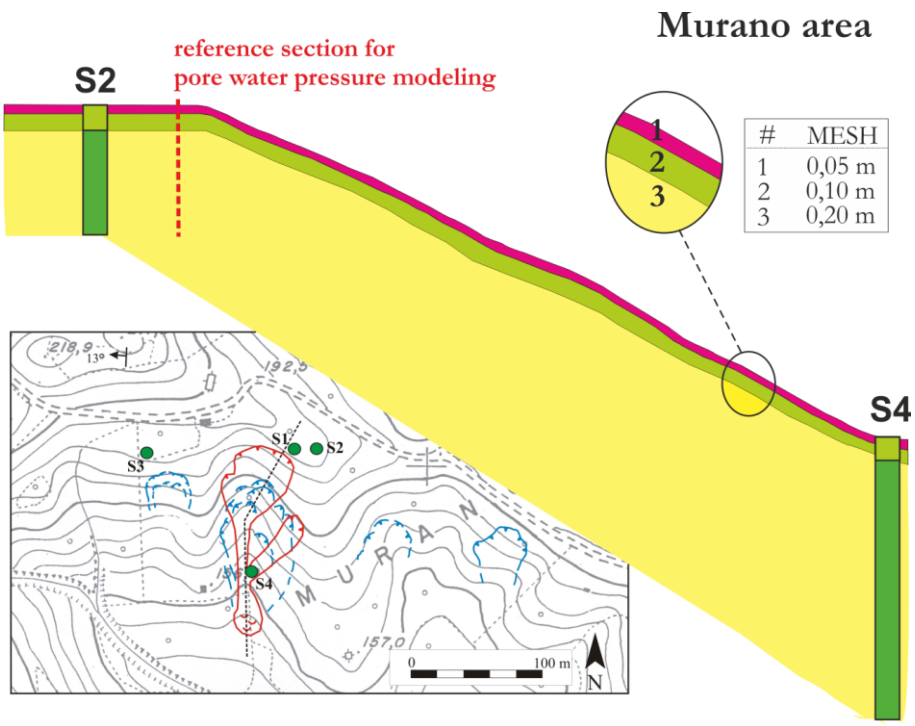

Figure 9.20 Reference section for modelling.

Table 9.1 Boundary conditions applied at the ground surface.

		T (°C)		RH (%)		Wind	P
data	giorno	T max	T min	max	min	(m/s)	(mm)
19/12/01	1	9.5	0.8	62.2	38.8	2.1	0
20/12/01	2	11.9	5.1	71.7	49.3	1.3	0
21/12/01	3	12.2	6.1	89	58.9	2	2
22/12/01	4	12.9	6.3	96.7	60.4	2.9	17.2
23/12/01	5	14.5	7.8	94.6	56.1	1.7	6
24/12/01	6	13.2	6.9	99.7	64.4	2.1	15.2
25/12/01	7	10	6.5	98.2	55.5	2.2	2.8
26/12/01	8	10.6	6.3	93.3	62.6	2.3	0.6
27/12/01	9	10	4.2	92.6	58.3	3.2	30.8
28/12/01	10	10.1	4.2	73.6	42.8	3.6	0
29/12/01	11	13.6	7.1	95.5	71.1	3.2	3.6
30/12/01	12	17.2	11.4	88.4	41.2	4.8	0.2
31/12/01	13	15.3	13.3	92.6	70.4	5.2	0.2
01/01/02	14	13.9	3.3	99.8	20.6	3.3	12

As it concerns the choice of the SWCC, and consequently of the hydraulic conductivity functions that must be associated to each layer in Figure 9.20, the depth of the tested specimens and the index properties of the soil were initially considered. In particular, Figure 9.21, an SWCC was used which is characterized by a high θ value near (ua-uw)=0, up to a depth of 1m, and a low θ value at greater depths. Finally, the lack of knowledge on saturated permeability was solved by developing a parametric analysis taking into account different values of K_{sat}, Table 9.2.

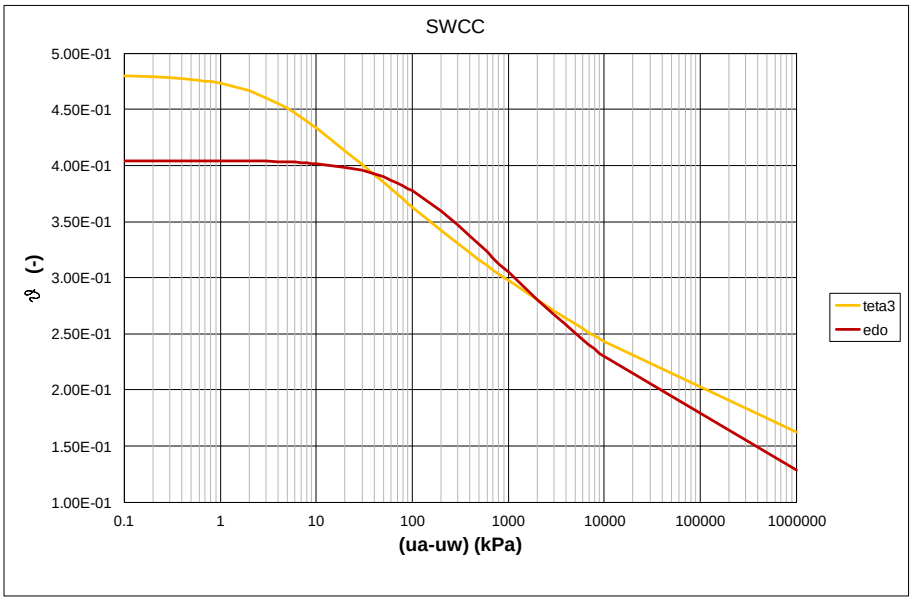

Figure 9.21 The SWCCs used in the first step of modelling.

Table 9.2 Hydraulic parameters.

	Degraded soil	Intact soil
SWCC	teta 2	edoa0212
Ksat	5E-04 m/s - 5E-07 m/s	5E-07 m/s - 5E-09 m/s

In this way, the combination that offers values closer to the trend of the available measurements is represented by Ksat=5e-06 m/s, for the degraded soil, and Ksat=5e-09 m/s for the intact one, Figure 9.22. At any rate, by looking at the diagram in the figure below, it could be reasonably argued that the hydraulic conductivity function obtained through lab tests is not actually representative of the hydraulic response recorded in situ and, with reference to scientific literature, a more

advanced characterization of the degraded and fissured soils is necessary to improve the quality of the modelled data.

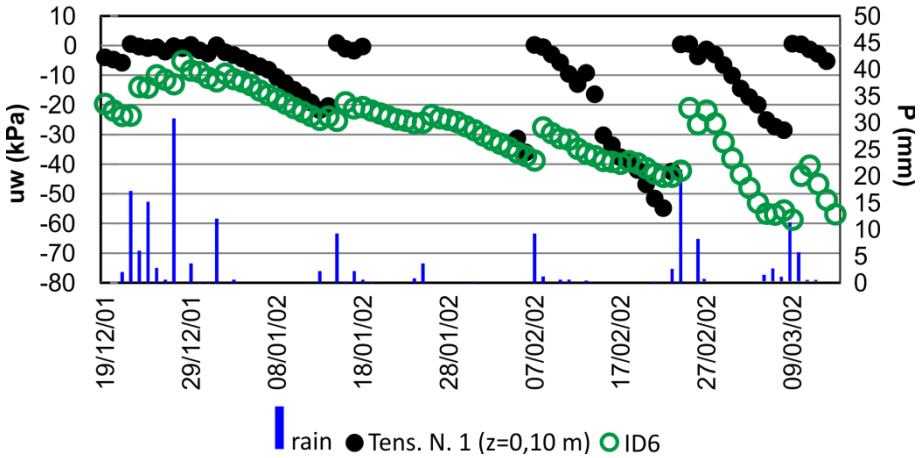

Figure 9.22 Results obtained by modelling. In black measured data, in green modelled data.

9.4.2 Literature review on SWCC for cracked soil

Few papers in literature focus on the unsaturated soil property functions of the cracked soils given the difficulties that such studies require, as clearly stressed by Fredlund et al. (2010). To compensate for such a gap in literature, some authors suggest to use rock mechanics theory dealing with materials containing cracks (Zhang and Fredlund 2004). These authors explain that a fractured rock produces a bimodal material with both matrix and fractured phases; therefore, the output soil-water characteristic curve is the sum of the effects of the two material phases weighted according to their respective porosities (Fredlund et al., 2010).
Other authors superimpose the SWCC obtained for the soil matrix by means of another independent analysis for the fractured portion. The resulting SWCC has also been used to estimate the hydraulic conductivity of a cracked soil (Peters and Klavetter 1988; Mallant et al. 1997; Zhang and Fredlund 2004).
Fredlund et al. (2010) propose the use of a different analysis domain from the scale of the lab soil specimen which is compatible with the presence of fractures and fissures; they identify a representative unit of $1m^3$, they measure the dimension and the spacing of the cracks and

identify both the soil water characteristic curves and the hydraulic conductivity function for the entire cracked soil referring to a bimodal fitting equation, Figure 9.23. In Figure 9.23(A), the soil water characteristic curve is computed by taking into account 1 mm wide at 0.5 cm spacing between cracks; in Figure 9.23(B), the conductivity is estimated by taking into account 0.1 mm wide at 0.5 cm spacing between cracks.

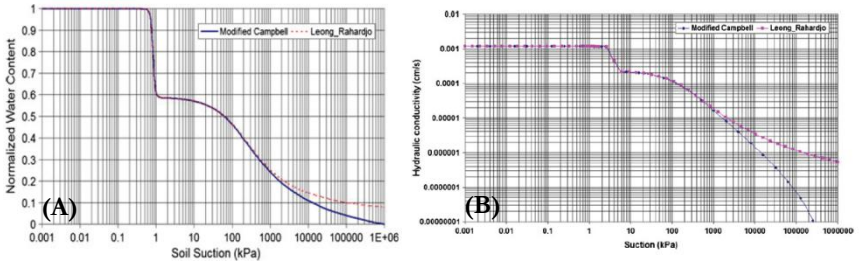

Figure 9.23 (A)Soil-water characteristics curve for fractured clay (1 mm @ 0.5 cm); (B) Soil suction versus hydraulic conductivity for a fractured soil (crack of 0.1 mm wide at 0.5 cm spacing between cracks) Fredlund 2010.

The Figure shows two distinct air-entry values and two residual points on the bimodal SWCCs. Such a behavior is reflected in the hydraulic conductivity function which shows a distinct jump between the facture-dominated material and the intact-dominated material. To this regard, Fredlund et al. (2010) observe that: *"The computed hydraulic conductivity functions for the selected soil crack scenarios studied show that there is an increase of approximately one order of magnitude in hydraulic conductivity when the relative volume of cracks enlarges from 9% to 30%"* Obviously, the air-entry value of the crack-dominated soil is strongly influenced by the widths of cracks. Particularly, Fredlund et al. (2010) found out that the air entry value decreases from 7 kPa to 0.7 kPa when the crack width increases from 0.05 mm to 1 mm.

In order to prove that cracks are paramount especially at more superficial levels, an analogous modelling of pore water pressure regime as the one described in paragraph 9.4.1 has been carried out, modifying the hydraulic conductivity function following Fredlund et al. (2010). However, even the results obtained by using this procedure diverge from actual data, Figure 9.24; furthermore, this modelling does not differ

much from the one previously carried out referring to the hydraulic properties of the matrix.

On the basis of the numerical results obtained, it can be concluded that i) only the bimodal behaviour of the soil which has been hypothesized for low suction values is not representative of the hydraulic behaviour of soils at the scale of mesostructure and ii) further efforts are necessary to properly characterize the hydraulic conductivity function of a fissured soil. This characterization is the preliminary step to develop a proper back analysis of the data recorded in situ, and to forecast the future soil suction trend during wet and dry seasons.

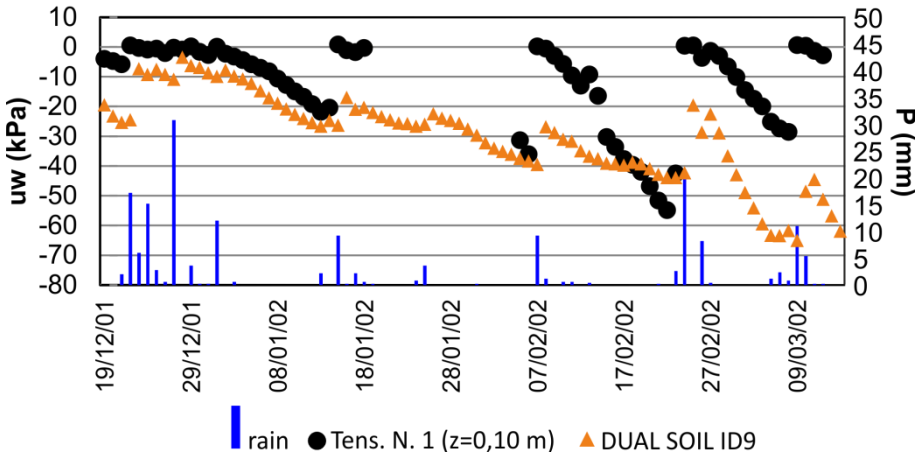

Figure 9.24 Comparison between measured data (in black in figure) and modelled data (in orange) considering bi-modal SWCC.

9.4.3 Proposed hydraulic conductivity function

Section 9.1 stresses that clayey soil is characterized in situ by a diffuse and unpredictable pattern of fissures and fractures which renders the hydraulic characterization of the soil at the scale of the mesostructure extremely difficult.

In effect, the scale of laboratory specimen used to characterize the hydraulic behaviour of the matrix, can provide some useful indications about the changes in the SWCC of samples artificially degraded in lab.

In effect, after one cycle of drying and wetting, the SWCC obtained shows a substantial change in ψ_{aev} (i.e. the soil suction corresponding to

the air-entry value; AEV) which goes from values of 26 kPa (for undisturbed specimens) to values of 13 kPa (for artificially degraded specimens). In addition, a substantial change in the slope of the SWCC for suction values higher than ψ_{aev} can be noted passing from SWCC of the undisturbed sample to that of the artificially degraded sample, Figure 9.26.

Determining the behaviour of the soil becomes even more complex when the dimensions of fissures and fractures are modified as a result of saturation processes which, in some cases, produce swellings (typical of non-collapsible soils) which result in the closure of the fissures.

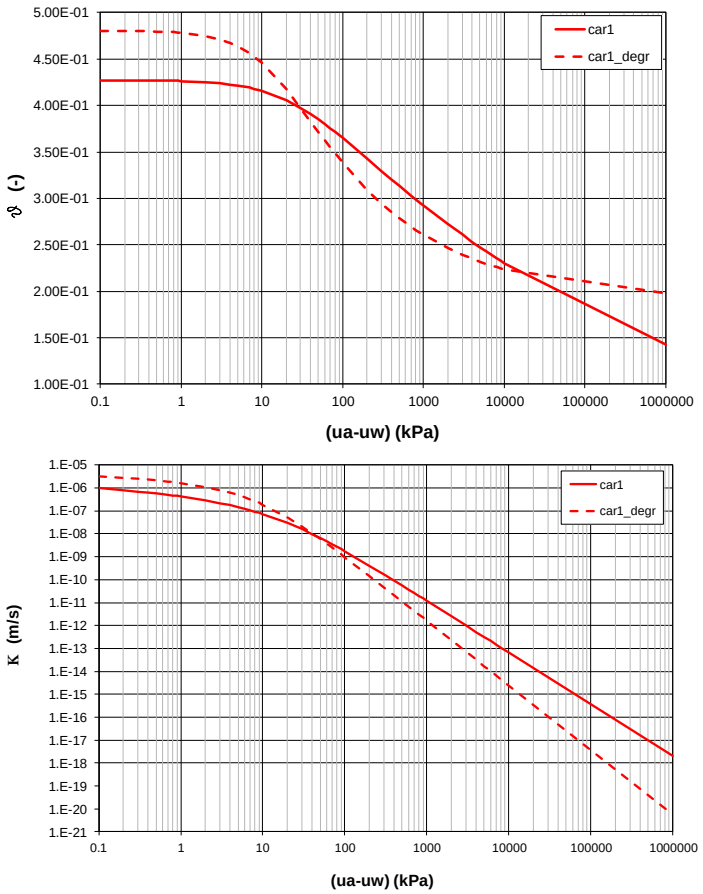

Figure 9.25 SWCCs and hydraulic conductivity functions for undisturbed and artificially degraded sample (car 1 and car1_degr).

Despite all these difficulties, an insight on how these phenomena can affect the soil properties is obtained by observing that the soil reacts quickly even after short rainfalls, with u_a-u_w values next to zero; the desaturation process at the end of the wet period is equally fast.
Generally, for low suction values, the capacity of the soil to absorb water depends on capillarity and, thus, on the distribution of pore dimensions, while for high suction values the specific surface of solid particles conditions the shape of this curve.
In this case, the conductivity function proposed here coincides with the conductivity function obtained on the artificially degraded soil specimen within the suction range 10 and 300 kPa, Figure 9.26.
The proposed conductivity function differs from the previous one in the extreme suction ranges, showing an air-entry value near 3 kPa and lower gradient for suction values higher than 300 kPa. The modification applied to the air-entry value is directly linked to the presence, in situ, of a more complex fissures pattern that can be simulated in the lab. The modification in the final range of the curve (for higher suction values than 300 Kpa) can reasonably be attributed to the fact that, within high suction ranges, the hydraulic behaviour of the soil must be governed by the matrix.

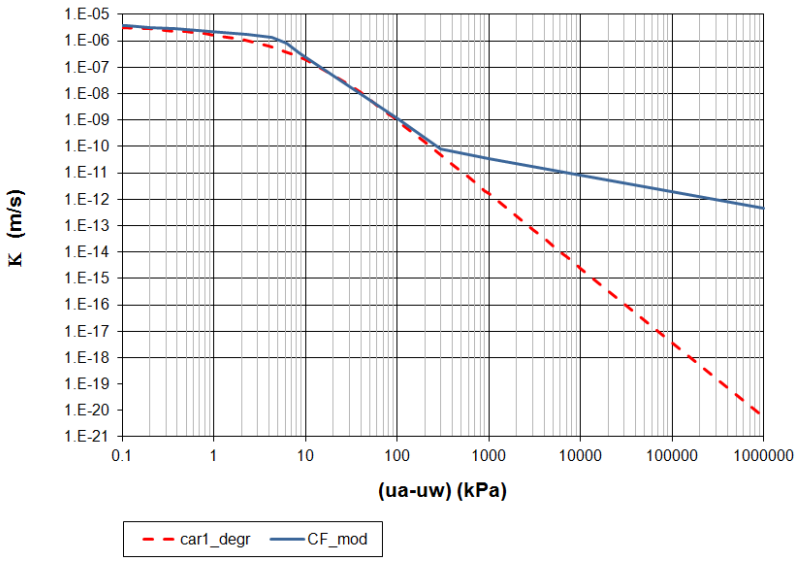

Figure 9.26 Comparison between the proposed hyfraulic conducivity function and the hydraulic conductivity function obtained for artificially degraded specimens.

In order to evaluate the representativeness of the SWCC thus obtained, the modelling of the in situ data has been carried out as previously done in sections 9.4.1 and 9.4.2, developing a calibration, Figure 9.27 (A), and a validation, Figure 9.27 (B). The results obtained reveal that i) the mesured and the simulated data are perfectly compatible with each other, especially in the most superficial layers and ii) they also reproduce the recorded peaks that cannot be modelled otherwise.

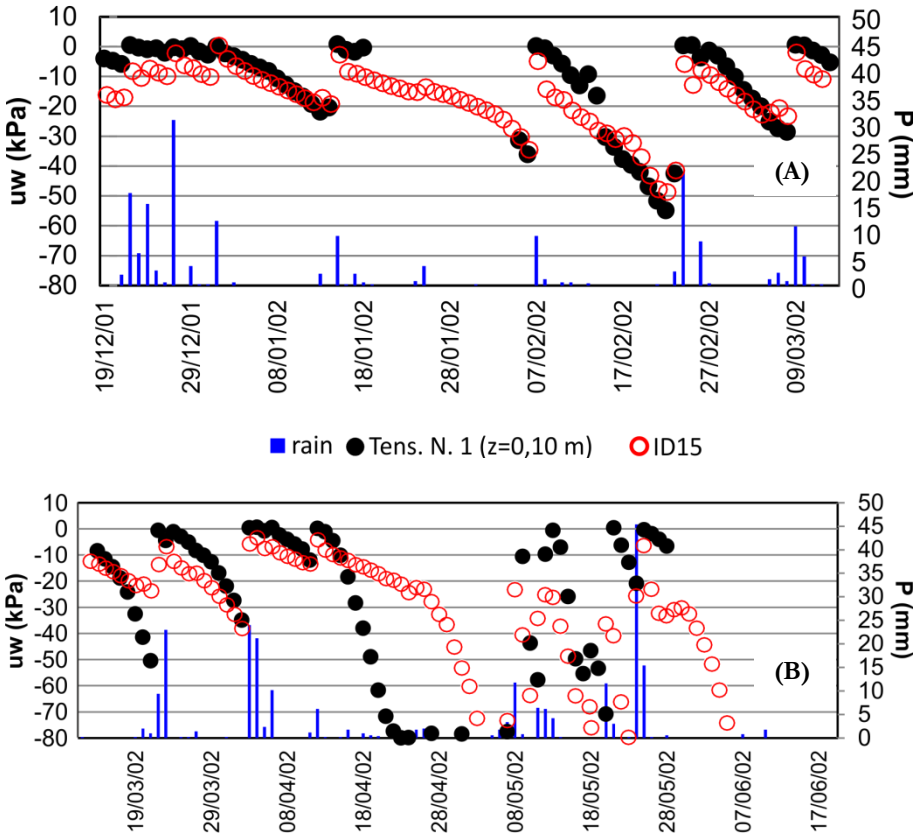

Figure 9.27 Measured and modelled pore water pressure using the proposed conductivity function. (A) calibration, (B) validation.

In order to get further insight on the proposed hydraulic conductivity curve, which seems extremely useful to simulate the behaviour of the soil at slope scale, some preliminary in situ permeability tests have been carried out through a Guelph permeameter, described in chapter 5, and by measuring the suction values by means of the monitoring station. The

permeability at stationary flux conditions has been computed through the "Single-Height", or "One-Ponding-Depth" using Gardner formula (1958) and the Laplace transforms:

$$K_{fs} = \frac{CQ_s}{2\pi H^2 + \pi a^2 C + \frac{2\pi H}{\alpha^*}} \quad (1)$$

$$K_{fs} = \frac{CQ_s}{2\pi H^2 + C\pi a^2} \quad (2)$$

The results obtained with these two equations indicate permeability values equal toK_{fs}=8.17E-07 m/s and K_{fs}=3.70E-06 m/s at stationary flux conditions.

The K_{fs} mesured are close to the saturated permeability value obtained thought parametric analysis. Further indications can be given onces the suction value in situ is known at the time when the test is carried out.On te same date and at the same test depth, the monitoring station registered a suction value of 2,4 kPa (inferior to ψ_{aev}). K_{fs} values measured near these suction values are below and abow the characteristic curve proposed, Figure 9.28.

This figure thus shows a good match between the saturated permeability value estimated on a parametric basis and the data measured.

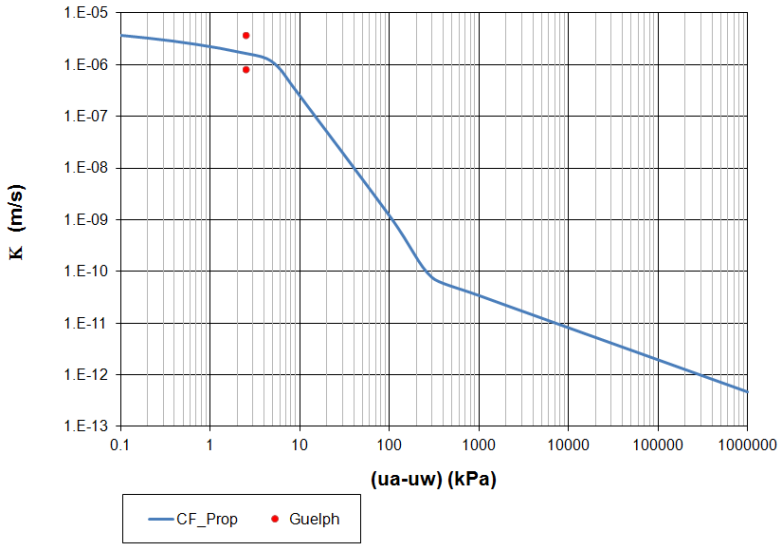

Figure 9.28 The proposed conductivity function (blue line) and K_{fs} values obtained from Guelph test.

10 NUMERICAL MODELLING AND RESULTS

The last stage of Phase II analysis at large and slope scale, which corresponds to the last step of the methodological approach proposed in chapter 4 (Figure 4.1), consists of the modelling of stability conditions to be performed by using i) all the available geological, geomorphological and hydrological information acquired through the analyses at small and medium scale, and ii) through the geotechnical input data provided by the in situ investigations and lab tests, described in the previous chapter.
In order to get the most reliable results, the modelling is preceded by the calibration of the shear strength parameters pursued on the basis of limit equilibrium analyses at slope scale. Then, the physically-based models are used to analyze the stability condition at basin scale, after having calibrated the model on the phenomena occurred in the past. In both cases, a brief description of the most significant theoretical aspects concerning the model used is provided in App. B.
In the present chapter the numerical analysis and the obtained results will be provide.

10.1 STABILITY ANALYSIS AT SLOPE SCALE-ADOPTED PROCEDURE

Chapter 8 individuated three different triggering mechanisms respectively called MORSLE1, MORSLE2 and MORSLE3. Each of these mechanisms is modelled in this chapter referring to both saturated and unsaturated conditions. For this purpose, pore water pressures regime is initially analysed and then used to perform limit-equilibrium analyses. Numerical results are obtained in both cases referring to a representative section for each mechanism on the basis of the available topographic map and the in situ and laboratory data set.

10.1.1 Selection of the most representative slope sections

The elements which contribute to defining the stability conditions of shallow landslides are several and include geometrical aspects, such as the slope angle of the triggering zones, and purely geotechnical aspects, such as the shear strength and the hydraulic parameters of the lithotypes involved. Thus, the geotechnical analyses at large and detailed scales must necessarily investigate the slope geometry factor which, at these scales, must be defined by referring to accurate topographic maps.
To this end, a DTM (5x5m cells) and a DTM obtained by LIDAR (1x1m cells), the latter where available, have been used in an area of about 8 km^2 including the hollows of the University and of the St. Antonio area, Figure 10.1, i.e. the test area at large and detailed scale.

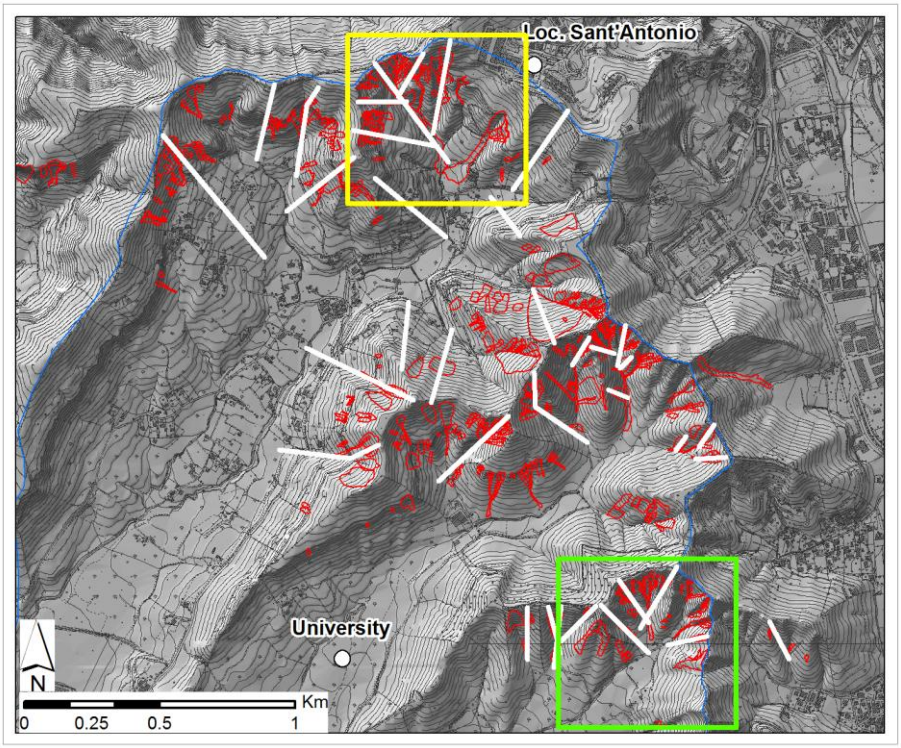

Figure 10.1 The test area at large and detailed scale. DTM (5x5m cells) is available for the area framed with the yellow square, DTMs (5x5m and 1x1m) are available for the area framed with the green square. White lines represent the sections used for the analysis of slope angle.

Here, the slope angle is analysed with reference to fifty topographical sections pertaining to the whole area in Figure 10.1 where all the instability phenomena can occur. The results obtained indicate that for MORSLE1 and MORSLE2 the maximum average slope angle value is about 35°, the mean slope angle is around 30° and the minimum slope angle reaches a value of about 24°. Different values characterize the average slope angle of the sections involved in MORSLE 3 where the maximum slope angle value is around 25°, the minimum value is 23° and the mean value is about 24°, Table 10.1.

Table 10.1 max, min and mean slope angle for a total of fifty sections analysed.

MORSLE 1			MORSLE 2			MORSLE 3		
max	min	mean	max	min	mean	max	min	mean
34.49	23.35	29.18	34.08	24.35	29.82	24.91	23.04	23.84

In order to verify the accuracy of the topographic maps, a comparison of the slope angle provided by these maps and the LIDAR maps has been carried out in the sample area indicated in Figure 10.1 (green border). The results obtained are summarized in Figure 10.2 (A) which highlights the substantial differences in the mean slope angle values. Further differences can be found by comparing the same topographic section obtained by using CTR and LIDAR maps as evidenced in Figure 10.2 (B) which reveals a series of significant changes in slope profile.

(A)

	LIDAR	CTR
Section number	average slope angle	
27	36	27
30	36	29
31	34	27
32	28	21
34	33	28
35	34	24
51	34	31
52	35	28
53	34	27
54	31	26
55	35	31
56	27	22
57	31	26

(B)

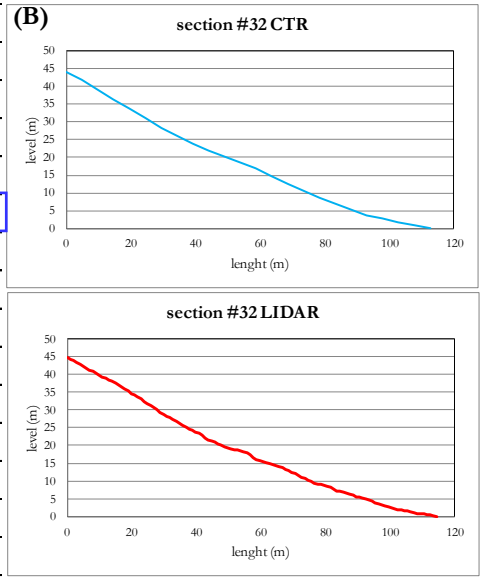

Figure 10.2 (A) min, max and mean values of slope angle for different sections. (B) The section n° 32 obtained using CTR and Lidar data.

On the basis of these results, three different topographical sections, which can be considered representative of the three landslide mechanisms, have been selected and used to develop the limit-equilibrium analysis at slope scale introduced and discussed in the following section.

The topographical sections have been integrated by a typical stratigraphic profile obtained by referring to the available borehole and the observation wells in the area which reveal the presence of two well-defined layers of soils, represented by an intact formation and a superficial degraded material respectively. As far as the thickness of the superficial degraded soil is concerned, different values have been assumed essentially on the basis of the triggering mechanisms analysed and their location along the slope, Figure 10.3.

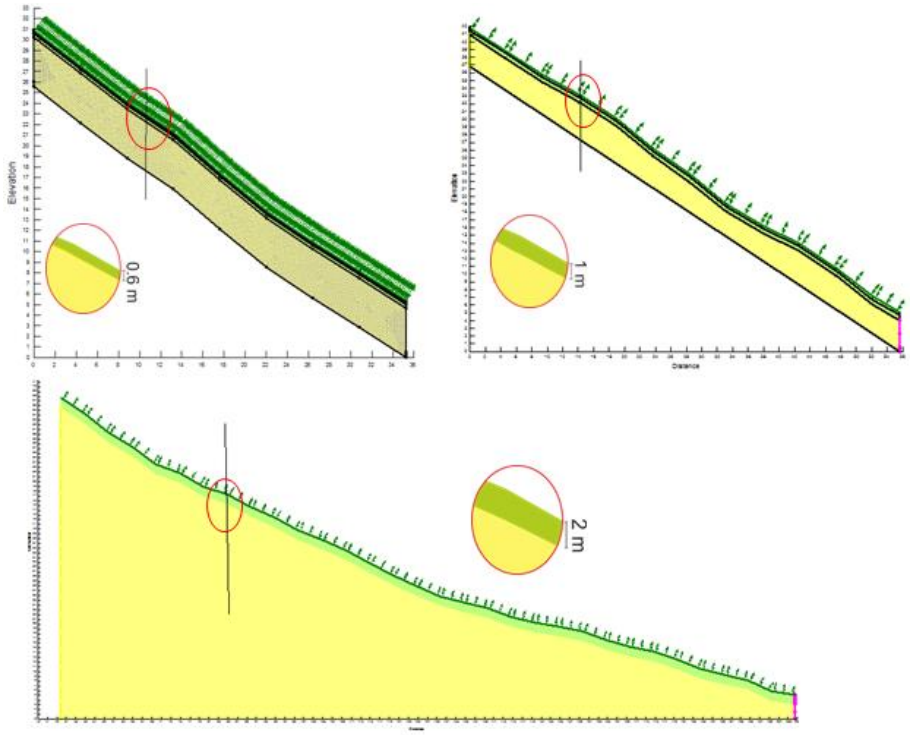

Figure 10.3 Sections considered in the modelling. (numbers specify depths in meters).

The hydraulic and shear strength properties used for each layer as input data in the numerical modelling are listed in Table 10.2 which essentially summarizes the values of the parameters discussed in sections 9.3 and 9.4.

Table 10.2 Mechanical properties of soils.

#	γ	hydraulic properties	Ksat	shear strength properties	
	[kN/m3]	Soil water characteristics curves	[m/s]	c' [kPa]	φ' [°]
degraded soil	18	Proposed in chapter 9	5.00E-06	2.0-8.0	10.0-60
intact soil	20	from laboratory test (edo)	5.00E-09	impenetrable	

10.1.2 Analysis and results

With refererence to the typical stratigraphic sections identified for each triggering mechanism the modelling of the pore water pressure has been performed on the basis of initial and boundary conditions deriving from

the available data set. In particular, these conditions are obtained referring to both i) the data recorded by the tensiometers and the rain gauge in the Murano area (Gullà et al., 2004), Figure 9.20, and ii) the available measurements in the Casagrande piezometers installed in the St. Antonio area (Cascini et al., 2010), Table 10.3

Table 10.3 Pore water pressures measures (Cascini et al., 2010).

Date	S1.P				S2.P				S1.I	S2.I	S3.I
22/4/08	7.7	7.7	17.2	17.2			20.5	20.5	3.75	6.1	12.4
24/4/08	2.8	2.8	13.1	13.1	10	10.05	23.1	23.7	3.7	6.1	12.4
26/4/08	2.8	2.81	13.1	13.1		10.02	22.5	22.6	3.7	6.1	12.4
28/4/08	2.8	2.83	13.1	13.13		10.02	21.8	21.8	3.7	6.1	12.4
30/4/08	2.8	2.85	13.2	13.2	10	10.02	19.65	19.65	3.72	6.05	12.4
2/5/08	2.95	2.95	13.9	13.9		9.96	19.68	19.68	3.75	6.05	12.36
5/5/08	2.91	2.9	14.22	14.2		10	19.72	19.7	3.75	6	12.38
6/5/08	2.9	2.9	14.5	14.5	10	9.98	19.75	19.72	3.75	6	12.38
7/5/08	2.9	2.9	14.73	14.73	10	9.99	19.75	19.72	3.75	6	12.35
9/5/08	2.9	2.95	15.05	15.05		10	19.85	19.95	3.75	6	12.4
16/5/08	2.95	3	16.1	16.1		10	20.1	20.15	3.72	5.95	12.4
23/5/08	2.95	3.05	16.1	16.1		10	20.1	20.2	3.75	6	12.4
4/6/09						9.96	20.12	20.1	2.9	5.1	11.57
24/7/09						9.99	20.15	20.16	3.05	5.22	11.52

As regards the tensiometers, the analysis of data performed in chapter 9 provides pore water pressure values equal to or higher than zero already at a depth of 1.20 m from the ground surface in the wet period going from October to April. Moreover, the data recorded by the most superficial tensiometers (z=0.10 m, 0.15 m, 0.30 m e 0.45 m) clearly evidence quick and significant increases in pore water pressure values, which strongly depend on daily rainfall events (Gullà et al., 2004), as shown in Figure 9.19.

As regards the piezometric measurements performed by Cascini et al. 2010, between April and July, two different ground water tables have been identified; the deepest of which located in the bedrock at a depth of 12-14 m below the ground surface and the other located at a variable depth from the same topographic surface in a range between 2.8 m -7 m.

On the basis of all the available data, the numerical analyses have been carried out essentially considering two different initial conditions called COMB 1 and COMB 2 which assume a groundwater depth of 1.20 m and 2.8 m -7 m from the ground surface respectively.

Boundary conditions at the ground surface have been taken into account by referring to the dates of the rainfall events (1st Jan 2003 and 18th Jan 2003) that triggered multiple shallow landslides in several areas of Catanzaro Graben, for which Gullà et al. (2004) identified critical triggering rainfall having a value of 23-mm during 1-day and a total cumulated rainfall of 43 mm with a total duration of 2 days. By "critical triggering rainfall" Gullà et al. (2004) means the rainfall which is necessary to trigger shallow landslides when particular in situ conditions occur. However, the reconstruction of these initial conditions is a very difficult task and, in the present thesis, they have been estimated thanks to the availability of the data recorded by the monitoring station Table 10.4. The table below shows the climatic data available from 24/11/02 to 18/01/03 which can be used to reconstruct these conditions before the occurrence of a multiple shallow landslides event.
With reference to the first triggering date 01/01/03, the rainfall analysis carried out over the 38 days preceding the landslide shows cumulated rainfall of 200 mm before the triggering event, whereas with reference to the date 10/01/03 the cumulated rainfall preceding the triggering event was 300 mm, Figure 10.4.

Table 10.4 Climatic data.

		T		RH		W	P		
DATA	#	max	min	max	min	(m/s)	(mm)	start	end
24/11/02	1	17.02	12.34	94	61.76	2.3	0	0	24
25/11/02	2	19.46	16.92	94.3	79.8	3.2	0	0	24
26/11/02	3	17.54	16.26	95.3	88.2	3.6	3.8	0	24
27/11/02	4	16.09	13.46	97.6	88.5	3.2	31	0	24
28/11/02	5	19.75	14.09	86.1	59.91	4.8	0	0	24
29/11/02	6	19.26	13.9	94.5	75.2	5.2	0	0	24
30/11/02	7	14.52	11.45	95	76.2	3.3	3.8	0	24
1/12/02	8	12.28	10.13	96.4	83.2	3.9	3.4	0	24
2/12/02	9	15.64	11.25	93.4	71.8	2.4	3.2	0	24
3/12/02	10	13.27	11.32	92.3	75.2	3.6	0	0	24
4/12/02	11	16.65	9.7	82.4	52.79	3.2	0	0	24
5/12/02	12	12.74	9.11	95.1	77.3	2.2	8	0	24
6/12/02	13	12.08	9.8	94.8	77.8	1.9	0	0	24
7/12/02	14	10.5	8.2	94.8	77.8	1.9	22.2	0	24
8/12/02	15	15.74	10.4	88.2	62.67	1.2	0	0	24
9/12/02	16	15.3	9.31	84.4	60.55	1.3	0	0	24
10/12/02	17	14.87	9.21	83.8	63.98	1.6	0.4	0	24
11/12/02	18	16.59	8.98	90.1	57.02	2	0	0	24
12/12/02	19	14.26	8.62	96	70.4	1.9	5.2	0	24
13/12/02	20	14.95	10.92	95.7	78.8	1.2	19.4	0	24
14/12/02	21	16.2	10.17	85.6	63.49	1.6	0.2	0	24
15/12/02	22	16.07	9.55	96	67.44	1.5	4.8	0	24
16/12/02	23	16.09	11.68	96.9	72.2	1.6	5.8	0	24
17/12/02	24	16.12	11.68	85	69.4	1.8	0	0	24
18/12/02	25	13.7	10.6	88.2	62.67	1.9	5.8	0	24
19/12/02	26	13.9	6.3	84.4	60.55	1.2	0.2	0	24
20/12/02	27	10.3	4.4	83.8	63.98	1.6	0	0	24
21/12/02	28	11.3	4.7	90.1	57.02	1.5	0	0	24
22/12/02	29	11.9	7.8	96	70.4	1.6	0	0	24
23/12/02	30	13.5	10.1	95.7	78.8	1.8	0.8	0	24
24/12/02	31	16.9	11.6	85.6	63.49	3.2	0.6	0	24
25/12/02	32	14	10.5	96	67.44	4.8	9.6	0	24
26/12/02	33	13.8	10.1	96.9	72.2	5.2	1.2	0	24
27/12/02	34	15.5	9.3	98.8	78.9	3.3	0	0	24
28/12/02	35	16.3	10.6	94.2	63.29	3.9	2.6	0	24
29/12/02	36	11.9	8.3	89.1	64.71	2.4	14	0	24
30/12/02	37	14.4	10.1	94	61.76	3.2	0	0	24
31/12/02	38	14.5	8.7	98.3	79.8	4.8	22.4	0	24
1/1/03	39	15.2	9.6	95.3	88.2	5.2	25	0	24
2/1/03	40	15.3	10.3	97.6	88.5	3.3	0	0	24
3/1/03	41	15.1	11.5	86.1	59.91	3.9	1.2	0	24
4/1/03	42	15.2	11.8	94.5	75.2	2.4	0	0	24
5/1/03	43	14.2	9.8	95	76.2	3.2	11	0	24
6/1/03	44	13.4	9.4	96.4	83.2	4.8	0.6	0	24
7/1/03	45	12.8	8.3	94	61.76	5.2	21.4	0	24
8/1/03	46	14.8	8.3	89	79.8	3.3	0.8	0	24
9/1/03	47	13.2	8.9	95.3	88.2	3.9	4	0	24
10/1/03	48	13	7.4	97.6	88.5	2.4	5	0	24
11/1/03	49	14.4	6	86.1	59.91	3.9	14.4	0	24
12/1/03	50	12.28	7.04	90.4	57.83	2.1	0.6	0	24
13/1/03	51	9.83	6.447	91.9	71.6	0	0.2	0	24
14/1/03	52	12.82	5.325	89	49.79	0	0	0	24
15/1/03	53	13.88	5.722	77.2	57.39	0	0	0	24
16/1/03	54	14.34	8.16	82.4	64.31	0	0	0	24
17/1/03	55	12.41	8.22	92.7	56.27	0	6.8	0	24
18/1/03	56	16.98	9.83	97.8	55.6	0	28.8	0	24
19/1/03	57	15.5	9.5	94.2	62.83	0	10.2	0	24

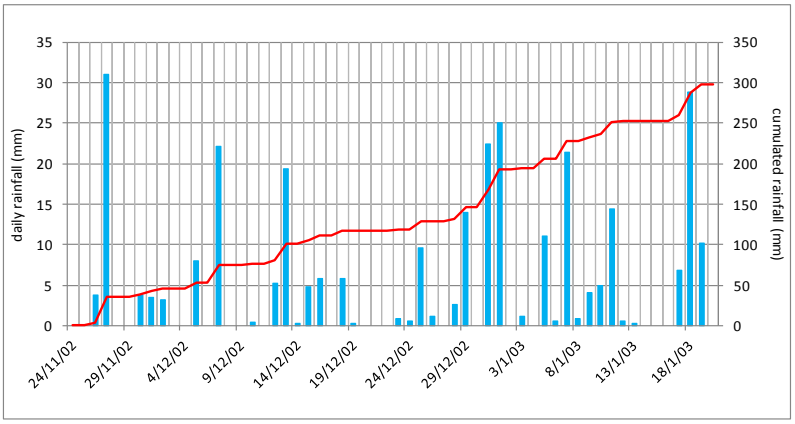

Figure 10.4 *In-situ* measured rainfall.

Therefore, specific analyses to model the critical pore water pressures regime have been performed using: the selected stratigraphic sections, COMB1 and COMB2 as initial conditions, and the climate data, previously defined, as boundaries conditions. In particular, the analysis of pore water pressure regimes performed with reference to COMB 1 shows that, for all the three mechanisms, the water table rise up to the ground surface on both triggering dates.

Instead, the pore water pressure modelled in COMB 2 evidences the formation of a suspended water table up to a depth of 1 m for MORSLE 1 mechanism, while the pore pressures trend shows a range of negative values up to a depth of 0.50 m, beyond which, and until a depth of 1.20 m, pore water pressures assume predominantly positive values for MORSLE2, Figure 10.5.

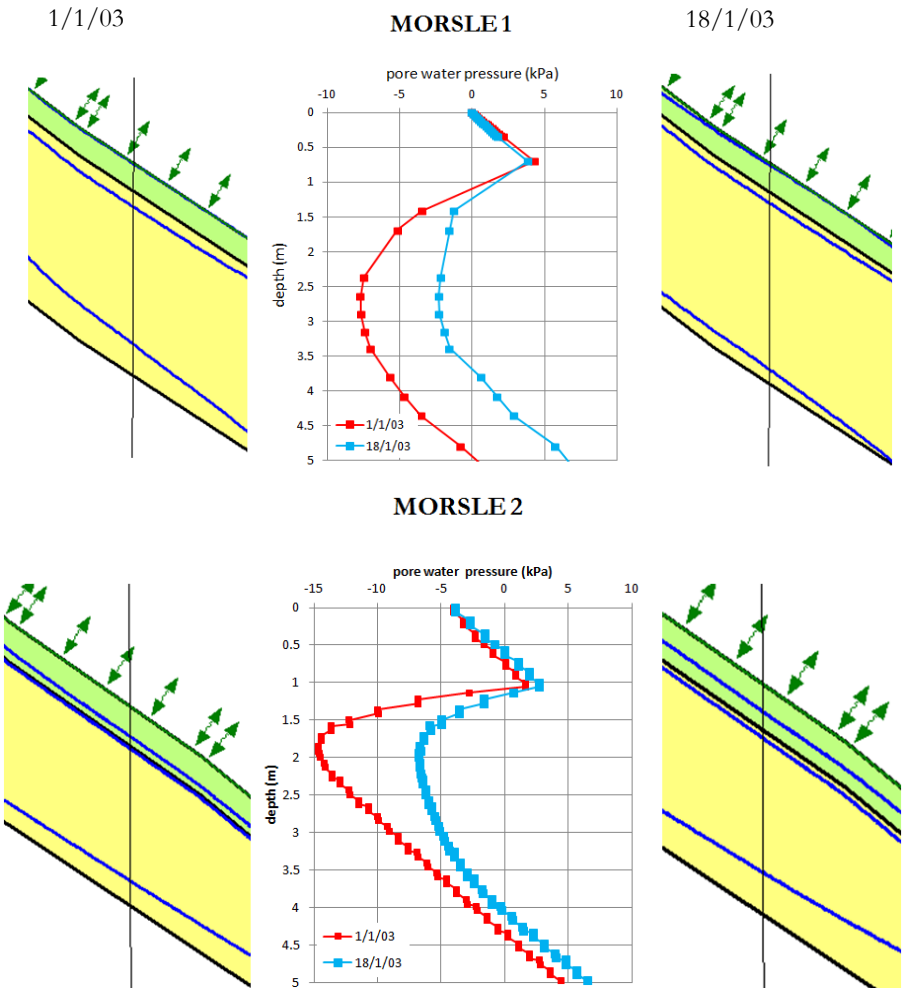

Figure 10.5 Pore water pressure analysis: MORSLE 1 and MORSLE 2.

For MORSLE 3 mechanism, it must be underlined that two layers considered in the stratigraphic section do not show any significant rise in water table resulting from a rainfall regime compatible with the triggering conditions and, as a consequence, no triggering conditions can be simulated in the slope.

For this reason, a new stratigraphic section has been developed for the deepest mechanism which, according to some in situ evidence is formed by three layers having the hydraulic characteristics listed in Table 10.5.

Table 10.5 Mechanical properties of soils

#	hydraulic properties	
	Soil water characteristic curve	Ksat [m/s]
1	Proposed CF	5.00E-06
2	Proposed CF	5.00E-08
3	From laboratory test (edo)	5.00E-09

The modelling performed taking these three layers into account shows a rise in water table up to depths between 0.5 m and 1.0 m, thus a mean depth of 0.80 m from ground surface can be assumed in the following analysis, Figure 10.6.

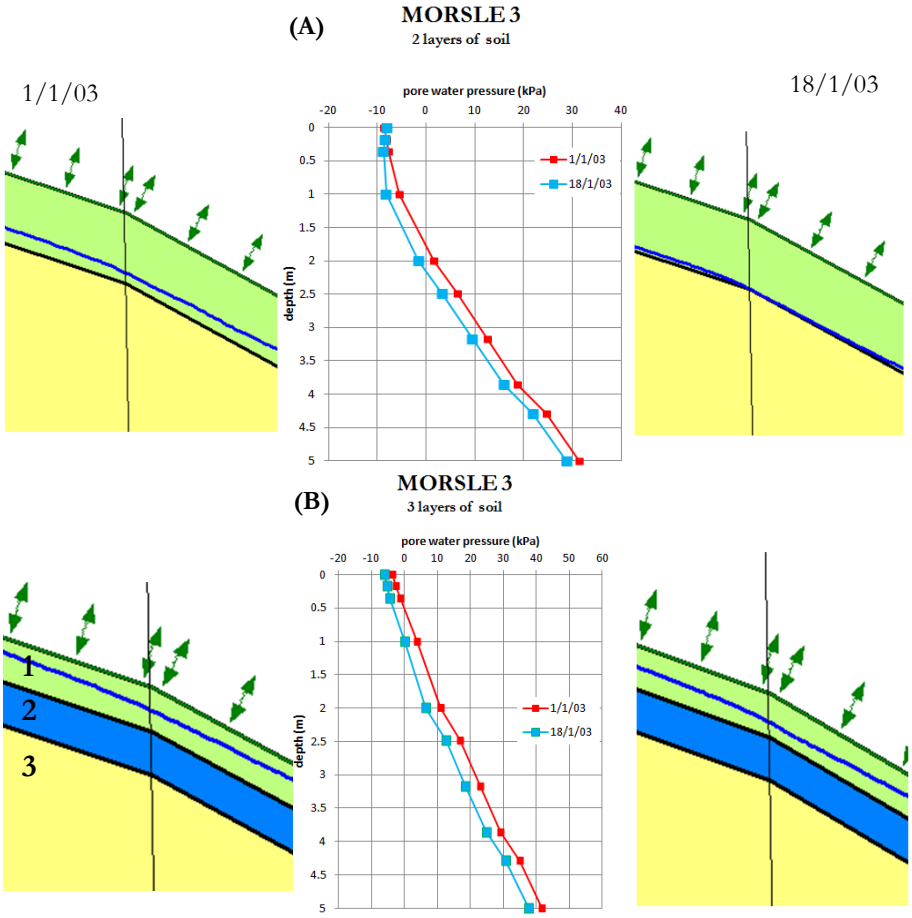

Figure 10.6 Pore water pressure analysis: MORSLE 3 (A) two layers of soil, (B) three layers of soil.

On the basis of the groundwater modelled for the three reference mechanisms, the next step is represented by the calculation of the mean values of shear strength parameters (c', φ') which are activated along the slip surface during the critical events. For this purpose a parametric back analysis of past reactivations events has been developed with the aid of limit equilibrium methods. Particularly, using the rigorous method proposed by Morgenstern and Price implemented in the code SLOPE/W ,distributed by GEO-SLOPE International Ltd. (LAM et al., 1987), the shear strength mobilised along the slip surface has been estimated in both saturated and partially saturated conditions extending Mohr-Coulomb criterion, as proposes by Fredlund et al. (1978).
For the sections examined, the soil layers have been considered homogeneous, isotropic and characterized by the mechanical and physical properties listed in Table 10.2.
The analyses have been performed using i) the critical water table previously calculated in correspondence with the critical triggering scenarios, ii) considering a friction angle of 27° compatible with the average of the available data set and varying effective cohesion c' in the range 2 and 8 kPa, which is representative of highly degraded covers, Figure 10.7.

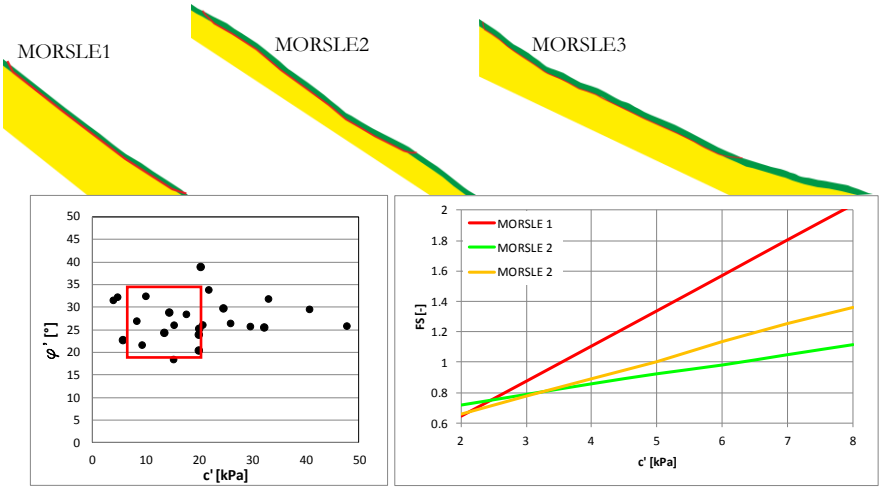

Figure 10.7 Slope stability analysis. (A) Available data set (B)Factor of safety versus cohesion.

As regards more superficial mechanisms, MORSLE1 (surface depth of 0.50 m) and MORSLE2 (sliding surface located at 1.0 m) limit-

equilibrium conditions (FS=1) are obtained for a cohesion value in the range c'=3-5 kPa. As regards MORSLE 3 mechanism, with a sliding surface at a depth of 2 m, the condition FS=1 is obtained for c' equal to 7 kPa. It is interesting to observe that the values obtained for c' seem to be compatible with a soil profile that is characterized by a degradation stage decreasing with depth from the ground surface.
In order to investigate the role of the friction angle in limit equilibrium conditions, a stability analysis has been performed once more fixing a cohesion value of 5 kPa and varying the friction angle of the material, (Fig. 10.8).
Figure 10.8 shows that the most superficial mechanism (MORSLE1) always reaches FS>1 for cohesion values equal to 5 kPa even for friction angle lower than 10° (which are neither compatible with the lab tests available, nor with reference to the materials artificially degraded by Gullà (2005).
MORSLE2 e MORSLE3 reach limit equilibrium conditions(FS=1) for friction angles respectively of φ'=25 and φ'=28°.
In conclusion, all the analyses performed indicate that these types of shallow landslides are strictly related to the degradation process and, particularly, to the influence of this process on the cohesion value rather than on the friction angle. Moreover, the pairs of values for which F=1 well fit the minimum value provided by Gullà et al. (2005) for the specimens artificially degraded in the laboratory.

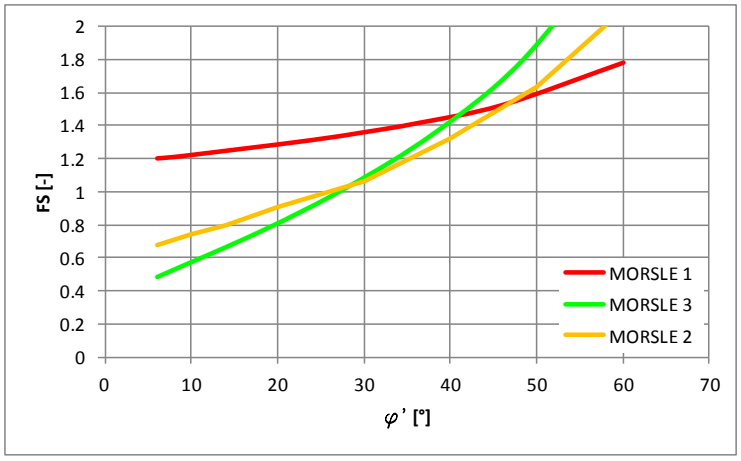

Figure 10.8 Slope stability analysis. Factor of safety versus friction angle.

10.2 STABILITY ANALYSIS AT LARGE SCALE

The results obtained at slope scale have been used to identify the input parameters necessary for large scale modelling. The analysis of stability conditions of this kind of phenomena at large scale has been performed using physically-based models which generally couple a hydrological model, for the analysis of pore water pressure regime, with an infinite slope stability model for the computation of the Factor of safety (Ward et al. 1982, Montgomery and Dietrich 1994, Dietrich et al. 1995, Terlien et al. 1995, van Ash et al. 1999, Baum et al. 2002, Savage et al. 2004).
According to this approach, groundwater modelling is devoted to the estimation of pore water pressure regime; then, the resulting pressure values are used to compute the Factor of Safety by means of one of the Limit Equilibrium Methods.
They can be conceptually classified with respect to the assumptions of the hydrological model used to compute pore water pressures (Fig. 10.9).

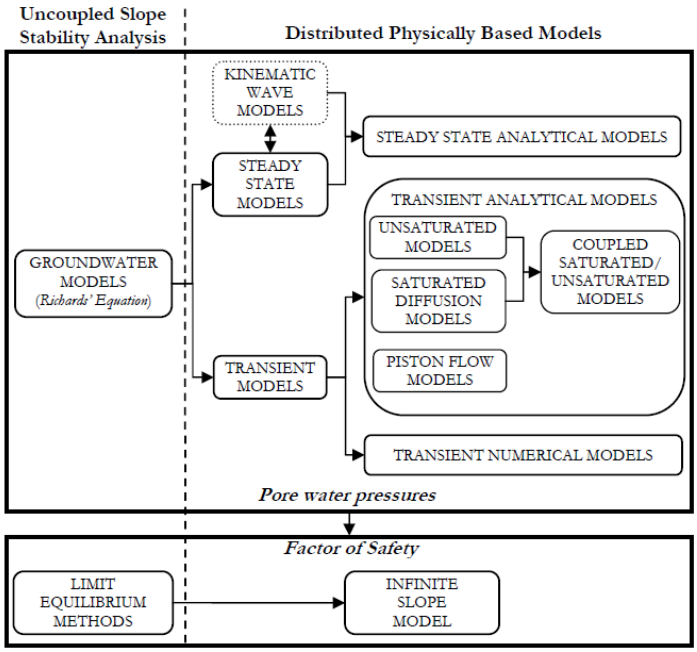

Figure 10.9 Physically based models.

Generally, physically-based models for pore water pressures modelling use steady-state analytical models, transient analytical models and

transient numerical models. Others use Richards' one-dimensional equation for pore water pressure modelling, others are based on the kinematic wave theory.
The greatest advantage of such models rests in the fact that they are grid-based methods which makes them easy to use also with GIS (Geographic Information Systems).
Among the physically-based models available in literature are: SHALSTAB (Montgomery & Dietrich 1994), SINMAP (Pack et al. 1998), dSLAM (Wu & Sidle 1995), TRIGRS (Baum et al. 2002) and TRIGRS unsaturated (Savage et al., 2004). Here the focus will be on TRIGRS and TRIGRS unsaturated which show high potentialities due to their conceptual and operational features (Sica, 2008).

10.2.1 Input data

The TRIGRS model divides the territory examined into cells of variable dimensions, depending on the accuracy of input data and calculates the distribution of pore water pressures and the factor of safety at different depths for each cells. Such computation requires the knowledge of a series of elements including topographic, geological, geomorphological, stratigraphic and hydrological features and typically geotechnical features such as shear strength parameters, hydraulic parameters, initial pore water pressures condition, and climatic factors such as rainfall intensity.

Topography With regard to this aspect, already introduced in paragraph 5.1, the data used are a DTM (5mx5m) taken from the technical regional map and a DTM (1mx1m) obtained through a LIDAR survey. In both cases, DTMs from which errors such as cell depressions or pit artifacts have been eliminated must be used. The accuracy of the DTM highly influences both elevation and other DTM-derived parameters, such as slope angle, which is considered significant for the analysis of shallow landslide triggering (Fig. 10.10).
Figure10.10 shows the slope map obtained for the same morphological hollow starting from two different DTMs obtained through CTR (5mx5m) and LIDAR (1mx1m). The first data tend to locally underestimate the slope angles, whose maximum slope value is no greater than 40°.

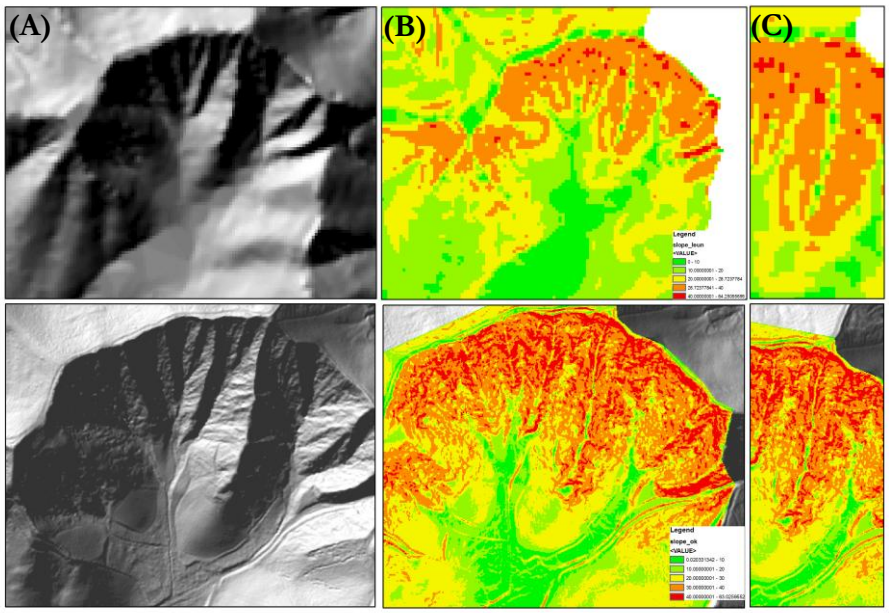

Figure 10.10 Cartographic database. (A) DTM, (B) Slope, (C) zoom Slope.

Geology and Geomorphology. The two hollows investigated, as discussed in detail in ch. 8, are composed of clayey soils in which the most superficial layers are physically degraded and directly involved in shallow landslides. The distribution of the degraded soils at large scale is paramount for triggering conditions modelling.
In terms of geomorphological data, they include both the alternation of hollows, and locally open slopes and the distribution of past landslides, cracks, discontinuities and all the morphological features characterising the landscape.
Geotechnics and Hydrology. As it regards the mechanical characterization already performed via in situ and lab tests, par. 9.3, it has been integrated with parametric analyses at slope scale through LEM. Such analyses have allowed to select the shear strength parameters of the soils in limit-equilibrium conditions.

The hydraulic characterization has been performed through lab tests (on both undisturbed and degraded samples) integrated through the modelling of pore pressures regime over time, par. 9.4.
The hydraulic parameters of the soil are those which significantly influence physically-based models. In the TRIGRS-based analysis the parameters considered are only saturated permeability values and θs already calculated at slope scale analysis, while TRIGRS-unsaturated considers θs, θr, ksat, $D(\psi)$.
With regard to the hydrological features, surface runoff and precipitation trend are necessary for the stability analysis at large scale. However, TRIGRS and TRIGRS-unsaturated are not suitable for modelling long-term effects of alternating periods of rainfall and evapotranspiration, and choosing the correct initial conditions for a given rainfall event is fundamental in order to obtain accurate results. For this purpose, as the initial condition, a water table at the contact between degraded and intact soil was considered. As the boundary condition at ground surface, with reference to the triggering dates already investigated at slope scale, a rainfall intensity of 43 mm in 2 days for the entire study area has been taken into account, as estimated by Gullà et al. (2004).

10.2.2 Results of TRIGRS analyses

The results provided by TRIGRS and TRIGRS unsaturated give detailed information on the limit-equilibrium conditions of the triggering mechanisms analysed.
In particular, TRIGRS modelling clarifies the role that each parameter plays in the definition of limit equilibrium conditions and highlights the strict relation between the soil cover thickness map and the results obtained. Given the relevance of the degraded soil cover, on the basis of the results obtained, an original method is proposed in this thesis to develop reliable soil cover thickness map only using simple and available input data.
Finally, TRIGRS unsaturated allows to establish the influence that hydraulic parameters have on the outputs of the numerical analysis performed.
The most significant scenarios resulting from TRIGRS and TRIGRS unsaturated applications are now going to be introduced and discussed.

10.2.2.1 Preliminary parametric analysis (1:5000)

The first TRIGRS analyses have been performed on the basis of the available dataset and the back analysis at slope scale, discussed in the previous section, which provides a reference value of 5kPa for the cohesion values and 27° for the friction angle. Moreover, the water table has been taken as the initial condition at the contact with the intact soil, i.e. the condition which is compatible with all the available data. Instead, the hydraulic parameters used in the modelling are: K_{sat}=5.0E-07m/s and D=3.49E-05m^2/s.

As regards the thickness of the degraded soil, a constant depth of 5 m has been associated to the areas at the toe of the slope, while at the top of the slope a parametric modelling has been performed associating constant soil cover of 2 m, 1.0 m, 0.5m, Figure 10.11.

The results obtained show that, regardless of the conditions considered, the landslides occurred in 2009-2010 are systematically undestimated or overestimated and no differences arise if a ponding condition is reached along the slope.

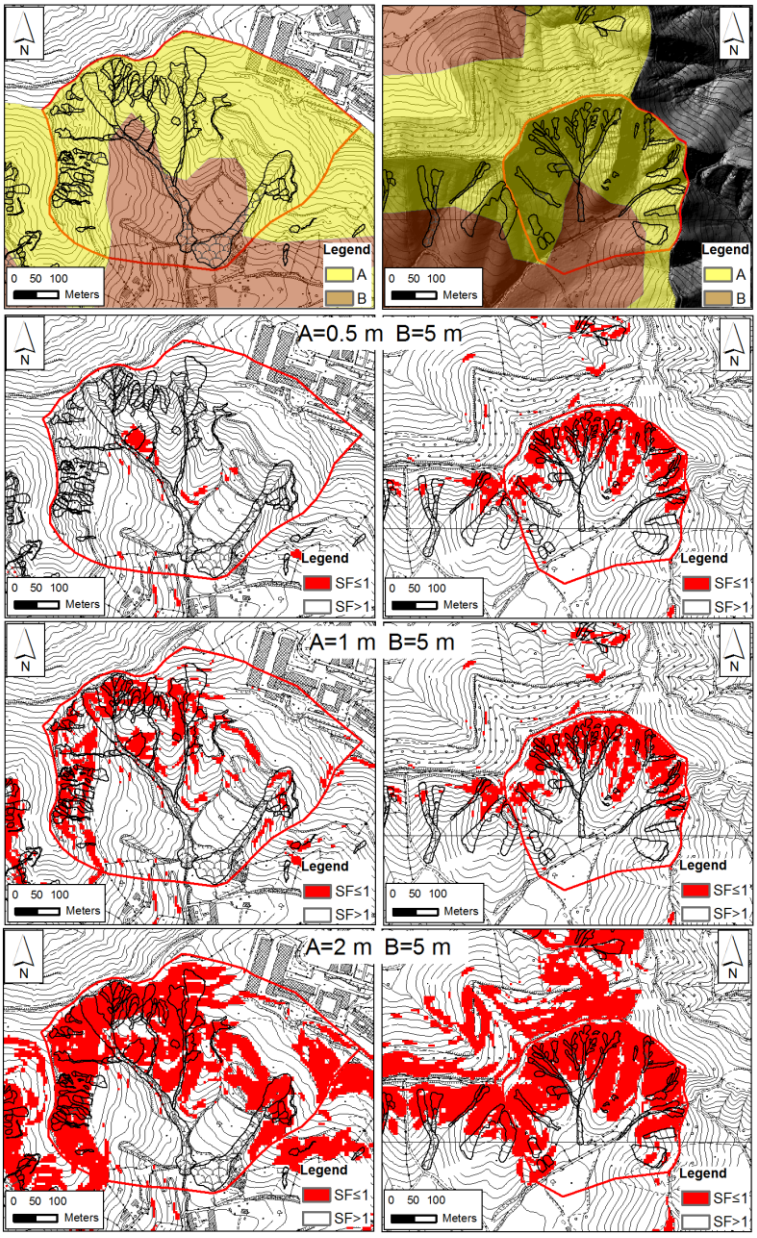

Figure 10.11 Soil cover thickness map and TRIGRS results.

10.2.2.2 Analysis based on the triggering mechanisms (5000)

Given the influence that the soil cover thickness map has on the results provided by the modelling, some criteria must be identified in order to obtain the most accurate soil cover thickness map possible.

For this purpose, from a morphological point of view, a significant distinction can be made between hollows, ridges, and locally open slopes that can be characterized by different degraded thickness. Another distinctive factor can be obtained by referring to the topographic maps and, specifically, to the distance between two following level curves. In particular, level curves that are very close to each other indicate steeper slopes along which the degraded soils are particularly thin. On the contrary, very distant curves are typical of highly degraded soils often made up of deposits coming from the top of the slope.

The soil cover thickness map obtained on the basis of these criteria, Figure 10.12, is characterized by a 0.80 m thickness near the top of the slope, while this thickness increases as the distance between the level curves increases. On the left part of the map, a zone of thickness equal to zero is localized which corresponds to the morphoselection scarp.

At the toe of the slope, where the level curves tend to be very distant, the degraded thickness considered can reach values of 5m.

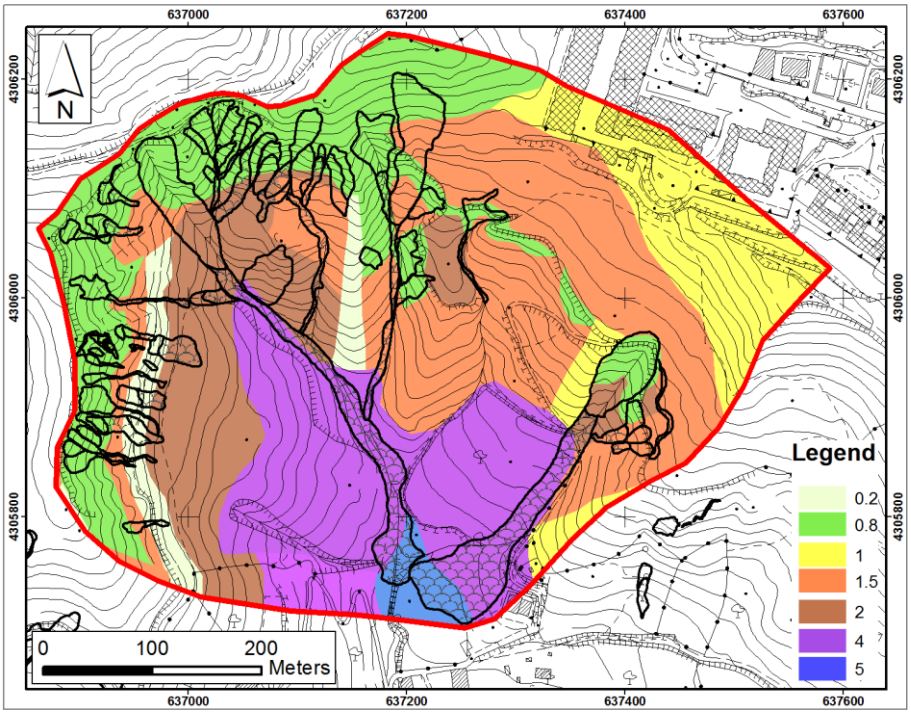

Figure 10.12 Soil cover thickness map (numbers specify depths in meters).

The analysis performed, on the basis of the same shear strength and hydraulic parameters previously considered as input data, shows a significant variation in the numerical results highlighting, in general, a better match between the landslides inventory and unstable cells modelling with TRIGRS, Figure 10.13.

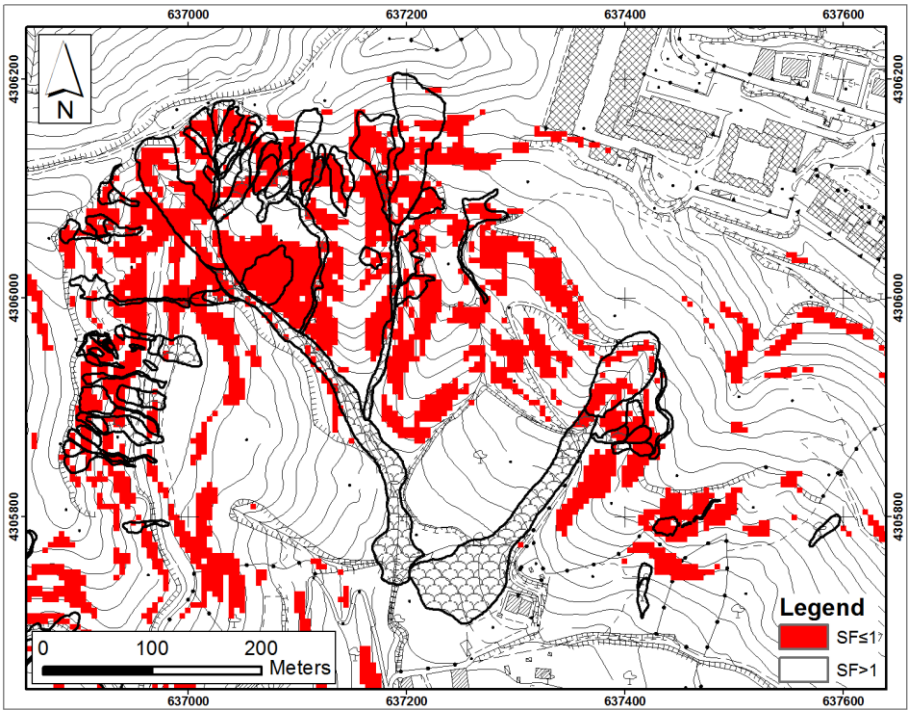

Figure 10.13 TRIGRS results.

In order to quantify the reliability of the analysis performed, following the suggestions given by Sorbino et al. (2007), two percentage indexes named "Success Index (SI)" and "Error Index "EI", have been introduced, Figure 10.14, and used referring to the event occurred in the period 2009-2010. For each source area, SI is the portion (in percentage) of the observed source area computed as unstable by the models and, in this case, is equal to 54%. The EI represents the percentage ratio between the areas computed as unstable located outside the observed triggering areas (*Aout*), and the area not affected by triggering phenomena (*Astab*); in the case studied, it is equal to 19%.

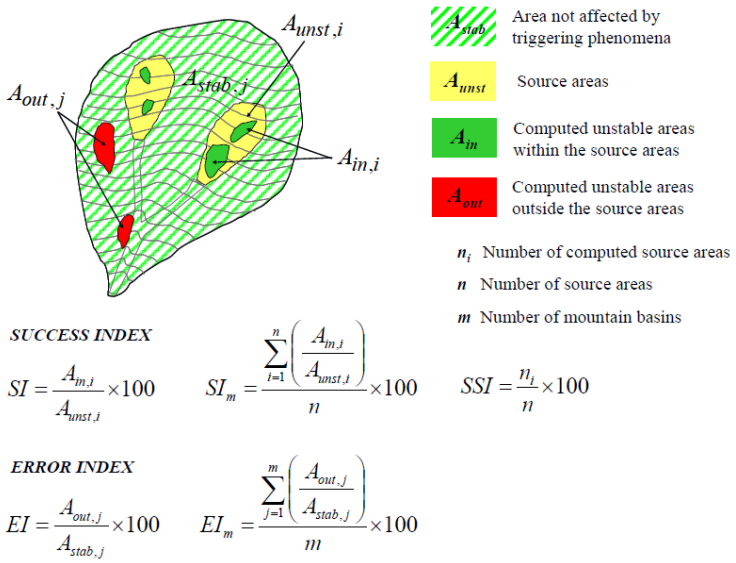

Figure 10.14 Quantitative indexes (Sorbino et al., 2007).

10.2.2.3 Analysis based on in situ investigations and triggering mechanisms (1:5000 scale)

In order to improve the quality of the numerical results, the soil cover thickness map realised on the basis of the criteria previously described has been validated by means of in situ investigations carried out with the use of a steel bar, a low-cost apparatus described in chapter 5.

In this way, 200 verticals were easily investigated, Figure 10.15 (A), thus allowing the compilation of a soil cover thickness map that modifies the thickness hypothesized in the upper part of the morphological hollow, Figure 10.15 (B).

The numerical analysis performed on the basis of this soil cover thickness map, and the same parameters previously introduced, shows an increase in success index being SI equal to 65%, while the EI decreases to 15% (Fig. 10.16).

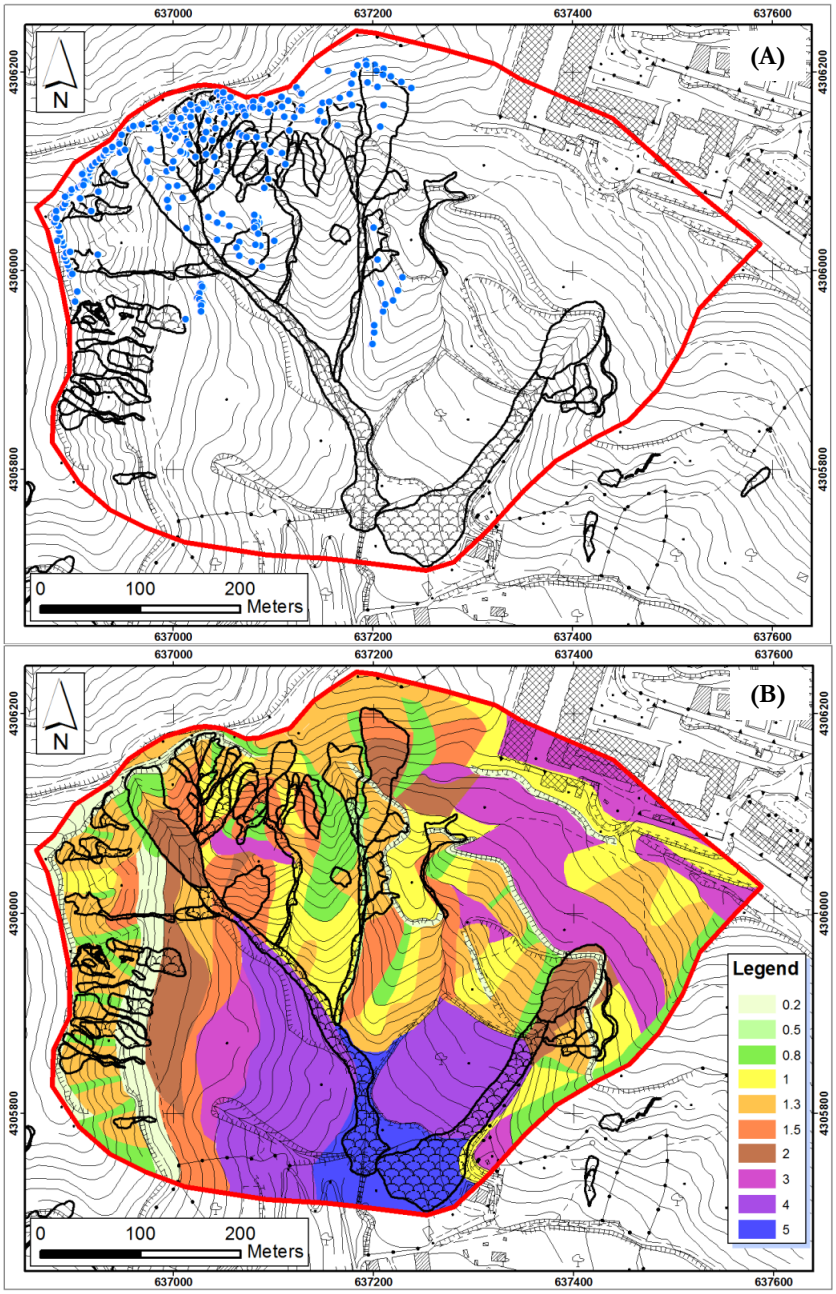

Figure 10.15 (A) Investigated verticals, (B) soil cover thickness map obtained.

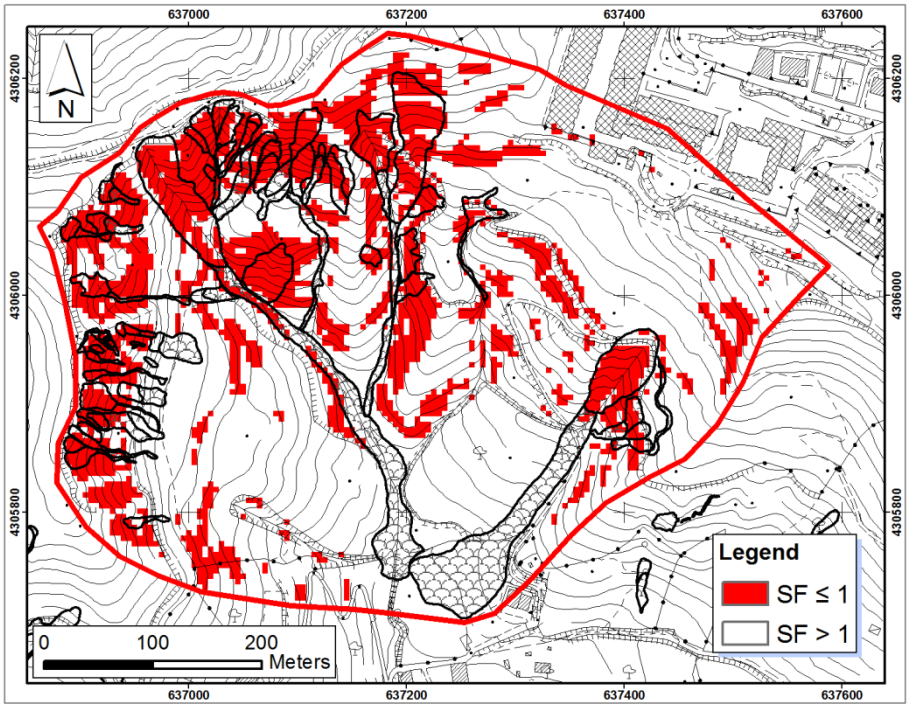

Figure 10.16 TRIGRS results. SI=65% and EI=15%.

The numerical analysis has been repeated assuming i) a friction angle of 27° and cohesion values between 2 kPa - 10 kPa and ii) a cohesion value of 5 kPa and a friction angle between 20°and 40°.
For each combination of shear strength parameters, the SI and the EI have been calculated obtaining the diagram in Figure 10.17

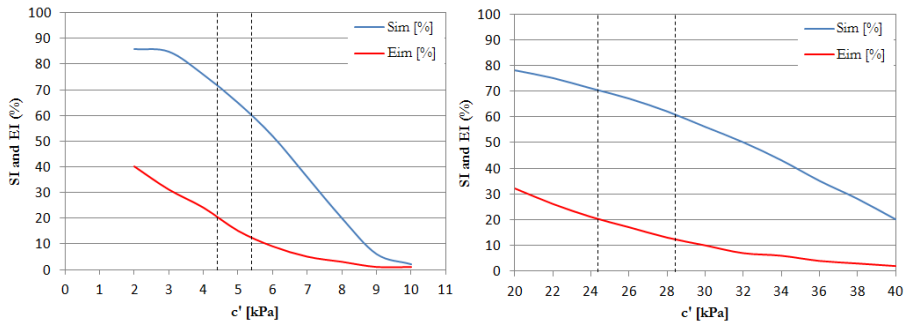

Figure 10.17 SI and EI values versus cohesion and friction angle.

It is interesting to observe that the values of c' and φ' which provide the best results, characterized by a SI over 60% and an EI below 20%, are respectively given by c'_p=4.2 kPa - 5.5 kPa and φ'_p=24° - 28° and fall within the range provided by the laboratory tests.
Finally, with reference to the triggering mechanisms, the highest SI and the lowest EI values are obtained by assuming c'_p=5 kPa e φ'_p=26°. Moreover, Figure 10.18 shows that the best results are obtained for MORSLE2 and MORSLE3 that are essentially related to the slope angle and to sub-surface runoff, i.e. the factors taken into account in TRIGRS.

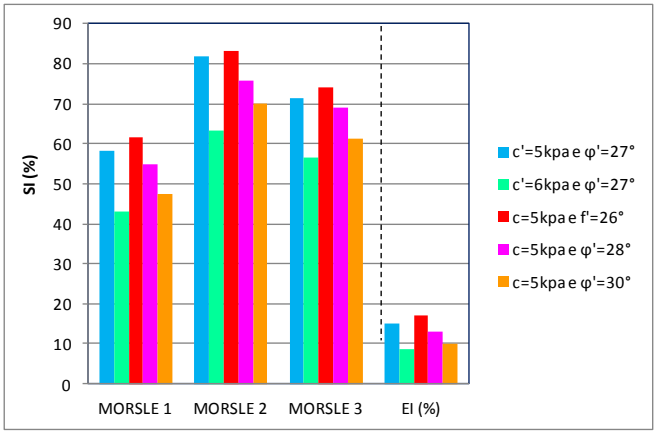

Figure 10.18 SI and EI values versus landslides mechanisms.

10.2.2.4 Analysis based on in situ investigations and triggering mechanisms (1:1000 scale)

In order to test how the accuracy of the topographical maps influences the results obtained, the analysis previously described has been repeated using a DTM deriving from an accurate LIDAR at 1:1000 scale. On the basis of this DTM, the soil soil cover thickness map developed following the criteria previously illustrated, Figure 10.19 (A), shows thickness of 0.30 m along the main ridges which tends to assume a value of 0.50 m in the upper part of the hollows and progressively increases down slope from 0.70 m to a maximum of 2 m in depth.
This analysis has been developed using the following input data:

- c'_p=5 kPa and φ'_p=26°, i.e. the shear strength parameters that at 1:5000 scale provide the highest success index and the error index below 20%;
- hydraulic parameters similar to those of the previous cases.

Figure 10.19 (B) highlights a substantial overestimation of the results obtained which could be related to the elevation and slope angle errors that can be considered typical errors in high resolution LiDAR DTM.
On the basis of this consideration, the soil cover thickness map thus created has been subsequently validated through in situ investigations similar to those performed a 1:5000 scale. Figure 10.19 (C) indicates the localization of 80 verticals investigated over an area of about 18,000 m^2. A comparison between the soil cover thickness map developed before and after the in situ investigations is shown in Figure 10.19 (A) and Figure 10.19 (D) and highlights a good match between the thickness hypothesized and that measured in the upper part of the slope. A less satisfactory match can be observed in the lower part of the slope, which, at any rate, is of no interest for the analysis of the stability conditions for shallow landslides.

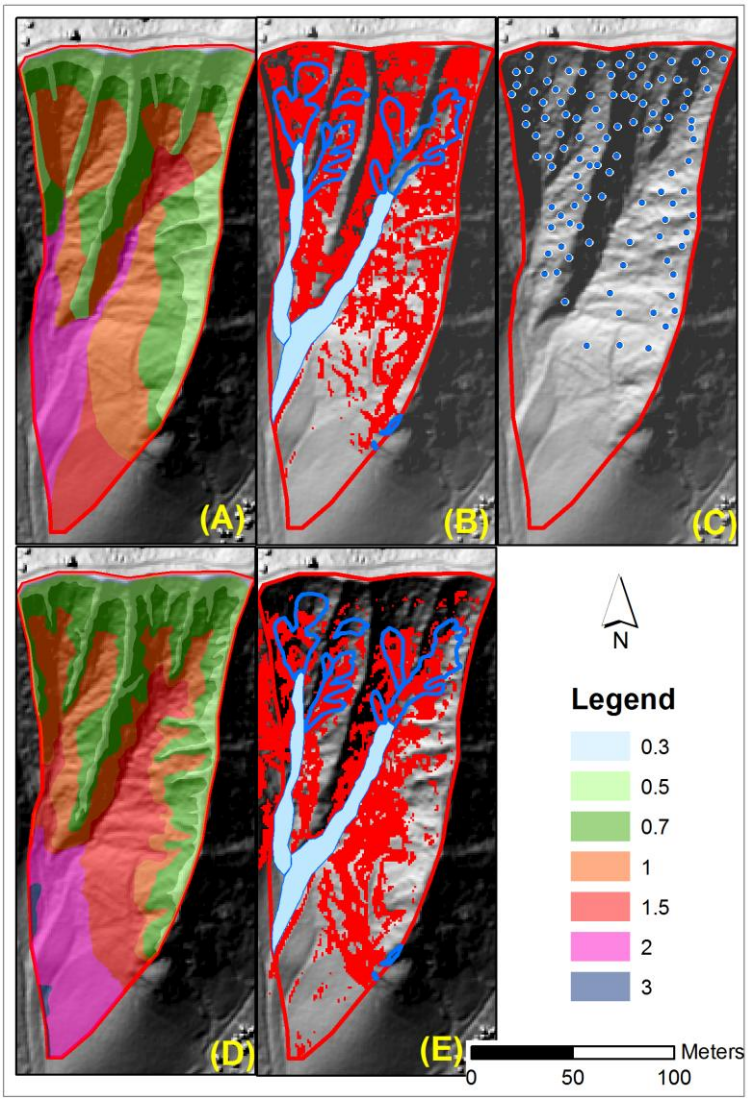

Figure 10.19 (A) and (B) soil cover thickness map ante *in situ* investigation and TRIGRS results, (C) Verticals investigated, (D) and (E) soil cover thickness map post *in situ* investigation and TRIGRS results.

The results of the modelling obtained using the new soil cover thickness map still shows a high overestimation of the mass movements that are likely to occur in areas where a diffuse pattern of deep cracks can be observed This last observation seems to indicate that the adopted procedure can be better used for the back analysis of shallow landslides

and, at the same time, to forecast the new ones, as a consequence of possible future critical rainfall events. From this point of view, the maps obtained should be considered as susceptibility shallow landslides maps rather than inventory maps.

10.2.3 Results of TRIGRS-unsaturated analysis

TRIGRS-based modelling allowed to identify the criteria for the creation of a soil cover thickness map and to perform a back analysis of shear strength parameters (c'=5kPa e φ'=26°) typical of the triggering mechanisms of shallow landslides for which a higher SI value and an EI lower than 20% can be obtained.

Strating from these results, and in order to determine how unsaturated conditions influence the triggering mechanisms of these phenomena, a TRIGRS-unsaturated modelling is carried out. Such modeling uses the same data as before, however it considers different hydraulic parameters values which nonetheless fall within the range calculated through lab test results, Table 10.6.

Table 10.6 Parameters used for the modeling (Catanzaro).

Unit weight	Effective cohesion	Friction angle	Soil Depth	Hydraulic conducivity	Diffusivity	θs (-)	θr (-)
γ (kN/m^3)	c' (kPa)	φ' (°)	h trigrs (m)	K (m/s)	D TRIGRS_unsaturated (m^2/s)		
18	5	26	variable	5.00E-07	1.68E-06 - 8.12 E-06	0.49	0.10

The modeling performed with reference to both morphological hollows shows the influence of the diffusivity value on the overall results obtained considering D=8.12e-06 m/s as the most significant value since there is a good match between these results and what can be observed in situ (Fig. 10.20A).
The comparison between the results obtained with the two models seems to show that while TRIGRS unsaturated identifies the landslides occurred, TRIGRS seems able to estimate the susceptibility to shallow landslides (Fig. 10.20 A,B).

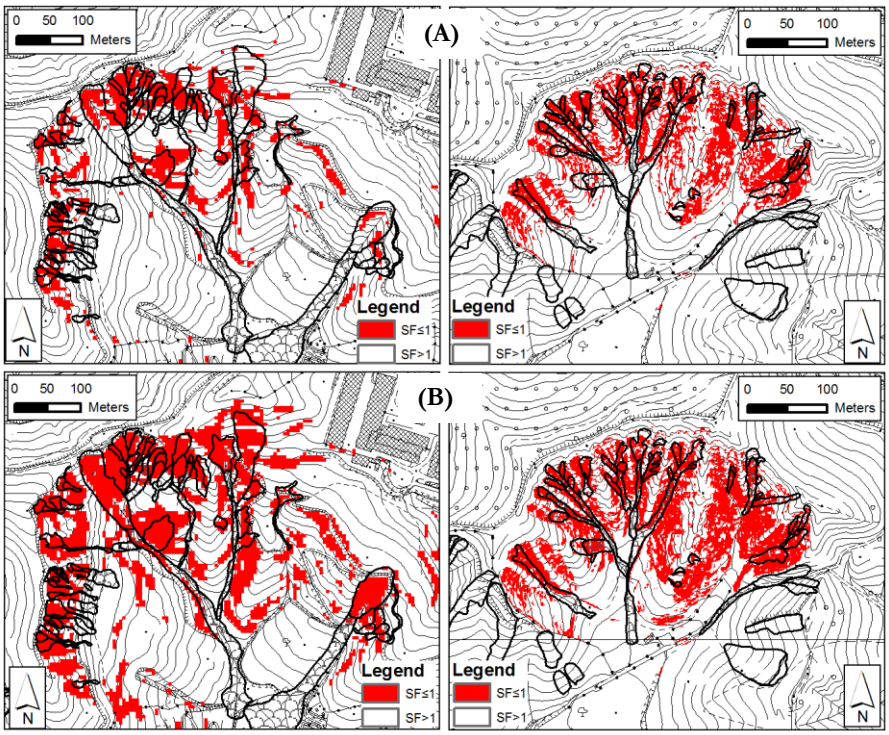

Figure 10.20 TRIGRS results. (A) Results obtained thought TRIGRS unsaturated, (B) Results obtained thought TRIGRS.

11 CONSIDERATIONS AND FUTURE DEVELOPMENTS

Few papers in literature address the analysis of shallow landslides in fine-grained soils and this is probably due to both the complexity of these phenomena and the little consideration given to their consequences, which seem to be less significant than those caused by the landslides occurring in collapsible soils very often resulting in human losses.
The lack of a single, universally accepted term to describe the same event, for which the expressions shallow landslides, soil slips, translational slides, etc. are interchangeably used, confirms the fact that little research is available on these events. The only term used to indicate the diffusion of these events at large scale is the acronym MORSLE, multiple occurrence regional shallow landslides events, proposed by Crozier (2005).
Also, the specific materials involved in such events, i.e. non-collapsible, physically weathered fine-grained soils, are never discussed in a substantial and systematic way in any of the works consulted. Only the weathering process is introduced and discussed sporadically. At any rate, no general indication which can be useful to investigate the triggering mechanisms is provided.
Finally, the lack of methodological proposals for the analysis of these events, aimed at providing a susceptibility zoning of shallow landslides, must be pointed out. Susceptibility zoning is instead carried out through either mono-disciplinary approaches or at a single scale of analysis.

The work carried out in this thesis is aimed at compensating many of the gaps in this field of research, although it cannot offer exhaustive solutions to all the issues concerning shallow landslides. To this end, the present work firstly proposes a multi-scalar approach, going from small (1:100,000) to slope scale (1:1000), following other authors who have used this approach to study landslides characterized by a medium-large magnitude (Cascini et al., 2008).
The main objective of this methodology is the identification of both the predisposition factors and the triggering causes of shallow landslides

through the combined use of regional, slope and REV scale analyses able to harmonize the geological and geomorphological studies at small scale (1:100,000) with the typical or advanced engineering modelling at large (1:5000) and slope scales (1:1000). To reach this goal, this thesis proposes a deductive methodology which starts with the identification of the predisposing factors and ends with the analysis of the triggering causes at large and slope scale.
At each scale, the analyses are carried out developing two distinct phases, respectively called identification and quantification, and the output of the preceding scale becomes the input of the following one in order to validate each single step and the whole procedure proposed.
The essential elements of the procedure, its primary aim, together with the other aims pursued in the present work are now going to be summarized and the most likely developments in the near future are going to be illustrated.

11.1 SMALL AND MEDIUM SCALE ANALYSIS

Within the procedure proposed at small scale, aimed at identifying the factors predisposing the morphological evolution of the area where shallow landslides can occur, regional geological features are very important.
Referring to the study area located in the Calabria region, southern Italy, some works evidence the presence of **tectonic structures** of the first order inside the area, delimiting morphological and structural sectors with a different uplift rate (Ghisetti 1979, Sorriso et al., 1991) and the consequent formation of the main morphological graben and horst.
On the other hand, the analysis of the main **outcropping lithotypes** in every sector examined leads to a selection of the study area which has been mainly affected by shallow landslides which are not visible, and thus unmappable, at this scale, but which are represented by symbols with attributed characteristics.
The structural and geological aspects of the study area have been further investigated in this thesis by examining their role in the development of the stream network that, together with the factors previously mentioned, play a role in the geological and morphological evolution of the entire study area.

The quantification of the predisposing factors identified through weighted values, and their potential concomitant occurrence, subsequently enabled the quantification of each factor and their potential combination in each part of the studies area.
At small scale, the important features of the study area are represented by regional morpho-structures separated by the main tectonic lineations along which the main rivers flow.
At medium scale (1:25,000) these features are evident in the typical profile of the reliefs which clearly show the influence of the evolutionary tectonics of the same reliefs. These reliefs will require further geomorphological and structural investigations. Such investigations, coupled with a knowledge of the distribution of the areas affected by shallow landslides, contributed to the definition of the predisposing factors of the evolution of the reliefs, and the role played by these factors at this scale has been determined through the identification of an evolutionary and morphological model of the same reliefs. Once acquired and re-interpreted, all these elements allowed to single out the morpho-structure with the greatest concentration of shallow landslides mainly located within well-defined morphological hollows formed as a result of the interfering perpendicular fault planes and the consequent erosion of talwegs.
Such processes can easily occur in geological contexts similar to the one under scrutiny. By contrast, the analysis that must be performed in different situations, and the themes to be considered, may vary from those proposed here if the objective is the definition of the typical aspects which predispose an area to shallow landslides. The quantification of the predisposing factors through quantitative procedures (as suggested by Fell et al., 2008) nonetheless remains urgent and necessary.

11.2 LARGE AND DETAILED SCALE ANALYSIS

The predisposing factors discussed in the previous paragraph have been further analysed at large and detailed scale in the attempt to understand their influence on morphological hollows and, consequently, to identify the triggering mechanisms of such landslides.

The analysis at these scales allows to identify the diagnostic elements that are characteristic of shallow landslides and to classify them on the basis of the different types of phenomena observed. In the study area, three common triggering mechanisms called MORSLE1, MORSLE2 and MORSLE3 have been identified.
For these mechanisms, the key instability factors have also been found through the combined use of geomorphological and hydro-geological studies, and of geotechnical models. Indeed, the geomorphological and hydro-geological analyses underline the importance of causal factors which, depending on the slope morphology, emerge as responsible for high or low degradation.
The distribution and depth of cracks pattern in the study area highlight the degradation process in space, while some observation wells can clarify the distribution of the depths of cracks in the most degraded thickness.

In particular, being the exposition and solar irradiation equal, MORSLE1 mechanism occurs on a open slope marked by a straight surface and subsurface drainage along the highest slope direction which is responsible for the degradation of the most superficial thickness up to a depth of 0.80 m.
MOSLE2 is typical of very narrow morphological hollows characterized by a convergent surface and subsurface runoff towards the main drainage line, where the overall degradation process is very high.
MOSLE3 is typical of wider morphological hollows characterized by a radial convergent surface and subsurface runoff towards the main drainage line, where the degradation process is very high and influenced by lateral runoff. Consequently, the degraded layer is 3 m deep.

These mechanisms differ in terms of areas, volumes involved and run-out, and their distribution in the hollows is not causal. They can be identified through an evolution model of the hollows which can be developed by means of geological analyses. Such analyses will subsequently be quantified via common geotechnical models.
The prerequisites for the application of such models are, respectively, the availability of: a map of degraded thickness as accurate as possible; geotechnical data referring to the shear strength parameters of the materials involved; hydraulic parameters representative of the soil behaviour at the scale of study. Specifically, in the latter case, the

measurement of pore water pressures in situ over a sufficiently long time is particularly relevant for estimating a seasonal variation trend.
Input data, which in turn allow to investigate in depth the stability conditions at large scale, can be acquired thanks to the proposed methodology, even in the absence of detailed in situ investigations. Of course, the accuracy of the database strongly influences the modelling results.
Given the relevance of the soil cover thickness map to reach this goal and the lack of proposals in literature for the creation of this map, the following sections focus on: the map of thickness for the study area on the basis of limited information; the analyses at slope scale providing the fundamental elements for a more advanced map of thickness; and the potentialities of the proposed methodology which can provide significant results in areas that are completely different from the test area studied in this thesis.

11.2.1 A methodological proposal to develop the soil cover thickness map

As already noted in the previous paragraph, the influence of the degradation process on landslides becomes even clearer starting from an initial modelling which does not take into account the evolution of the hollow, but which refers to constant degraded thickness marked by different values in the most important sections of the hollow (top part of the slope and valley bottom). The input data for these analyses and the results obtained are shown in paragraph 10.2.
Better results can be obtained considering that, given the same climatic parameters, degraded thickness is significantly influenced by the reliefs morphology and by the role that the latter plays on surface and subsurface runoff. In particular, in the case of locally open slopes, a straight surface and subsurface runoff running along the main slope direction occurs, which is generally responsible for the formation of low degraded thickness. In the case of morphological hollows, the surface runoff is convergent facilitating the degradation process with the consequent formation of more degraded thickness. Finally, in the cases of ridges, the divergent surface and subsurface runoff entails the formation of very low degraded thickness.
It can be argued that the depth of degraded thickness with the same morphology increases the more one moves from the top of the slope

towards the bottom where the soil coming from the slope is usually deposited.
Within such a context, slope is inversely proportionate to the degraded thickness since very steep slopes usually present modestly degraded thickness, while gentle slopes indicate the presence of significantly degraded thickness.
These observations are usually confirmed when the exact location of the triggering mechanisms is found; they can also benefit from an accurate topographic map which clearly shows the alternation of hollows, ridges and open slopes. Large scale maps, such as those obtained through LIDAR, can be considered fundamental from this point of view.
The map of thickness thus obtained can be further improved through in situ investigations which allow the calibration, validation and exportation of this map. These investigation must be simple but accurate and must take into consideration the events which have affected the area in the past.
Using this map, large scale modelling has been carried out through the use of TRIGRS and TRIGRS unsaturated, which both show a good correlation in terms of success and error indices respectively with reference to both the parameters used for the modelling previously discussed and the single triggering mechanisms.
The results obtained, Figure 10.20, show that TRIGRS unsaturated model identifies the landslides occurred in the past in the study area, whereas TRIGRS appears to overestimate landslide areas. Such an overestimation may be due to partial saturation conditions that persist until the original condition of the slope has not been significantly modified. In contradistinction, high instability, together with a cracks pattern, may influence the pore water pressure regime as a result of the change in saturated permeability value at the scale of macrostructure. Within such a purview, TRIGRS-obtained results seem to offer a representation of the overall development of the area and, for this reason, they may be taken as an estimate of slopes susceptibility to shallow landslides.
This deduction can be easily verified by simply observing the evolution of the landslide in the studied hollow over the time.

11.2.2 Detailed and REV scale

In situ investigations and lab tests show that the degradation process and the progressive development of a cracks pattern modify the shear strength parameters of the clayey soils (Gullà et al. 2006) as well as the hydraulic parameters (Fredlund et al., 2010) of the lithotypes affected by shallow landslides.

Given the typical features of the lithotypes under investigation, the experimental program carried out (see chapter 9) included a series of tests on intact samples and on samples artificially degraded in lab. These tests led to the identification of the variation bands proper of SWCCs. Back analyses of the pore water pressures data coming from the tensiometers installed have been carried out to calibrate the results obtained in the lab. These analyses have been supported by permeability measurements performed in situ with Guelph permeameter.

The conductivity function, modified during the modelling, is very different from the one available in other works, yet its shape and the gradient identified make it compatible with the actual behaviour of such a complex soil. Indeed, the results obtained show a good match between the pore water pressure data measured by the monitoring station and those modelled with VADOSE/W code (Figure 9.27).

Furthermore, the interpretation of the mechanisms identified at slope scale in section 8.2 was performed by a back analysis, initially modelling the pore water pressure regime and after the limit-equilibrium conditions of the slope. The results of these analyses give fundamental indications on the shear strength of these complex soils such as degradation soils, for which long and difficult in situ and lab tests are not sufficient.

Ultimately, the data obtained revealed that complex events such as shallow landslides – involving soils which are difficult to characterize though traditional methodologies– must be necessarily examined by applying a complete methodology which balances the experimental and the modelling phases using either traditional or cutting-edge procedures.

11.3 APPLICABILITY AND FUTURE DEVELOPMENTS

11.3.1 Applicability of the proposed procedures (New Zealand case study)

The potentialities of the proposed methodology can be verified in a different area than the one considered in this thesis. For this purpose, an area in New Zealand has been chosen, which is systematically affected by multiple landslides events triggered by rainfall such as the one occurred in February 2004 which caused from thousands to ten thousands of landslides over areas extending up to 20,000 km^2, Figure 11.1 (Crozier, 2005).

These multiple events predominantly involve eluvial soils and can be classified as shallow earth or debris slides and flows. They mainly occur in morphological hollows with a sliding surface at a depth of 10m from ground surface and an overall length of the trigger zone of more than 30 m Figure 11.2.

Figure 11.1 Earth slides and earthflow of the landslide event of 15–17 February 2004, Wanganui-Manawatu, North Island, New Zealand (Crozier 2005).

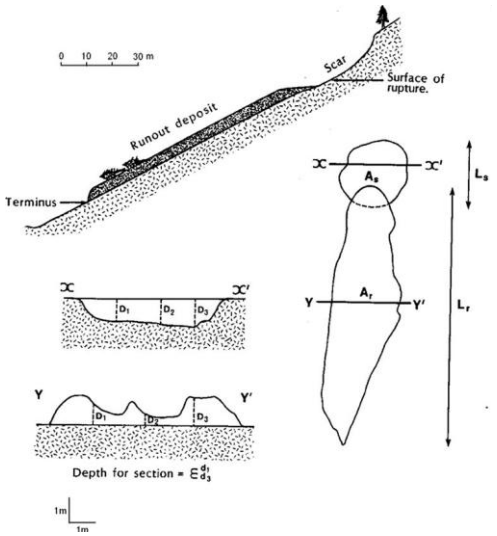

Figure 11.2 Typical morphology and dimensions of an individual landslide belonging to a multiple-occurrence regional landslide event. Notation: *A*s is Area of scar; *A*r area of runout deposit; *L*s is length of scar; *L*r length of runout; and D is depth modified (Crozier 1996).

Considering that in such a case the database available in literature does not provide detailed elements, the analysis was performed by referring, although not very accurately, to a DTM (20x20 m cells) which was the only topographical data available online on the GSN website(http://www.gns.cri.nz). The hydrological data have been taken directly from Crozier (2005) who, underlining the exceptionality of the event that took place between 15 and 17 February 2004, reports a rainfall intensity between 160 and 300 mm over two days. Crozier points out that the values recorded during this event are between 4 and 6 times more intense than those generally registered in February.
Finally, Table 11.1 summarizes the hydraulic and shear strength parameters used as input data in the modelling; the latter have been taken from previous works, whereas the former coincide with those obtained through the procedure used in the study area. A TRIGRS-based modelling has been performed on an area within the Wanganui-Manawatu region, after the realization of a soil cover thickness map which has been created following a similar procedure to the one described in section 10.2.2, but taking into account the fact that the thickness involved is generally thicker given a deeper sliding surface, Figure 11.3.

Table 11.1 Parameters used for modelling (New Zealand)

Parameters used for modelling				
Unit weight	Effective cohesion	Friction angle	Hidraulic conducivity	Soil Depth h TRIGRS
γ (kN/m3)	c' (kPa)	ϕ' (°)	k (m/s)	(m)
15,54	11,5	32	5.00E-07	variable

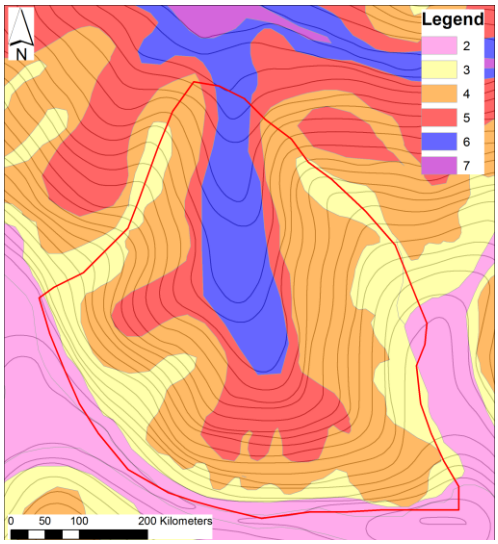

Figure 11.3 Soil cover thickness map (numbers specify depths in meters).

Overall, the obtained results show that, despite the lack of advanced input data, a good match exists with the occurred landslide event. Infact, in the areas where the Google Earth image does not seem to reveal the presence of landslides, a zoom of the same image shows a diffuse cracks pattern along the topographical surface, Figure 11.4.

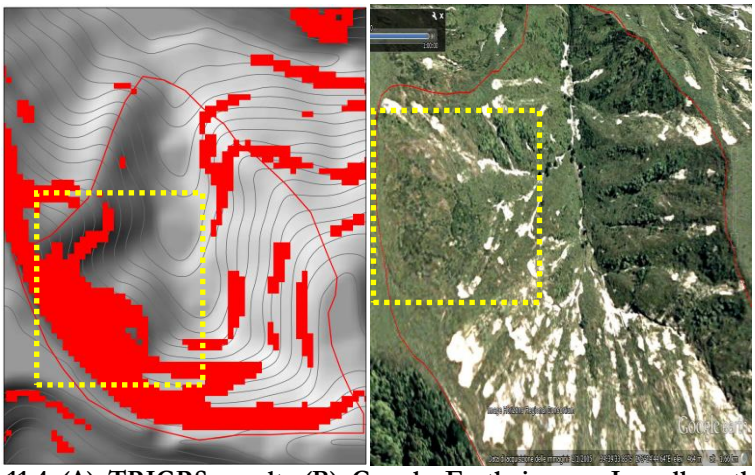

Figure 11.4 (A) TRIGRS result, (B) Google Earth image. In yellow the area involved by a diffuse cracks pattern.

The results obtained are shown in Figure 11.4 which also illustrates how TRIGRS modelling, in the absence of accurate input data, can identify the areas where landslides occur with sufficient approximation, confirming the overall validity of the methodology proposed in this work. Of course, more accurate input data could greatly improve the results of the analyses for which topographical data are paramount, as pointed out in section 10.2.2.

11.3.2 Future developments

The study carried out in this thesis underlines that several issues must be faced in order to improve the analysis of shallow landslides at various scales. General and specific indications will now be provided as to what concerns the different scales of analysis used in the present work. Only the small scale analysis is not going to be considered, since this strongly depends on the geodynamic evolution of the area to be studied, and the formulation of general criteria are beyond the scope of the thesis.

In terms of medium scale analysis, the knowledge deriving from the approach proposed here can be increased by applying intermediate methods such as statistical analyses. The latter, together with an understanding of the predisposing factors identified, can offer significant

results in relation to shallow landslides, and can clarify the links existing between predisposing factors and shallow landslides.
At large scale, the modelling of surface and subsurface runoff can be further investigated in cases of convergent flows through the use of 3D analyses which can account for the increase in degraded thickness as a result of the effects of water infiltration.
Certainly, it is essential, at this scale, to collect useful data on the degraded thickness involved in order to carry out analyses which are similar to those performed in the present thesis. Choosing low-cost in situ investigations can be extremely useful to reconstruct a map of degraded thickness on significantly wide areas. However, this technique has not been standardized, and there are no relations linking in situ measured data with shear strength parameters. Standardising the dimension of the device could be extremely demanding, and yet interesting, and so could be the creation of charts relating in situ measured data and geotechnical parameters.
At slope scale, the key factor for an understanding of the behaviour of the soil at actual scale are the pore water pressure values in situ over a sufficiently long timespan to show seasonal trends.
The number of instruments for monitoring negative pore water pressure measures could be increased in order to reconstruct the pore water pressure regime along the slope.
Further analyses are paramount in relation to the combined measures of permeability values in situ and of negative pore pressures in order to measure the conductivity function directly and to calibrate the curve proposed here.
In addition, at this scale, the use of a totally uncoupled approach is not sufficient for an understanding of the actual shallow landslide triggering because the latter is the result of two simultaneous processes (pore water pressure and failure).
In effect, currently, the lack of the necessary elements for the use of a coupled model renders the methodology used in the present study the most adequate. Significant efforts should be made in order to use a coupled hydro-mechanical model valid for degraded, fine-grained, non-collapsible soils and capable of analysing the triggering causes of these landslides at slope scale.
Finally, at REV scale, it is necessary to estimate further SWCC on specimens submitted to several cycles of artificially degradation in lab (continuous drying and wetting) in order to verify the decrease in suction

value near when the air-entry value is calculated, as hypothesized in the proposed conductivity curve. It might be useful to measure permeability on both intact and artificially degraded samples in order to calculate to what extent this process modifies the conductivity function measured.

12 CONCLUDING REMARKS

The research carried out in the present thesis is based on a deductive, multiscale methodological approach already used in other works, but whose innovative and original character, both at national and international level, rests in its application to shallow landslides.
One of the most significant aspects characterising the methodology proposed here is its user-friendliness which allows to choose the best areas in which further investigations can be carried out. This aspect is particularly evident in the passage from small to large scale.
Another fundamental result of the work carried out consists in the possibility to model instability at large scale with good results even without a complete database, but rather by using incomplete information gathered from geographically distant areas possessing the same geological and environmental characteristics as the one investigated.
Similarly, the geotechnical characterization of the soils affected by landslide events obtained through the combined use of in situ investigations, lab tests and slope scale modelling constitutes another significant result of this study. Furthermore, the overall information obtained at the scale of the micro, meso and macrostructure, and the synergy among the various analyses, reduces the uncertainties which inevitably characterize a modelling carried out without a significant geotechnical database.
Finally, all the analyses performed validate the potentialities embedded in the methodology proposed and recommend its use in contexts that differ from the one studied here, provided that a high-quality topographic database is acquired in order to obtain accurate results.

REFERENCES

Aleotti P., Baldelli P., Polloni G. (1996). Landsliding and flooding event triggering by heavy rains in the Tanaro Basin (Italy). *International Symposion on interpraevent 1996-Garmish-Partenkirchen Tagungspuplikation,* Band 1: 435-446.

Amodio Morelli L., Bonardi G., Colonna V., Dietrich D.,Giunta G., Perrone, V., Piccaretta G., Russo M., Scandone P., Zanettin Lorenzoni, E. and Zuppetta A., (1976*).* L'Arco calabro-peloritano nell'orogene appenninico maghrebide. *Mem. Sot. Geol. Ital.*. 17: l-60.

Antronico et (2004) Shallow instabilities for sliding flow: regional influence and area affects. *Atti del convegno "IX International Symposium on Landslides",* Rio Sayao: London, 2: 1381-1388. de Janeiro, Brasile*,* 28 Giugno/2 Luglio, 2004, Lacerda E., Fontoura and

Antronico L. and Gulla G. (2000). Slopes affected by Soil Slips: validation of evolutive model. *Landslides in research, theory and practice. Proceedings of the 8th Iternational symposium on landslides held in Cardiff on 26-30 June 2000,* 1: 77-84.

Antronico L., Gullà G., Oddo B. (2001). Considerazioni preliminari sui risultati relativi alla caratterizzazione di soil slip in alcune zone di studio della Stretta di Catanzaro (Calabria). *Mem. Soc. Geol. It.,* 56: 1-10.

Baum R.L., Savage W.Z., Godt J.W. (2002). TRIGRS - *a FORTRAN* program for transient rainfall infiltration and grid-based regional slope-stability analysis. *U. S. Geological Survey Open-File Report* 02-0424.

Benites L. A. (1968). Geotechnical properties of the soils affected by piping near the Beson area, Cochise County, Arizona. University of Arizona, Tucson.

Blight G. E. (1997). Interactions between the atmosphere and the Earth Geotechnique 47, No. 4: 715-767.

Blong R.J. (1973). A numerical classification of selected landslides of debris slide-avalanche-flow type. *Engineering Geology,* 7: 99-114.

Borga M., Dalla Fontana G., Gregoretti C. and Marchi L. (2002). Assessment of shallow landsliding by using a physically based model of hillslope stability. *Hydrological processes*: 16: 2833–2851.

Boschi E., Ferrari G., Gasperini P., Guidoboni E., Smriglio G., Valensise G., 1995. Catalogo dei forti terremoti in Italia dal 461 a. C. al 1980 (Strong earthquakes in Italy from 461 b.C. to 1980), n. 1 CD-ROM. ING and SGA, Roma, 973 pp.

Boschi E., Guidoboni E., Ferrari G., Valensise G., Gasperini P., 1997. Catalogo dei forti terremoti in Italia dal 461 a. C. al 1990, vol. 2 (Strong earthquakes in Italy from 461 b.C. to 1990, vol. 2), n. 1 CD-ROM. ING and SGA, Roma, 644 pp.

Brabb E.E. (1984). Innovative approaches to landslide hazard and risk mapping. *Proc. of the IV International Symposium on Landslides, Toronto*, 1: 307–323.

Burbank W. & Anderson R. (2001) - Tectonic Geomorphology; *Blackwell Science,* pp. 274.

Calvello M., Cascini L., Cuomo S., Della Sala M. (2012). Applicazione dei metodi di base ed intermedi all'areale delle piroclastiti. In: Cascini L. (Editor). Criteri di zonazione della suscettibilità e della pericolosità da frane innescate da eventi estremi (piogge e sisma): 46-50.

Campbell R.H. 1975. Soil slip, debris flow and rainstorms in the Santa Monica Mountains and vicinity, Southern California. U.S. *Geological Survey Professional Paper* 851: 1-51.

Carrara A. (1992). Landslide hazard assessment. *Proceeding 1st Symposio Internationale Sensores Remotos y Sistema de Informativo Geografico para el Studio de Resources Naturales, 10-12 March, Bogotá,* 329-355

Carrara A. (1983). A multivariate model for landslide hazard evaluation. *Mathematical Geology,* 15: 403-426.

Carrara A., Cardinali M., Guzzetti F. and Reichenbach, P. (1995). GIS technology in mapping landslide hazard. In: Carrara, A. and Guzzetti, F. (eds.) *Geographycal Information Systems in Assessing Natural Hazards*. Kluwer Academic Publisher, Dordrecht, The Netherlands, 135-175.

Carrara A., D'Elia B., Semenza E. (1985). Classificazione e nomenclatura dei fenomeni franosi. *Geol. Appl. Ed Idrogeol*, 20 (II), 223-243.

Carraro F. (1976). Appunti sulla tettonica quaternaria. Gruppo di studio del Quaternario Padano. Quaderno n.3 Torino pp.1-19.

Cascini L. (2008). Applicability of landslide susceptibility and hazard zoning at different scales. *Engineering Geology* 102 (3-4): 164-177.

Cascini L. (2004). The flowslides of May 1998 in the Campania region, Italy: the scientific emergency management. *Rivista Italiana di Geotecnica*, 2: 11 – 44.

Cascini L., Bonnard C.h., Corominas J., Jibson R., Montero-Olarte J. (2005). Landslide hazard and risk zoning for urban planning and development. State of the Art Report (SOA7). In: Hungr, O., Fell, R., Couture, R., Eberthardt, E. (Eds.), Proceedings of the International Conference on "Landslide Risk Management", Vancouver (Canada) Taylor and Francis, London, pp. 199–235.

Cascini L., Cuomo S. and Sorbino, G. (2005a). Flow-like mass movements in pyroclastic soils: remarks on the modelling of triggering mechanisms. Italian Geotechnical Journal 4: 11-31.

Cascini L., Critelli S., Di Nocera S., Gullà G., Matano F. (1992). Grado di alterazione e franosità negli gneiss del massiccio Silano: l'area di San Pietro in Guarano (CS). *Geologia applicata e Idrogeologia*, XXVII: 49-76.

Cascini L., Cuomo S, Sorbino G. (2005). Flow-like mass movements in pyroclastic soils: remarks on the modelling of triggering mechanisms. *Italian Geotech. Journal. Patron Ed.*

Cascini L., Ferlisi S., Tagliaferro G. (2002). Il contributo delle indagini storiche nella definizione del rischio da frana: un caso di studio. *Proceedings of the XXI Italian Geotechnical Congress. Pàtron Editore, 135–142.*

Cascini L., Gullà G., Sorbino G. (1991) Modellazione delle acque sotterranee in una coltre di detrito in frana: risultati preliminari. *Atti del Seminario Annuale del Gruppo Nazionale di Coordinamento degli Studi di Ingegneria Geotecnica, C.N.R.,* Roma, giugno, pp.149-151.

Cascini L. and Matano F. (2010). Scivolamento del muro in conci prefabbricati realizzato a valle della Centrale tecnologica, nell'ambito dei lavori di completamento del nuovo complesso demaniale della legione dei Carabinieri di Catanzaro. *Relazione Tecnica.*

Casmez (1967). Carta geologica della Calabria. Poligrafica e cartevalori, Ercolano – Napoli.

Castellanos Abella E. A. (2008). Multi-scale landslide risk assessment in Cuba. PhD thesis. University of Utrecht.

Chung C.-J. and Fabbri A.G. (2003). Validation of Spatial Prediction Models for Landslide Hazard Mapping. *Natural Hazards*, 30: 451-472.

Claessens L., Schoorl J.M., Veldkamp A. (2007). Modelling the location of shallow landslides and their effects on landscape dynamics in large watersheds: An application for Northern New Zealand. *Geomorphology* 87: 16-27.

Clevenger, W. A. (1956). Experiences with loess as foundation materials. *Journal of Soil Mechanics and Foundation Division*, 82 (3): 1025-26.

Coe J.A., Godt J.W., Baum R.L.,Bucknam R.C., Michael J.A. (2004). Landslide susceptibility from topography in Guatemala. *Landslides: Evaluation and Stabilization, Lacerda, Ehrlich, Fontoura & Sayao (ed*s), 2, 69-77.

Corominas J. (1996). The angle of reach as a mobility index for small and large landslides. *Canadian Geotechnical Journal*, 33: 260-271

Corominas J., Copons R., Vilaplana J.M., Altimir J., Amigo J. (2003). Integrated landslide susceptibility and hazard assessment in the Principality of Andorra. *Natural Hazards*, 30: 421–35.

Corte A. E. and Higashi, A. (1964). Experimental research on desiccation cracks in soil, *Research Report 66*. Hanover, NH: US Army Cold Regions Research and Engineering Laboratory, Army Material Command.

Cotecchia F., Santaloia F., Lollino P., Mitaritonna G. e Vitone C. (2012). Applicazione delle Linee Guida del JTC-1 secondo un approccio multi-

scalare. In: Cascini L. (Editor). Criteri di zonazione della suscettibilità e della pericolosità da frane innescate da eventi estremi (piogge e sisma): 46-50.

Crozier M.J. (2005). Multiple-occurrence regional landslide events in New Zealand: Hazard management issues. *Landslides,* 2: 247-256.

Crozier M.J. (1986). Landslides: causes, consequences and environment. *Croom Helm Pub.*

Cruden D.M., Varnes D.J. (1996). Landslide Types and Processes. *Landslides Investigation and Mitigation* (Turner A.K., Schster R.L. eds). Transp. Res. Board Spec. Rep. 247, National Research Council, National Academy Press, Washington D.C., pp. 36 – 75.

Das B. M. (2007). Principles of foundation engineering, PWS publishing company, Boston, MA.

D'Elia B., Picarelli L., Leroueil, S. & Vaunat J. (1998). Geotechnical characterization of slope movements in structurally complex clay soils and stiff jointed clays. *Italian Geotech. J.* No. 32: 5-32.

Demangeot J. (1973). Neotectonique et depots quaterneres dans l'Apennin. *Acc. Naz., Lincei, Quad. n. 183* " Moderne vedute sulla geologia dell'Appennino", Roma , pp. 215-240.

Denisov N. Y. (1951). The engineering properties of loess and loess loams, Gosstroiizdat, Moscow.

Dexter A.R., 1988. Advances in characterization of soil structure. *Soil and Tillage Research,* 199-238.

Dietrich E.W., Reiss R., Hsu M-L., Montgomery D.R. (1995). A process–based model for colluvial soil depth and shallow landsliding using digital elevation data. *Hydrological Process*, 9: 383-400.

Dubois R. (1970). Phases de serrage, nappes de socle et metamorphisme alpin a la jonction Calabre-Apetmin: la suture calabro-apenninique. *Rev. Geogr. Phys. Geol. Dyn.*. 2, 12(3): 221-254.

Dunn J.R. and Hudec P.P. (1966). Water, clay and rock soundness, Ohio J. Sci., 66: 68-153.

Eden W.J. and Mitchell R.J. (1969). The mechanics of landslides in Leda clay. *Canadian Geotechnical Journal*, 7: 286-296.

Eigenbrod K.D. and KaluzaD. (1999). Shallow slope failures in clays as a result of decreased evapotranspiration subsequent to forest clearing, 36: 111-118.

Fannin R.J. (2000). Piezometric observations: implications for debris flow initiation on forested. Landslides in research theory and practice. *Vol. 2. Proceedings of the 8th International symposium on on landslides held in Cardiff on* 26-30 *June* 2000 (537-542).

Feda, J. (1964). Colloidal activity, shrinking and swelling of come clays. *Proceedings Soil Mechanics Seminar*, 531–546.

Fell R., Corominas J., Bonnard C., Cascini L., Leroi E., Savage W.Z. on behalf of the JTC-1 Joint Technical Committee on Landslides and Engineered Slopes (2008a). Guidelines for landslide susceptibility, hazard and risk zoning for land-use planning. *Engineering Geology* 102, 85–98.

Fell R., Corominas J., Bonnard C., Cascini L., Leroi E., Savage W.Z. on behalf of the JTC-1 Joint Technical Committee on Landslides and Engineered Slopes (2008b). Commentary of Guidelines for landslide susceptibility, hazard and risk zoning for land-use planning. *Engineering Geology* 102, 99–111.

Finetti I., Del Ben A. (1986). Geophysical study of the tyrrhenian opening. *Boll. Geof. Teor. Appl.*, 28, 75-155.

Fredlund D.G., Houston S. L.,• D. Fredlund Q. N. • M. (2010). Moisture Movement Through Cracked Clay Soil Profiles. *Geotechnical and Geological Engineering* 28:865-888.

Fredlund D.G., Morgenstern N.R., Widger R.A. (1978) The shear strength of unsaturated soils. *Canadian Geotechnical Journal*, 15, pp. 313 – 321.

Ghisetti, F., 1979. Evoluzione neotettonica dei principali sistemi di faglie della Calabria centrale (Neotectonic evolution of main fault systems of Central Calabria). *Boll. Soc. Geol. It.* 98, 387–430.

Gibbs, H. J. (1961). Properties which divide loess and dense uncemented soils. *Earth laboratory report EM-658*, Bureau of Reclamation, U.S. Department of the Interior, Washington D.C.

Glade T., Anderson M., Crozier M.J. (2005). Landslide Hazard and Risk. England John Wiley & Sons.

Golfetto F., Merlini S., Riva M., Torricelli S., Toscano C., Zerilli A. (2000). A regional structural model for the northern sector of the Calabrian Arc (southern Italy). *Tectonophysics* 324: 267–320

Gullà G., Aceto L. and Niceforo D. (2004). Geotechnical characterisation of fine-grained soils affected by soil slips. *Proc. of the 9th International Symposium on Landslides,* Rio de Janeiro, June 28 - July *7, 2004,* 663-668.

Gullà G., Aceto L., Critelli S., Perri F. (2008a) – Geotechnical and mineralogical characterization of fine grained soils affected by soil slips. *Proc. of the 10th International Symposium on Landslides*, June 30 - July 4, 2008, Xi'an, China, 373-379.

Gullà G., Antronico L., Iaquinta P., Terranova O. (2008). Susceptibility and triggering scenarios at a regional scale for shallow landslides. *Geomorphology* 99: 39–58

Gullà G., Mandaglio M.C., Moraci N. (2006) – Effect of weathering on the compressibility and shear strength of a natural clay. *Canadian Geotechnical Journal, Volume* 43*, Number* 6, June 2006, 618-625.

Gullà G., Mandaglio M.C., Moraci N. (2005). Influence of degradation cycles

on the mechanical characteristics of natural clays. *Proc. of the 16th International Conference on Soil Mechanics and Geotechnical Engineering,* September 12-16, 2005, Osaka, Japan, 2521-2524.

Gullà G., Niceforo D., Ferraina G. Aceto L., Antronico L. (2004). Monitoring station of soil slips in a rappresentative area of Calabria (Italy). *Proc. Of the 9th International Symposium on Landslides*, Rio de Janeiro, June 28-July 7, 2004, 591-596.

Guzzetti F. (2008). The rainfall intensity–duration control of shallow landslides and debris flows: an update. *Landslides* 5:3–17.

Guzzetti F. (2005 a).Landslide hazard and risk assessment. PhD Thesis.

Guzzetti F., Cardinali M. and Reichenbach P. (1994) The AVI Project: a bibliographical and archive inventory of landslides and floods in Italy. Environmental Management, 18:4 623-633.

Guzzetti F., Mondini A. C., Cardinali M., Fiorucci F, Santangelo M., Chang K.-T. (2012) Landslide inventory maps: New tools for an old problem. *Earth Science Reviews* 112 (2012) 42–66.

Guzzetti F., Cardinali M., Reichenbach P., Carrara A., (2000). Comparing landslide maps: a case study in the upper Tiber River Basin, Central Italy. *Environmental Management* 25 (3), 247–363.

Guzzetti F., Carrara A., Cardinali M. and Reichenbach P. (1999). Landslide hazard evaluation: a review of current techniques and their application in a multi-scale study, Central Italy. *Geomorphology,* 31: 181-216.

Guzzetti F. and Tonelli G. (2004) SICI: an information system on historical landslides and floods in Italy. *Natural Hazards and Earth System Sciences*, 4:2 213-232.

Hancox G.T., Wright K. (2005). Analysis of terrain and landsliding caused by the 15–17 February 2004 rainstorm in the Wanganui-Manawatu hill country, southern North Island, New Zealand. *Institute of Geological & Nuclear Sciences Science Report* 2005/11.

Handy R. L. (1973). Collasible loess in Iowa. *Proceedings, Soil Science Society of America*, 37: 281–284.

Hansen A., 1984a. Engineering geomorphology: the application of an evolutionary model of Hong Kong. *Zeitschrift für Geomorphologie* 51, 39–50.

Hansen A., 1984b. Strategies for classification of landslides. In: Brunsden, D., Prior, D.B. (Eds.), Slope Instability. *Wiley, New York, pp*. 523–602.

Hicks D.L. (1995). Control of soil erosion on farmland. *New Zealand Ministry of Agriculture an Fisheries Policy* technical paper 95/4.

Howayek A. El, Huang P.T., Bisnett R. Santagata M.C. (2011). Identification and Behavior of Collapsible Soils. *Joint Transportation Research Program*.

Hungr O., Evans S.G., Bovis M.J., Hutchinson J.N. (2001). *A review of the classification of landslides of the flow type.* Environ. & Eng. Geosci., VII (3), 221-238.

Hutchinson J.N. (1988). Morphological and Geotechnical parameters of Landslides in relation to Geology and Hydrogeology. *State of the art Report.* Proc. V Intl. Symposium on Landslides, Lausanne, Vol. 1, pp. 3 – 35.

Iverson R.M. (2000). Landslide triggering by rain infiltration. *Water Resources Research*, vol. 36, no. 7, pag 1897–1910

Jahns R. H. (1978). Landslides. National Academy of Science; Geophysical Predictions: 58-65.

Kennard M. F., Knill J. L. and Vaughan P.R. (1967) The geotechnical properties and behavior of Carboniferous shale at the Balderhead dam, J. Engng. Geol., 1: 3-24.

Klukanova, A., and Frankovaska J. "The Slovak Carpathians loess sediments, their fabric and properties." Proceesings of the NATO Advanced Research Workshop on Genesis and Properties of Collapsible Soils, Loughborough, U.K., 413.

Lachenbruch A. H. (1962). Mechanics of thermal contraction cracks and ice-wedge polygons in permafrost, Special Paper No. 70, pp. 1±60. Washington, DC: Geological Society of America.

Lanzafame G., Tortorici L., 1981. La tettonica recente della valle del Fiume Crati (Calabria) (Recent tectonics in the R. Crati valley (Calabria)). *Geografia Fisica e Dinamica Quaternaria* 4, 11–21.

Leoni E. (2008). Contributo della modellistica idrologica all'analisi di suscettività alle frane superficiali in argilla. *PhD Thesis University of Bologna.*

Leroueil S., Vaunat J., Picarelli L., Locat J., Lee H.J., Faure R. (1996). Geotechnical characterization of slope movements. *Proc. 7th Int. Symp. on Landslides*, Trondheim, v.l, pp. 53-74.

Lim T.T., Rahardjo H., Chang M.F., Fredlund D.G. (1996). Effect of rainfall on matric suctions in a residual soil slope. Can. *Geotech. J.* 33: 618-628.

Lollino G. Mitaritonna C. Vitone, F. Cotecchia e F. Santaloia (2012). Applicazione dei metodi avanzati al fronte appenninico apulo-lucano: analisi di II livello della metodologia multi-scalare. *In: Cascini L. (Editor).* Criteri di zonazione della suscettibilità e della pericolosità da frane innescate da eventi estremi (piogge e sisma): 219-230.

Lorenzoni S. and Zanettin Lorenzoni, E., 1975. The "Granitic" Unit of the Sila Piccola (Calabria, Italy). *Its position and tectonic significance. Neues Jahrb. Geol. Paleontol. Abh.*, 148(2): 133-251.

Lutenegger A. J. (1988). Determination of collapse potential of soils. *Geotechnical Testing Journal*, 11(3), 173 178.

Mallant D, Tseng PH, Torde N, Timmerman A, Feyen J (1997) Evaluation of multimodal hydraulic function in charactering a heterogeneous field soil. *J Hydrol* 195:172–199.

Martha T. R. (2011) Detection of landslides by object-oriented image analysis. *PhD thesis University of Twente.*

Massari F., Rio, D., Sgavetti, M., Prosser, G., D'Alessandro, A., Asioli, A., Capraro, L., Fornaciari, E., Tateo, F., 2002. Interplay between tectonics and gladio-eustasy: Pleistocene succession of the Crotone basin, Calabria (southern Italy). *Geol. Soc. Amer. Bull.* 114/10, 1183– 1209.

McCalpin J., 1984. Preliminary age classification of landslides for inventory mapping. Proceedings 21st annual Engineering Geology and Soils Engineering Symposium. *University Press, Moscow, Idaho*, pp. 99–111.

Meisina C. (2006). Characterisation of weathered clayey soils responsible for shallow landslides. *Nat. Hazards Earth Syst. Sci.*, 6: 825–838.

Mescerjakov J.P. (1968). Le concepts de morphostructure et de morphosculpture: un nuvel instrument de l'analyse geomorphologique . *Ann de Geogr.*, 423, pp. 539-552.

Metternicht G., Hurni, L., Gogu, R., 2005. Remote sensing of landslides: an analysis of the potential contribution to geo-spatial systems for hazard assessment in mountainous environments. *Remote Sensing of Environment* 98 (23), 284–303.

Mitchell J. K. and Soga K. (2005). Fundamentals of soil behavior, *John Wiley & Sons*, Hoboken, N.J.

Monaco C., Tansi C. (1992). Strutture transpressive lungo la zona trascorrente sinistra nel versante Nord-orientale del Pollino (Appennino calabro-lucano).*Boll. Soc. Geol. It.*, 111: 291-301.

Monaco C., Tapponnier, P., Tortorici, L., Gillot, P.Y., 1997. Late Quaternary slip rates on the Acireale-Piedimonte normal faults and tectonic origin of Mt. Etna (Sicily). *Earth Planet. Sci. Lett.* 147, 125–139.

Monaco C., Tortorici, L., 2000. Active faulting in the Calabrian Arc and eastern Sicily. *J. Geodyn.* 29, 407–424.

Montgomery D.R. Dietrich W.E. (1994) - A physically based model for the topographic control on shallow landsliding. *Water Resources Research*, 30, 1153-1171.

Musso A., Olivares L. (2004) – *Flowslides in pyroclastic soils: transition from "static liquefaction" to "fluidization"*. Proc. of the Int. Workshop "Flows 2003 – Occurrence and Mechanisms of Flows in Natural Slopes and Earthfill pp. 117 – 127.

Nichol J., Wong, M.S., 2005. Detection and interpretation of landslides using satellite images. *Land Degradation & Development* 16, 243–255.

Olivares L., Picarelli L. (2003) – Shallow flowslides triggered by intense rainfalls on natural slopes covered by loose unsaturated pyroclastic soils. *Géotechnique* 53, No. 2, pp. 283 – 287.

Ollier C. (2002). Tectonics and landforms Longman, London 1981. Bartolini C. and Peccerillo A. I fattori geologici delle forme del rilievo (lezioni di geomorfologia strutturale). pp. 228.

Ollier C. (1984). Weathering, Geomorphology text 2nd ed. Longman London and New York.

Ollier C. (1981). Tectonics and landforms Longman, London.

Pan G. and Harris D.P. 2000b. Mineral resources information system, Information synthesis for mineral exploration. *Oxford University Press, New York*, pp. 13-43.

Page M., Trustrum N., Gomez B. (2000). Implications of a century of anthropogenic erosion in Gisborne-East Coast region of New Zealand. *NZ Geogr* 56(2):13–24.

Panizza M.(2005). Manuale di geomorfologia applicata, *Angelini*, Bologna.

Panizza M. (1992) – *Geomorfologia; Pitagora Editrice Bologna*, pp. 397.

Pašek J., 1975. Landslide inventory. *International Association Engineering Geologist Bulletin* 12, 73–74.

Pastor M., Fernandez Merodo J.A., Gonzalez E., Mira P., Li T., Liu X. (2003A). Modelling of landslides: (I) Failure mechanisms. Degradations and Instabilities in Geomaterials, *CISM Cours*e, June 16-20 2003, Udine, pp. 31.

Pastor M., Quecedo M., Gonzalez E., Herroros M.I., Fernandez Merodo J.A., Mira P. (2003B). Modelling of landslides: (II) Propagation. Degradations and Instabilities in Geomaterials, *CISM Course*, June 16 - 20 2003, Udine, pp. 49.

Pasuto A. and Silvano S. (1997). Rainfall as a trigger of shallow mass movements. A case study in the Dolomites, Italy. *Environmental Geology* 35: 2–3.

Peters RR, Klavetter EA (1988) A continuum model for water movement in unsaturated fractured rock mass. *Water Resour Res* 24(3):416–430

Picarelli L. (1991). Resistenza e meccanismi di rottura nei terreni naturali. *Convegno dei ricercatori sul tema: Deformazioni in prossimità della rottura e resistenza dei terreni naturali e delle rocce, Ravello* 2, II.7-II.61.

Polynov B.B. 1937. Cycle of weathering (Trans. A. Muir). Murby, London.

Postpischl D. (1985). Catalogo dei forti terremoti italiani dall'anno 1000 al 1980 (Catalogue of strong Italian earthquakes from a.D. 1000 to 1980). CNR, Progetto Finalizzato Geodinamica, Graficcop, Bologna, 239 pp.

Priklonski V. A. (1952). *Gruntoedenia-Vtroarid Chast, Gosgeolzdat, Moscow.*

Rahardjo H., Li X.W., Toll D.G., Leong E.C. (2001). The effect of antecedent rainfall on slope stability. *Geotechnical and geological Engineering,* 19: 371–399.

Razak K.A., Straatsma, M.W., van Westen, C.J., Malet, J.-P., de Jong, S.M., 2011. Airborne laser scanning of forested landslides characterization: terrain model quality and visualization. *Geomorphology* 126, 186–200. doi:10.1016/ j.geomorph.2010.11.003.

Ritchie J.T. and Adams J.E. 1974. Field measurements of evaporation from soil shrinkage cracks. *Soil Sci. Soc. Am. Proc.* 38: 131-134.

Rogers N. W., Selby M. J. (1980) Mechanisms of shallow translational landsliding during summer rainstorms: North Island, New Zealand. *Geografiska Annaler* 62 A 1-2.

Santaloia F., Cotecchia F. e Vitone C. (2012a). Le aree test dell'approccio multi-scalare. In: Cascini L. (Editor) . *Criteri di zonazione della suscettibilità e della pericolosità da frane innescate da eventi estremi (piogge e sisma)*: 46-50.

Santaloia F., Cotecchia F. e Vitone C. (2012b). Applicazione di metodi avanzati al fronte appenninico apulo-lucano: analisi di I livello. In: Cascini L. (Editor) . *Criteri di zonazione della suscettibilità e della pericolosità da frane innescate da eventi estremi (piogge e sisma)*: 130-138.

Savage W.Z., Godt J.W., Baum R.L. (2003). A model for spatially and temporally distributed shallow landslide initiation by rainfall infiltration. in press. *Proc. 3rd Int. Conf. on Debris Flow Hazards Mitigation: Mechanics, Prediction, and Assessment*, Davos, Switzerland, pp. 179 – 187.

Savage W.Z., Godt J.W., Baum R.L. (2004). Modeling time-dependent areal slope stability. *In: Landslides – Evaluation and Stabilization Proceedings of the 9th International Symposium on Landslides. Lacerda, W.A., Erlich, M., Fontoura, S.A.B., Sayao, A.S.F., (Eds.). Balkema*, 1, 23-36.

Shan J., Toth, C.K. (Eds.), 2009. Topographic Laser Ranging and Scanning: Principles and Processing. *CRC Press, Taylor and Francis Group, p.* 590.

Sica C. (2008). Modelling the triggering of flow-type slope movements over large areas: limitations and potential of distributed physically based models. *PhD thesis University of Salerno*.

Sivakumar V. (1993). A critical state framework for unsaturated soil. *PhD thesis, University of Sheffield.*

Skempton A.W. (1953). Soil mechanics in relation to geology. *Proc. Yorkshire Geological Society* 29 (1): 33-62.

Soeters R. and Van Westen, C.J. (1996). S*lope instability recognition, analysis and zonation*. In A.K. Turner and R.L. Schuster (eds.).

Sorbino G., Sica C., Cascini L. (2009). Susceptibility analysis of shallow landslides source areas using physically based models. *Nat Hazards*.

Sorbino G., Sica C., Cascini L. and Cuomo S. (2007). On the forecasting of flowslides triggering areas using physically based models. *Conference Presentations:* 1*st North American Landslide Conference, Vail, Colorado***.**

Sorriso-Valvo M., Antronico L., Gaudio R., Gullà G., Iovine G., Merenda L., Minervino I., Nicoletti P.G., Petrucci O., Terranova O. (2004). Carta dei dissesti causati in Calabria meridionale dall'evento meteorologico dell'8- 10 settembre 2000. *Gruppo Nazionale per la difesa dalle catastrofi idrogeologiche* (n°2859).

Sorriso-Valvo M. and Sylvester A. (1993). The relationship between geology and landforms along a costal mountain front, nothern Calabria, Italy. *Earth Surface Processes and Landforms*, 18: 257-273.

Sorriso-Valvo M., Tansi C. (1996). Grandi frane e deformazioni gravitative profonde di versante della Calabria. Note illustrative della Carta 1:250,000. *Geogr. Fis. Din. Quat.* 19, 395-408.

Tansi C., Muto F., Critelli S., Iovine G. (2006). Neogene-Quaternary strike-slip tectonics in the central Calabrian Arc (southern Italy). *Journal of Geodynamics* 43: 393-414.

Terlien M.T.J . (1998). The determination of statistical and deterministic hydrological landslidetriggering thresholds. *Environmental Geology* 35 (2–3), pag. 124 – 130.

Tortorici L., 1982. Lineamenti geologico-strutturali dell'Arco Calabro Peloritano (Geologic-structural lineaments of the Calabrian-Peloritan Arc). *Società Italiana di Mineralogia e Petrografia* 38, 927–940.

Tortorici L., Monaco, C., Tansi, C., Cocina, O., 1995. Recent and active tectonics in the Calabrian Arc (southern Italy). *Tectonophysics* 243, 37–55.

Tortorici L., 1982. Lineamenti geologico-strutturali dell'Arco Calabro Peloritano (Geologic-structural lineaments of the Calabrian-Peloritan Arc). *Società Italiana di Mineralogia e Petrografia* 38, 927–940.

Towner G. D. (1987). The mechanics of cracking of drying clay. J. *Agric. Eng. Res.,* 36: 115-124.

Tribe S., Leir M., 2004. The role of aerial photograph interpretation in natural hazard and risk assessment. *Proceedings of the International Pipeline Conference*, October 4–8, Calgary, Canada. 6 pp.

Van Asch TH.W.J., Buma J., Van Beek L.P.H. (1999). A view on some hydrological triggering systems in landslides. *Geomorphology* 30 1999 25–32.

Van Dijk and Okkes Mark (1991). Neogene tectonostratigraphy and kinematics of Calabrian basins; implications for the geodynamics of the Central Mediterranean. *Tectonophysics*, 196: 23-60.

Van Dijk J.P., Bello M., Brancaleoni G.P., Cantarella G., Costa V., Frixa A.,

Van Westen C.J., 2004. Geo-information tools for landslide risk assessment — an overview of recent developments. In: Lacerda,W., Ehrlich, M., Fontoura, S., Sayao, A. (Eds.), Landslides, Evaluation & Stabilization. Proceedings of the 9th International Symposium on Landslides, Rio de Janeiro, 28th June–2nd July, pp. 39–56.

Van Westen, C.J., Castellanos, E. and Kuriakose, S.L., 2008. Spatial data for landslide susceptibility, hazard, and vulnerability assessment: *An overview. Engineering Geology*, 102(3-4): 112-131.

Van Westen C.J. and Lulie Getahun, F., 2003. Analyzing the evolution of the Tessina landslide using aerial photographs and digital elevation models. *Geomorphology*, 54(1-2): 77-89.

Vanapalli S. K., Fredlund D. G., Pufahl D. E. and Clifton A. W. (1996). Model for the prediction of shear strength with respect to soil suction. *Can. Geotech. J.* 33: 379-392

Varnes D.J. (1978). Slope movements types and processes. *Landslides: Analysis and Control, Transportation Research Board*, Nat. Acad. of Sciences, Trasp. Res. Board, Washington, Special Report 76: 11–35.

Varnes, D.J., 1978. Slope movements types and processes. In: R.L. Schuster and R.L. Krizek (Editors), Landslides: Analysis and Control. Special Report 176. *Transportation Research Board, National Academy of Sciences, Washington D.C., pp.* 11-33.

Vaunat J., Leroueil, S. & Tavenas, F. (1992). Hazard and risk analysis of slope instability. Proc. 1st Can. Symp. *Geotechnique and Natural Hazards, Vancouver,* 397-404.

Walker F., Blong R.J., McGregor J.P. (1987)- Landslide classification, geomorphology, and site investigations. *Soil Slope Instability and Stabilisation. Balkema, Rotterdam*: 1-52.

Wang F.W., Sassa K., Wang G. (2002) – Mechanism of a long-runout landslide triggered by the August 1998 heavy rainfall in Fukushima Prefecture, Japan. *Eng. Geology* 63, pp. 169 – 185.

Wang F.W., Sassa K., Fukuoka H. (2003). Downslope volume enlargement of a debris slide– debris flow in the 1999 Hiroshima, Japan, rainstorm. *Engineering Geology,* 69: 309–330.

Ward T.J., Li R.M., Simons D.B. (1982). Mapping landslides in forested watersheds. *ASCE Journal Geotechnical Enginnering Division*, 8: 319-324.

Wieczorek, G.F., 1984. Preparing a detailed landslide-inventory map for hazard evaluation and reduction. *Bulletin of the Association of Engineering Geologists* 21 (3), 337–342.

Wilson J.P., Gallant J.C. (2000). Primary topographic attributes, in Wilson, J.P., and Gallant, J.C., eds., Terrain Analysis: Principles and Applications: John Wiley and Sons, New York, 51-76.

Zecchin M., Nalin R., Roda C. (2004). Raised Pleistocene marine terraces of the Crotone peninsula (Calabria Souther Italy): facies analysis and organization of their deposits. *Sedimentary geology* 1072: 165-185.

Zhang L, Fredlund DG (2004) Characteristics of water characteristic curves for unsaturated fractured rocks. *In: The second Asian conference on unsaturated soils, Unsat-Asia, Osaka, Japan*, pp 425–428.

APPENDIX A
Geological features

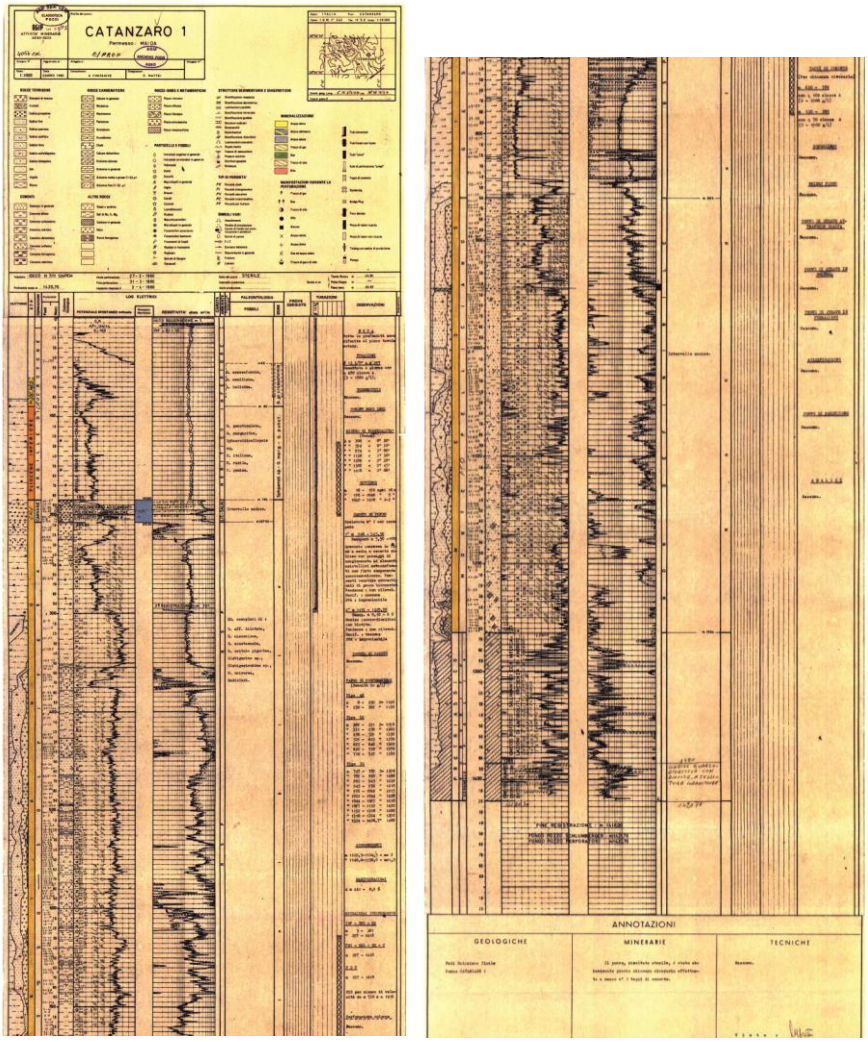

Figure A.1 AGIP Borehole (Catanzaro).

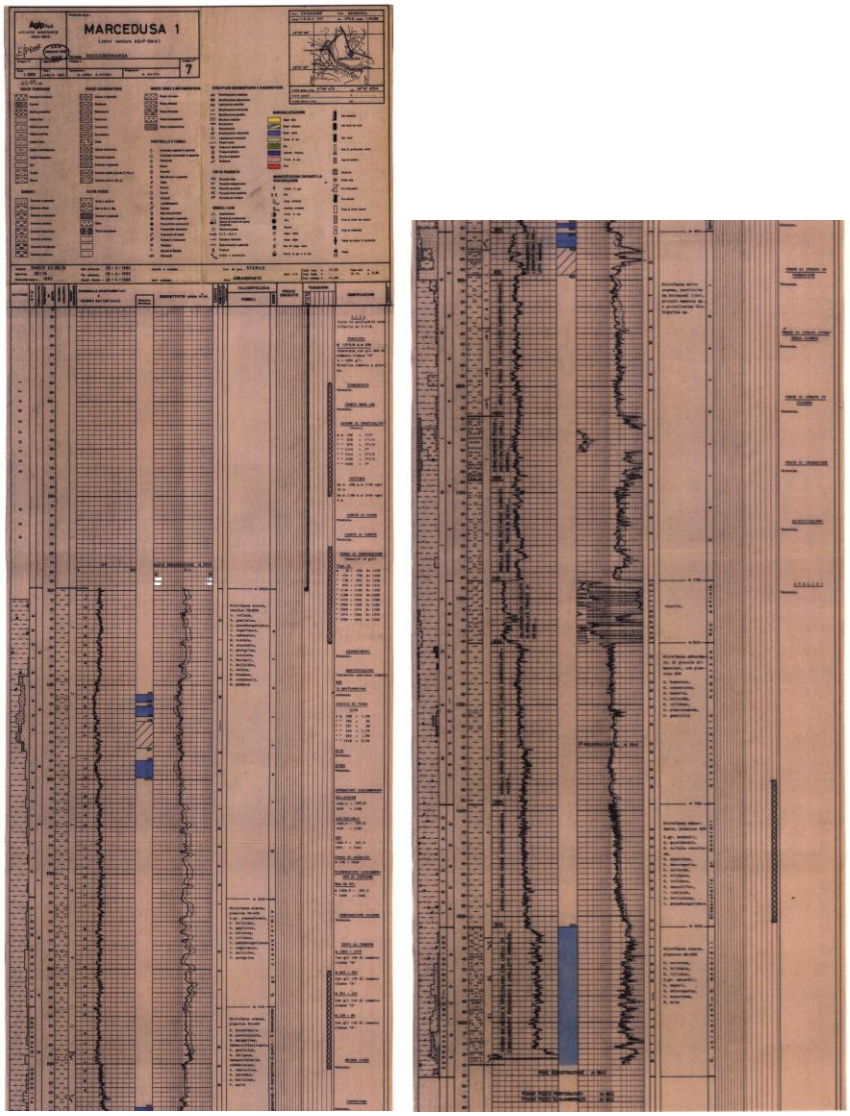

Figure A.2 AGIP Borehole (near Crotone).

http://unmig.sviluppoeconomico.gov.it/deposito/pozzi/l

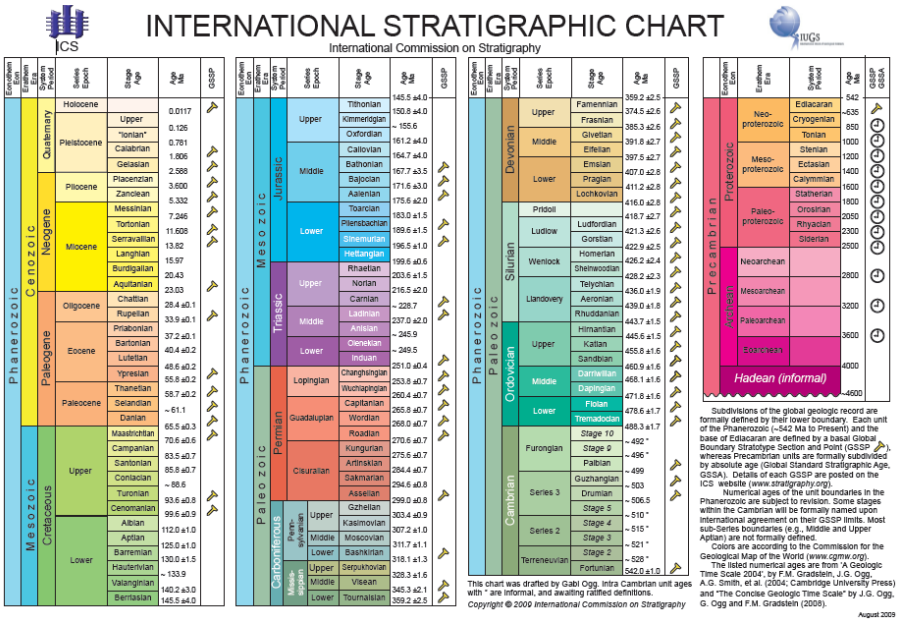

Figure A.3 International stratigraphic chart.

APPENDIX B
Theoretical aspects in the modeling

In this appendix, some aspects are addressed concerning the geotechnical methods used in Sect. 10 to model the triggering stage of shallow landslides in fine-grained soils (Sect. 8-9). Of course, this Section does provide an exhaustive discussion of the topic, and must be considered as a support to the analyses and the discussions described in the present thesis. The following pages briefly address the theoretical frameworks used in this work.

Slope scale analysis

The groundwater modelling in both saturated and unsaturated conditions was analyzed by finite element code VADOSE/W, while the triggering stage was analysed through limit-equilibrium methods using the SLOPE/W code both distributed by GEOSLOPE International Ltd (LAM et al., 1987).

Pore water pressure

The most significant variable requiring quantification is the magnitude of surface infiltration and actual evaporation, or in modelling terms, the surface unit flux boundary. VADOSE/W, determines this value by coupling moisture and heat stress states at the ground surface with climate conditions present above the ground surface.

Groundwater modelling was essentially based on heat and mass equations that can be fully coupled.

The mass transfer equation is derived directly from Richards equation for transient flow in unsaturated soils with adaptations for vapour flow added by Wilson (1990) (VADOSE/W).

Both general governing differential equations for two-dimensional seepage analysis can be expressed as:

$$\frac{1}{\rho}\frac{\partial}{\partial x}\left(D_v\frac{\partial P_v}{\partial x}\right)+\frac{1}{\rho}\frac{\partial}{\partial y}\left(D_v\frac{\partial P_v}{\partial y}\right)+$$

$$\frac{\partial}{\partial x}\left(k_x\frac{\partial\left(\frac{P}{\rho g}+y\right)}{\partial x}\right)+\frac{\partial}{\partial y}\left(k_y\frac{\partial\left(\frac{P}{\rho g}+y\right)}{\partial y}\right)$$

$$+Q=\lambda\frac{\partial P}{\partial t}$$

where:
P = pressure,
Pv= vapour pressure of soil moisture,
mv = slope of the volumetric water content function,
Kx= hydraulic conductivity in the x-direction,
Ky= hydraulic conductivity in the y-direction,
Q = applied boundary flux,
Dv= vapour diffusion coefficient as described by Wilson (1990),
y = elevation head,
ϱ = density of water,
g = acceleration due to gravity, and
t = time.

For heat transfer:

$$L_v\frac{\partial}{\partial x}\left(D_v\frac{\partial P_v}{\partial x}\right)+L_v\frac{\partial}{\partial y}\left(D_v\frac{\partial P_v}{\partial y}\right)+$$

$$\frac{\partial}{\partial x}\left(k_{tx}\frac{\partial T}{\partial x}\right)+\frac{\partial}{\partial y}\left(k_{ty}\frac{\partial T}{\partial y}\right)+Q_t$$

$$+\rho cV_x\frac{\partial T}{\partial x}+\rho cV_y\frac{\partial T}{\partial y}=\lambda_t\frac{\partial T}{\partial t}$$

ϱc= volumetric specific heat value,
Kx= thermal conductivity in the x-direction,
Ky= thermal conductivity in the y-direction and assumed equal to Ktx,
Vxy= the Darcy water velocity in x and y directions,
Qt = applied thermal boundary flux, and
Lv= latent heat of vaporization.

Under steady-state conditions, the flux entering and leaving an elemental volume is the same at all times. The last term of the equation consequently can be eliminated and the equation for mass transfer, neglecting vapour flow for the sake of clarity, becomes:

$$\frac{\partial}{\partial x}\left[k_x \frac{\partial\left(\frac{P}{\rho g}+y\right)}{\partial x}\right]+\frac{\partial}{\partial y}\left[k_y \frac{\partial\left(\frac{P}{\rho g}+y\right)}{\partial y}\right]+Q=0$$

The parameters, namely pressure (P), temperature (T), and vapour pressure (Pv) are unknown; thus, in order to solve the equations reported above, VADOSE uses the relationship proposed by Edlefsen and Anderson (1943):

$$P_v = P_{vs}\left(e^{\frac{-P \cdot w}{\rho \cdot R \cdot T}}\right) = P_{vs} h_{rair}$$

Which Joshi (1993) reformed as:

$$\nabla P_v = d_1 \nabla(-P) + d_2 \nabla T$$

Where:
Pvs= saturated vapour pressure of pure free water,
W= molecular mass of water vapour,
R = universal gas constant,
T = temperature (K) for the term in the exponent, and
hrair=relative humidity of air.

For further detailed information on the equations reproduced above, please refer to VADOSE/W engineering book.

Limit-equilibrium analysis
Limit-equilibrium analyses were developed by means of SLOPE/W code (Geoslope, 2007) using the rigorous methods proposed by Morgenstern & Price (1965). Limit-equilibrium conditions have been calculated by solving two factors of the safety equations; one equation satisfies the force equilibrium and the other satisfies the moment equilibrium. Failure

conditions are obtained when the factor of safety F reaches a value lower than one.
In these analyses, a rigid, perfectly plastic behaviour is assumed and soil shear strength and mobilized shear are related to the soil suction through the extended Mohr-Coulomb criterion (Fredlund, 1978):

$$S_m = \frac{\beta}{F}\left(c' + \left(\sigma_n - u_a\right)\tan\phi' + \left(u_a - u_w\right)\tan\phi^b\right)$$

In general, methods of slices can be classified in terms of: the statics used in deriving the factor of safety equation, and the interslice force assumption used to render the problem determinate.
The Morgenstern & Price method uses the following statics equations in solving for the factor of safety:
•The normal force at the base of the slice, N, is computed by the summation of forces in a vertical direction for each slice:

$$N = \frac{W + (X_R - X_L) - \dfrac{c'\beta\sin\alpha + u_a\beta\sin\alpha\left(\tan\phi' - \tan\phi^b\right) + u_w\beta\sin\alpha\tan\phi^b}{F} + D\sin\omega}{\cos\alpha + \dfrac{\sin\alpha\tan\phi'}{F}}$$

• The interslice normal force, E is computed by the summation of forces in a horizontal direction for each slice:

$$E_R = E_L + \frac{(c'\beta - u\beta\tan\phi')\cos\alpha}{F} + N\left(\frac{\tan\phi'\cos\alpha}{F} - \sin\alpha\right) - kW + D\cos\omega$$

• The summation of moments about a common point for all slices. The equation can be rearranged and solved for the moment equilibrium factor of safety, *Fm*.

$$F_m = \frac{\sum\left(c'\beta R + \left[N - u_w\beta\dfrac{\tan\phi^b}{\tan\phi'} - u_a\beta\left(1 - \dfrac{\tan\phi^b}{\tan\phi'}\right)\right]R\tan\phi'\right)}{\sum Wx - \sum Nf + \sum kWe \pm \sum Dd \pm \sum Aa}$$

• The summation of forces in a horizontal direction for all slices, giving rise to a force equilibrium factor of safety, *Ff*.

$$F_f = \frac{\sum \left(c'\beta \cos\alpha + \left[N - u_w \beta \frac{\tan\phi^b}{\tan\phi'} - u_a \beta \left(1 - \frac{\tan\phi^b}{\tan\phi'} \right) \right] \tan\phi' \cos\alpha \right)}{\sum N \sin\alpha + \sum kW - \sum D \cos\omega \pm \sum A}$$

where β is the base length of each slice, α is the angle between the tangent at the base of each slice and the horizontal.
Limit-equilibrium methods assume a constant factor of safety value along the entire sliding surface, which is in fact a simplification especially when such surface intersects several layers with different mechanical characteristics.

Large scale analysis
Large scale analysis can be conducted using the physically based models TRIGR and TRIGRS unsaturated. TRIGRS is a physically based model that couples a hydrological model, for the analysis of pore water pressure regime, with an infinite slope stability model for the computation of the Factor of safety.
The most important theoretical aspect concerning pore water pressure modelling for both the models and the stability condition analysis on large scale are going to be summarizedin the rest of the appendix.

Pore water pressure TRIGRS
TRIGRS and TRIGRS-unsaturated are able to analyse vertical infiltration in transient conditions of the pore pressure regime, integrating linearised solutions of Richards' equation, respectively, for saturated soils and for both saturated and unsaturated soils (Sica, 2008) .
TRIGRS model performs transient seepage analysis using the linearized solution of Richards' equation proposed by Iverson (2000), induced by constant rainfall intensities over a homogeneous hill-slope in saturated conditions. Following Iverson (2000) and Savage et al. (2003), the groundwater flow field is modelled by the superposition of a steady component, $\psi_0(Z,0)$ and a transient component $\Delta\psi(Z,t)$:

$$\begin{aligned}
&\psi(Z,t) = (Z-d)\beta \\
&+2\sum_{n=1}^{N} \frac{I_{nZ}}{K_S} H(t-t_n)[D_1(t-t_n)]^{\frac{1}{2}} \sum_{m=1}^{\infty} \left\{ \text{ierfc}\left[\frac{(2m-1)d_{LZ} - (d_{LZ} - Z)}{2[D_1(t-t_n)]^{\frac{1}{2}}} \right] + \text{ierfc}\left[\frac{(2m-1)d_{LZ} + (d_{LZ} - Z)}{2[D_1(t-t_n)]^{\frac{1}{2}}} \right] \right\} \\
&-2\sum_{n=1}^{N} \frac{I_{nZ}}{K_S} H(t-t_{n+1})[D_1(t-t_{n+1})]^{\frac{1}{2}} \sum_{m=1}^{\infty} \left\{ \text{ierfc}\left[\frac{(2m-1)d_{LZ} - (d_{LZ} - Z)}{2[D_1(t-t_{n+1})]^{\frac{1}{2}}} \right] + \text{ierfc}\left[\frac{(2m-1)d_{LZ} + (d_{LZ} - Z)}{2[D_1(t-t_{n+1})]^{\frac{1}{2}}} \right] \right\}
\end{aligned} \tag{1}$$

Where:
Z=z/cosδ, where Z is the vertical direction (positive downward) and depth below the ground surface, z is the slope-normal coordinate direction (also positive downward), and δ is the slope angle.
D is the steady-state depth of the water table measured in the vertical direction;
$\beta = \cos^2\delta - (I_{ZL,T}/K_s)$
K_s is the saturated conductivity in the Z direction;
I_{nz} is the surface flux of a given intensity for the n^{th} time interval;
$D_l = D_0/\cos^2\delta$, where D0 is the saturated hydraulic diffusivity;
N is the total number of time intervals; and
$H(t-t_n)$ is the Heaviside step function and t_n is the time at the n^{th} time interval in the rainfall infiltration sequence.
The function ierfc is of the form

$$\mathrm{ierfc}(\eta) = \frac{1}{\sqrt{\pi}}\exp(-\eta^2) - \eta\,\mathrm{erfc}(\eta),$$

Dlz is the depth of the impermeable basal boundary measured in the Z direction.
The first term in equation (1) represents the steady part of the solution and the remaining terms represent the transient part.
The equation (1) is valid in the case of an impermeable basal boundary at a finite depth dlz. Generally, this equation is applied where loose, relatively permeable slope deposits overlie relatively impermeable bedrock.

Pore water pressure TRIGRS-unsaturated
With the aim to analyse large scale stability conditions involving soils characterized by various saturation conditions, the TRIGRS unsaturated model has been used. This model treats the soil as a two-layer system consisting of a saturated zone with a capillary fringe above the water table overlain by an unsaturated zone that extends to the ground surface (Savage et al., 2004), Figure B1.

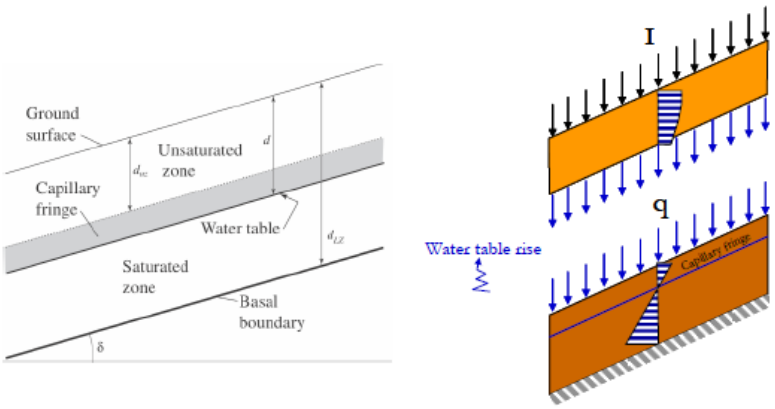

Figure B1 TRIGRS-unsaturated scheme (Savage et al., 2004)

The behaviour of an unsaturated zone can be schematized starting from the considerations made by Baum et al (2009) for whom the unsaturated zone absorbs the water a part of which infiltrates from the surface and the other part accumulates above the water table, Figure

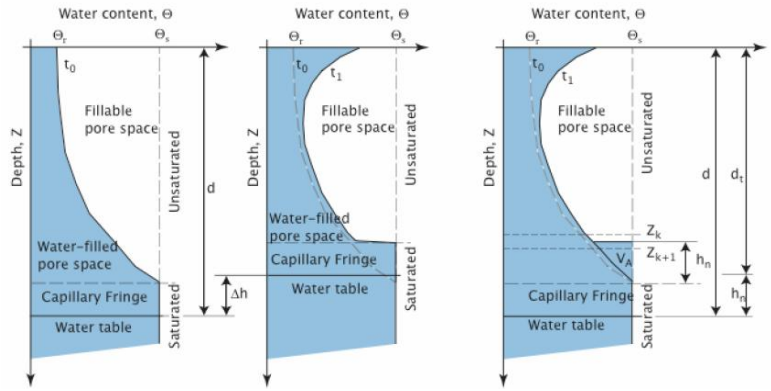

Figure B2 Water table rise (Sica 2008)

The equations governing the infiltration process are Richards' one-dimensional equations (Freeze and Cherry 1979),which use the local coordinate system proposed by Iverson 2000 in order to take into account the effects of slope over the soil.

$$\frac{\partial \theta}{\partial t} = \frac{\partial}{\partial Z}\left[K(\psi)\left(\frac{1}{\cos^2 \delta}\frac{\partial \psi}{\partial Z} - 1\right)\right] \qquad (2)$$

Where the function between conductivity and negative pressure head is given by Gardner (1958).

$$K(\psi) = K_S \exp(\alpha\psi) \qquad (3)$$

The presence of one layer of saturated material and one of partially saturated material is such that the overall formulation governing the process is different: the most general formulation used by the model takes on the form of the solution by Srivastava and Yeh (1991)

$$K(Z,t) = \sum_{n=1}^{N} H(t-t_n)\left\{\begin{array}{l} I_{nZ} - [I_{nZ} - K_s \exp(\alpha_1\psi_0)]\exp[-\alpha_1(d_u - Z)] \\ -4(I_{nZ} - I_{ZLT})\exp\left(\frac{\alpha_1 Z}{2}\right)\exp\left[-D_\psi \frac{(t-t_n)}{4}\right] \\ \cdot\sum_{m=1}^{\infty} \frac{\sin[\Lambda_m\alpha_1(d_u - Z)]\sin(\Lambda_m\alpha_1 d_u)}{1+\frac{\alpha_1 d_u}{2}+2\Lambda_m^2\alpha_1 d_u}\exp\left[-\Lambda_m^2 D_\psi (t-t_n)\right] \end{array}\right\} \qquad (4)$$

$$-\sum_{n=1}^{N} H(t-t_{n+1})\left\{\begin{array}{l} I_{nZ} - [I_{nZ} - K_s \exp(\alpha_1\psi_0)]\exp[-\alpha_1(d_u - Z)] \\ -4(I_{nZ} - I_{ZLT})\exp\left(\frac{\alpha_1 Z}{2}\right)\exp\left[-D_\psi \frac{(t-t_{n+1})}{4}\right] \\ \cdot\sum_{m=1}^{\infty} \frac{\sin[\Lambda_m\alpha_1(d_u - Z)]\sin(\Lambda_m\alpha_1 d_u)}{1+\frac{\alpha_1 d_u}{2}+2\Lambda_m^2\alpha_1 d_u}\exp\left[-\Lambda_m^2 D_\psi (t-t_{n+1})\right] \end{array}\right\}$$

In which:

$$D_\psi = \frac{\alpha_1 K_S}{(\theta_s - \theta_r)}$$

Λ_m are the positive roots of the pseudoperiodic characteristic equation: $\tan(\Lambda d)+2\Lambda=0$.

Pressure head in the unsaturated zone is obtained from equations 3 and 4.

Slope stability

Both the models defined (TRIGRS and TRIGRS unsaturated) use an infinite-slope stability analysis (Taylor, 1984) for stability conditions modelling. The failure of an infinite slope is characterized by the ratio of resisting basal Coulomb friction to gravitationally induced downslope basal driving stress, *Fs*, calculated at a depth *Z* by:

$$F_S(Z,t) = \frac{\tan\phi'}{\tan\delta} + \frac{c' - \psi(Z,t)\gamma_W \tan\phi'}{\gamma_S Z \sin\delta\cos\delta}$$

Where c' is soil cohesion for effective stress, φ' is the soil friction angle for effective stress, γ_w is unit weight of groundwater, and γ_s is soil unit weight.Factors of safety are calculated at different depths and then in different conditions of saturation. The failure is predicted when Fs<1 and obviously stability when Fs≥1. The depth *Z* in whichF_S<1will be the depth of landslide initiation, this depth depends on soil properties and on the time and depth variation of pressure head and, also, on rainfall history.

In unsaturated zones, TRIGRS unsaturated uses a simple approximation by Bishop (1959) introducing an effective stress parameter, χ, when computing the factor of safety . In particular TRIGRS unsaturated uses the approximation suggested by Vanapalli and Fredlund (2000) in which: $\chi = (\theta - \theta_r)/(\theta_s - \theta_r)$. Thus to calculate FS in the unsaturated portion, the value of ψ(Z,t)γ_{wi} multiplied for χ.

Table B1: Boundary condition at the groud surface.

Date	#	T (°C)		RH (%)		Wind	R
		T max	T min	max	min	(m/s)	(mm)
19/12/01	1	9.5	0.8	62.2	38.8	2.1	0
20/12/01	2	11.9	5.1	71.7	49.3	1.3	0
21/12/01	3	12.2	6.1	89	58.9	2	2
22/12/01	4	12.9	6.3	96.7	60.4	2.9	17.2
23/12/01	5	14.5	7.8	94.6	56.1	1.7	6
24/12/01	6	13.2	6.9	99.7	64.4	2.1	15.2
25/12/01	7	10	6.5	98.2	55.5	2.2	2.8
26/12/01	8	10.6	6.3	93.3	62.6	2.3	0.6
27/12/01	9	10	4.2	92.6	58.3	3.2	30.8
28/12/01	10	10.1	4.2	73.6	42.8	3.6	0
29/12/01	11	13.6	7.1	95.5	71.1	3.2	3.6
30/12/01	12	17.2	11.4	88.4	41.2	4.8	0.2
31/12/01	13	15.3	13.3	92.6	70.4	5.2	0.2
01/01/02	14	13.9	3.3	99.8	20.6	3.3	12
02/01/02	15	7.8	-0.2	69.3	37.9	3.9	0
03/01/02	16	7.8	2.8	92.7	31.8	2.4	0.6
04/01/02	17	4.6	0.3	91.2	33.6	3.6	0
05/01/02	18	9.3	1.6	55.4	31.8	3.2	0
06/01/02	19	11.4	2.7	67.2	36.1	2.2	0
07/01/02	20	12.4	5.3	78.5	52.7	1.9	0
08/01/02	21	13.4	5.1	76.1	47.8	1.2	0
09/01/02	22	13.7	5	77.9	44.6	1.4	0
10/01/02	23	13.3	5.6	79	53.6	1.6	0
11/01/02	24	14	7.2	82.2	55.9	2	0
12/01/02	25	14.2	7	82	59.1	1.9	0
13/01/02	26	12.8	6.5	93.4	68.6	1.2	2.2
14/01/02	27	14.5	7.4	92.3	59.5	1.6	0
15/01/02	28	12.1	6.3	94.9	70.6	1.5	9.2
16/01/02	29	11.1	5	81	61.6	1.6	0.2
17/01/02	30	12.1	7.6	96.1	74.9	1.8	2.2
18/01/02	31	11.7	7	96.1	59.1	2	0.6
19/01/02	32	9.6	2.6	88	50	0	0.2
20/01/02	33	11.7	6.5	79	54	0	0
21/01/02	34	12.7	5.8	89	64	0	0
22/01/02	35	11.9	8.5	78	58	0	0

02/02/02	46	15.2	9.1	90	69	0	0
03/02/02	47	16.1	9.9	91	42	0	0
04/02/02	48	16.3	10.9	90.3	61.5	3.6	0
05/02/02	49	15.4	10.1	94.1	62.4	3.8	0
06/02/02	50	17.5	9.6	92.1	42.7	1.7	0
07/02/02	51	11.6	9.6	98.1	79.1	1.4	9.2
08/02/02	52	17.2	9.7	98.6	59.1	2.2	1.2
09/02/02	53	15.5	9.7	91.5	68.1	2.7	0
10/02/02	54	13.9	11	93.1	69.2	4.1	0.6
11/02/02	55	17.8	10	90.4	25.1	4.5	0.6
12/02/02	56	15.8	9.8	85.9	64.2	3.7	0
13/02/02	57	15.6	10	91.3	62.9	3.4	0.4
14/02/02	58	17.4	9.9	91.5	60	2.3	0
15/02/02	59	14.2	10.2	97.5	76.5	3	0
16/02/02	60	16.1	12.3	96.8	77	3.5	0
17/02/02	61	14.2	13.3	96.3	90.8	5.5	0
18/02/02	62	15.6	13.1	97.6	80.9	5.2	0
19/02/02	63	15.9	9.9	93.7	64	3.5	0
20/02/02	64	14.8	8.3	86.3	53.7	3.5	0
21/02/02	65	14.6	9.9	88.2	55.1	3.3	0.2
22/02/02	66	12.5	9.4	91.9	75.1	2	0
23/02/02	67	15	8.9	93	63.5	3.5	2.6
24/02/02	68	14.6	10.7	92.5	69.3	6.5	21.2
25/02/02	69	14.2	9.3	91.1	47.8	2.3	0
26/02/02	70	13.6	10.2	96.6	71.8	2.6	8.2
27/02/02	71	15.9	11.4	90.7	53.5	4.6	0.4
28/02/02	72	21.2	11.4	72.5	23.5	4.5	0
01/03/02	73	26.3	12.3	96.2	15.6	1.7	0
02/03/02	74	24.4	12.8	96	27.9	1.7	0
03/03/02	75	21.2	10.6	99.3	31.1	1.3	0
04/03/02	76	19.7	10.9	99.9	36.3	2.8	0
05/03/02	77	17.5	11.2	97.5	73	4.5	0
06/03/02	78	16.6	13.9	97.8	69.4	3.5	1.2
7/3/02	79	16.2	12.9	99.6	64	2.5	2.4
8/3/02	80	16.3	11.8	88.2	47.8	2.1	0.8
9/3/02	81	18.4	12.9	99.4	46.4	3.1	11
10/3/02	82	13.6	11.3	99.5	75.5	4.1	5.4

11/3/02	83	15.2	11.2	78.5	32.7	3.6	0.2
12/3/02	84	15.6	10	82.1	39.1	3.7	0.2
13/3/02	85	18	8.7	89	46.8	1.4	0
14/3/02	86	16.8	9.9	93.5	73.7	2.4	0
15/3/02	87	17.7	11.4	94.9	73.2	1.9	0
16/3/02	88	17.8	11.7	97.3	74.7	2.1	0
17/3/02	89	17.1	11.7	96.1	70.3	2.9	0
18/3/02	90	17.8	10.5	94.1	69.1	2.5	0
19/3/02	91	16.9	12.9	91.5	68.3	5	0.2
20/3/02	92	18.1	13.1	92.3	74	5.7	2
21/3/02	93	20.1	13.7	92.5	59.7	4.5	1
22/3/02	94	16.1	13	93.6	69.8	6.1	9.4
23/3/02	95	15.9	5.5	95.5	44.7	4	23
24/3/02	96	10.5	4.8	65.5	31.7	4.2	0
25/3/02	97	13.3	5.2	64.8	44.5	4.2	0.2
26/3/02	98	14	6.1	70.3	42.7	3.6	0.2
27/3/02	99	12.2	6.5	93	64.3	1.5	1.4
28/3/02	100	15.2	5.9	83.5	33.1	1.7	0
29/3/02	101	14.5	6.4	76.7	40.3	2.5	0
30/3/02	102	16.9	6.9	75.3	37.6	1.9	0
31/3/02	103	15.5	7.4	84	39.7	3.3	0.2
1/4/02	104	16.8	8.7	89.5	57	3.1	0
2/4/02	105	19.9	10.3	94	44.5	2.4	0
3/4/02	106	12.7	8.9	100	55.8	3.8	24
4/4/02	107	13.9	7.3	100	81.7	3.1	21.2
5/4/02	108	13.7	7	93.7	70.2	4	2.4
6/4/02	109	16.6	9.2	92.9	70.1	3.9	10.2
7/4/02	110	19.9	12.3	83.8	46.1	2	0
8/4/02	111	17.3	10.2	95.8	71.1	3.1	0
9/4/02	112	16.9	11.5	98	76.5	2.6	0
10/4/02	113	19.4	13.1	93.4	61.6	2.5	0
11/4/02	114	17.9	11.9	99.3	69.6	3.6	1.2
12/4/02	115	17.5	14.1	100	86.8	3.4	6.2

13/4/02	116	23.9	13.3	100	46.9	2.5	0.2
14/4/02	117	18.2	13.2	92.3	62.9	4.3	0
15/4/02	118	16.9	12.2	94.6	62.7	4.9	0.2
16/4/02	119	16.4	11.3	79.3	54.2	5.6	1.8
17/4/02	120	16.4	11.7	83.2	59.9	4.8	0
18/4/02	121	15.9	10	88.4	64.8	4.8	1
19/4/02	122	16.7	11.1	90.3	65.4	5	0.6
20/4/02	123	17.2	11.9	90.7	64.9	4.4	0.4
21/4/02	124	18.3	10.9	94.5	55.3	2.7	0
22/4/02	125	19.3	11.7	89.9	43.9	3.2	1.6
23/4/02	126	17.5	11.8	89.9	64.6	4.5	0.8
24/4/02	127	18.9	12.3	91.8	60.8	4.5	0
25/4/02	128	16.4	10.7	92.3	71.7	1.5	1.8
26/4/02	129	18.9	10	98.5	53.4	2.6	2
27/4/02	130	19.5	11.7	90.6	44.3	2.9	0.2
28/4/02	131	21.1	13.4	93.2	48.4	2.7	0
29/4/02	132	20.6	11.8	94.3	68	1.7	0
30/4/02	133	23.1	14.4	87.5	32.8	2.2	0
1/5/02	134	22.9	14.7	91.1	49.6	1.7	0
2/5/02	135	21.4	14.3	96.1	67.2	3	0
3/5/02	136	22.9	15	93.9	51.2	3.3	0
4/5/02	137	23.4	15.3	92.2	54.9	3.6	0
5/5/02	138	19.5	12.8	92.2	57.9	4.1	0.6
6/5/02	139	21.7	11.9	88.5	44.4	2.3	1.8
7/5/02	140	21.3	12.8	95.4	42.7	3.2	3.4
8/5/02	141	18.8	15.6	97.3	56.3	5.2	11.8
9/5/02	142	19.9	15.8	96	54.3	3.9	0.8
10/5/02	143	24	16	93	29.2	2.3	0
11/5/02	144	19.8	14.8	93.7	70.1	3.3	6.4
12/5/02	145	19.1	13.3	94.1	72.8	4.3	6.2
13/5/02	146	18	13.3	95.2	79.6	5	4.2
14/5/02	147	19.1	14.5	92.6	71.3	4.2	0.2
15/5/02	148	19.9	14.6	87.8	70.3	4	0
16/5/02	149	22.1	15.2	90.9	63.3	3.9	0
17/5/02	150	26.4	16.1	88.2	44.5	1.5	0
18/5/02	151	27.3	16	84	41.3	2.2	0
19/5/02	152	20.7	15.7	90.2	53.6	3.3	0
20/5/02	153	20.7	15.4	94	69.2	3.1	11.6
21/5/02	154	22.2	15.9	93.7	63	3.1	3
22/5/02	155	23.7	15.9	95.7	58.6	1.8	0

29/5/02	162	19.3	14.4	69	53	0	0
30/5/02	163	20.6	14.6	73	60	0	0
31/5/02	164	22.8	14.7	83	62	0	0
1/6/02	165	25.9	15.5	85	60	0	0
2/6/02	166	24.9	16.3	84	60	0	0
3/6/02	167	23.7	16.9	81	61	0	0
4/6/02	168	24.1	16.5	80	56	0	0
5/6/02	169	25.6	18	77	27	0	0
6/6/02	170	23.2	17.9	79	45	0	0
7/6/02	171	20.7	16.1	80	62	0	0.8
8/6/02	172	25.2	16	80	62	0	0
9/6/02	173	22.5	15.1	85	59	0	0
10/6/02	174	21.3	13.8	84	57	0	1.8
11/6/02	175	22.2	15.6	77	55	0	0
12/6/02	176	24.1	16.3	76	58	0	0
13/6/02	177	23	16.9	81	58	0	0
14/6/02	178	23.9	16.9	80	60	0	0